Evaluation of an In Situ Polymerizing Hydrogel Scaffold as a Brain Delivery System for Parkinson's Disease therapeutics

Francesco Gubinelli

université PARIS-SACLAY

NNT : 2019SACLS439

UNIVERSITÉ PARIS SUD
Comprendre le monde, construire l'avenir

Evaluation of an *in situ* polymerizing hydrogel scaffold as a brain delivery system for Parkinson's disease therapeutics

Thèse de doctorat de l'Université Paris-Saclay
préparée à CEA - MIRCen, UMR 9199

École doctorale n°568 : signalisations et réseaux intégratifs en biologie (Biosigne)
Spécialité de doctorat: Sciences de la vie et de la santé

Thèse présentée et soutenue à Fontenay-aux-Roses le 10 Décembre 2019, par

Francesco Gubinelli

Composition du Jury :

Prof. Michael Schumacher Research Director INSERM, Paris-Saclay University	President
Dr. Gaillard Afsaneh Research Director INSERM, University of Poitiers	Rapporteur
Dr. Eilis Dowd Senior Lecturer and Team Leader National University of Ireland	Rapporteur
Prof. Stephane Palfi University Professor and Hospital Practitioner Mondor Biomedical Research Institute	Examinateur
Dr. David Blum Research Director INSERM University of Lille Nord de France	Examinateur
Dr. Emmanuel Brouillet Research Director CNRS Paris-Saclay University	Directeur de these

Thèse de doctorat

And how can we win,
When fools can be kings?
Don't waste your time
Or time will waste you.

(Muse, King of Cydonia, 2006)

This project has been funded by the European Union Horizon 2020 Programme (H2020-MSCA-ITN-2015) under the Marie Skłodowska-Curie Innovative Training Network and Grant Agreement No. 676408.

Acknowledgments

Various people have been participating is such exciting and unexpected scientific voyage.
First of all, I would like to thank my supervisor for giving me the possibility to be part of the BrainMatTrain consortium, and all the ESRs, managers and supervisors with whom I spent lovely scientific and personal time during the last 3 years.
I would also personally thank our collaborators (mainly National University of Galway, Collagen Solution and Strathclyde University of Glasgow) for the exciting and prolific scientific exchange we had in these 3 years.
Inside my home institution, I would like to thank all the people of MIRCen that directly or indirectly helped me to professionally grow up and be a more experienced researcher.
Special thanks go to Sylvie, Cecile and Marie-Laure because they were never bothered with my requests, in English or broken French.
Within all the people of MIRCen, I would particularly thank:

- Histology team: Caroline Fanny and Pauline G., for your patience and your unconditional help at any time and moment
- In vivo team: Martine and Mylene, because any crazy request I did was accepted not only with a smile, but also with great technical and practical support
- MRI team: Julien and JB, for being always available to answer my naïve questions
- Human stem cells team: Anselme, Morgane and Emilie, our collaboration was very short but definitely intense and exciting.
- Marie-Claude, Gwen and Maria C., because even if you had other important things to do, you always found time to give me suggestions, or to directly help me.

In addition to all this, there are few extra people I would love to thank personally from the deepest of soul.

- Pauline R., for surviving 3 years with me – in the office, and at home. She had also to stand to a lot of complains and request of help, especially for word and power point.
- Marianna, because the crazy experiments we did together would not have been possible without your visits in MIRCen. In addition, coffee in two is much tastier than alone.
- Didier, because he is the da Vinci of computer, electronic, robotic, 3D printing and whatever you might need. If something does not exist yet, ask Didier.
- Nadja, the problem solver. Scientific or non-scientific problem, she always finds a solution! If the solution is not straightforward, she is always ready to make it happen, and this has been extremely precious for me. Few lines are not enough to describe my appreciation, but I hope I showed you my gratitude in these 3 years.
- Gilles, because he is something like a scientific motivational coach. When you are lost in the cloud, he is the perfect lighthouse to show you the good direction.
- Geraldine, something like a second mum. In addition to the great science she does, she always found the time to talk about personal and scientific problems I faced. With her words and encouragements, I was always able to see a new light at the end of the tunnel.
- And then, we arrive to AnSo: I am sure this is not enough to thank a person that has been crucial for many of the results achieved during my PhD. Your hints, irony, experience, scientific and human suggestions have been extremely important for all my work. In addition, she is the only one who can fully tame and dominate the wild beast - the AxioScan.
  I will never forget the funny and deep conversations we had while waiting the pre-scan of the slices into the AxioScan, with a room temperature of 15° C.
  I am very very grateful to you, and I will not forget it easily.

Table of contents

List of figures

List of tables

1. Introduction

1.1 The numbers of Parkinson's disease today

Parkinson's disease (PD) is the second most common neurodegenerative disease after Alzheimer's disease (AD), causing severe disability and reduced quality of life in the patients, and a significant burden on family, caregivers and national healthcare system (Findley, 2007; Lau and Breteler, 2006). Onset of the disease is rare before 50 years of age, increasing drastically after an age of 60 years (Lau and Breteler, 2006), and it is considered to affect, with variations between studies and countries, around 0.3% of the general population, reaching 1% in the group aged over 60 (Blin et al., 2015). At the moment, 10-20 years after onset of the disease between 40% and 75% of the patients die, while 50% of the surviving ones need strong and intense home-care (Xia and Mao, 2012). Statistically, 90% of PD cases are considered to be sporadic, while the remaining 10% is considered to be derived from causative genetic mutations (Lau and Breteler, 2006).

The disease starts with early death of dopaminergic (DA) neurons in the substantia nigra pars compacta (SNpc) (Kalia and Lang, 2015) that project to the basal ganglia (Dickson, 2018), and accumulation of Lewy's bodies (LB) within the surviving neurons (Lesage and Brice, 2009) composed of alpha-synuclein (α-syn) protein (Spillantini et al., 1997). The disease is characterized by two types of typical symptoms: motor deficits such as bradykinesia, resting tremors, rigidity and postural instability (Kalia and Lang, 2015) and non-motor deficits such as apathy, constipation, sleep and mood disturbance, loss of smell and taste, fatigue and anxiety (Sveinbjornsdottir, 2016). At the moment, patients' lifestyle is partially improved by symptomatic pharmacological (e.g. L-DOPA) and/or non-pharmacological treatments (e.g. deep brain stimulation), while there is no therapy available that directly targets the neurodegenerative process (Singh et al., 2007).

Due to the lack of effective treatment that directly targets the development of the disease, there is an increase in costs for patients, family and society: extensive studies on such topic are lacking but a document published by the World Health Organization (WHO) in 2006 states that in average the annual cost for a PD patient is more than double compared to the control population (World Health Organization, 2006). Approximately $14 billion was spent in 2010 in the US by subjects affected with

PD, accounting for $8.1 billion more than the same population without PD. Of all the extra medical costs for PD, approximately 24% were paid by the national health insurance program (Medicare), 24% by other government programs (as Medicaid), 19% by personal commercial insurances, and 33% were directly paid by the PD patients and families (Kowal et al., 2013).

In Europe the weighted mean estimated cost from all countries and diagnoses for subjects affected by PD is 11.153 € year/person, while the total estimated cost for all the PD affected patients is 13.933 million € (Gustavsson et al., 2011). Specifically around 50% of all expenses are direct healthcare costs (goods and services related to the prevention, diagnosis and treatment of the disease), around 40% are direct non-medical costs (goods and services related to the disorder as social services, special accommodation) and around 10% are considered indirect costs (early retirement and loss of productivity at work) (Gustavsson et al., 2011).

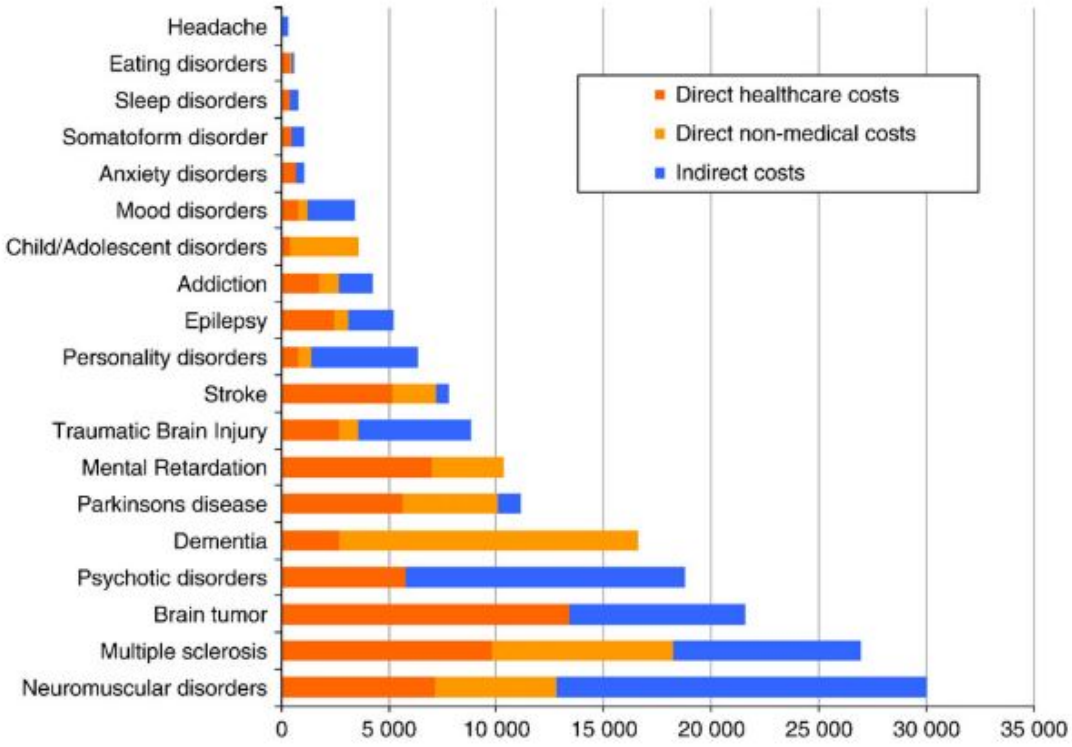

Figure 1: Financial burden of brain diseases in European Union.

Estimation of annual types of costs (€/patient) of different brain diseases in European population in 2010.

(Gustavsson et al., 2011)

1.2 History of Parkinson's disease

1.2.1 Parkinsonism in ancient history

The first written descriptions of tremor as a consequence of troubles in the movement centre appear in one of the only two surviving scripts about the Indian traditional medicine - the *Charaka Samhita* (2500 BC). In chapter 20, different tremors are described, ascribing some of them with a disbalance of the vatas' (one of the three energies, specifically controlling movements in the mind and in the body) (Lees, 2007).

Some descriptions of Parkinsonism and PD related movement disorders can also be found in a document written between 1350 BC and 1200 BC, during the 19th Egyptian dynasty, describing the uncontrolled salivation of an old king and his inability to maintain saliva in the mouth, resembling the drooling visible in Parkinson's Disease patients (Lees, 2007).

Another mention of tremors is shortly given in the *Tanakh* (the Hebrew Bible), where the aging process is associated and described as *trembling* (Lees, 2007).

A more comprehensive attestation of tremors as a pathological condition is ascribed to Aelius Galenus (commonly known as Galen of Pergamon) - a famous Greek philosopher, physician and surgeon who lived in the Roman Empire between 129 AD and 210 AD. In a short work called "*De Tremore*" Galen described unwanted tremors (together with spasms, palpitations and rigor) as the consequence of movements' organ's disease. The author clearly distinguishes tremor from palpitation: the first one occurs only when the subject consciously wants to produce a movement and is aware of it, while the latter affects parts of the body that are at resting state. Galen described palpitations as caused by thick and vaporous pneuma induced by cold that localize in a cavity (supposedly in the muscles): winter, cold regions or food were considered as risk factor, and the treatment suggested by Galen included warm spring water/seawater, warm drinks and different kinds of drugs (Galen, republished in 1824).

1.2.2 Parkinsonism in the early modern history

In the 15th century Leonardo da Vinci, on a note in the side of the page of the anatomical drawings from the Royal Library Windsor Castle, described how sometimes nerves produce movements without any command of the body or the soul (as the trembling of people feeling cold or the ones of paralytics): such movements are involuntary and cannot be anyhow prevented (Lees, 2007).

In the "*De cerebri morbis*" (one of the first neurology book) published in the 16th century, Pratensis presents an evolution of Galen's theory; the author describes tremors as obstruction of nerves caused by cold, that can occur also at resting state when the patient does not attempt to move a part. Tremors are not always pathological (an example is seen after carrying heavy objects) and causes of each single event should be deeply investigated into patient's personal life (J. Pratensis, 1549).

In 17th and 18th century, while there is a more detailed differentiation between involuntary movements during action and at rest, additional causes are considered to lead to tremors: these include exposure to mercury vapours, narcotics and alcoholics (especially if taken on an empty stomach). Tremors can also be a prognostic sign of paralysis or epilepsy, and could lead to seizure. Differentiation between external causes – disappearing spontaneously over time - and internal causes – considered incurable with usually bad prognosis, were done during those years; interestingly tremor in old people was considered incurable. Treatments, following Galen's directions, suggested to keep the patient away from sunlight, moonshine or humid places; moreover affected subjects were suggested to sleep after meals, avoid emotions and exercise (Koehler and Keyser, 1997; Lanska, 2009).

1.2.3 From "The Shaking Palsy" to Parkinson's disease

The first most important, extensive and methodological transcript of the disease dates back to 1817, when James Parkinson, a bright surgeon and luminary in different scientific fields, published a document called "*An Essay on the Shaking Palsy*", where he describes the behaviour of 6 subjects he had the chance to get in touch with. All the subjects had similar behaviour and they all exhibited – quoting the author himself – "*involuntary tremulous motion, with lessened muscular power, in parts not in action and even when supported; with a propensity to bend the trunk forwards, and to pass from a walking to a running pace: the senses and intellects being un-injured*" (Parkinson, republished in 2002). The disease at that time was reported with the name of *paralysis agitans*.

To prove even more the high intellectual and professional capability of James Parkinson, it is worth mentioning story of how the author met his 6 described subjects **(Table 1).**

Table 1: How J. Parkinson met his "patients" *(Parkinson, republished in 2002).*

The first case was never met by James Parkinson, but he received all the information by a physician who examined the subject. The second and third case were casually met in the street and stopped to have a brief discussion about their condition. The fourth and sixth case instead was presented at James Parkinson, who was able to collect their story and to make a short examination. More interesting is the story of the fifth case: the described subject was seen and followed by the author in the streets, but unfortunately no contacts have been taken between the two.

"*An Essay on the Shaking Palsy*" obviously attracted international attention but only years after its first publication.

Concurrently with James Parkinson, two other doctors in France, Charcot and Vulpian became interested in Parkinson's disease, publishing interesting additional material about it. For example, they recognized and confirmed the key hallmarks of the disease as bradykinesia, resting tremors, impairment of balance and rigidity (Goedert and Compston, 2017). In addition, Charcot noticed that some subjected diagnosed with PD presented atypical neurological signs as lack of tremor or rigid posture instead of stooped one: this led, from one side, to a more accurate and precise disease's diagnosis, and on the other side introduced the concept that other pathological conditions could be added (or misdiagnosed) for PD, leading to different prognosis and treatment (Przedborski, 2017). Moreover they also noted that intellectual faculties, at the beginning of the disease, were mostly unaffected (Goedert and Compston, 2017). In honour of James Parkinson, they decided to call this medical condition Parkinson's disease.

Table 2: A patient's point of view about Parkinson's Disease *(Horowski et al., 1995).*

Between 1829 and 1834 Wilhelm von Humboldt, a German diplomat in the Congress of Vienna, wrote different letters to friends describing his "*special clumsiness*". His letters are the first real insight and touching testament of the feelings and difficulties of a PD patient, while at the same time capturing the most relevant clinical symptoms. Strikingly, in most all the letters Von Humboldt is asking the addressee for forgiveness for his unclear hand-writing, explaining that it occurs when not fully concentrated on writing. He says that his hands are affected, but not the eyes. The doctor's attributed this to a weakness in the spinal cord, as it was believed to be the place where nerves originate. In subsequent letters Wilhelm von Humboldt described newly arising difficulties in every-day tasks, such as buttoning up while dressing. Interestingly the author discriminates other behaviours like holding, grabbing and carrying that are not impaired. In addition, he described a cyclical transitory unpleasant trembling in the feet, both while standing and sitting, that does not impair walking, and trembling in the hands that is present only when one or both of them are inactive. It occurs mostly when he is under pressure or in rush. Wilhelm von Humboldt describes himself as not suffering from any disease but a "*premature advanced aging*"

1.2.4 Parkinson's disease in modern medicine

An important achievement in the modern history of PD dates back to 1912: the discovery of Lewy's body (LB). Friedrich Jakob Heinrich Lewy, analysing different human brains, noticed the presence of some typical characteristic inclusions in different parts of the brain (i.e. periventricular nucleus of the thalamus, dorsal motor nucleus of the vagus nerve, globus pallidus, lateral nucleus of the thalamus and basal nucleus of Meynert). Such inclusions were very characteristic and not soluble in ethanol or any other solvent, meaning they were formed of protein/proteins. Few years later, in 1919, Konstantin Tretiakoff found the same inclusions in the substantia nigra (SN) of PD patients: he decided to name these as Lewy's body, in honour of the first discoverer. A few years later, Tretiakoff, as well as Rolf Hassler in 1938 (Parent and Parent, 2010), linked the development of PD with loss of nerve cells and degeneration of the substantia nigra. They both located the site of major loss in the ventrolateral and caudal part of the SN, definitely proving that the globus pallidus and the striatum were mostly unaltered in this disease. Lewy never fully accepted Tretiakoff's theory on the origin of the disease, remaining with the idea that Parkinson originated in the globus pallidus (Goedert et al., 2013).

Arvid Carlsson is another import player in the history of Parkinson's disease: a former pharmacologist and a Nobel Prize winner in 2000, he is today considered as the first scientist to effectively prove the link between loss of dopamine and parkinsonism. In 1957, he first theorized that

dopamine in the brain is a neurotransmitter and not simply a precursor of norepinephrine. Moreover he discovered that reserpine (an indole alkaloid) was able to deplete dopamine, leading to a loss of movement control very similar to the one visible in Parkinson's disease (Yeragani et al., 2010). In the same year Carlsson, together with other researchers from different laboratories, showed that Levodopa (L-dopa), a naturally occurring L-isomer of the amino acid D, L-dihydroxyphenylalanine, was able to restore normal levels of dopamine in animals previously depleted of all the three catecholamines; interestingly, levodopa restored only dopamine levels, leaving the levels of adrenaline and noradrenaline almost untouched (Yeragani et al., 2010). Thanks to Hornykiewicz and Birkmayer, these findings were quickly translated into human testing, as a dopamine restoring therapy: various studies (also done investigating a placebo effect of L-dopa) clearly showed the great anti-akinetic effect of the treatment on PD patients (Yeragani et al., 2010).

1967 was the year L-dopa became routinely administered for the treatment of PD: before '67, in fact, levodopa was partially used with PD patients but many reports were fairly sceptical about its real effect. In addition, there were various concerns about its gastrointestinal side effects observed even with tiny doses. George Cotzias developed an oral L-dopa intake based on high dosage together with a very slow release over time, that is still nowadays worldwide used (Hornykiewicz, 2010; Lees et al., 2015).

A key event in the story of PD is the discovery of alpha-synuclein in 1997. In a large Greek family emigrated to Italy with members living in the United States, researchers were able to identify the first genetic missense mutation in the gene *SNCA* (named A53T) directly connected with the autosomal dominant form of the disease (Fahn, 2018; Polymeropoulos et al., 1997). This breakthrough was completed a few months later by the short paper published in Nature by Spillantini and colleagues, showing that Lewy bodies were mostly constituted by aggregated form of α-syn (Spillantini et al., 1997). In addition the authors noticed that such aggregations were not only visible in subjects with the *SNCA* mutation, but also in patients with sporadic form of PD; this led to the concept that α-syn is a key player in the pathogenesis of PD, and not only a rare genetic player (Nussbaum, 2017; Spillantini et al., 1997).

In the last 30 years huge achievements have been reached in the field of Parkinson's disease both in clinical and applied/translational research: these advances include – but are not limited to -

neuroprotective agents, cells transplantation, surgical procedures, gene therapy (Oertel, 2017; Singh et al., 2007), biochemistry (Fahn, 2018), pharmacological research (Hauser, 2011; Jankovic and Poewe, 2012), to end up with the modern, and still under development biomaterials' approach (Giordano et al., 2009; Moriarty and Dowd, 2018; Newland et al., 2013).

Another important event is the clinical application of deep brain stimulation (DBS) in the treatment of PD: DBS is a surgical technique where electrodes are implanted in a target brain region, and thanks to an impulse generator, electrical stimuli are delivered into the brain to disrupt or modulate neural signalling (Okun, 2012). Even if the use of DBS dates back to 1870, Food and Drug Administration (FDA) approved DBS of the subthalamic nucleus for PD only in 2002 aiming to reduce symptoms caused by levodopa intake (in particular dyskinesia, tremors and on-off fluctuations) when pharmacological adjustments are not effective (Kringelbach et al., 2007; Okun, 2012). Even if complications and side effects caused by surgery have to be considered (but are nowadays quickly being overcome thanks to advances in surgical procedures), positive clinical outcomes of DBS were confirmed by numerous clinical trials, demonstrating a great improvement in analysed patients, long lasting positive effect on symptoms and significant improvement in quality of life (Groiss et al., 2009).

Nowadays more and more public, private, no profit and governmental institutions are offering grants and funding to investigate different aspects of Parkinson's disease. In Europe, an interesting project focused on Parkinson's disease was financed in 2016 by the Research Executive Agency (REA) of the European Commission within the Horizon 2020 program. The project, called *BrainMatTrain* (BMT), aims to understand the mechanisms behind PD, from the basis to translation, involving four research institutions, two hospitals and two small and medium-sized enterprises (SMEs). The consortium aims to develop a multi-modal injectable collagen hydrogel scaffold that would incorporate therapeutic moieties able to target directly two aspects that are considered crucial in triggering and developing PD: neuro-inflammation and neurodegeneration. The consortium is managing one of the few interdisciplinary projects that involves the use of biomaterials to directly target PD, mixing basic and translational research with biomaterial and cellular engineering, hoping for the development of a commercializable functional medical device against Parkinson's disease.

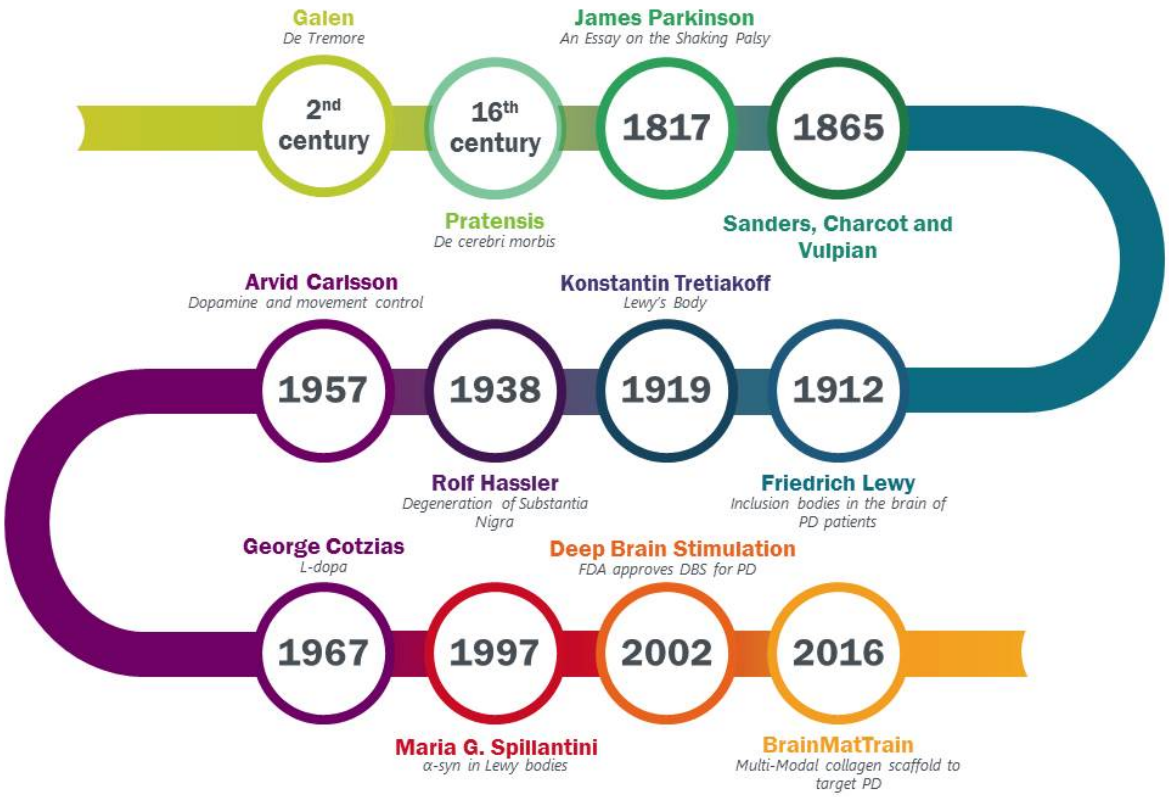

Figure 2: History of PD at glance

Summary of key events in the history of Parkinson's disease over time scientific and non-scientific literature.

1.3 Aetiology and Risk factors of Parkinson's disease

Aetiology of PD is still today partially unknown, but certainly it includes both genetic and environmental factors (Wirdefeldt et al., 2011).

1.3.1 Genetic factors

In the last 20 years researchers worked intensively trying to identify the specific genes involved in the development of Parkinson's disease and their specific functions. A total of 43 genetic loci are currently considered to represent risk factors or causes of PD (Billingsley et al., 2018). It is interesting to note that basing on the involved gene triggering the disease, there is an early (as with Parkin) or late (as with LRRK2 – Leucine-rich repeat kinase 2) onset, as well as direct influence on impairment of some protein functions more than others (Corti et al., 2011).

Table 3: Genes and loci involved in Parkinson's disease (modified from *Corti et al., 2011*)

Loci	Gene	Disease Onset	Inheritance
PARK1/PARK4	*SNCA*	Early	Dominant; Rarely sporadic
PARK2	*Parkin*	Juvenile; Early	Recessive: Sporadic
PARK3	*Unknown*	Late	Dominant
PARK5	*UCHL1*	Late	Dominant
PARK6	*PINK1*	Early	Recessive
PARK7	*DJ-1*	Early	Recessive
PARK8	*LRRK2*	Late	Dominant; Sporadic
PARK9	*ATP13A2*	Early	Recessive
PARK10	*Unknown*	Late	Unclear
PARK11	*GIGYF2*	Late	Dominant
PARK12	*Unknown*	Late	Unclear
PARK13	*Omi/HTRA2*	Late	Unclear
PARK14	*PLA2G6*	Juvenile levodopa responsive dystonia parkinsonism	Recessive
PARK15	*FBXO7*	Early-onset parkinsonian pyramidal syndrome	Recessive
PARK16	*Unknown*	Unclear	Unclear
Not assigned	SCA2	Dominant	Unclear
Not assigned	GBA	Recessive	Unclear

1.3.1.1 α-synuclein

α-synuclein is a 14 kD protein localized mainly in CNS (in particular in the presynaptic terminals and the nucleus, cytosol and some cellular membranes) (Recasens and Dehay, 2014). Together with beta and gamma synucleins, alpha-syn is part of the family of small acid proteins expressed only in vertebrates. It has a structure consisting of three major domains: a *N*-terminal domain, a median domain (non-amyloid component – NAC) and an acid non folded *C*-terminal domain (Bobela et al., 2015). All the three domains have specific roles and constant interaction and are all essential for the protein's structure (Xu and Pu, 2016). Mutations on the *N*-terminal domain are known to be associated with the familiar PD form, accelerating protein's aggregation via direct destabilization of the *N*-terminal conformation (Burrè et al., 2015). The NAC domain is important for α-syn's self-propagation. *C*-terminal domain has direct role in the interaction of α-syn with other proteins and small molecules, but also in aggregation (truncated *C*-terminal domain forms aggregate faster) and in solubility (*C*-terminal domain is necessary to maintain it) (Xu and Pu, 2016).

α-syn in humans is mainly expressed in the SNpc and in the hippocampus, and, even if its role is not yet totally understood, it is believed to be involved in different activities - mainly in vesicle trafficking during neurotransmission (Recasens and Dehay, 2014). At the moment, point mutations (as p.A53T, p.A30P, p.H50Q, p.G51D, p.A53E and p.E46K) (Recasens and Dehay, 2014) as well as whole locus multiplication in the *SNCA* gene encoding for human α-synuclein protein are known to result in the autosomal dominant form of PD: in the last years also some missense mutations were identified, but at the moment are considered rare and not enough data are yet available (Rocha et al., 2018). Aggregated forms of α-syn (amyloid fibrils) are found to be the major component of Lewy's bodies (LBs) and Lewy's neurites (LNs) (Ghosh et al., 2017).

α-synuclein in physiological condition exists as an unfolded monomeric protein: in PD, once misfolded, it creates oligomers that subsequently self-assemble into highly ordered amyloid fibrils which then accumulate in LBs and LNs (Ghosh et al., 2017). Both oligomers and amyloid fibrils are extremely toxic and play a key role in the development of the diseases via various mechanisms including disruption of α-syn's normal neurotransmission release, impairment of the ER-Golgi vesicular transport, specific protein-degradation mechanisms, and interference with mitophagy and mitochondria's dynamics and structure (Recasens and Dehay, 2014).

Until not long ago, α-syn was considered to be only an intracellular protein due to the absence of the signal peptide to directly drive it into the secretory pathway (Recasens and Dehay, 2014). This view changed when in 2008 two independent studies showed that 10 years after successful cellular transplantation of foetal dopaminergic neurons, some patients developed again α-synuclein-positive LB pathology in grafted cells (Kordower et al., 2008; Li et al., 2008). Such event made the scientific community accept the theory that pathological forms of α-syn are able to spread through the brain in a prion-like manner. Prions are infectious proteins assemblies that, behaving as a template, are able to convert normal proteins into a pathogenic conformation, leading to a specific biological effect (Vaquer-Alicea and Diamond, 2019). Consequently, toxic α-syn is able to enter cells and to start aggregation of unfolded protein into LBs, contributing to the progression of the disease (Ghosh et al., 2017; Marques and Outeiro, 2012). At the moment it is widely accepted that α-syn is secreted *in vitro* by different types of neurons, and it is released via exosomes in a calcium-dependent manner (Recasens and Dehay, 2014).

How α-syn is toxic and leads to cellular death is mostly unknown: dysfunctions in the systems in charge to clear toxic α-syn as autophagy and ubiquitin-proteasome system (UPS) might lead to neuronal death. Truncation of C-terminal domain might lead to an increased creation of fibrils, leading to a gain of toxicity. Nitration and oxidation might also play an important role in advance of the disease, significantly reducing α-syn's capacity to form stable conformations. Also inflammation plays an important role in the toxicity of α-syn, via direct transfer of the misfolded protein form neurons to glial cells that subsequently are activated, induce chronic inflammation and contribute in the spreading of the disease in the brain (Xu and Pu, 2016).

1.3.1.2 Leucine-rich kinase domain 2

LRRK2 was first described in 2002 as a locus on chromosome 12 linked to PD in a Japanese family (Funayama et al., 2002) and then in 2004 an autosomal dominant mutation on the LRRK2 gene was identified and confirmed by two independent groups (Paisán-Ruíz et al., 2004; Zimprich et al., 2004). *LRRK2* gene codes for a large 2527 amino acidic protein from the ROCO family formed by *1)* the core signalling region that includes a Ras of-complex (ROC) and a C-terminal of Roc (COR) (always occurring in tandem with the G-domain), formed by an highly conserved N-terminal part that interacts with ROC and a C-terminal behaving as a dimerization device, and *2)* a protein-protein interaction domains that include an armadillo repeats (ARM), ankyrin repeats (ANK), leucine-rich repeats (LRR), a kinase and a WD40 domain (Gilsbach and Kortholt, 2014; Li et al., 2014). The high conservation during evolution of the ROC-COR (ROCO) section suggest a very thigh interactions and functional interdependence of these two domains (Li et al., 2014).

Studies done at the protein and mRNA level showed that LRRK2 is mainly expressed in the brain and in the peripheral tissues; in particular in adult rodents the highest levels of LRRK2 are found in the lung, kidneys and lymph nodes, while in the brain its level increase only during post-natal time, in particular in the areas innervated by dopaminergic neurons, especially the striatum (Rideout and Stefanis, 2014).

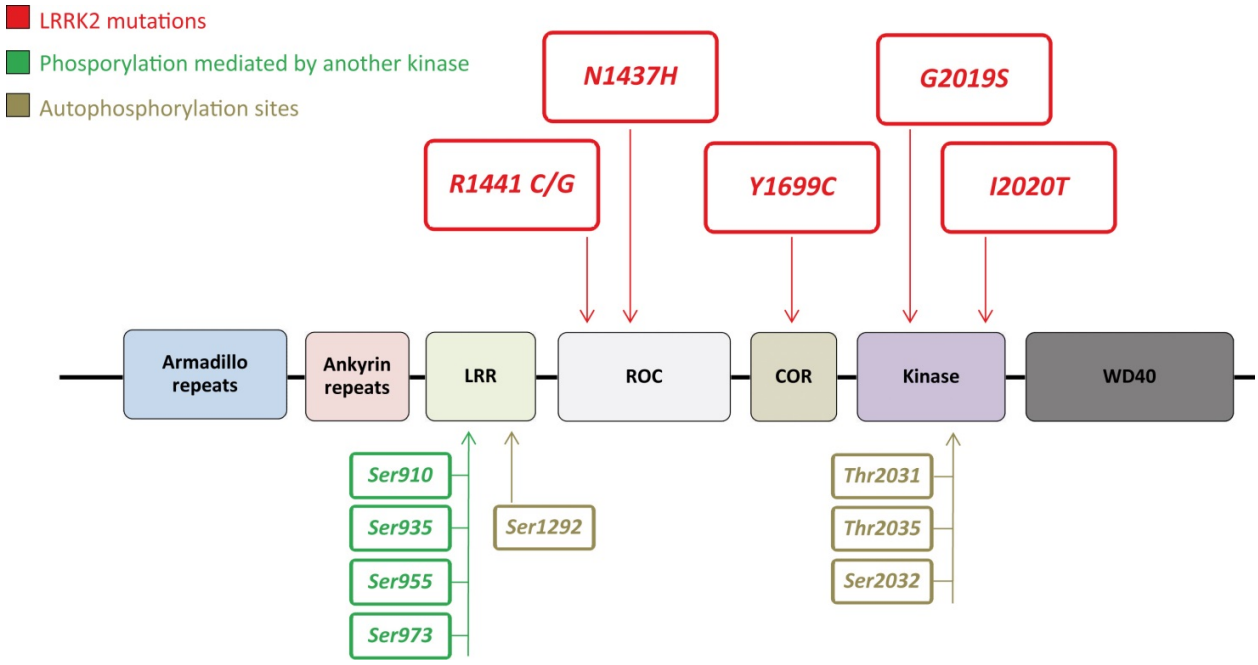

Figure 3: LRRK2 protein structure

LRRK2 is a 2527 amino acidic protein from the ROCO family. Different LRRK2 mutations (in red) are known to be connected with development of PD. LRRK2 can undergo autophosphorylation at specific sites (in brown), or be phosphorylated by other kinases (in green).

Seven different LRRK2 mutations are known to be directly linked with PD: these are G2019S, R1441C/G/H, Y1699C, I2020T and N1437H (Huang et al., 2018).

Among those, the most common mutation - G2019S – is located in the kinase domain and has been found in both sporadic and familiar forms of PD (Li et al., 2014); this specific mutation is pathologically indistinguishable from sporadic PD cases, with patients showing the typical LBs pathology (Martin et al., 2014). Interestingly other LRRK2 mutations do not lead to LBs pathology, but in some cases neurofibrillary tau tangles have been reported (Martin et al., 2014).

How LRRK2 and its mutated forms are toxic is still under debate: in last years have been shown (almost only *in vitro*) that alterations in the enzymatic activity of mutated LRRK2 are the core event to fully understand the progression of PD (Price et al., 2018). Due to the complex LRRK2 structure, specific domains, interactions with other proteins and different cellular processes linked with it, it is very challenging to characterize and identify the disease-relevant network: for a matter of simplicity is possible to organize pathways and signalling events in proximal signal events and distal signalling events (Price et al., 2018).

Proximal signal events include those events having a direct interaction with LRRK2 for example via enzymatic activities and/or protein/protein interactions. Various experimental evidences showed that LRRK2 can undergo both phosphorylation (at Ser860, Ser910, Ser935, Ser955 and Ser973), autophosphorylation (at Ser1292, Ser2032, Thr2031 and Thr2035) and dephosphorylation (via protein phosphatase 1) (Price et al., 2018).

Phosphorylation (in particular at Ser910 and Ser935) is connected with the ability of LRRK2 to directly interact with the 14-3-3 proteins family, showing that there are very tight bounds between phospho-regulation, protein functions and protein/protein interactions, controlling a wide range of LRRK2 activities (as its localization within the cell, enzymatic activities and partners to interact with) (Price et al., 2018).

The physiological reason why autophosphorylation occurs has still to be unrevealed: studies done on autophosphorylation at the Ser1292 showed that it occurs *in vivo* (Sheng et al., 2012) and that it regulates the activity of the GTPase domain (affecting for example cellular processes, signal transduction and translation) (Price et al., 2018; Sheng et al., 2012).

G2019S mutation for example, has been shown to increase LRRK2 kinase activity when compared with wild type or with any other LRRK2 mutated form: surprisingly all the LRRK2 mutations lead to apoptosis in a kinase dependent manner when expressed in cultured neuroblastoma cells or primary neurons, even if only G2019S shows strong increased kinase activity (Rideout and Stefanis, 2014).

A lot of resources have been put into the identification of LRRK2 substrates and proteins that might be phosphorylated by LRRK2; unfortunately most of the substrates were only able to be phosphorylated *in vitro* (Araki et al., 2018). The first group of proteins to be identified as a substrate for LRRK2 was part of the ERM family: even if phosphorylation by LRRK2 of the ERM family was independently confirmed and reproduced, it was never reproducible in physiological conditions (Araki et al., 2018). Other studies showed that LRRK2 phosphorylates tau, and it might lead to disruption of microtubule network: this specific substrate is considered to be one of the most disease-relevant as some PD patients with LRRK2 mutations show tau accumulation (Araki et al., 2018; Rideout and Stefanis, 2014). Only in 2016, using a challenging approach and advanced techniques, pathologically relevant LRRK2 substrates have been identified: these were Rab proteins, including Rab8A/B and Rab10 (Steger et al., 2016). Following this discovery the same group identified other Rab family LRRK2

potential substrates, including Rab3A/B/C/D, Rab12, Rab35 and Rab43 (Steger et al., 2017). Another substrate recently discovered is the p62/sequestome-1: basically p62 interacts with the ARM/ANK LRRK2's domain (Park et al., 2016) and LRRK2 phosphorylate p62 at the Thr138 (Kalogeropulou et al., 2018).

Distal signalling events are those happening at distance, via multiple intermediaries; LRRK2 has been shown to influence and have direct effect on mitochondrial dysfunction, autophagy, vesicles trafficking, transcriptional regulation and also to be involved in the immune response.

Different reports showed that LRRK2 is directly involved in mitochondrial dysfunction, and it directly modulates mitochondrial functions: in cellular models of LRRK2-G2019S PD as well as in clinical tissues, there is an increase consumption of oxygen, reduction in mitochondrial membrane potential and suppression in mitochondrial derived ATP and cellular ATP (Rideout and Stefanis, 2014). Even if not totally understood and accepted, it is believed that mitochondria undergo morphological changes: while some studies showed intact mitochondrial structure (Papkovskaia et al., 2012), others showed an increase in mitochondrial elongation and interconnectivity (Mortiboys et al., 2010), as well as increased mitochondrial fragmentation but no elongation (Wang et al., 2012). The reason why there are so many contrasting results might be linked to the different experimental approach used by the different groups, as amount of expressed protein and/or the different cellular models (Rideout and Stefanis, 2014).

Dysfunction and changes in the autophagy/lysosomal protein degradation pathway is another pathological event occurring in PD. On cells, expression of G2019S LRRK2 leads to decrease in neuritic length and increase in neuritic and somatic autophagic vacuoles. Overexpression of G2019S LRRK2 leads to accumulation of autophagic and lysosomal structure in neuronal cells lines as well as in transgenic G2019S (and partially R1441C) mice models (Esteves et al., 2014). iPSCs dopaminergic neurons derived from human fibroblast, when compared to control fibroblasts, exhibited increased autophagic properties (Manzoni et al., 2013) due to MAPK1/3 (Bravo-San Pedro et al., 2013). Recent theories introduced the link between LRRK2 impaired autophagic degradation and calcium (Ca^{2+}), suggesting that LRRK2, localised in the lysosomes, interacts with nicotinic acid adenine dinucleotide phosphate (NAAD) receptors that stimulate Ca^{2+}release; calcium then disrupt endoplasmic reticulum

(ER) dependant Ca^{2+}homeostasis followed by release of Ca^{2+} that in turn activates the CaMK/AMPK pathway, leading to lysosomal alkalinisation and increase autophagy (Esteves et al., 2014).

LRRK2 is known to localize within neurons, in vesicular and membranous structures and it has a direct effect on synaptic vesicles trafficking. First of all, LRRK2 due to its kinase activity is involved in synapses vesicles formation, through the LRRK2-mediated EndoA phosphorylation at Ser75. Moreover, knockdown or overexpression of LRRK2 in primary neurons impairs synaptic vesicles endocytosis, that can be reversed with co-expression Rab5b: such effect can be ascribed to the fact that LRRK2 in cooperation with Rab5b directly modulate synaptic vesicles endocytosis (Esteves et al., 2014).

LRRK2 has also a potential effect in transcriptional regulation: in a study, the G2019S mutation showed an upregulated transcriptional activity when expressed in mice and compared to WT form or knockout (Nikonova et al., 2012), while another study done *in vitro* showed no altered gene expression (Devine et al., 2011).

Last but not least, LRRK2 is also involved in inflammation and immune system regulation. First of all, high levels of LRRK2 mRNA and protein expression have been detected in brain immune cells, and in peripheral blood mononuclear cells of both human and rodent (Russo et al., 2014). On LPS-based rat inflammatory model, reduction of LRRK2 in microglia leads to a general attenuation of pro-inflammatory cytokines and proteins. On the same direction, LRRK2 silencing on dermal fibroblast derived from PD patients carrying mutations stimulates reduction of cyclooxygenase-2 (COX-2) mRNA levels (Esteves et al., 2014).

In addition, different studies proved the tight link between LRRK2 and pro-inflammatory responses directly on PD patients: post-mortem analysis of PD-derived brain tissues showed increased microglial activation together with changes in natural killer cells, lymphocytes and monocytes. Moreover high levels of inflammatory cytokines have been detected in blood, brain tissues and cerebrospinal fluid derived from PD patients (Collins et al., 2012).

1.3.1.3 Interaction between α-syn and LRRK2

The idea of a tight deleterious interaction between α-syn and LRRK2 in the last year gained more and more attention in the field of PD, and has been partially showed in human as well as animal models. The mechanism of action of such interaction not yet totally understood, but it could be based on a direct cell to cell interaction within cells expressing both α-syn and LRRK2, or could be based more

on an indirect pathway where other players as neuroinflammation, autophagy and mitochondrial defects are involved.

A detailed review about the interaction of α-syn with LRRK2, and the possible mechanism of actions undergoing in Parkinson's disease can be found in supplementary material *(Chapter 8.1)*.

1.3.2 Genetic risk factors

A huge multicentre study done on 5000 PD patients and 5000 control patients showed that the major genetic risk factor is a mutation in the glucocerebrocidase (*GBA)* gene (Kalia and Lang, 2015). *GBA* mutation was first identified in patients suffering of Gaucher disease (GD), a lysosomal-storage disease characterised by impaired glucocerebrosidase enzyme (GCase) activity leading to accumulation of glycolipid substrate. GBA1 gene is 7.6kb in length and is found on chromosome 1q21: around 300 mutations have been already documented, but the most famous ones are the L444P and N370S (O'Regan et al., 2017).

How GBA mutation may be a great risk factor for development of PD is still poorly known. Some theories explain such predisposition through a strong loss and gain-of function interaction with α-synuclein: in fact, decrease of GCase (via mutation of CBE treatment) leads to an increase in intracellular alpha synuclein, but also overexpression of α-asyn showed a reduction in GCase levels (Manning-Boğ et al., 2009; O'Regan et al., 2017; Schapira, 2015). Other theories implicate impairment of the autophagy-lysosomal pathway for the interactions between GBA and the autophagy-lysosomal system. This system, in normal conditions, has the role to control the degradation of dysfunctional or unnecessary proteins. Another theory involve the accumulation of mutated GCase into the endoplasmic reticulum (ER) leading to reduced levels of GCase in the lysosome and increased levels of unfolded protein response together with the ER associated degradation (ERAD) (O'Regan et al., 2017). Another hypothesis is based on the idea that α-syn aggregates may have a prion-like mechanism of cell-to-cell transmission, involving macrophages (the most affected cells in GD) as a carrier and due to a new somatic GBA mutation the α-syn accumulation and spread could start (Sidransky and Lopez, 2012).

1.3.3 Other factors

The non-genetic risk factors of PD are various but the most important include 1) *gender* (with the ration male-female being approximately 3:2), 2) *age* (a strong increase and peak is reached after 80

years of age, 3) *ethnicity* (in the US higher incidence is in the Hispanic group, followed by non-Hispanic Whites, Asians and Blacks), and 4) *environmental factors* (exposure to pesticides, prior head injury, rural living, β-blockers use, etc.) (Kalia and Lang, 2015).

An interesting theory proposes that exposure to bacterial and viral infection could be a modifier of PD; such idea comes from the analysis of PD cases that are considered to "lie outside of the expected" (Jang et al., 2009). A long history of studies showed a correlation between changes in the CNS induced by viral infection (e.g. influenza A and HSV-I) and development of PD pathologies (Olsen et al., 2018), but still detailed investigation have to be done to confirm such link and to prove that direct interventions on the viral infection could reduce the incidence of PD. In this regard, different studies showed that the use of nonaspirin nonsteroidal anti-inflammatory drug (NSAID) or ibuprofen might have a protective effect on the risk of PD; in particular long term and regular users of NSAIDs or ibuprofen had a more protective and evident effect, while users of acetaminophen or aspirin did not show any protective effect (Gagne and Power, 2010).

1.4 Anatomy and Physiology of Parkinson's disease

1.4.1 The role of Basal Ganglia (BG)

As briefly introduced before, PD can be sporadic or inherited and in both forms it leads to a progressive loss of dopaminergic neurons in the SNpc, with a consequent impairment of the nigrostriatal pathway (formed by A9 cell group) and development of motor and non-motor symptoms (Dickson, 2018). Interestingly, in addition to dopaminergic loss, it has been shown that degeneration of the cholinergic system (Bohnen and Albin, 2011), as well as loss of noradrenaline neurons of the locus coeruleus (Delaville et al., 2011) are involved in the development of motor and non-motor symptoms of the disease,

Dysfunctions of the basal ganglia (BG) are considered to have a direct influence with PD. The major role of BG is to initiate voluntary movements (Bartels and Leenders, 2009) and its anatomical areas include: *1)* substantia nigra (both pars compacta – SNpc with pigmented dopamine-containing neurons, and GABAergic pars reticulata – SNr), *2)* the subthalamic nucleus (STN), *3)* the internal and external pallidal segment (GPi and GPe), and *4)* the neostriatum (formed by caudate nucleus and putamen) (DeLong and Wichmann, 2010; Galvan and Wichmann, 2008).

BG receives cortical inputs from the striatum and subthalamic nucleus, forwarding them to the SNr and GPi. The modern view of BG functional organization includes the interaction of cortex and BG via parallel, segregated cortical-subcortical re-entrant circuits; abnormal activities of specific circuits leads to the so called "circuits-disorders" (PD, hyperkinetic disorders, Tourette's syndrome, etc.) (DeLong and Wichmann, 2010).

Two pathways – direct and indirect - have been described connecting the striatum to GPi and SNr (DeLong and Wichmann, 2010); the activity of each of them is differentially regulated by dopamine released from SNc.

In the *direct pathway,* activation by dopamine of striatal neurons with excitatory D1-like receptors leads to increased activity of the pathway via corticostriatal transmission, leading to decreased inhibitory thalamocortical neuronal activity (DeLong and Wichmann, 2010; Obeso et al., 2008; Purves et al., 2001).

In the *indirect pathway,* striatal neurons express D2-like receptors and, in presence of DA, this specific neuronal activity is decreased, leading to a greater inhibitory activity of thalamocortical neurons. This pathway can be considered as a "break signal" to direct pathway's normal functions (DeLong and Wichmann, 2010; Obeso et al., 2008; Purves et al., 2001)

Basing on such view, inhibition of direct pathway would allow movements to proceed due to inhibition of specific pallidal and nigral neurons, while unintended movements would be suppressed by increased concomitant excitatory input to Snr and GPi neurons via the indirect pathway (DeLong and Wichmann, 2007). Thus, in PD the loss of dopamine tends to produce hyperactivity of the STN, which increases the inhibitory effects of GABAergic neurons of the internal GP, which in turn abnormally inhibits VA and VL thalamic nuclei and reduce the excitatory glutamatergic inputs in the motor cortex, producing akinesia.

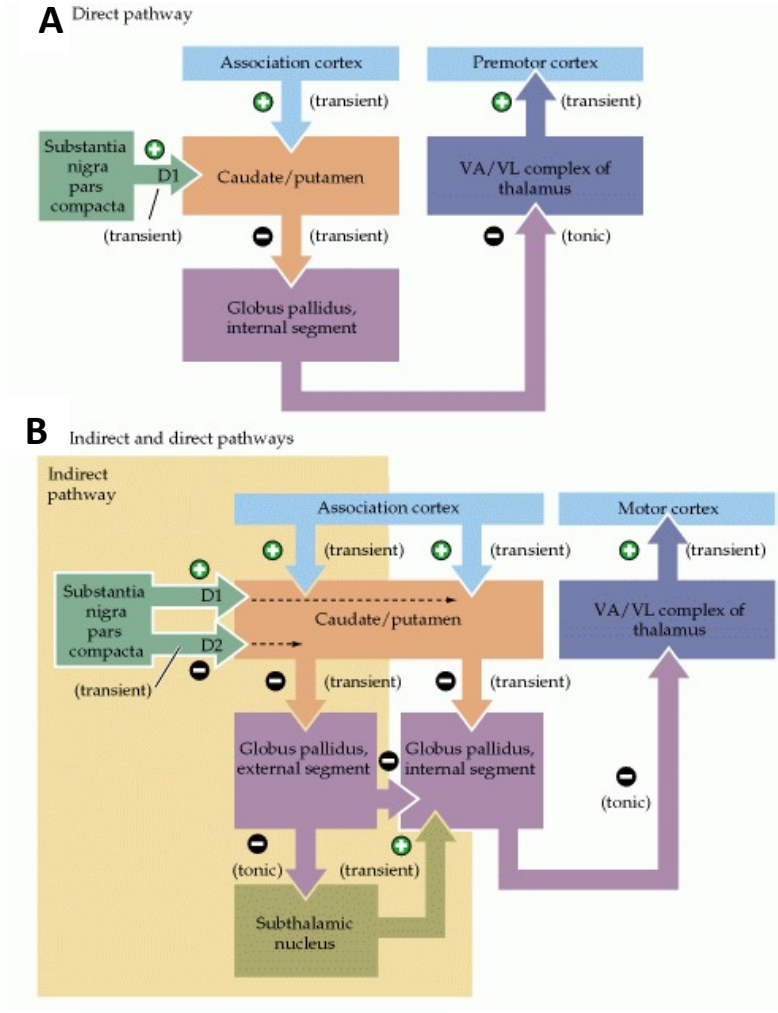

Figure 4: Direct and indirect pathways connecting the striatum to the substantia nigra.

(A) Direct pathway: dopamine activates striatal neurons expressing D1-like receptors, resulting in an increased activity of the pathway and subsequent decreased inhibitory thalamocortical neuronal activity.

(B) Indirect pathway: dopamine decreases activity of striatal neurons expressing D2-like receptors resulting in a bigger inhibition of thalamocortical neuronal activity.

(Purves et al., 2001)

1.4.2 Possible mechanisms of neuronal death in PD

Different cellular, biochemical and molecular mechanisms are thought to be involved in the development of PD, leading together to a progressive loss of DA in the SNpc.

1.4.2.1 Protein accumulations

Proteins' aggregation is known to be one of the major mechanisms involved in neuronal death.

At the cellular level, there is a great continuous production of abnormal proteins, including misfolded, incomplete, mutant and damaged proteins (Sherman and Goldberg, 2001); for this reason, physiologically, there is a continuous control on the quality of the produced proteins, with mechanisms of repairing and removal in case of abnormalities (Martinez-Vicente and Cuervo, 2007).

This specific control in production and degradation is even more important in the brain, since the long lifespan of neuronal cells, together with their limited regenerative capacity makes the neurons more susceptible and fragile to damages (Keller et al., 2004). In PD, different types of proteins aggregates in the SNc, including various species of α-syn, ubiquitin and phosphorylated proteins; the most abundant is α-syn, which aggregates and forms LBs and LNs (Melki, 2018, 2015).

Why proteins accumulate in PD is still under debate: aggregation of abnormal proteins into intracellular inclusions might be a way to deal with the high levels of unwanted proteins, reducing their toxicity and facilitating their clearance. This view seems to be coherent with the clinical cases of sporadic PD patients, where symptoms have a late onset, but high levels of LBs are detected (McNaught and Olanow, 2006). In addition it might be speculated that as proteins accumulates in LBs, dysfunctions in proteins handling is a core feature of PD (Gundersen, 2010).

1.4.2.1.1 Lewy's bodies and Lewy's neurites

LBs and LNs are neuronal spherical inclusions with a length of 200–600 nm and a width of 5–10 nm (Spillantini et al., 1998) mainly composed of α-syn that accumulates respectively into the nerve cells and within the cellular processes as aggregates of insoluble filaments (Bourin, 2018; Dickson, 2018). Different other proteins are found in the LBs and LNs including proteins related to familiar form of PD the (parkin, ubiquitin, PINK1 and UCH-L1), proteins related to the ubiquitin-proteasome system (dorfin, NUB1), proteins associated to microtubules (tau, MAB1B, MAB2, MAB5) and also kinase proteins (G-protein-coupled receptor kinase 5) (Wakabayashi et al., 2007).

A new theory proposed in a recent work published by Shahmoradian and colleagues states that LBs and LNs do not contain mainly filaments of α-syn, but they are formed by "a crowded membranous medley of vesicular structures and dysmorphic organelles" (Shahmoradian et al., 2019).

LBs and LNs are widely distributed into the central nervous system, but also in the peripheral nervous system and in neurons of the cerebral cortex and amygdaloid nucleus (Wakabayashi et al., 2007). They are one of the main hallmarks of PD and can be found in the SN of PD patients, but

interestingly they are also an hallmark of other diseases categorized as dementia with Lewy's bodies (DLB) (McKeith et al., 2017).

LBs' formation and development can be easily revealed by α-syn immunohistochemistry. This is a stage-process: in healthy condition α-syn immunoreactivity is absent in the neuronal cytoplasm. In the 1st stage it is visible a diffuse pale cytoplasmic staining most of the times in morphologically normal-looking neurons. In the 2nd stage it is visible an uneven and irregular shaped staining where neurons are often poorly pigmented. The 3rd stage correspond to the staining of pale bodies, that most of the times also display a peripheral condensation which will disappear on stage 4. The 4th stage correspond to the traditional LBs staining, consisting in a central core and a surrounding circular halo, and a ring-like staining (Wakabayashi et al., 2013).

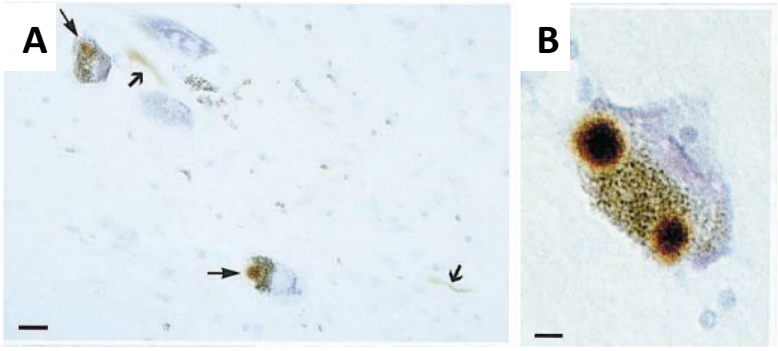

Figure 5: α-synuclein positive immunohistochemistry in the SN of Parkinson's patient

Lewy bodies and Lewy neurites are two typical hallmarks of Parkinson's disease. They are mainly formed by aggregated forms of α-syn as well as other different types of proteins. **(A)**: Lewy body (thin arrow) and Lewy neurites (thick arrow) stained for α-synuclein. **(B)**: Nerve cell with α-syn positive Lewy bodies

(Spillantini et al., 1997).

1.4.2.1.2 Braak's theory and the Threshold theory

An interesting, and very endorsed theory on the development and spreading of Lewy's bodies in sporadic Parkinson's disease cases was published by Braak's group in 2003: briefly authors hypothesized that an unknown pathogen (virus or bacteria) in the gut could be responsible for the initiation of the disease (H. Braak et al., 2003). Few years after an updated theory – known as *double hit theory* – was published stating that the beginning of sporadic PD starts both in the gut and in the nasal cavity: from the initial location α-syn spreads all around the brain and the central nervous system through the olfactory tract and the vagal nerve, leading to the development of Lewy's bodies (Hawkes et al., 2009).

The authors theorized 6 different stages: in stage 1 and 2 LBs appear in the lower nuclei of the brainstem and in the olfactory bulb, and the patient is asymptomatic except for some olfactory disorders. In stage 3 and 4 the LBs reach the substantia nigra, the subthalamic nucleus, amygdala and forebrain: at this stage patients present sleep disturbance and motor dysfunction. At stage 5 and 6 LBs spread through the neocortex and they are associated with cognitive and emotional deficits (Heiko Braak et al., 2003).

Table 4: Braak's stages of the evolution of sporadic Parkinson's disease in details *(Heiko Braak et al., 2003)*

Stage	Location	Description
I	medulla oblongata	Lesions in the dorsal IX/X motor nucleus and/or intermediate reticular zone
II	medulla oblongata and pontine tegmentum	Pathology of stage 1 plus lesions in caudal raphe nuclei, giganto-cellular reticular nucleus, and coeruleus subcoeruleus complex
III	midbrain	Pathology of stage 2 plus midbrain lesions, in particular in the pars compacta of the substantia nigra
IV	basal prosencephalon and mesocortex	Pathology of stage 3 plus prosencephalic lesions. Cortical involvement is confined to the temporal mesocortex (transentorhinal region) and allocortex (CA2-plexus). The neocortex is unaffected
V	neocortex	Pathology of stage 4 plus lesions in high order sensory association areas of the neocortex and prefrontal neocortex
VI	neocortex	Pathology of stage 5 plus lesions in first order sensory association areas of the neocortex and premotor areas, occasionally mild changes in primary sensory areas and the primary motor field

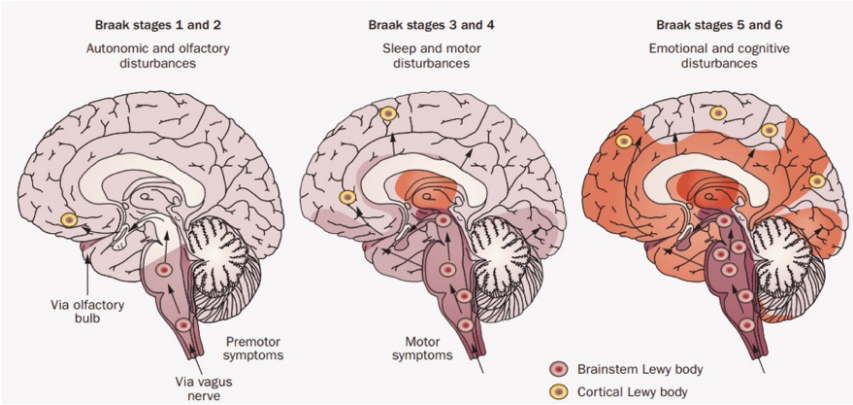

Figure 6: Braak's double hit theory of Parkinson's disease

α-syn spreading starts from the olfactory bulb and the vagus nerve, invading then the brain. During the stage 1 and 2 of the disease patients are asymptomatic, while motor symptoms appear only from stage 3 and 4, after aggregation of α-syn into Lewy's bodies in the SNc *(Doty, 2012).*

Until 2017, Braak's theory of PD as a prion like disease (where neuronal damage in PD occurs in an ascending way, from peripheral nervous system - PNS - to CNS) was totally accepted by the scientific community: a paper published by Engelender and Iscacson proposed a different approach called *Threshold theory* (Engelender and Isacson, 2017).

The authors believe that Parkinson's disease is a global systemic disease where at the same time different neurons in the CNS as well as in the PNS are influenced: crucial in this view is the individual vulnerability of neurons in a specific area and their resistance to dysfunction and/or death. Consequently, the appearance of symptoms derives from the level of neurons' damage in relation with the network they form with other neuronal groups: this means that the more sensitive areas will show earlier signs of dysfunction compared to more resistant areas and symptoms will only start when there is inability of network compensation (Engelender and Isacson, 2017). To support this new approach, the authors presented interesting data from different studies: for example, basing on this theory, even a small number of healthy and functional dopaminergic neurons and synapses (even less or equal to 10%) would be enough to start normal movements in patients (Engelender and Isacson, 2017). This view was indeed confirmed in a human study published in the beginning of 90's where dissociated foetal ventral midbrain (VM) tissue was transplanted into the striatum of Parkinson's disease patients who were addicted to heroin and acutely developed the disease after accidental injection of 1-methyl-4-phenyl-1,2,3,6-tetrahydropyridine (MPTP), an uncontrolled by-product of the heroin analogue meperidine. The subjects not only showed an increased uptake of ^{18}F-fluorodopa (a radiotracer used to

directly target the nigrostriatal dopaminergic pathway) in the striatum after positron emission tomography (PET) analysis, but they also exhibited visible motor improvements (Widner et al., 1992). In another study, around 7% of patients from the UK brain bank showed high α-synuclein pathology in the SN, but not in the dorsal motor nucleus of the vagus (Kalaitzakis et al., 2008). Another interesting finding challenging the Braak's ascending theory is the fact that even if constipation is thought to be the most prevalent early PD symptom occurring in almost half of the patients (Adams-Carr et al., 2016; Stocchi and Torti, 2017; Sung et al., 2014), Lewy bodies were more abundant in the stomach than in the colon (Annerino et al., 2012)

1.4.2.2 Autophagy dysfunctions

Another mechanism involved in neurodegeneration includes disruption in autophagy. Autophagy is a cellular surveillance system controlling the recycling and removal of intracellular and extracellular components. Key role in degradation and recycling is played by the lysosomes; basing on how components are delivered to the lysosomes, autophagy can be divided in macroautophagy, microautophagy and chaperone-mediated autophagy (CMA) (Martinez-Vicente and Cuervo, 2007).

Macroautophagy is the most conserved form of autophagy and it preferentially occur under stressful conditions mainly to create energy during starving situations or to remove altered intracellular components (Martinez-Vicente and Cuervo, 2007). It is a step process: the autophagosome, a membrane of around 500 nm (Nair and Klionsky, 2005), sequesters the intracellular components that then are fused with the lysosomes where degradation is initiated (B. Wang et al., 2016).

Microautophagy is a simpler process that mainly occurs in normal cellular conditions, consisting in the direct fusion of substrates into the lysosomes without mediation of other structures (B. Wang et al., 2016).

CMA is the most selective autophagic process and it steps in as a supplier of aminoacids for proteins' production when macroautophagy is impaired due to prolonged starving conditions: selective CMA's substrates present a specific lysosomal targeting motif (KFERQ) on their surface that is recognised and binds with a chaperone in the cytosol. Subsequently the substrate is delivered to the lysosomes surface where is unfolded and translocated into the lysosomes for degradation via LAMP-2A (lysosome associated membrane protein type 2A) (Martinez-Vicente and Cuervo, 2007; B. Wang et al., 2016) .

Another important system in degradation of unfolded monomeric protein is played by the ubiquitin-proteasome system (UPS); in normal conditions such system is the preferred degradation's route as much more effective than the macroautophagic system (Sánchez-Pérez et al., 2012). In neurodegenerative diseases some altered proteins start to impair the clearing regular functions of UPS and CMA, leading to proteins' aggregation in oligomers, protofibers and fibers (Martinez-Vicente and Cuervo, 2007). At this point, the UPS and the CMA are not able anymore to deal with aggregated proteins and macroautophagy becomes the preferential degradation route (Sánchez-Pérez et al., 2012). Unfortunately, over time also macroautophagy starts to fail, leading to abnormal protein accumulation, cellular toxicity and consequent neurodegeneration (Martinez-Vicente and Cuervo, 2007).

In PD, α-syn is generally degraded by UPS and CMA; α-syn aggregation begins when the mutant α-syn's forms bind to the CMA complex and to the lysosomal membrane but without being internalized and destroyed (Cuervo et al., 2004). In parallel, as the main degrading pathway is impaired, also other proteins start to accumulate and aggregate inside the cells (Cuervo, 2006).

All this pushes the macroautophagic system to take over and upregulate its activity, trying to degrade the accumulating proteins; this is a compensatory process that will irremediably lead to cellular imbalance and subsequent neuronal toxicity (Martinez-Vicente and Cuervo, 2007).

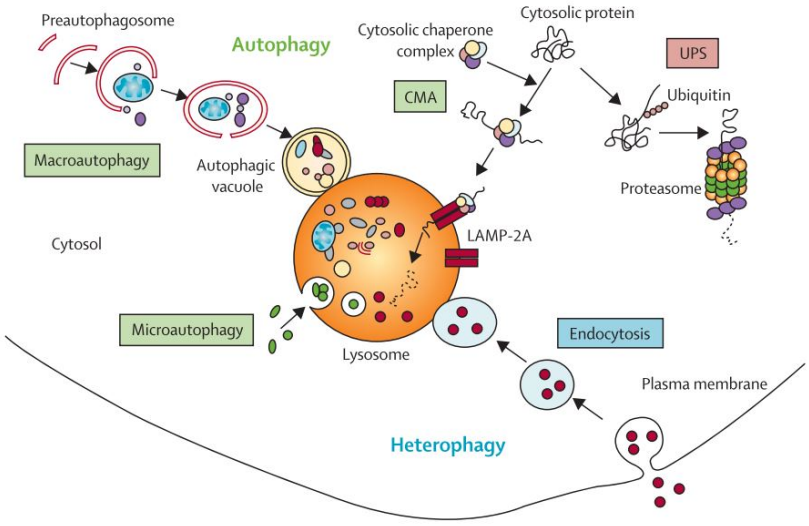

Figure 7: Proteolytic system representation

In mammalian cells threee different types of autophagy are known: microautophagy, macroautophagy and CMA. In addition, the UPS is another pathway for degradation of intracellular proteins into the cells *(Martinez-Vicente and Cuervo, 2007)*.

1.4.2.3 Mitochondrial dysfunction

Also mitochondrial dysfunctions play an important role in neurodegeneration and development of PD.

The first evidences was found in the '70 when, accidental exposure to MPTP caused the inhibition of the mitochondrial respiratory complex I and subsequent neurodegeneration of dopaminergic neurons and parkinsonism (Langston et al., 1983; Schapira et al., 1989). The direct negative impact of MPTP, which main metabolite is MPP+, a selective inhibitor of complex I like rotenone, on dopaminergic neurons of the SNc was then confirmed in both mice (Przedborski et al., 2004) and non-human primates (J. Langston et al., 1984) studies; still today MPTP is used to create toxin-related PD animal models. Another set of data supporting the mitochondrial hypothesis for PD came from immunohistological studies of post-mortem human brain samples. The group led by Mizuno showed an interesting complex type I deficiency in the striatum of PD patients (Mizuno et al., 1989); similar results were confirmed one year later by Schapira's group, but in the SNpc (Schapira et al., 1990). The tight link between mitochondria and parkinsonism can be also seen in both humans and rats when exposure to MPTP or rotenone (a well-known inhibitors of mitochondria complex I) (Cresto et al., 2018). Genes as PINK1, Parkin and DJ-1 are known to play a crucial role in the mitochondrial quality control: mutations in these genes leads also to the autosomal recessive form of PD (Dawson et al., 2010). Interaction of α-syn with the translocase of the outer mitochondrial membrane (TOM20) revealed an inhibition of the protein import (Di Maio et al., 2016), and accumulation of α-syn to the mitochondrial membrane have been detected in the cortex striatum and SNpc of PD brains (Devi et al., 2008).

In addition to toxins, also pathogenic mutations in the mitochondrial DNA (mtDNA) are known to facilitate mitochondrial dysfunction and be directly connected with neurodegeneration: in fact, high levels of mutated mtDNA were found on the SN neurons of PD patients when compared with healthy normal-aged patients (Bender et al., 2006).

A great interested toward mitochondria arose when two well-known PD-related genes, Parkin and PINK1, were discovered to be directly controlling the mitochondrial quality control pathway (Narendra et al., 2012). In physiological conditions, PINK1 detects and accumulates on the dysfunctional mitochondria, releasing signals to Parkin. Parkin is then recruited on the site of damage and after identification and isolation of dysfunctional mitochondria, it engulfs them, and activates their degradation through mitophagy (Pickrell and Youle, 2015). In PD, mutation of these two genes may

lead to dysfunctions in mitophagy with subsequent toxicity caused by accumulation of damaged mitochondria (Michel et al., 2016).

Another important gene connected both with PD development and mitochondrial functions is DJ-1: in particular, this gene behaves as redox-chaperone protein and a sensor for oxidative stress (Puspita et al., 2017). Production of reactive oxygen species (ROS) in mitochondria is a physiological controlled event that is involved in the aging process: antioxidant proteins have the role to control the stability and the levels of ROS into the cells. When antioxidants fail in their control, there is an imbalance between the produced and removed ROS, with accumulation and cellular damage and death (Puspita et al., 2017). How ROS can lead to neurodegeneration is still under debate; for sure ROS leads to spontaneous mutation that make cells vulnerable to dysfunctions. In addition, some types of cells (like cells of the SN) are physiologically more prone to oxidative stress and subsequent neurodegeneration (Floor and Wetzel, 2002) due to their direct role in synthesis of dopamine (Kuhn et al., 2006).

In this view, PD development might be seen as the interplay between different pathogenic conditions directly linked to cellular stress (Puspita et al., 2017).

1.4.2.4 Neuroinflammation

Neuroinflammation is also linked with PD, and its consequences in the development of the disease are well known. What remains still unclear is if neuroinflammation is the cause or the consequence of dopaminergic neurons degeneration (Glass et al., 2010) and, in particular, if the role of activated microglial cells is beneficial (removal of toxic proteins, prevention of neurodegeneration and myelin restoration) or deleterious (direct connection of prolonged neuroinflammation with neurodegeneration) (Gao and Hong, 2008).

Neuronal death in PD is considered to be mediated by two different pathological mechanisms: cell-autonomous and non-cell-autonomous. The first one includes accumulation of damage into the degenerating neurons that lead to their death. The latter sees the neuronal degeneration as a consequence of negative interaction of the neurons with the surrounding environment and cells as glial cells and infiltrating immune cells (Gelders et al., 2018).

Briefly, neuroinflammation is a complex response that involves different types of immune cells of the CNS as astrocytes, microglia, and infiltrating T-lymphocytes. Astrocytes are abundant glial cells in the CNS playing different roles in controlling neuronal functions; in addition, astrocytes have a direct

communication with microglial cells during immune response, amplifying their response and activity. Microglial cells, even if represent only a small portion of CNS cells, are the first type of cells responding to different type of signals, including brain injury, ischemia, pathogen invasion, environmental toxin, or aggregated proteins. Under normal conditions microglia surveils the environment maintaining stable physiological conditions (Le et al., 2016). Upon activation, microglial cells quickly undergo specific modification in the surrounding of the injury; these include mutations in genes expression (promoting expression or over-expression of genes involved in tissue repair), in function (production of bioactive molecules and increased phagocytic activity), in number (proliferation of resident cells and infiltration of bone-marrow derived precursors), and in morphology (from resting ramified to amoeboid active shape) (Gao and Hong, 2008). In addition, activated microglial cells also release tropic factors that are able to promote neuronal survival and rescue injured neurons (Le et al., 2016).

How neuroinflammation directly leads to neurodegeneration in PD is still under debate. Microglial activation might be triggered in response to misfolded proteins (as α-syn) or proteins with aberrant activities (e.g. LRRK2, etc.) (Le et al., 2016), or by different mediators, including cytokines, chemokines and nitric oxide (NO) (Shimoji et al., 2009). Binding of these pro-inflammatory factors to the dopaminergic neurons (than express the same type of receptors) might lead to nigrostriatal pathway injury (Gelders et al., 2018) and subsequent degeneration. The idea that abundant levels of activated microglial cells and astrocytes are present in PD subjects has been confirmed by *in vivo* and post mortem studies: for example, high levels of PK-11195 (a ligand selective for activated microglia) binding were detected with PET in PD brains, showing increased levels of activated microglial cells (Gerhard et al., 2006). In addition, also high levels of reactive microglial cells positive to HLA-DR (McGeer et al., 1988), as well as high levels of ROS , NO (Hunot et al., 1999) and various interleukins (Mogi et al., 1996) were detected in post mortem studies of PD's SNpc. Increased levels of pro-inflammatory cytokines were also detected in the CFS (Blum-Degena et al., 1995) and in the serum (Brodacki et al., 2008) of various PD patients. The involvement of inflammation and chronic inflammation in PD has been shown also in a recent study by Gaillard's team: injection of neuropeptide Y (a neuropeptide physiologically widely expressed in the mammalian brain and known to be an inflammatory mediator) immediately after 6-OHDA lesion in rats, showed a greater survival of TH+ and DAT+ cells in the SN and ST; these data, while from one side show the great neuroprotective role of

neuropeptide Y (possibly via p38 signalling pathway), on the other show that this neuropeptide is able to directly inhibit microglial cells, and such inhibition have beneficial effects on the neurodegeneration of DA neurons (Pain et al., 2019).

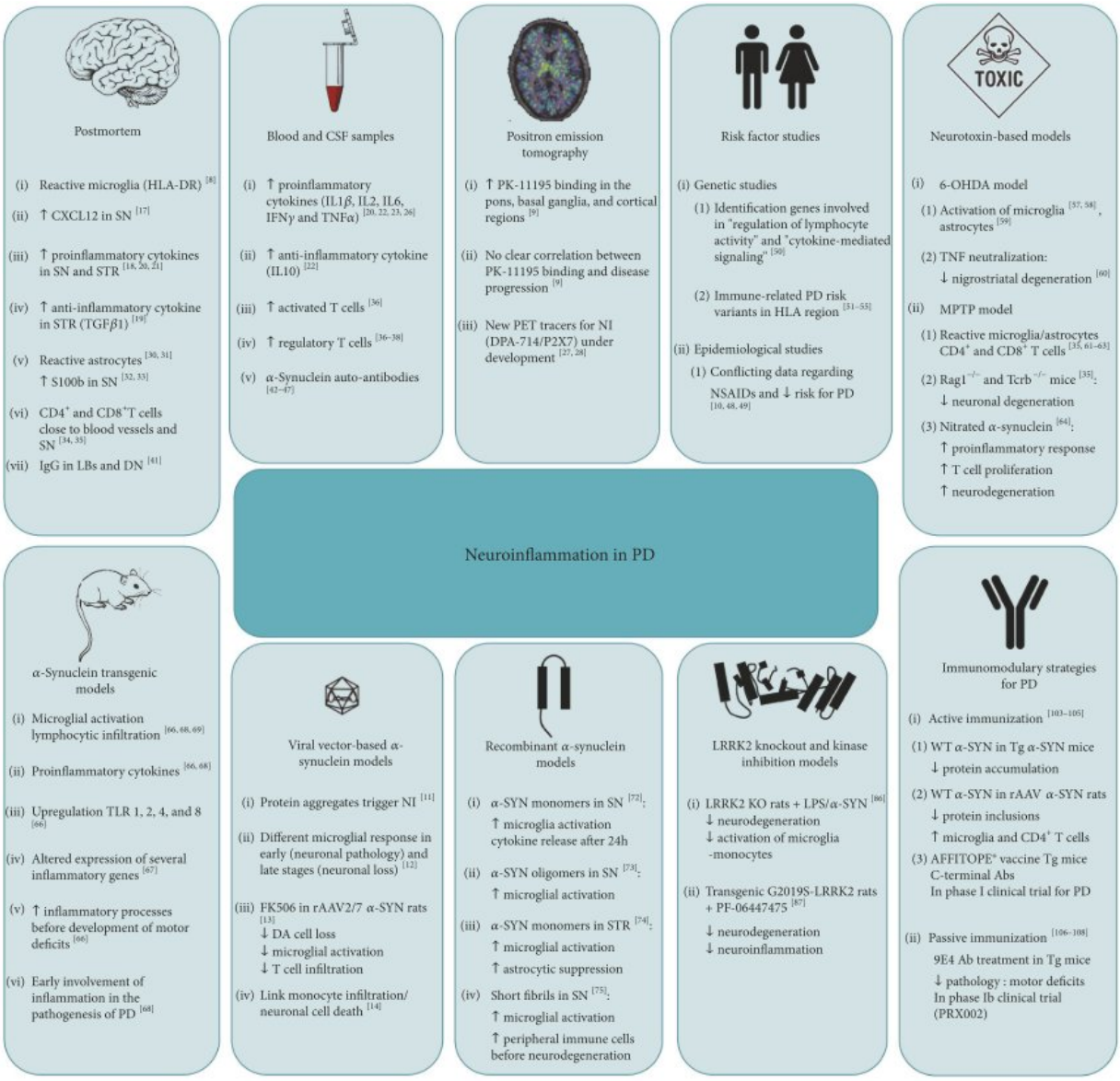

Figure 8: Clinical and preclinical evidences of the role of neuroinflammation in the development of PD and consequent neuronal degeneration

The link between neurodegeneration and neuroinflammation has been showed by different preclinical studies as well as clinical investigations *(Gelders et al., 2018).*

1.5 Symptoms, Diagnosis and Biomarkers of Parkinson's disease

1.5.1 Symptoms

At the moment there is still a lack of reliable and easy-applicable test or biomarker to check whether a patient is affected by PD or not (Lau and Breteler, 2006), and the same time to follow up the progression of the disease over time and/or any potential applicable therapy (Oertel, 2017). In clinic it is widely accepted that when the first traditional and quantifiable symptoms of the disease are visible (and so the diagnosis is formulated) between 30% (Chen et al., 2013; Rizek et al., 2016) to 80% (DeMaagd and Philip, 2015; Lang and Lozano, 1998; Sveinbjornsdottir, 2016) of dopaminergic neurons in the nigro-striatal pathway are dead; even if 80-90% of the diagnosed cases correlate with a post-mortem proof (Lau and Breteler, 2006) brain autopsy must still be done to have a confirmation of the previous correct diagnosis.

1.5.2 Diagnosis

Diagnosis of the disease should be evaluated specifically for each patient (Jankovic, 2008) basing on his/her clinical history and accurate physical examinations (DeMaagd and Philip, 2015; Rizek et al., 2016), focusing primary in ruling out alternative wrong diagnosis as essential tremor or multiple-system atrophy (DeMaagd and Philip, 2015).

Physicians, since the beginning of 60's have available different and numerous PD evaluation scales done both for clinical and research purposes. Unfortunately, until 1987 the available scales were not totally validated and most of the time specifically modified by the developers or other users to fit the need of their study; this led to a great amount of data that were not completely comparable between them. From 1987, then, two new scales - the *Unified Parkinson's Disease Rating Scale (UPDRS)* and the I*ntermediate Scale for Assessment of Parkinson's Disease (ISAPD)* were developed and validated to create standardized tools that could be used in most of the studies, and since then intensively used. In 2008 the *UPDRS* scale has been substituted by its updated version, the *Movement Disorder Society-Unified Parkinson's Disease Rating Scale (MDS-UPDRS)* (Bhidayasiri and Martinez-Martin, 2017; Perlmutter, 2009). The importance of such scales are not only related to a good diagnosis based on quantification of symptoms and disability, but are also an important tools for patients' and caregivers' quantification and follow-up of the ongoing treatment (Perlmutter, 2009).

Cardinal hallmarks of the disease can be grouped under the acronym *TRAP* (Jankovic, 2008) standing for *T*remor at rest, *R*igidity, *A*kinesia (also called bradykinesia) and *P*ostural instability. Between all these symptoms the latter is the "weakest" and less correlated to a strong diagnosis, as in most cases it is not present at the moment of diagnosis (Reichmann, 2010), but occurs within 5 years in 50% of patients (DeMaagd and Philip, 2015). Other useful symptoms for a complete disease's description include freezing and flexed posture (Jankovic, 2008), hypophonia (soft voice), micrographia (small handwriting), difficulties with balance and shuffling steps (Rizek et al., 2016). In the last 10-20 years clinicians started to focus their attention also on the non-motor symptoms of the disease as olfactory and erectile dysfunction (Xia and Mao, 2012), constipation, impaired colour discrimination and blurred vision, sleep disorders (Reichmann, 2010), gastrointestinal and neuropsychiatric issues, autonomic and sensory symptoms (Xia and Mao, 2012). Taken all together, these entities are believed to be directly connected with the progression of the pathology, and could be used to partially predict Parkinson's disease as the non-movement related symptoms may even long before the appearance of motor-related problems (Xia and Mao, 2012).

Nowadays, neuroimaging techniques are widely used to help clinicians in confirming and validate the clinical diagnosis of the disease (Titova et al., 2017). The most used approaches are based on magnetic resonance imaging (MRI), positron emission tomography (PET) or SPECT (single Photon emission tomography) with the long period emitter ^{123}I-DATScan. The first one is a widely available and inexpensive imagine technique based on strong magnetic fields and radio waves that, stimulating water molecules of the body, are able to produce detailed physiological and anatomical images on the organs. For example, nigral iron deposition, degeneration of nigrostriatal pathway or of the white matter can be detected using specific acquisitions sequences (Titova et al., 2017). PET is used to study metabolic processes in the body and is based on the detection of gamma rays emitted by a radioactive tracer injected directly in the patient bloodstream. Dopaminergic system is widely investigated with PET, even if in the last years radiotracers targeting other systems have been developed (Titova et al., 2017). SPECT, together with MRI, is routinely used in clinics; it integrates computer tomography scans and nuclear imaging scans through gamma rays, showing how the blood flows through organs and tissues.

1.5.3 Biomarkers for prevention

Prevention of PD, when compared to other common diseases as cancer or cardiovascular diseases is difficult and still in the early phases: first of all, there is not a full characterization of the disease's causes and it is still unknown what triggers the beginning on the neurodegeneration. In addition Parkinson's disease field is still in huge need of reliable biomarkers to finally understand the disease, its development and its specific features: biomarkers were originally defined as "*cellular, biochemical or molecular alterations that are measurable in biological media such as human tissues, cells, or fluids*" (Hulka and Wilcosky, 1988), but most recently (2000) this definition was implemented (or updated) by the National Institute of Health (NIH) as "*a characteristic that is objectively measured and evaluated as an indicator of normal biological processes, pathogenic processes, or pharmacologic responses to a therapeutic intervention*" (Chen-Plotkin et al., 2018).

Biomarkers have been widely used since time in many fields of medicine - to mention few - cancer biology, cardiovascular disease, immunological genetic disorders and nervous system disorders (Mayeux, 2004). They can be generally classified in different categories: *1) in vivo biomarkers* (neurophysiology, neuroimaging, polysomnography); *2) in vitro biomarkers* (biochemical and genetics from tissue samples); *3) pathological biomarkers* (iron/α-syn accumulation, dopamine transporter loss); *4) neurobehavioral biomarkers* (fatigue, depression) and *5) clinical biomarkers* (sleep disturbance, constipation etc.) (Titova et al., 2017).

Up to date there is not approved or validated tissue or blood biomarker, even if some of them are very promising. Although imperfect and with many limitations, imaging biomarkers are currently the best available approach in clinical trials. Looking at the future, it is highly possible to imagine the development of batteries of tests that will include different types of approaches for a complete readout of the disease (Algarni and Stoessl, 2016).

1.6 Treatments for Parkinson's disease

1.6.1 L-DOPA and deep brain stimulation

Currently there are no drugs or therapy known to be disease modifying or neuroprotective (Jankovic and Poewe, 2012); treatment of Parkinson's disease in 2019 is still based on L-DOPA, a molecule characterized in 1938 (Hornykiewicz, 2010) and routinely administered in high oral dose to treat PD since 1967 (Cotzias et al., 1967). L-dopa treatment sole role is to control motor symptoms by

delivering into the brain a precursor of dopamine that is then synthesized and compensate the lack of production by the death dopaminergic neurons; this external delivery and compensation of dopamine makes patient's life partially better (Jankovic, 2002). During the first years of the disease it is possible to substitute dopaminergic drugs with amantadine or anticholinergic drug, but once the PD-related symptoms start to interfere with patient's life, therapy with monoamine oxidase type B (MAO-B) inhibitors and dopaminergic medicament is mandatory (Jankovic and Poewe, 2012). However, after years of treatment, many patients develop side effects connected with L-dopa intake - including motor fluctuations, on-off effects, freezing, awake or asleep myoclonus (uncontrolled twitching of a muscle or group of muscles), punding (repetition of a complex motor behaviour most of the times without any purpose) and dyskinesia (Jankovic, 2005; Okun, 2012). To control advanced motor fluctuations in PD patients under the high regime of L-dopa different approaches may be taken: first of all physicians suggest a change in L-dopa pharmacokinetics and delivery via COMT-inhibition, the additional use of MAO-B inhibitors or dopamine antagonists, injection or infusion of apomorphine, and at the end deep brain stimulation (Jankovic and Poewe, 2012).

DBS is a surgical technique widely used in clinic to help PD patients with intractable tremor or very strong drug-induced motor complications: the most common procedure consists in implanting unilaterally (or bilaterally for the most severe form of PD) an electrode in the motor portion of the STN or GPi (Wichmann and DeLong, 2011): once the electrode is in place, it delivers electric stimuli to the surrounding brain tissues (Okun, 2012). Although clinical evidences strongly support the positive outcome of DBS it is still unclear how this technique has direct benefits on reducing symptoms of PD (Okun, 2012; Wichmann and DeLong, 2011). It is generally accepted that due to the electric stimulus there is an inhibition of neuronal cell bodies and excitation of the nearest axons. Moreover, from one side astrocytes are excited to release glutamate and adenosine, and from the other side there is an increase in the blood flow and an increase in neurogenesis. All this effects and reactions begin in the area around the implant, but are quickly able to extend and reach the large neural network (Okun, 2012). The risk of post-surgical problems is very low with DBS: the most common problems include intracerebral haemorrhage (ICH) (0.2-5 % of reported cases) and postoperative infections (1.8-15.2 % of reported cases), most often in the area surrounding the pulse generator (Groiss et al., 2009). In some cases involuntary movements, worsening of speech or gait, cognitive and moods and side effects,

post-operative depression (in some cases leading to suicide in patients with untreated or unrecognized previous depression), mania, anxiety and apathy have been reported: most of them may be correlated with involuntary stimulation of the limbic circuit elements that can be fixed tuning the stimulation parameters (Wichmann and DeLong, 2011).

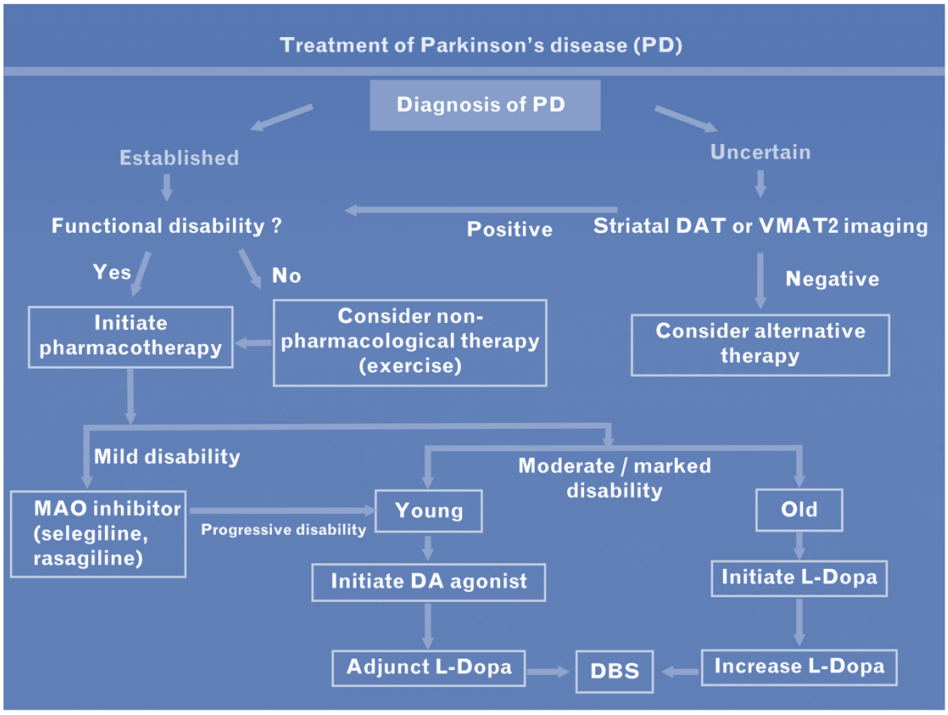

Figure 9: Suggested possible approaches in the diagnosis and treatment of PD from diagnosis to advanced stages *(Jankovic and Poewe, 2012).*

1.6.2 Gene therapy

Goal of gene therapy in Parkinson's disease is to deliver, via viral vectors, genes into the patient's brain (Stoker and Barker, 2018). Some therapies aimed in changing directly the behaviour of neurons, enhancing for example their activity in the release of dopamine, while some other focused on changing behaviour of specific genes, or delivered genes demonstrated to control cellular growing factors release (Albert et al., 2017; Stoker and Barker, 2018; Valdés and Schneider, 2016).

Even if the number of clinical trials with gene therapy for PD is relatively small, in the last years some of them have been done and showed interesting results: considering that in PD there is a significant loss of aromatic L-amino acid decarboxylase (AADC) – the enzyme that has the role to convert levodopa into dopamine – Aminoff's and Bankiewicz groups in 2009 used adeno-associated

viral type 2 vector with the human aromatic L-amino acid decarboxylase gene (AAV-hAADC). Ten total PD patients (divided in low and high dose group, 5 per group) were bilaterally intraputaminal injected with AAV-hAADC. Even if 3 patients presented intracranial haemorrhages post-surgery the overall study was successful: in fact, the viral infusion was well tolerated by the patients, there was a general improvement tested with the UPDRS scale (unified Parkinson's disease rating scale) of around 30% and confirmed also in the motor state diaries. In addition PET scan specific for the AADC enzyme done at 1 and 6 month post infusion showed an average increase of AADC expression equal to 75% for high dose patient's cohort (and 30% low dose cohort) (Christine et al., 2009). Another study published in 2018 used AAV mediated gene delivery of AADC: results led to similar outcomes as in the previous described study. Injection of viral vector was well tolerated by the patients, surgery related haemorrhagic events observed in Aminoff's study were not present (except for one patient who had venous haemorrhage below the burr hole); authors evaluated a PET increased FMT activity up to 96 weeks (56%) and a motor function improvement of 46% basing on UPDRS scale (Pardo et al., 2014).

Another elegant set of studies was done by Palfi's group back in 2009: MPTP injected macaque monkeys received a bilateral interstriatal injection of lentiviral vector coding for guanosine 5′-triphosphate cyclohy-drolase 1 (CH1), tyrosine hydroxylase (TH) and aromatic L-amino acid decarboxylase (AADC) - genes known to be crucial for the production of dopamine. Results showed a great restoration of dopamine production together with reduction of motor deficit without associated dyskinesia up to 12 months post injection (Jarraya et al., 2009). Basing on these results, a phase 1/2 open-label trial was carried out in France and UK to test the safety of the therapy (called ProSavin); PD patients were bilaterally injected into the putamen with low, medium or high dose of lentiviral vector coding for TH, AADC and CH1. Results showed a significant improvement of the motor scores off medication evaluated by the UPDRS part III scale at 6 and 12 months post lentiviral delivery when compared with the baseline (Palfi et al., 2014). A follow up of the study was done up to 5 and 8 years post injection: a significant improvement in the motor score off medication was seen also after 2 years. At 4 years follow up, only 8 patients out of 15 showed significant improvement, and at 5 years a moderate improvement over the baseline was seen in the majority of analysed patients (Palfi et al., 2018). To note, the ProSavin administration in PD patients resulted to be always safe and well

tolerated, even if some adverse effects were detected (e.g. on-off phenomena and dyskinesia), but were not related to the viral delivery (Palfi et al., 2018, 2014)

1.6.3 Neurotropic factors

Neurotropic factors (NTFs) are active biomolecules involved in synaptic plasticity, neurite branching, neuronal survival and in regulation of neuronal number (Domanskyi et al., 2015). NTFs can be generally divided in three families: *1)* the glial cell-line derived NFCs (GDNF), *2)* neurotrophins and *3)* neuropoietic cytokines (Deister and Schmidt, 2006).

Since their discovery, many NTFs have been studied both *in vivo* and *in vitro* to be used against Parkinson's disease due to their known regeneration ability (Barker, 2009; Valdés and Schneider, 2016): the ones showing the best preclinical results are GDNF and neurturin (NRTN), (Sullivan and O'Keeffe, 2016).

GDNF investigations showed contrasting results: when injected intraventricularly in 50 patients in a randomized controlled study, no relevant clinical positive effect where visible even if doses where high and side effects (included Lhermitte's signs) were visible (Nutt et al., 2003). Two other open label studies used direct continuous infusion of GDNF into the brain: the therapy was well tolerated and minimal side effects occurred. A significant improvement was visible both by UPDRS score and PET analysis (Sullivan and O'Keeffe, 2016). A placebo randomized controlled trial involving 34 patients who received bilateral continuous delivery of GDNF (or placebo) did not show any significant improvement in the UPDRS scale. Surprisingly there was an increase on ^{18}F-dopa detected by PET, although without associated clinical benefit and apparent effective release of dopamine (Lang et al., 2006).

NRTN, an analogue of GDNF acting through the co-receptor GFRα2 instead of GFRα1, showed as well variable results: while had great results on animal models (both non-human primates and rodents), in human clinical trials results were contrasting. In the open label phase 1 study (supported by Ceregene Inc.), 12 PD patients were intraputaminal injected with AAV2-NRTN both at high or low dose. Even if no changes were detectable using PET, a 36% UPDRS scale improvement was registered at 1 year; in addition no adverse side effects were detectable at 1 year post surgery (Marks et al., 2008). Subsequently a phase 2 double bling sham-surgery controlled randomized trial was launched in 2018: 58 patients received a bilateral injection into the putamen of either AAV2-NRTN or a sham surgery. At the first evaluation time-point (12 months post-surgery) there was not any improvement

compared with the sham surgery. At secondary time-point (18 months post-surgery) some beneficial significant effects were visible in motor scores and self-reported activities of daily living (ADL), but the whole study was non-blinded even for the patients, with consequent increased risk of evaluation bias. It is important to mention that many adverse side effects occurred in this study (even if not all of them were connected with injection itself): different subjects developed tumour (both in the sham or AAV group), and transient post-surgery effects were visible (confusion, haemorrhage, cerebral oedema) (Marks et al., 2010)

1.6.4 Regenerative medicine

1.6.4.1 Pioneering research on cells transplantation for PD

The long story of cells transplantation for PD starts in the late 70's with the first transplantations of foetal cells - in detail foetal ventral mesencephalic cells (FVM): in one study rat FVM cells (containing SN cells) or adult sciatic nerve cells were injected into the lateral cerebral ventricle in a 6-hydroxydopamine (6-OHDA) model: 4 weeks after transplantation animals injected with foetal cells showed an improvement (around 50%) in apomorphine behavioural test. In addition, DA cells were able to graft into the host brain (Perlow et al., 1979). Similar independent results were obtained by another group that injected the same kind of cells into the cavity at the surface of the striatum and tested the motor asymmetry using amphetamine; also in this study transplanted cells were able to graft, survive and extend projections in the surrounding host area (Bjorklund and Stenevi, 1979).

The first clinical cells transplantation in human affected by PD dates back in 1987 when Olson's group (Lindvall et al., 1987) published a report of unilateral transplantation of autologous adrenal medullary tissue into the striatum of two advanced stage Parkinson's disease patients. Unfortunately, even if for the first few days beneficial effects of the procedure seemed to be present, in short time the authors noticed that the partial restoration of motor function was only transitory (Lindvall et al., 1987).

In 1990 Lindval and colleagues showed that striatal transplantation of foetal dopamine rich mesencephalic tissue led to reinnervation of the striatum, increased DA production and storage in the area of the graft, and improvement of motor functions (Lindvall et al., 1990) In the same years (and for mostly all the '90's), also human FVM cells were involved in numerous human trials: results were contrasting, showing both improvements (sometimes very good recovery or positive outcome detectable also after 20 years) and no real significant changes (especially when compared with standard therapies as DBS). Moreover some adverse effect (graft-induced dyskinesia - GIDs) and ethical

issues raised questions about the choice of this type of cell source: all this did not completely dismissed the method but general opinion was that it should not be pursed (Barker et al., 2015; Lindvall, 2015; Yasuhara et al., 2017).

1.6.4.2 Current directions for cells transplantation for PD

Regenerative medicine is a branch of applied research that has the goal to "replace or regenerate human cells, tissue or organs, to restore or establish normal function" (Mason and Dunnill, 2008). The idea that regenerative medicine would become a personalized medicine, revolutionizing the healthcare of the future, has always been of great appeal for physicians and researchers (Blair et al., 2017). Both in clinic and in applied research, different sources of cells and various types of diseases are studied using stem cells and cells transplantation: many studies entered the clinical trial phase, and are studied for direct application in humans (Trounson and McDonald, 2015). An additional boost and a new gain of interest in the field was given in 2006 (and again in 2012 winning the Nobel Prize in physiology and medicine) by Yamanaka when, during a lecture at the International Society for Stem Cells Research, unrevealed the possibility to reprogram adult developed cells into embryonic-stem-like-cells (later renamed induced pluripotent stem cells – iPSc) thank to a cocktail of genetic factors (Scudellari, 2016; Takahashi and Yamanaka, 2006). The idea that in a very close future traditional organs transplantation would be replaced by a single transplantation of cells in combination with some natural or synthetic scaffold did not sound anymore as an optimistic dream, but a simple matter of time (Ratajczak et al., 2014).

During the last 30 years, a huge amount of cell transplantation studies have been done both *in vitro* and, mostly, *in vivo*. Researcher main goal was to control stem cells fate and drive their differentiation into dopaminergic neurons (Barrow, 2015), and establish a reliable source of cells that could be used on demand and not be based on unpredictable supply (Stoker and Barker, 2018). Once these problems are overcame, transplantation into the patients might be done to substitute the lost neurons and restore dopaminergic release (Barrow, 2015).

Important to keep in mind is that each study done so far has its own characteristic and peculiarity, so it should be singularly analysed and comparison is not encouraged; generally variables in studies include – but are not limited to – *a)* site of injection, *b)* time points for evaluation after transplantation, *c)* type of PD animal model used or stage of parkinsonism of the patient enrolled into the trial, *d)* type of transplanted cells and/or source and type of stem cells used to generate

dopaminergic neurons and/or differentiation procedure. The most used type of stem cells in the PD field include iPSCs, hematopoietic stem cells (HSCs), mesenchymal stem cells (MSCs), embryonic stem cells (ESCs), neuronal stem cells (NSCs) and FSCs (Barker et al., 2015, 2013; Blair et al., 2017; Cresto et al., 2018; Lindvall, 2016; Moriarty et al., 2018b; Trounson and McDonald, 2015; Yasuhara et al., 2017; Zhang et al., 2017).

Major issues with stem cells transplantation are ethical issues (especially for embryonic cells) (Stoker and Barker, 2018), integration of viral vector used for reprogramming cells into the cell genome (in particular for iPSCs) (Herberts et al., 2011) that together with the strong self-renewal and high rate proliferation activity of the cells leads to teratoma formation (du Pré et al., 2013), and low survival of selected cells before (due to the preparation procedures with subsequent detachment from the extracellular matrix), during (due grow factor deprivation and unhospitable environment) and after the transplantation (strong immune response of the body with consequent rejection of the graft) (Herberts et al., 2011; Moriarty et al., 2018a; Moriarty and Dowd, 2018).

Although the use of NTFs and stem cells transplantation alone might not be fully successful to strike advance of PD, their use could be extremely helpful and lead to a positive outcome when combined together with newly developed hydrogels and biomaterials (Bruggeman et al., 2019).

1.6.5 Biomaterials

Biomaterials are a class of materials used and adapted for medical applications and are designed to interact with different biological systems (Orive et al., 2009). In the last years, different kind and types of biomaterials have been used for various medical applications, mainly for drug delivery, organ and tissue repair (behaving as a scaffold for stem cells therapy protecting them and enhancing their attachment and proliferation) (Orive et al., 2009; Sekuła and Zuba-Surma, 2018) (Orive et al., 2009; Sekuła and Zuba-Surma, 2018). Common characteristics that all types of biocompatible materials must respect include: *a):* biocompatibility (ability to integrate into the host's system without adverse effects), *b):* biofunctionality (ability to perform specific biological tasks), *c):* biodegradation (decomposition of material in natural way and no toxic effect when it remains in the body) or bioreasorbability (decomposition of the material by the body in a certain time after transplantation and removal form the body via metabolic pathways), *d):* non toxicity (no release of potential toxic components used to create the biomaterial) and *e):* mechanical properties (the ability to mimic

mechanical properties of the anatomical site of implantation (Orive et al., 2009; Sekuła and Zuba-Surma, 2018).

Biomaterials used in healthcare can be easily derived from different type of natural sources or be designed and engineered on demand.

Natural elements as collagen, agarose, alginate, and fibrin, are widely used due to their low immune response in tissue engineering. Among them collagen results to be the most used and preferred candidates due to its ability to be naturally resorbed by the body without any toxicity; in addition, it possesses flexibility and mechanical strength to be adapted in various biomedical fields and stimulates the survival, interactions, attachment and adhesion of cells leading to restoration of the tissue.

An alternative to natural elements might be synthetic materials: many types are currently used in research and medicine. Poly(ethylene) (PE), polylactides (PLA), poly(glycolide) (PGA) and polyurethanes (PUR) are intensively used due to their well-known chemical composition and the ability to control their properties on demand; moreover, such class of polymers is widely used on therapies with specific stem cells population (neurons, cardiac cells, muscles cells) for tissue repair. Titanium and ceramic bases biomaterials are mostly used in the field of bone regeneration as they have relative long durability, good mechanical properties, high biocompatibility and have been discovered to stimulate osteoblast recruitment and proliferation around the scaffold, leading to successful healing (Sekuła and Zuba-Surma, 2018).

Another interesting class of biomaterials are the so called “smart materials”: their feature is the ability to change physical properties as shape, colour, stickiness or stiffness in response to external stimuli as magnetic or electric field, pH, temperature, hydrostatic pressure radiation. Once the stimulus is finished, they have the ability to go back to the original state (Sekuła and Zuba-Surma, 2018) .

Hydrogels are another type of biomaterials: they are formed by a 3D network of polymer chains and water; due to their biocompatibility and ability to swell in solutions, they can be easily injected in the body (Sekuła and Zuba-Surma, 2018). Hydrogels by definitions are “*the broad class of crosslinked polymeric networks those absorb large amount of water or any other biological fluid without showing any alternations in their 3-D architecture*” (Bhat and Kumar, 2013). Currently hydrogels have miscellaneous applications, ranging from food additives, water purification, decontamination of organic

wastes to biomedical implants, cells encapsulation, regenerative medicine and tissue engineering, biosensors, diagnostic, controlled drug delivery and release, contact lenses and so on (Varaprasad et al., 2017). They can be categorized basing on different properties, including their physical state (solid, liquid and semi-solid) (Varaprasad et al., 2017), their cross-linking preparation (physically crosslinked, chemically crosslinked and dual network) (Ullah et al., 2015; Varaprasad et al., 2017), and source (natural, synthetic hybrid) (Ullah et al., 2015)

The most used classification is the one based on hydrogel's cross-linking preparation: in physically crosslinked hydrogels, no external crosslinking agent is used, and the reaction is achieved via physical process as crystallization, chain aggregation, hydrophobic association, and hydrogen bounding; physical interaction between the different polymer's chains prevent dissolution of the hydrogel crosslinking itself (Ullah et al., 2015; Varaprasad et al., 2017).

Chemically crosslinking hydrogels use covalent bonds between the different polymer chains; they are very stable and can be dissolved only when the covalent crosslinking points are cleaved (Ullah et al., 2015; Varaprasad et al., 2017) Dual network hydrogels are a mix formed by chemical and physical hydrogels, due to an electrostatic interaction: they are used in situations when a higher liquid intake capacity is needed and/or higher pH sensitivity is required. In addition in 2003 a self-healing properties of the dual network hydrogels has been reported (Ullah et al., 2015).

Since 2016 a lot of effort is put in the development of a specific hydrogel to help therapy development against Parkinson's Disease (BrainMatTrain - Official Website, n.d.): this European consortium is focusing on the development of an hydrogel, formed by crosslinking collagen type I with 4-star poly(ethylene glycol) ether tetrasuccinimidyl glutarate (4s-StarPEG).

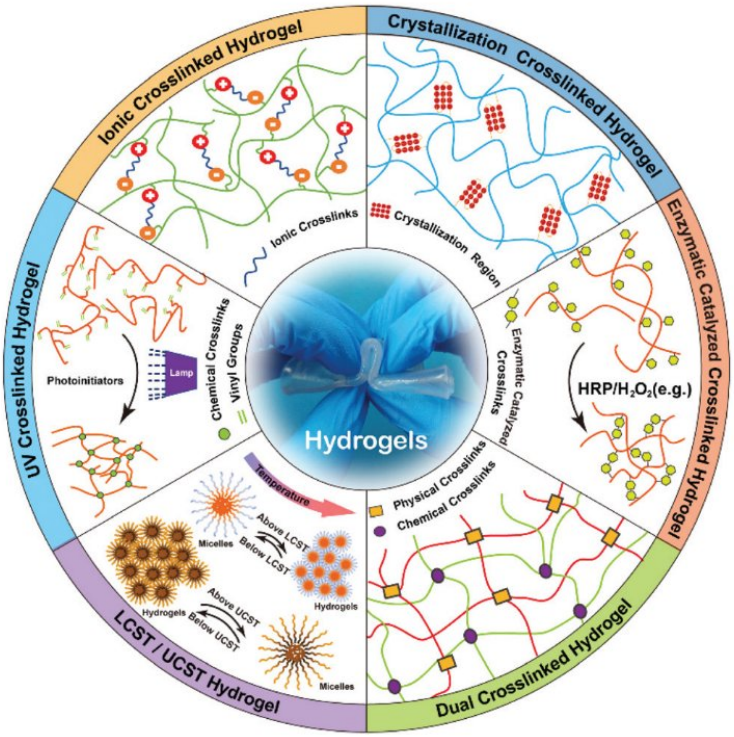

Figure 10: Crosslinking strategies for hydrogel.

Different types of crosslinking strategies are available at the moment to create hydrogel. Our hydrogel of interest is collagen based and chemically crosslinked with 4s-StarPEG *(Hu et al., 2019).*

Collagen, formed by a triple helix of three polypeptide chains, is one of the most abundant proteins in the human body and is involved in providing mechanical stability, strength and elasticity to the organism (Chang et al., 2012; Gelse et al., 2003). So far 28 different types of collagens are known, and they can be classified into distinct categories basing on their supramolecular organization and structure (Ricard-Blum, 2011). The most abundant family is the so-called fibril-forming collagen, that includes collagen type I, II, III, V, XI, XXIV and XXVII (Ricard-Blum, 2011).

Type I collagen, formed by two α-1 chains and one α-2 chain (Chang et al., 2012), is the most abundant collagen in the human body and can be found in bones, tendons, cornea, skin, ligaments, and interstitial connective tissues (but in very low quantity in the brain) (Gelse et al., 2003). Collagen is daily used in various creams and cosmetics: moreover, different studies proved that due to its safety, ingestion of hydrolysed collagen protein lead to stimulation of fibres' production leading to a recovery and reduction of the skin ageing (the so-called visible wrinkle effect) (Avila Rodríguez et al., 2018). Collagen nowadays is derived from both natural and synthetic sources; the latter ones are types of collagens that mimic the real natural collagen behaviour and structure, possessing a very low immune

response and wide applications in the field of healing and blood clothing. Natural derived collagens are the most used ones: they may be derived both from vegetable (tobacco and barley mainly) or animal sources. The most common derived collagen is from animal sources, namely bovine and porcine. In addition, even if used only for specific applications, it is possible to derive collagen from chickens, equine's tendons, alligators, frogs, kangaroos' skin and tail. Another source of collagen that only in recent years arrived to market is the one derived from marine animals which include starfishes, jellyfishes, octopuses, sponges, anemones, squids, prawns and bones, fins, scales or skin of fresh or saltwater fishes: such type of collagen has high yield and almost no risk of disease transmission as well as low immune response; at the same time it possesses low thermal stability that reduce its direct applications (Avila Rodríguez et al., 2018).

Collagen based biomaterials recently gained healthcare's attention and already today are widely applied in some fields of regenerative medicine as tendon repair and skin grafts (Abou Neel et al., 2013), wound healing (Chattopadhyay and Raines, 2014), bones and spinal cord regeneration (Ferreira et al., 2012). In August 2019, a team from Carnegie Mellon University in Pittsburgh, USA, reported their ability to 3D print components of human heart (from capillaries to bigger structures) based on collagen (A. Lee et al., 2019).

Even if collagen is able to self-assembly and create supramolecular structures, their bonds are too weak to make stable structure with well-known and tailorable properties as sponges, gels or hydrogels; that is the reason why to have usable biomaterials a crosslinker has to be added (Sanami et al., 2016; Sekuła and Zuba-Surma, 2018).

PEG is a class of molecules with different polymer chain lengths (tailored for the specific need) used in different biological and industrial fields (French et al., 2009); in biomedicine it is mostly used to initiate the polymerization of proteins as collagen into a gel and control its degradation rate (Moriarty et al., 2017; Moriarty and Dowd, 2018). On demand degradation rate of PEG chains (and then of the gel) can be achieved using different crosslinker concentrations: this permits the fabrication of known structure with specific network's properties over time (Lin and Anseth, 2009). Even if different types of crosslinking methods are available on the market, multi-functional poly(ethylene glycol systems) have been widely used in medical devices and regenerative medicine due to their satisfying properties: in the specific, 4s-StarPEG appear to have the greatest properties as a collagen crosslinker when

compared to traditional crosslinking methods, showing stability, good mechanical and thermal properties, no cytotoxic effects and enhanced cells' growth and proliferation (Sanami et al., 2016).

The use of biomaterials for enhance cellular replacement therapy for Parkinson's disease, seems to be very promising and attractive. *In vitro* test done on a collagen type I hydrogel showed no adverse effects of the hydrogel on cells survival or any sign of toxicity. The peculiarity of this specific hydrogel is its ability to be liquid at 4°C, and polymerizes *in-situ* at 37°C. Transplantation of dopaminergic neurons encapsulated in such collagen hydrogel enriched with GDNF showed that after transplantation in the striatum of a 6-OHDA rats, there was an increase in cells survival, as well as an improvement in the lesioned striatal re-innervation (Moriarty et al., 2017). Enhance survival of cells after transplantation was seen when hPSCs-derived neural progenitors were embedded in a HA-based hydrogel and transplanted in the rat striatum (Adil et al., 2017). Increased cellular survival and increase re-innervation of the striatum was also observed when VM cells were mixed to a composite scaffold enriched with GDNF, and then transplanted in the striatum of 6-OHDA rats (T.-Y. Wang et al., 2016).

2. Animal models for Parkinson's disease

Whether to understand the whole disease or some specific features of it, scientists need well defined and reliable models: while from one side, *in vitro* and *ex vivo* experimentation is routinely used, they might not give results that correspond to what really occurs in a living organism. This is the reason why studies on animal models – *in vivo* – have to follow not only to confirm the preliminary results, but also to investigate the potential effect on a complete organism.

Certainly, *in vivo* studies are still far from being perfect and far from unravelling all the mechanisms of diseases, but at the moment these are the only way to obtain data possibly relevant to a clinical context.

For PD, different animal species (non-human primates, rodents, drosophila, and fish) have been developed during years: to remain in the scope of the present thesis only PD rodent models will be described.

2.1 Neurotoxic models: MPTP and 6-OHDA

The two traditional neurotoxic models of PD used in research are based on 6-Hydroxydopamine (6-OHDA) (for rats and mice), and 1-methyl-4-phenyl-1,2,3,6- tetrahydropyridine (MPTP) (for mice and NHP only). These models are relatively fast and easy to produce, and are routinely used as models to test neurorestorative and neuroprotective therapies.

MPTP was discovered by chance by Dr. Langston in 1982 when he was presented with a case of a 40 years old subject with apparent catatonic schizophrenia and PD-like symptoms. After a short investigation, he discovered that there were 6 similar cases in different part of the USA; they had all had consumed a new drug – synthetic heroin. Analysis of this drug showed that it was almost pure MPTP, a by-product of MPPP, which had deleterious and toxic effects on the SNpc (Langston, 2017). The mechanism of action of MPTP is quite simple: MPTP molecules are able to cross the BBB and enter the brain stem, where they are sequestered by astrocytes and converted to MPP+ (Langston et al., 1984; Markey et al., 1984). MPP+ is selectively toxic for DA neurons but not for astrocytes as it is an excellent substrate for dopamine transporter (DAT) (Meredith and Rademacher, 2011). Once MPP+ is taken by SNpc neurons, it starts to accumulate in the mitochondria, where it subsequently inhibits

complex I of the mitochondrial respiratory chain. Such inhibition leads to a reduction of ATP in the striatum and SNpc, and shortly after death of DA neurons due to necrosis and apoptosis (Meredith and Rademacher, 2011). In addition to strong mitochondrial dysfunction and neurodegeneration, MPTP is also able to produce both in mice (Vila et al., 2001) and primates (Kowall et al., 2000) accumulation of α-syn in the SNpc.

6-OHDA was first used in 1968 in rats (Ungerstedt, 1968), which showed a fast and strong loss of tyrosine-hydroxylase (TH) positive cells, and behavioural abnormalities which could be temporarily reversed with amphetamine or apomorphine administration (Jackson-Lewis et al., 2012). However, but no Lewy-bodies-like or any other type of inclusions that are typically seen in PD patients were observed (Blesa and Przedborski, 2014). As the toxin cannot cross the BBB, the model is produced by direct administration into the brain, preferably unilateral (bilateral injection is connected with higher mortality) in the SNpc (Jeon et al., 1995) or the striatum (Batassini et al., 2015), but alternatively also in the medial forebrain bundle (MFB) (Boix et al., 2015; Sahin et al., 2014; Torres et al., 2011). Onset and magnitude of dopaminergic degeneration are strictly connected with 6-OHDA's dose and site of injection: with moderate doses, loss of TH positive cells occurs within 24 hours up to 3 days, with a loss that can be quantified between 60 to 90% (Meredith et al., 2008). At the cellular level action of 6-OHDA starts when toxic molecules enter neurons and quickly auto-oxidase; this leads to an increase of intracellular oxidative stress and subsequent cellular death (Meredith et al., 2008).

2.2 Neuroinflammatory model: LPS

Neuroinflammation has been proved to have a very important role in the pathogenesis of PD, involving the activity of microglial and macroglial cells (Przedborski, 2007). It is still not fully understood if neuroinflammation is the cause or consequence of dopaminergic neurons loss: the most followed theory suggests that neuroinflammation is not the direct cause of cellular loss, but it is an essential secondary event in the neurotoxicity cycle (Hirsch and Hunot, 2009; Michel et al., 2016; Tieu, 2011).

To dig inside neuroinflammation and its direct effect on PD, lipopolysaccharide (LPS) model is widely used, even if it does not fully replicate real disease's conditions (Duty and Jenner, 2011).

LPS is an endotoxin found in the outer membrane of gram-negative bacteria (Dutta et al., 2008) that is able to strongly activate glial cells leading to induction of oxidative and nitrative stress as well as iNOS

expression, release of different types of cytokines (eg. TNFα, IL-6, IL1β) and trophic factors (mainly GDNF and BDNF) (Duty and Jenner, 2011). LPS' action starts once it binds to specific receptor complexes of the microglia as CD14/TLR4/LBP, leading to a strong uncontrolled cellular activation. This quickly releases different neurotoxic factors that accelerate neuronal damage and then death. Subsequently, damaged neurons are able to release injury signals as α-syn and neuromelanin that stimulate a further microglial activation (reactive microgliosis) leading to release of additional nontoxic factors and starting a self-amplifying cycle that might directly lead to neurodegeneration (Liu and Bing, 2011).

Different LPS's administration protocols are used to achieve neuroinflammation: high doses (between 5 to 10 μg/animal) of LPS directly injected in the striatum, SN, hippocampus or cortex lead to a strong activation of microglia with a consequent diffused inflammatory state in around 24 hours, loss of DA fibres in the striatum within few days, and, basing on the site of injection, DA cellular death in the SN within 30 days (Meredith et al., 2008).

Interestingly, microglia activated conformation is reverted in 30 days (Meredith et al., 2008). Permanent SN's dopaminergic cellular loss is seen also one year after intranigral injection (Batista et al., 2019; Flores-Martinez et al., 2018) while no cellular loss is seen after intrastriatal injection (Hoban et al., 2013a).

To achieve a more progressive model (with some technical challenges due to the surgical procedure), chronic intracerebral injection of LPS with an osmotic mini-pump might be done during few weeks: results lead to a fast-microglial activation and signs of oxidative stress, persisting for few weeks together with a significant but slow progressive loss of DA neurons. An alternative could be an acute systemic injection of high dose of LPS that leads to a fast microglial activation within 3 hours, and a delayed but also progressive DA loss (Meredith et al., 2008).

Another approach might be intrauterine LPS injection during gestation time, leading to an offspring with reduced striatal DA and reduced DA positive cells in the SN (Meredith et al., 2008).

2.3 Transgenic and genetic models

Various genetic models have been generated to better understand the genetic undergoing development of PD; in particular the most used to study the autosomal dominant form of PD are based on α-syn and LRRK2 mutations while PINK1/Parkin and DJ-1 mutation are used to study the autosomal recessive PD's form (Blesa et al., 2012). These genetic models, in most cases, led to the discovery of the important cellular and molecular deregulations produced by mutation of the causal genes, including altered mitophagy, protein misfolding, alteration of the proteasome function, abnormal reactive oxygen production, and mitochondrial defects (B. D. Lee et al., 2012). In most cases, alteration of the dopaminergic system and behavioural disturbances are often absent or minimal, occurring only in advanced ages (>18 months in mice) (B. D. Lee et al., 2012). Despite the major insights that these models brought to our understanding of the complex mechanisms likely related to PD pathogenesis, the fact that most of the models developed so far are not able to fully recapitulate the behavioural and pathological phenotypes typical of the human condition of PD, limits their use for development of experimental therapeutics aiming at either reconstructing the damaged nigrostriatal pathway or preventing the actual loss of SNc neurons that is seen in PD patients (Blesa and Przedborski, 2014).

2.3.1 α-synuclein models

Different types of α-syn (mutant or WT) (Dawson et al., 2010) as well as various promoters (including some specific for DA-neurons) have been used to create transgenic models based on α-syn (Y. Lee et al., 2012). The successful development of PD-like phenotypes in such models is strictly correlated with the transgene high-level expression and distribution, proving the important gain-of-function toxic mechanisms of α-syn (Visanji et al., 2016).

The mouse prion protein promoter (mPrP) did not lead to any loss of DA neurons in SNpc, even if the mice showed typical hallmarks of PD including accumulation of α-syn, phosphorylation and ubiquitination as well as motor alterations (Giasson et al., 2002).

PDGF-β promoter induced loss of dopamine and cellular terminals in the ST, but no loss of TH+ cells was detected in the SNpc (Masliah et al., 2000).

The specific TH promoter showed some loss of TH+ cells, but results were unfortunately variable and, in some cases, irreproducible. An alternative might be the Thy-1 promoter that is able to

reproduce loss of DA in the striatum, general α-syn pathology but also a very moderate loss of TH+ cells in the SNpc (Blesa and Przedborski, 2014).

Lin and colleagues showed that overexpression of α-syn-A53T in mice's dopaminergic neurons under the Pitx3 promoter leads to strong decrease of dopamine release, neurons neurodegeneration together with fragmentation of Golgi apparatus and defects in the autophagy/lysosome degradation pathways (Lin et al., 2012).

A bacterial artificial chromosome (BAC) mice model (SNCA-OVX) overexpressing WT human α-syn was used in 2013 by Janezic and colleagues to achieve an early impairment of dopamine release in the dorsal striatum, protein accumulation and reduced firing of SNpc dopaminergic neurons, with a consequent age-dependent loss of DA neurons in the SNpc (Janezic et al., 2013). Another BAC model is proposed by Nuber and colleagues: it is based on overexpression of full-length form of human WT-α-syn in rats, that leads to reduced striatal dopamine at 12 month of life, motor deficits (decreased rearing behaviour and increased time in accomplishing motor tasks) starting at 12 months of life, and consequent loss of nigral TH+ neurons at 18 months of age (Nuber et al., 2013). In addition, the authors found insoluble proteinase-K α-syn aggregates. Interestingly, the same animals showed also non-motor abnormalities including early impaired odour discrimination and novelty-seeking interest (Nuber et al., 2013).

An alternative approach (Peelaerts et al., 2015) might be the injection of preformed recombinant α-syn fibrils or brain extracts rich in α-syn aggregates in transgenic mice overexpressing human A53T α-syn: some preliminary studies showed that this leads to a progressive synucleinopathy and it might be an useful tool to better understand propagation and diffusion of α-syn (Visanji et al., 2016).

Table 5: Schematic classification of genetic rodent models of synucleinopathy with achieved PD traditional hallmarks

References	Mutation	Promoter/ Technology	Loss of fibers (ST)	Loss of DA neurons (SN)	α-syn inclusions	Motor alterations
(Giasson et al., 2002)	*A53T*	*mPrP*	*no*	*no*	*yes*	*yes*
(Lin et al., 2012)	*A53T*	*Pitx3*	*yes*	*yes*	*yes (only in axons)*	*yes*
(Masliah et al., 2000)	*WT*	*PDGF-β*	*yes*	*no*	*yes*	*yes*
(Ono et al., 2009), (Rockenstein et al., 2002)	*Various*	*Thy-1*	*yes*	*yes (very moderate)*	*yes*	*yes*
(Janezic et al., 2013)	*WT*	*BAC*	*yes*	*yes*	*yes*	*yes*
(Nuber et al., 2013)	*WT*	*BAC*	*yes*	*yes*	*yes*	*yes*

2.3.2 LRRK2

As for α-syn transgenic models, also LRRK2-based transgenic models of PD are not very robust, in particular if compared with other species as *Drosophilia* and *C. elegans* (Dawson et al., 2010). Different types of transgenic mice and rats based on WT or muted form of LRRK2 are available: unfortunately in such models it is very had to identify a significant loss of dopaminergic neurons in the SN (Creed and Goldberg, 2018). In many models behavioural changes are visible, but are hard to be correlated with real cellular loss or altered neuronal structure (if not some small and partial impairment in the striatal DA release) (Hinkle et al., 2012; Melrose et al., 2010; Sloan et al., 2016; Walker et al., 2014). In few study minor but significant histopathological features of the disease were seen, together will the all set of cognitive and behaviour symptoms (Li et al., 2009). Partial neurodegeneration was achieved overexpressing LRRK2 mutated form (G2019S), leading to a progressive time-dependant loss of DA neurons in the SNpc, but without abnormal locomotor activity (Chen et al., 2012; Ramonet et al., 2011).

2.4 Viral vector-based models

As previously described, difficulties in using transgenic models to mimic PD include high variability between animals and used approached, lack of real progressive development of the disease, as well as low or inexistent loss of DA neurons in the SNpc.

An approach to overcome such problems is the use of viral vector-based models of PD.

Viral vectors are able to deliver various types of cargo (genes, DNA, RNAs, *micro*RNAs, etc) in different species and strains of animals (rodents to primates), during all lifespan of animals (embryonic stages to adulthood), targeting specifically one or more area of interest. In addition, the degree of infection can be modulated basing on the dose of injected viral particles, leading to a controlled expression (or overexpression) of the transgene (Van der Perren et al., 2014).

In the last 10 years more and more publications included the use of different viral vectors to deliver α-syn and/or LRRK2, both mutated or WT form, *in vivo;* various protocols of injection, types of viral vectors, serotypes, viral titres, promoters and transgene were used. Interestingly AAV and LV vectors, even if with a limited cargo capacity, are the ones majorly used; their proprieties include a preference in targeting neurons (for AAV using specific neuronal serotype), together with a low or very low host's immune response and a relatively fast and stable expression of the transgene.

Very extensive reviews on the use of viral vector to generate animals models of PD may be found in these articles: (Albert et al., 2017; Creed and Goldberg, 2018; Fischer et al., 2016; Ulusoy et al., 2010; Van der Perren et al., 2014; Visanji et al., 2016).

Table 6: The mostly used viral vectors for modelling Parkinson's disease in rodents

Modified from (Fischer et al., 2016; Papale et al., 2009; Van der Perren et al., 2014)

	Lentiviral vector	Adeno-associated viral vector	Adenoviral vector
Genome type	*ss RNA*	*ss DNA*	*ds DNA*
Envelope	*yes*	*no*	*no*
Promoter flexibility	*yes*	*yes*	*yes*
Cargo capacity (kb)	*7-7.5*	*4.5-5*	*30*
Onset of expression (days) *in vivo*	*7-14*	*7-14*	*7*
Integration	*yes*	*yes (but low)*	*no*
Stability of expression	*long*	*long*	*short*
Immune reaction	*low*	*medium*	*high*

3. Aim of the PhD thesis

Aim of the PhD project is to investigate the possibility to use a temperature-dependant *in-situ* polymerizing collagen-based hydrogel as a delivery system for the treatment of Parkinson's disease.

The organization of the PhD project can be described as two converging roads, representing development of PD relevant animal models mimicking specific aspects of the disease on one side, and characterization of a collagen-based hydrogel on the other. The long-term objectives, beyond the present work, are to test the efficacy/added value of the functionalized scaffold (with added factors or cells) in the most relevant animal model of PD.

Neurodegeneration and loss of dopaminergic neurons in the SNc are hallmarks of Parkinson's disease, and it is widely accepted that mutations in LRRK2 and α-syn proteins play a crucial role in the development and advancement of the disease (Cresto et al., 2018).

I contributed to develop a novel model of neurodegeneration of the SNc using an AAV coding for the kinase domain of the mutated LRRK2 ($LRRK2^{G2019S}$) (publication available in supplementary material). To investigate the slow neurodegenerative processes ongoing during the development of PD and to address the likely role of both LRRK2 and a-syn in the pathogenesis of the disease, we established a semi-progressive rat model based on overexpression of mutated α-syn ($\alpha\text{-syn}^{A53T}$) with the kinase domain of the mutated LRRK2 ($LRRK2^{G2019S}$) proteins via viral vector. Although this experimental model does not mimic a genetic situation in PD, it gave us the opportunity to investigate over time the degeneration of dopaminergic neurons of the SNpc, and how such cellular death could be linked with the tight interaction between LRRK2 and α-syn.

Another key player in the development of PD is neuroinflammation: different theories propose that uncontrolled and prolonged neuroinflammation might weaken dopaminergic neurons, leading to their death (Y. Lee et al., 2019). Still today it is unknown if prolonged inflammation leads to neurodegeneration, or if cellular death activates the immune system that increase neurodegeneration, in a vicious circle manner (Gelders et al., 2018).

To study the role of neuroinflammation as a cause (or a co-cause) of disease's development, we improved the well-known LPS model. This model of acute neuroinflammation, although does not fully resemble the pathological conditions (slow and progressive for around 30 years, with significant

loss of DA neurons) could be very useful to test therapeutics based on reduction of inflammation in the brain.

Collagen-based hydrogel can be simply tuned and modify to delivery various types of cargos, including cells, active molecules, pharmacological treatments; basing on its chemical and physical proprieties, hydrogels can be designed to deliver specific loads in a time dependant manner, following the polymer's degradation. In regenerative medicine, biopolymers are thought to play a crucial role in protecting transplanted cells from the host's immune response, increasing the graft survival and reducing the risk of graft rejection. In addition, hydrogels are able to provide a safe environment and nutrients to the transplanted cells during and post-surgery (Madl and Heilshorn, 2018). Due to the collagen's proprieties (natural endogenous protein highly expressed in the body), collagen-based hydrogels fulfil the biomaterials proprieties of being completely degraded and reabsorbed by the body in a non-toxic manner (Sekuła and Zuba-Surma, 2018).

Collagen-based biomaterials in the last years have been widely used for different clinical applications (Dinescu et al., 2019), and numerous clinical trials are currently ongoing to test their reliability in humans (https://clinicaltrials.gov/ct2/home - keyword: *collagen scaffold*).

The use of collagen hydrogels for neurodegenerative diseases, and in particular for Parkinson's disease, is not yet investigated.

A very active group in this field is the one directed by Eilis Dowd (National University of Galway) : this group routinely transplants collagen type I hydrogels loaded with cells and/or bioactive molecules (as growing factors) in PD animal models to restore the loss of dopaminergic cells (Moriarty et al., 2018a, 2017). Dowd's team results are extremely promising: cells encapsulated in the collagen-hydrogel enriched with GDNF and transplanted in 6-OHDA lesioned animals, are able to survive longer and healthier when compared with naked cells. In addition, the cells protected by the biomaterial are fully functional, are able to re-innervate the striatum, and do not trigger any inflammatory reaction.

While the current results are very encouraging, and support the view that collagen hydrogel could provide a major positive therapeutic benefit for the treatment of Parkinson's disease, not much is known about the polymer behaviour in the brain after transplantation, and optimisations have to be made for using it in a safe and well-controlled manner:

1. We developed a versatile tool to control the polymerization process, a small automated cooling system connected to the needles used for stereotaxic brain injection of the crosslinker/collagen mixture, allowing to produce polymerization only *in-situ* in the brain, without risks of clog formation in the injection apparatus;
2. We examined whether injection and polymerization of the collagen-based hydrogel into the brain is not deleterious for the host brain. For this we studied different aspects of the scaffold, including its degradation time and the brain immune response to the scaffold;
3. In parallel, with the idea to translate its use in humans in the next future, we decided to use MRI as a non-invasive tool to detect the hydrogel, to evaluate any possible post-implantation side effect, and to follow its degradation over time. In addition, to study the immune response caused by the scaffold, we used diverse post-mortem histopathological techniques.

To sum-up, project's investigation might be divided in two main topics:

1. *Development of a relevant neurodegenerative animal model of PD and refinement of a LPS-derived neuroinflammatory model to test the proprieties of the collagen-based hydrogel*
2. *Development and characterization of collagen-based hydrogel in vitro and in vivo*

4. LPS-induced neuro-inflammatory model

In this section we refined the traditional LPS induced inflammatory rodent model of PD.

As previously described neuroinflammation is known to play a critical role in Parkinson's disease. LPS model has been widely studied and used to test therapeutics and to get a better insight into mechanism leading to possible neurodegeneration. While LPS derived neuroinflammation is relatively simple and fast to achieve, it has as a drawback a very high variability not only between animals and experiments, but also between laboratories and research teams.

To be able to fully understand the obtained data and to avoid biases derived by the model high variability, we had to quickly re-characterize the model in our hands.

4.1 Materials and Methods

4.1.1 Animals and Stereotactic injection

All surgical procedures were approved by the local ethics committee and registered with the French Research Ministry (committee #44, approval #12-100 and APAFIS#1372-2015080415269690v2).

Sprague-Dawley rats (7 weeks old) sourced by Janvier France were kept in the housing facility with a 12:12 hour light/dark cycle, 21° C regular temperature, 50% humidity and *ad libitum* access to food and water as for European Community (Directive 2010-63/EEC) and French (Code Rural R214/87-130) regulations.

All surgical procedures were completed with animals under 4% isoflurane anaesthesia, followed by a mixture of ketamine (75 mg/kg) and xylazine (5 mg/kg). Once deeply anesthetised, animals were placed in the stereotactic frame and a single, unilateral injection of either 2 µl of 5 µg/µl lipopolysaccharides (LPS, L2880, Sigma) or 2 µl of 1x Dubecco's Phosphate Buffer Saline (DPBS, Gibco) was done in the striatum. Injection coordinates were as following: Tooth bar: - 3.3mm; Anterio-Posterior (basing on bregma): + 0.5 mm; Lateral (basing on bregma): ± 3 mm; Ventral (basing on dura): - 4.3 mm. Injection procedures were achieved using an automatic pump (CMA-4004) with a speed of 0.5 µl/min, with a 34-gauge blunt-tipped needle connected by a polyethylene catheter to a 10 µl Hamilton syringe. At completed infusion the needle was left in place for 2 minutes and then was gently retracted.

4.1.2 Tissue processing

Animals were deeply anesthetized with isoflurane inhalation followed by lethal intraperitoneal injection of 1 ml/kg of sodium pentobarbital. Subsequently, they were transcardially perfused with 300 ml of 4% paraformaldehyde (PFA) in phosphate buffer at a rate of 30 ml/min.

After, brains were extracted and placed for 24 h in PFA at 4° C, and then subsequently transferred in 30 % sucrose for 48 hours. The brains were then cut using a freezing microtome (CM1900, Leica, Germany) with a thickness of 40 µm. Serials sections of the striatum and midbrain were stored in antifreeze solution (30% sucrose, 30% ethylene glycol in PBS) until use.

4.1.3 Immunohistological analysis and quantifications

Immunohistochemistry

Sections were removed from antifreeze solution washed in PBS for 30 minutes. After, slices were incubated at RT for 30 minutes with 1% hydrogen peroxide (H_2O_2) and then washed three times in PBS. Sections were then blocked at RT in dark for 30 minutes with 4.5% normal goat serum (NGS) in PBS-T (0.2% Triton X-100 in PBS). At the end of this step, without washing, slides were incubated overnight with primary antibody in 3% NGS in PBS-T at 4° C with gentle shaking (WAKO anti-IBA1 rabbit, 1:3000, Calbiochem anti-Vimentin mouse mAb V9 clone, 1:2000). The following day sections were removed from primary antibody, washed 3 times in PBS, and incubated for 1 hour at RT with specific secondary antibody (Vector Laboratories, Burlingame, 1:1000) in PBS-T. Sections were then washed three times in PBS and incubated for 1 hour at RT with ABC complex solution (Vectastatin, reagents A and B in a ration of 1:1) in PBS-T (1:250 with reagent A-B mix). Sections were washed again and incubated at RT with DAB solution (Vector) for 30s to 1 minute. After DAB incubation slices were properly washed in PBS and let dry overnight. The next day, sections were rehydrated in consecutive ethanol baths (50%, 70%, 96%, and absolute) and washed in Xylene before sealing with Eukitt mounting medium.

Acquisition was carried out digitalising slides using Zeiss Axioscan.Z1 at a magnification of 10x and 20x.

Immunofluorescence

Protocol is similar to the one used in immunohistochemistry; briefly sections were removed from antifreeze solution and washed 30 mins in PBS. Sections were then blocked at RT in dark for 30 minutes with 4.5% normal goat serum (NGS) in PBS-T (0.2% Triton X-100 in PBS). At the end of this step, without washing, slides were incubated overnight with primary antibody in 3% NGS in PBS-T at 4° C with gentle shaking (DAKO Polyclonal Rabbit Anti-Glial Fibrillary Acidic Protein – ref: 0334, 1:10000). The following day sections were removed from primary antibody, washed 3 times in PBS, and incubated for 1 hour at RT with specific secondary antibody (Invitrogen Alexa Fluor 594-labeled goat anti-rabbit IgG, 1:1000) in PBS-T. Sections were then washed in PBS, stained for DAPI (5 minutes at RT), washed again in PBS and mounted in a fluorescent mounting medium.

Acquisition was carried out using a laser confocal microscopy (SP8, Leica, Germany), or sections were digitalised using Zeiss Axioscan.Z1 at a magnification of 10x and 20x.

Quantifications

Stained sections were digitalised using Zeiss Axioscan.Z1 using its x10 or x20 objective.

The occupied area by IBA1+ cells was evaluated using Fiji-ImageJ software: the striatal area of interest was delineated, a specific threshold was applied, and the occupied area was evaluated. Between 4 and 6 brain slices per animal were used.

For GFAP and Vimentin quantifications, sections were scanned and digitalized using a Zeiss Axioscan.Z1 at a magnification of 20x. Astrocytes staining intensity (measured as optical density after back-ground subtraction) was evaluated on four to six slides per rat using Fiji-ImageJ software.

4.1.4 Real time quantitative PCR

Transcriptomic analysis was performed on the rat striatum, as it was the site of LPS injection.

Previously cut striatal sections were removed from antifreeze solution and washed in PBS for 30 minutes. Striatum was dissected under a binocular microscope using a surgical scalpel blade. mRNA extraction is carried out using E.Z.N.A. FFPE RNA Kit (Omega Bio-Tek, Georgia, USA) – a specific RNA kit for PFA-fixed material. Total RNA was treated with Dnase RQ1 kit and reverse transcriptase achieved using SuperScript 390 II reverse transcriptase kit (VILO, Life Technologies). All the procedures were done according to vendors' instructions. Different genes of interest were selected and checked in SYBR

Green based real time quantitative (RT-qPCR) with the *Taq* Platinum enzyme (SYBR Green qPCR kit, Invitrogen) using an Eppendorf Master cycler Realplex system. Various primers (list and sequence in table 6, additional material) were designed and tested before experiments.

Data were analysed using Biorad CFX-Maestro software, with Hypoxanthine-guanine phosphoribosyltransferase (HPRT) and Cyclophilin H (cyclo or PPIH) as housekeeping genes, and confirmed by independent manual analysis. Results are showed as relative normalized expression.

4.1.5 Statistical analysis

Statistical analysis was done by two-tailed, one-way analysis of variance (ANOVA) followed by Bonferroni post hoc correction for multiple comparisons (for parametric data) or Kruskal-Wallis test followed by Dunn's test of multiple comparisons (for non-parametric data) using GraphPad Prism software (GraphPad Software, San Diego, California, USA) and/or Statistica software (Statsoft Inc., Tulsa, Oklahoma, USA). Mann-Whitney U test was performed for pairwise comparisons in non-parametric data.

Level of significance annotations are as following: * $p<0.05$; ** $p<0.01$; *** $p<0.001$.

4.2 Results and Discussion

To evaluate the level of neuroinflammation following LPS striatal injection biochemical and histological methods were used.

Striatal sections were stained with different markers related to neuroinflammation and immune response as IBA1 (ionized calcium binding adaptor molecule 1), GFAP (glial fibrillar acidic protein), and Vim (vimentin).

Knowing that during inflammatory situations microglial cells undergo an increase in cellular size and cellular number (Sasaki, 2017), we evaluated the area occupied by IBA1 + cells.

Our result showed a clear and significant increase in the area by IBA1+ cells in the LPS injected hemisphere when compared with the same cells in the PBS injected side, or with the non-injected animals **(Fig. 11 A, B)**.

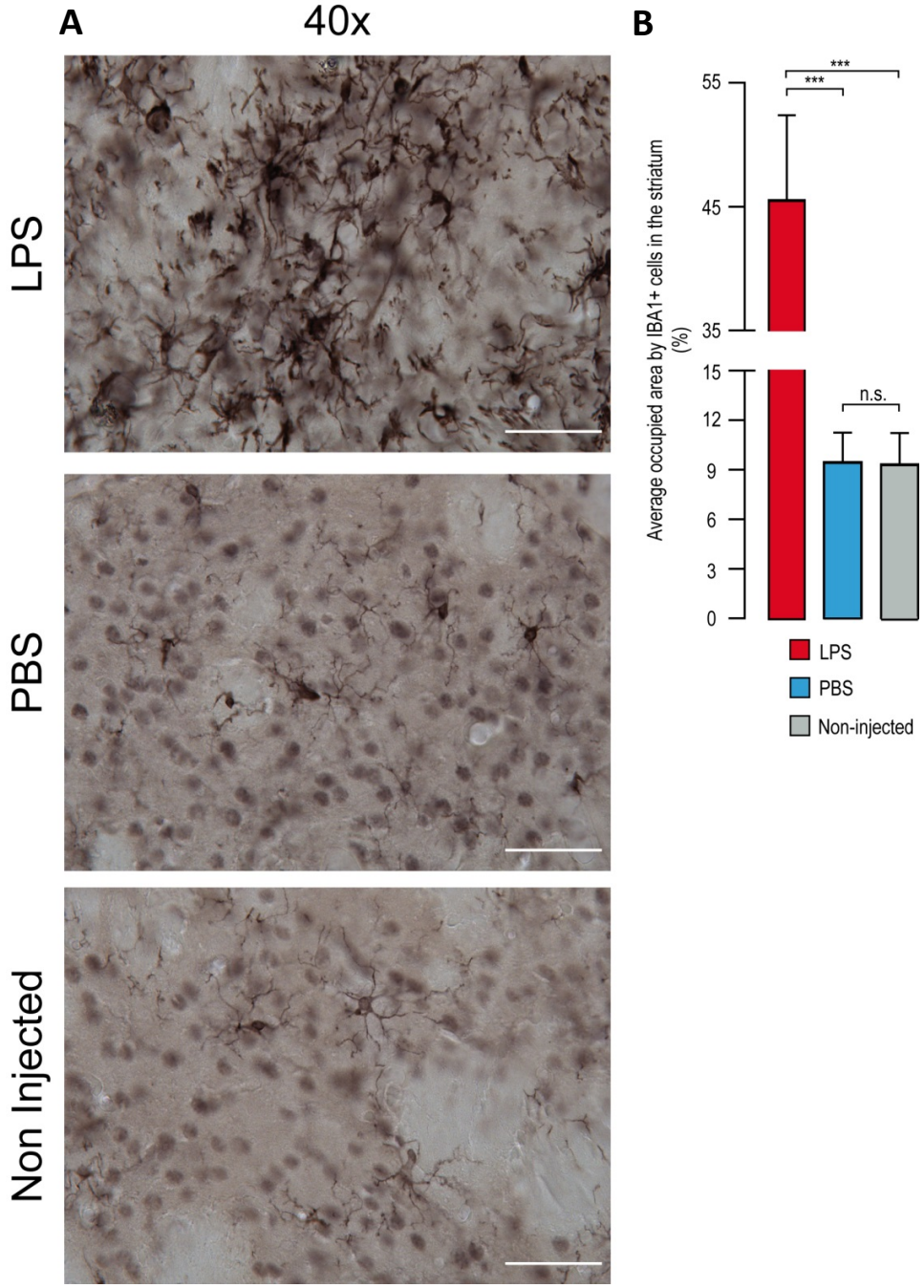

Figure 11: Striatal IBA1 histological evaluation of the effect of intrastriatal injection of LPS, PBS or no injection (sham) at 1-week timepoint

(A) Representative photomicrographs showing striatal IBA1 staining in the striatum of the animals of the three experimental groups. **(B)** Striatal area occupied by IBA1+ cells were evaluated in relation to the striatal area and expressed as percentage.

One-way ANOVA was used for between-group comparison and Bonferroni post hoc correction for multiple comparisons was applied. *n*=6/group. Scale bar: 50 µm

The strong inflammatory response produced by LPS injection was also confirmed by astrocytes evaluation. Astrocytes are the most numerous cellular population in the CNS and they play an important role in brain homeostasis, in controlling adaptive and innate immune responses in the CNS (Colombo and Farina, 2016) and different housekeeping functions of the neuron-glia system (Liu et al., 2014). Astrocytes play also a crucial role during CNS injury; in fact, in case of injury or trauma, they are activated and quickly release chemokines and cytokines that deal with the primary emergency situation. In addition, astrocytes also undergo molecular and morphological changes (named activated astrogliosis) and, in the most extreme cases, create scar formation to isolate and enclose the lesioned area (Colombo and Farina, 2016; Sofroniew, 2009), avoiding an uncontrolled spreading of damage to the surrounding healthy tissue (Liu et al., 2014).

Expression of GFAP and Vimentin proteins *in vivo* and *in vitro* are routinely used to identify respectively mature astrocytes and activated astrocytes (Pekny and Nilsson, 2005). Generally, in normal adult brains GFAP is the main expressed protein in astrocytes, while only low levels of vimentin are detected; a strong upregulation of GFAP and vimentin are considered an hallmark of astrogliosis and a sign of CNS pathologies (Colombo and Farina, 2016; Pekny and Nilsson, 2005).

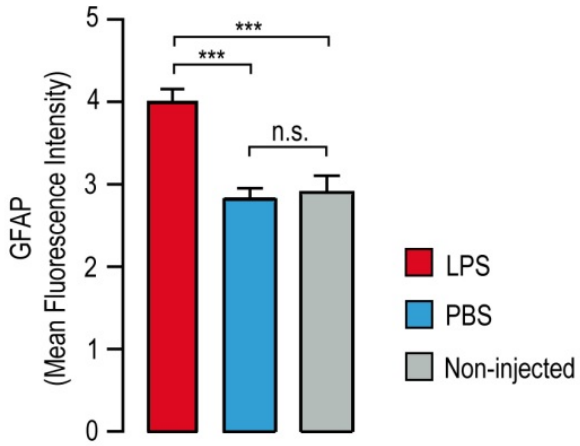

Figure 12: Striatal GFAP histological evaluation of the effect of intrastriatal injection of LPS, PBS or no injection (sham) at 1-week timepoint

One-way ANOVA was used for between-group comparison and Bonferroni post hoc correction for multiple comparisons was applied. *n*=6/group.

Our results showed a significant increase of GFAP positive cells 7 days post LPS injection when compared both with the PBS and non-injected groups **(Fig. 12, Fig. 13)**. Generally, recruitment of GFAP positive astrocytes in rats begins 12 hours after injury, surrounding the lesioned area 24 hours the injury and reaching its peak at 7 days (Lee et al., 2015).

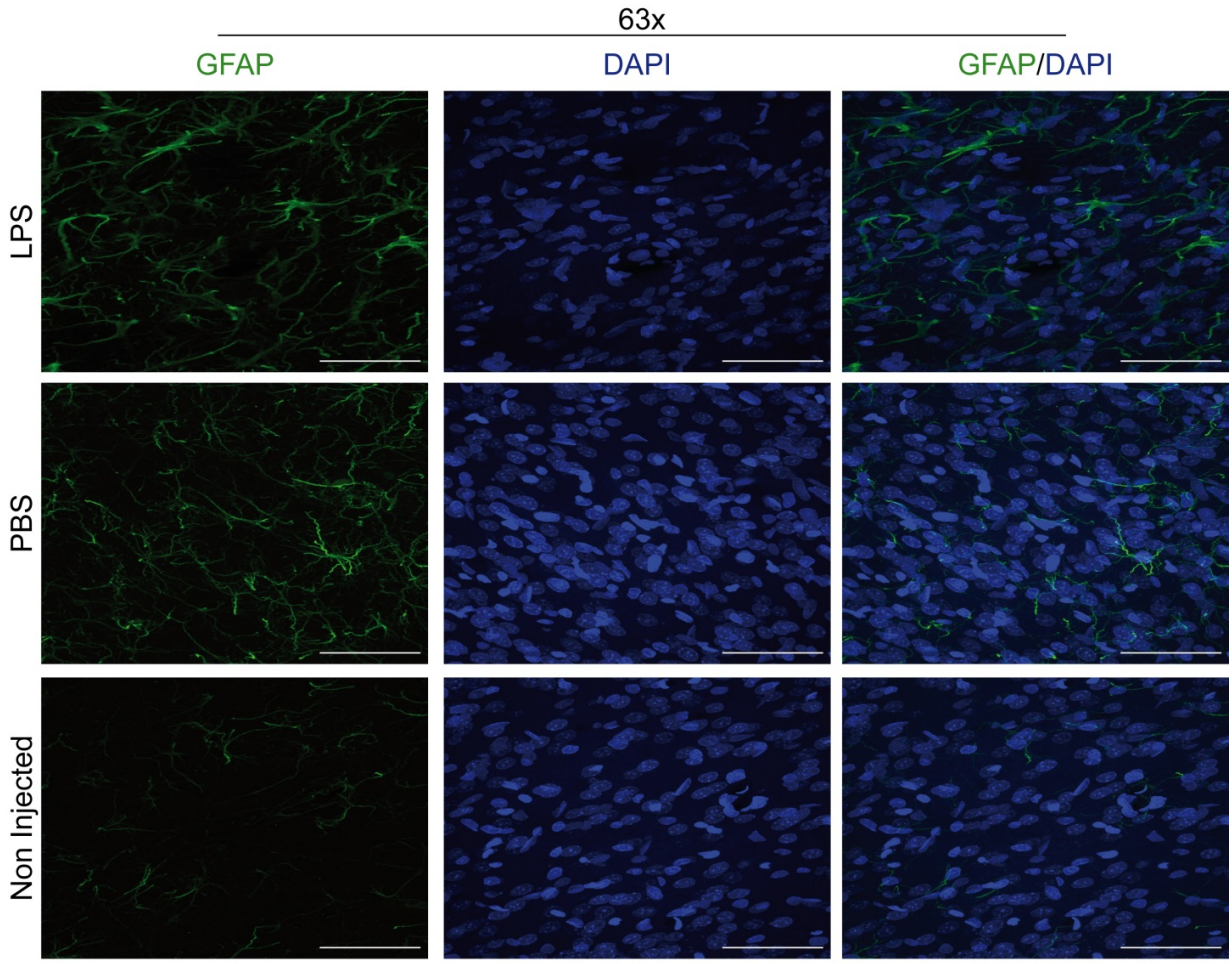

Figure 13: Representative striatal GFAP expression of the three evaluated groups

Confocal Z-stack pictures were taken in different points of the striatum and in the close area of the injection point.

Scale bar: 50 µm

In our study, also vimentin levels in the LPS injected group resulted to be increased when compared with the controls (PBS and non-injected animals) **(Fig. 14 A,B)**; in accordance with that published (Wang et al., 2004), reactive astrocytes were mainly distributed around the site of lesion, and were rarely found in other parts of the striatum. This results were expected as vimentin is generally linked to cellular motility, helping reactive astrocytes to migrate at the site of lesion and subsequently create the

scar (Lee et al., 2015). Vimentin is generally detected in the injured rats' brain at early stages (during the first 24 hours) and slowly decrease between 7 and 14 days post lesion, after migration to the lesioned site (Lee et al., 2015).

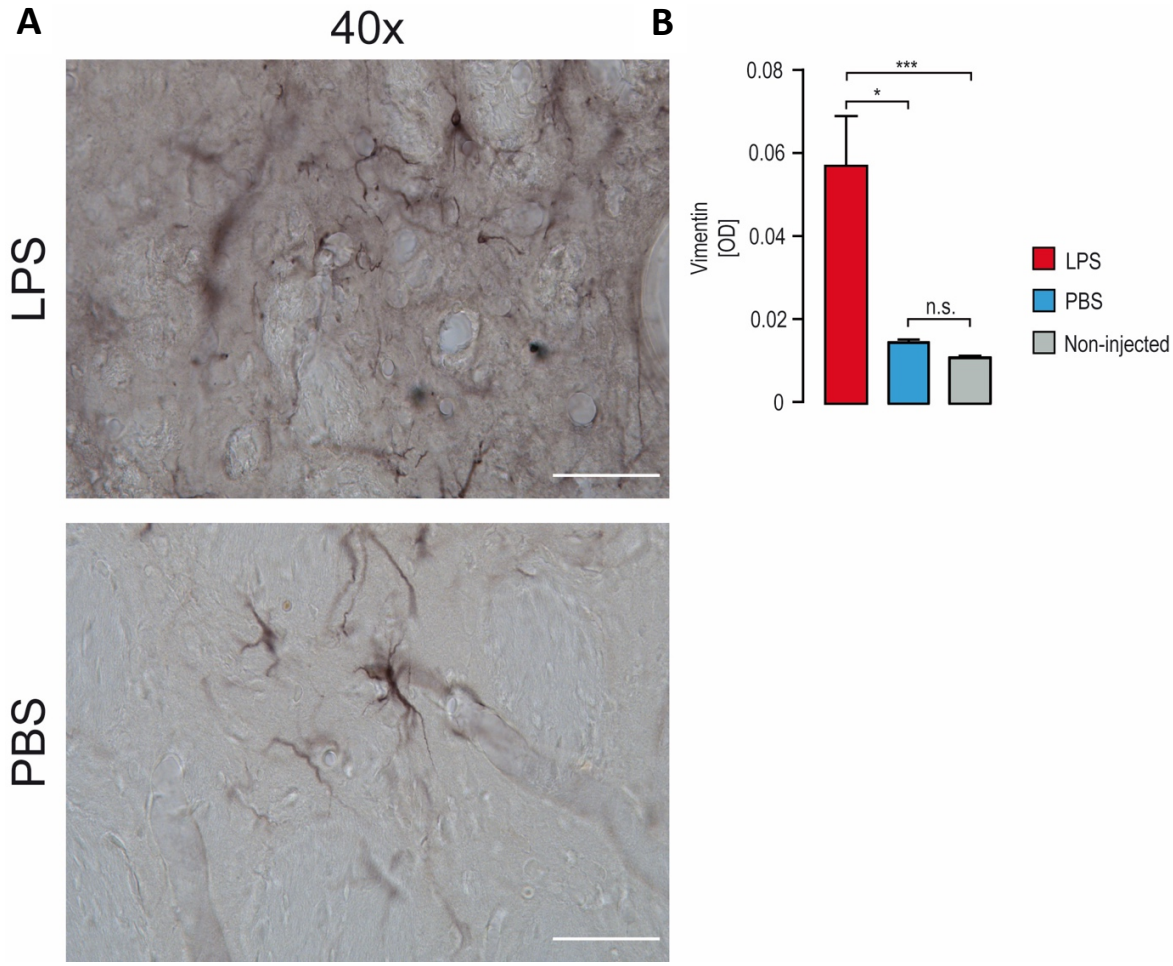

Figure 14: Vimentin histological evaluation of the effect of in intrastriatal injection of LPS, PBS or no injection (sham) at 1-week timepoint.

(A) Representative striatal Vimentin staining for section of the evaluated groups. (B) Striatal optical density for the three evaluated groups.

Kruskal-Wallis test was used for between-group comparison and Dunn's test of multiple comparisons was applied.

n=6/group. Scale bar: 50 µm

Using different inflammation-related markers (IBA1, GFAP and Vim) we proved that striatal injection of LPS in rats leads to the development of a significant inflammatory condition within 1 week. Our results also confirm the hypothesis that neuroinflammation is an event that involves different types of players synergistically working together.

Once confirmed that neuroinflammation was present and detectable at the cellular level, we wanted to investigate changes at the mRNA levels: to do so, we checked selected markers of neuroinflammation using RT-qPCR **(Fig. 15)**.

C1qa and *C1* (important components of the complement system), *CCL2* (chemokine recruiting cells on the site of insult), *Iba1* (a marker for microglia activation), *IL1b* (important mediator of inflammatory response controlling different cellular processes), *ITGAM* (marker of activated macrophages and phagocytosis), *NeuN* (specific marker of neurons expressed in all striatal neurons), and *TNFα* (proinflammatory cytokine produced by macrophages) mRNAs were analysed.

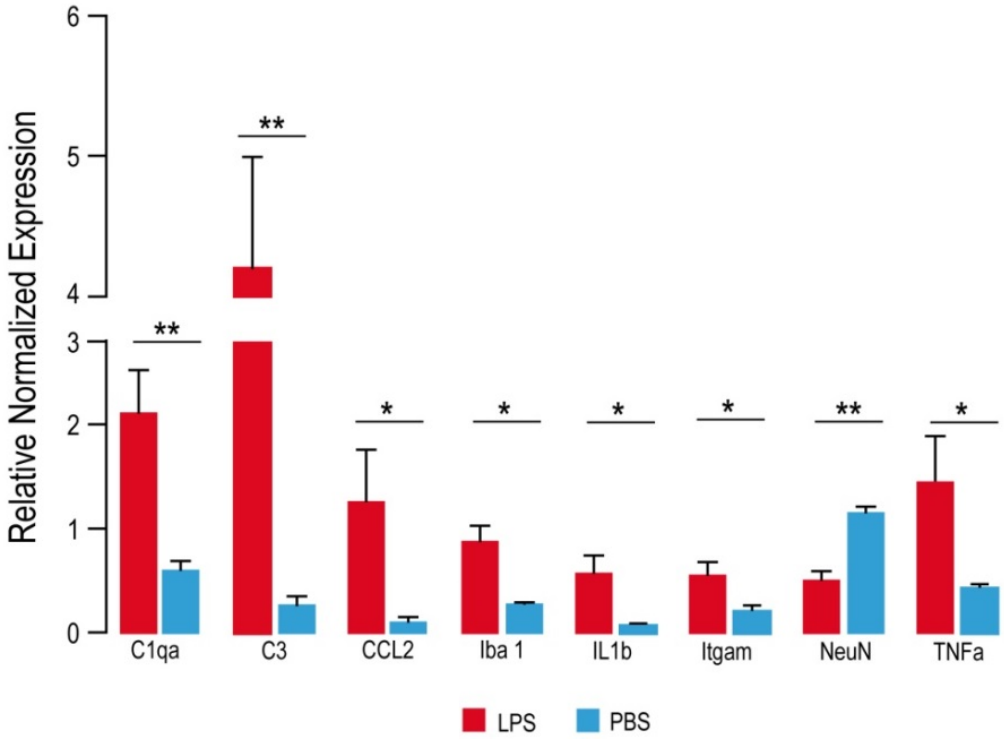

Figure 15: Striatal mRNA expression of different genes related to the inflammatory response

Mann-Whitney U test was used for between-group comparison.

n=6/group.

Results showed an upregulation of all the genes related to neuroinflammation, suggesting the presence of a relatively strong inflammation in the site of injection (striatum), with a consequent release of various factors trying to face the effect of LPS-related immune response. Interestingly, reduction of *NeuN* in the LPS injected group may indicate a functional change of neurons when compared with the PBS group. Import to keep in mind, is that this reduction of NeuN does not always indicate a neuronal cell loss, but more a "suffering of cells" (Ünal-Çevik et al., 2004).

4.3 Conclusion

In this preliminary study we were able to re-characterize the neuroinflammatory model based on striatal LPS injection in rats. Our results showed that 1 week after intrastriatal injection of 10 µg of LPS, we were able to create an inflammatory condition confirmed by increased levels in the striatum of microglial cells, increased levels of adult astrocytes and proliferation of reactive astrocytes.

Also changes at the striatal mRNA levels were detected, showing an upregulation of the genes linked to neuroinflammation and inflammatory conditions.

Taken together these results confirm we obtained a simple, fast and reproducible protocol to generate LPS-derived neuroinflammation *in vivo*. Such model could be easily used to test different therapeutic approaches, and possibly obtain a better understanding of the role of neuroinflammation in the development of PD. In addition, the LPS-based inflammatory model could be used to test different anti-inflammatory molecules loaded in the collagen hydrogel, and their potential beneficial effect over time.

4.4 Supplementary material

Table 7: List of primers

Primers	*Forward*	*Reverse*
Cyclo	*ATGGCAAATGCTGGACCAAA*	*GCCTTCTTTCACCTTCCCAAA*
HPRT	*GGACCTCTCGAAGTGTTGGATAC*	*CCCTGAAGTGCTCATTATAGTCAAG*
RPL-13	*CTGAAGCCTACCAGAAAGTTTGC*	*GGTACTTCCACCCGACCTCAT*
CCL2	*CCAGCCCAGAAACCAGCCA*	*CAACAGGCCCAGAAGCGTGA*
IBA1	*CCAGCCTAAGACAACCAGCGTC*	*GCTGTATTTGGGATCATCGAGGAA*
IL1b	*CCTTGTCGAGAATGGGCAGT*	*GTCAGAGGCAGGGAGGGAA*
Itgam	*ACACCAAGGACAGGCTGCGAGA*	*TTTCATCAAAGAAGGCTCGGACAAC*
NeuN	*CAACTCCACCCTTCCGACCC*	*TCCCGAATTGCCCGAACAT*
TNF-a	*AAATGGGCTCCCTCTCATCAGTTC*	*TCTGCTTGGTGGTTTGCTACGAC*
C1qa	*Biorad primer, ref. qRNoCED0052487*	*Biorad primer, ref. qRNoCED0052487*
C3	*Biorad primer, ref. qRNoCED0001280*	*Biorad primer, ref. qRNoCED0001280*

5. Neurodegenerative models of PD: LRRK2 and α-syn

5.1 Study 1: the role of C-terminal domain of LRRK2^{G2019S} in neurodegeneration

We focused our attention on the G2019S LRRK2 mutation, known to be the most prevalent PD mutation.

The mechanisms of how LRRK2 is toxic are still unknown; it is widely accepted that in presence of LRRK2 mutated form (G2019S), there is a gain of toxic function of the kinase domain that results toxic for the SNpc (West et al., 2005). The use of viral vectors to deliver mutated proteins and create PD-relevant animal models is an interesting and interesting alternative to transgenic mice models: in fact, although different transgenic models are available, they are unable to fully resemble all the pathological phenotypes of the disease. A model that could be interesting, unfortunately showed only a minor loss of DA neurons together with a long waiting time to achieve it (more than 12 months) (Ramonet et al., 2011); it is clear that the long experimental time, as well as the small neurodegeneration, do not make feasible any test of therapeutics.

The most appealing model has been obtained injecting LRRK2^{G2019S} in the mice striatum using a herpes simplex virus (HSV) with a retrograde transportation; in a short time (21 days) a great neurodegeneration is achieved (around 50%) (Lee et al., 2010). Even if results are promising, some additional aspects should be considered: difficulties in production and use of HSV are an issue, as well as the inflammatory response provoked by injection of this virus in the host system, the non-specificity of infection (it targets also astrocytes and oligodendrocytes), and the not always great efficacy of the HSV retrograde transport. Similar trends are found when using adenoviral vectors encoding for full length LRRK2 (Dusonchet et al., 2011).

Considering issues and necessities previously described, and aiming to study the real neuronal toxicity of the disease, we investigated the role of mutated form of LRRK2 (G2019S) in the neurons of the SNpc. As increased kinase activity of LRRK2^{G2019S} is known to have neurotoxic effects, we wanted to investigate if this specific kinase domain was sufficient to produce neurodegeneration, or if the full-length protein was absolutely required.

After generating a construct that corresponds to the C-terminal domain of the G2019S LRRK2 (ΔLRRK2^{G2019S}) and WT LRRK2 (ΔLRRK2^{WT}), we overexpressed it in the rats SNpc using either LVs or AAVs and evaluated neurodegeneration at different time-points.

Injection of LV-ΔLRRK2^{G2019S} and LV-ΔLRRK2^{WT} in the SNpc of adult rats did not show any detectable loss of dopaminergic neurons 6 months post injection.

To explore the possibility that higher levels of ΔLRRK2^{G2019S} could trigger neurodegeneration, we used AAV2/9 to deliver both ΔLRRK2^{G2019S} and ΔLRRK2^{WT} in the SNpc of adult rats. Our results showed that, 6 months post injection, a significant loss of TH+ and VMAT+ DA neurons was detected in the AAV-ΔLRRK2^{G2019S} group when compared with the ΔLRRK2^{WT} group.

Results are intriguing and they suggest that the mutated C-terminal part of LRRK2 is sufficient, when overexpressed, to induce neurodegeneration of DA neurons.

As co-author of the study 1, I have performed stereological count and quantifications of TH and VMAT cellular marker to evaluate neurodegeneration in the animals injected in the SNpc with AAV2/9-ΔLRRK2^{G2019S} and AAv2/9-ΔLRRK2^{WT} (Fig. 10). In addition, I performed photomicrographs of the SNc HA-tagged ΔLRRK2 neurons for the rats injected with AAV2/9-ΔLRRK2^{G2019S} and AAv2/9-ΔLRRK2^{WT} at 25 weeks time-point (Fig. 9).

The full study can be found in supplementary material *(Chapter 8.2, pages 146-171).*

5.2 Study 2: deleterious interaction between α-syn^{A53T} and C-terminal domain of LRRK2^{G2019S} in neurodegeneration

The idea of a tight and direct interaction between LRRK2 and α-syn gained more and more attention in the last years: what was before proposed as a possible mechanism of action, is today widely accepted by the scientific community (Cresto et al., 2018; Daher, 2017; Liu et al., 2012), although underlying mechanisms are unknown.

Such functional and physical interaction has been confirmed by numerous histological studies done on human tissues, where LRRK2 was identified to co-localise in Lewy's bodies (Perry et al., 2008; Vitte et al., 2010; Zimprich et al., 2004).

Interestingly, a study done by Alegre-Abarrategui and colleagues showed that mutated LRRK2 localises with granular α-syn deposits (considered to represent the early stages of the aggregation) and neurites

in PD patients (Alegre-Abarrategui et al., 2008). In addition, a study done by Vitte and colleagues showed that, in the locus coeruleus of idiopathic PD patients, 11% of Lewy's bodies co-localise with LRRK2, while, in the SN, this number reaches 24%. Surprisingly, the same study done in patients carrying the G2019S mutation of LRRK2 revealed a 50% co-localisation in both areas (Vitte et al., 2010).
Various studies tried to address the same question *in vivo*, producing contrasting results; in some cases, deletion or overexpression of G2019S LRRK2 did not change the negative phenotype of α-syn^{A53T} (Daher et al., 2012). Another study, in contrast, showed that overexpression of LRRK2 alone was not enough to produce neurodegeneration, but it accelerated neurodegeneration in α-syn^{A53T} transgenic mice at least in regions unrelated to SNpc; in addition, LRRK2 promoted aggregation and somatic accumulation of α-syn (Lin et al., 2009). Another report showed that expression of G2019S LRRK2 increases endogenous α-syn inclusions' formation; these results were confirmed both *in vitro* cultured neurons and *in vivo* SNpc rat dopaminergic neurons (Volpicelli-Daley et al., 2016).
In our first study we showed that the C-terminal part of the G2019S mutated LRRK2 preserves similar biochemical proprieties as the full length, and that its overexpression via AAV2/9 *in vivo* is able to produce a small but significant loss of DA neurons in SNpc at 25 weeks.
Basing on the results obtained in our first work, and trying to address the numerous unanswered questions, we investigated, in an *in vivo* PD relevant environment, whether the C-terminal part of LRRK2^{G2019S} is able to increase the toxicity induced by α-synuclein mutated form (A53T).
To do so, we generated different C-terminal LRRK2 fragments (ΔLRRK2): the first one has no mutations (ΔLRRK2^{WT}), the second one harbours the G2019S mutated kinase domain (ΔLRRK2^{G2019S}), and the last one harbours the G2019S mutation as well as the kinase inactivating mutation D1994A (ΔLRRK2$^{G2019S/D1994A}$). ΔLRRK2^{WT}, ΔLRRK2^{G2019S}, ΔLRRK2$^{G2019S/D1994A}$ or PBS were injected in the SNpc of adult rats using AAV2/6; our results did not show any type of SNpc DA cellular loss at 15 weeks post injection.
We then injected α-syn^{A53T} using AAV2/6 in the SNpc of adult rats: evaluation done at 12 and 15 weeks post-surgery showed significant loss of TH+ cells (around 30%) in the SNpc.
At this point, we wanted to evaluate the toxic effect of AAV-α-syn^{A53T} with or without AAV-ΔLRRK2^{G2019S}: to do so, we co-injected in the SNpc of adult rats AAV-α-syn^{A53T} together with AAV-GFP (as a viral load control) or AAV- ΔLRRK2^{G2019S}. Our data showed that at 15 weeks post injection, α-

syn^{A53T} produced a significant loss of TH+ cells in the SNpc; this loss was also higher than the one produced by AAV-GFP alone. At the same time, a greater and significant loss was detected in the SNpc of animals injected with AAV-α-syn^{A53T} and AAV- ΔLRRK2^{G2019S}.

To address the question whether the toxicity of AAV-α-syn^{A53T} is directly linked with the LRRK2^{G2019S} kinase activity, we co-injected in the SNpc of adult rats AAV-α-syn^{A53T} with AAV-ΔLRRK2^{G2019S} or AAV-ΔLRRK2$^{G2019S/D1994A}$. Our results showed that, at 6 weeks time-point, the SNpc was almost totally infected by the AAVs, and that around 70% of the neurons expressed both α-syn^{A53T} and ΔLRRK2 (both G2019S or G2019S/D1994A). Stereological analysis of TH+ cells in the SNpc showed that α-syn^{A53T} produced higher toxicity and consequent cellular death in presence of ΔLRRK2^{G2019S} than with ΔLRRK2$^{G2019S/D1994A}$.

These results taken together suggest that there is a very tight interaction between LRRK2 and α-syn, and that mutated LRRK2 could facilitate and increase α-syn toxicity in the DA neurons of the SNpc.

As co-author of the study 2, even if I joined in the middle of the study, I have been involved in different activities and discussions. For example, I performed immunohistochemistry, stereological counting and related quantification for the TH marker in the SNc of 15 and 6 weeks animals co-injected with α-synA53T and different forms ΔLRRK2 (Fig. 3A, 7 A). In addition, I also performed immunofluorescent staining, image quantification and analysis for microglial cells (IBA1) both in the striatum and substantia nigra of animals co-injected at 6 weeks with α-synA53T and different forms ΔLRRK2 (Supplementary Fig. 2).

The full study can be found in supplementary material *(Chapter 8.3, pages 172-190).*

5.2.1 Additional studies on the neurotoxic interaction between α-syn^{A53T} and C-terminal domain of LRRK2^{G2019S}

Basing on the data obtained in the Study 2, we thought that a faster model, with a dopaminergic loss within 8 weeks, could be interesting for the PD field.

In a preliminary set of experiments I have been able to show that, doubling the viral dose of AAV-α-syn^{A53T} and injecting it in two points that correspond to the beginning and end of SNpc (+3.4 mm and +2.4 mm anterior to the interaural zero and ±2.0 mm lateral to bregma, at a depth of -7.8 mm relative to the skull, with the tooth bar set at -3.3 mm), we could achieve, in a 8 weeks time-point, a loss of TH+ cells quantified via stereological counting of ±15% when compared with the non-injected group **(Fig. 16 A)**. In addition to neuronal loss, we detected a major motor impairment of ±35%, evaluated with the

cylinder test when compared to the non-injected group **(Fig. 16 B)**. In this study we also found (data not shown) reduced dopaminergic terminals in the striatum, assessed by PET with [^{18}F]-LBT9994 (LBT), a radio-ligand for dopamine transporter (DAT).

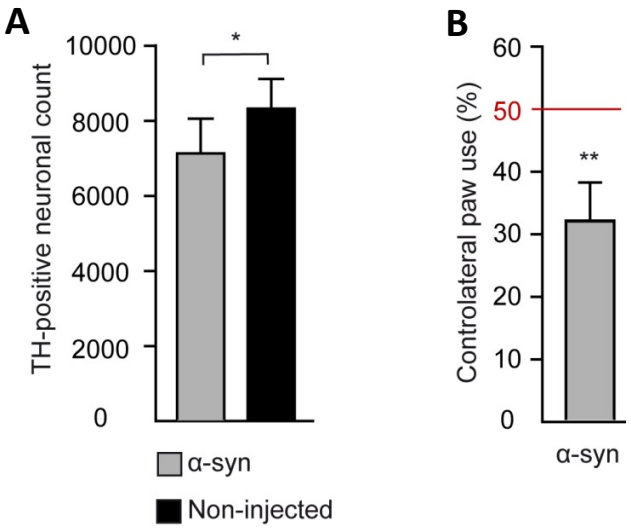

Figure 16: TH immunohistochemistry and cylinder behavioral test of rats injected with a double dose of AAV-A53T in the two sites of SNpc at 8 weeks time-point.

A: The number of TH+ cells was measured by stereology in the whole SNpc.

B: Number of touches with the right and left paw were evaluated using the cylinder test. Results are expressed as percentage of use of the contralateral paw compared to the total touches of the cylinder walls. 50% of contralateral paw use corresponds to an equal use of the paws, meaning no behavioral deficits.

Paired Student t-test was used for comparison between the injected and non-injected hemisphere of each animal.

n=7/group.

Once we proved that double dose of AAV-α-syn^{A53T} injected in two sites of the SNpc leads to a faster dopaminergic loss, we wanted to study the neurotoxic interaction with the C-terminal domain of mutated LRRK2's forms.

To do so, we mixed the setup of our latest preliminary study with the experimental design used in the Study 2: doubled dose of AAV-α-syn^{A53T} was co-injected with the previous used dose of AAV-ΔLRRK2^{G2019S} or AAV-ΔLRRK2$^{G2019S/D1994A}$. As previously described, to directly target the whole SNpc and facilitate a homogenous spreading and transduction of the viral vectors, we targeted two points that correspond the beginning and end of the SNpc (+3.4 mm and +2.4 mm anterior to the interaural zero

and ±2.0 mm lateral to bregma, at a depth of -7.8 mm relative to the skull, with the tooth bar set at -3.3 mm).

Our results **(Fig. 17)** were extremely interesting: even if higher dose of AAV-α-syn^{A53T} alone resulted to be neurotoxic and were able to create a significant loss of DA neurons in the SNpc at 8 weeks, AAV-GFP, AAV-ΔLRRK2^{G2019S} or AAV-ΔLRRK2$^{G2019S/D1994A}$ had no impact on the resulting neuronal loss in the SNpc.

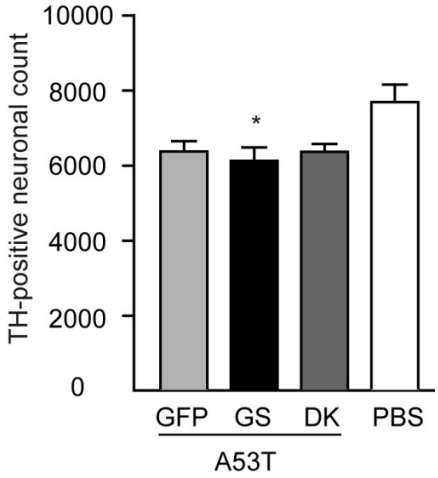

Figure 17: TH immunohistochemistry of rats injected with a double dose of AAV-A53T and AAV-GFP, AAV-ΔLRRK2^{G2019S} or AAV-ΔLRRK2$^{G2019S/D1994A}$ in the two sites of SNpc at 8 weeks time-point.

The number of TH+ cells was measured by stereology in the whole SNpc.

One-way ANOVA was used for between-group comparison and Bonferroni post hoc correction for multiple comparisons was applied.

n=12/group

These results suggest that, when neurodegeneration of DA neurons results from relatively low levels of α-syn^{A53T,} increased levels of the active C-terminal domain of LRRK2^{G2019S} can be sufficient to facilitate α-syn^{A53T} toxicity. In addition, the interaction between α-syn and LRRK2 seems to be dependent on the levels of mutant α-syn expression.

6. Development and characterization of an *in-situ* polymerizing collagen-based hydrogel *in vitro* and *in vivo*

In this study we elucidated the best methodological approach and protocols to test our collagen-based hydrogel both *in vivo* and *in vitro*. Collagen based hydrogels are still a novel approach and have not yet been fully characterized, especially in neurodegenerative diseases; for this reason, various preliminary experiments and methodological tuning were needed.

The most important aspect for a successful transplantation (organ, cells, or biomaterial) is the well tolerated effect of the transplant in the host organism and absent or extremely low immune response that prevents immunologic scaffold rejection. At the same time, it is crucial to have a reliable and simple method to detect the transplant and follow up its behaviour over time, as well as its regenerative effect. With the idea to translate the use of the collagen hydrogel into humans, we hypothesized that MRI would be the most appropriate method for a non-invasive and longitudinal follow up after intracerebral injection. Up to date, MRI has been used in the brain to detect cells grafting (Grealish et al., 2014), to enhance the pre-surgical targeting of the DBS electrodes and to evaluate their successful delivery (Duchin et al., 2018), as well as the possible side effects of the surgical procedures (e.g. oedema) (Borellini et al., 2019). In addition, MRI has been used to evaluate pathological processes as neuroinflammation (Albrecht et al., 2016), ischemic stroke (González, 2012), brain injuries (González, 2012) and myelin loss (Park et al., 2019). To our knowledge, the use of MRI for *in vivo* detection of an *in-situ* polymerizing collagen hydrogel have never been used before: that is the reason why we had to setup and develop a new methodological and experimental approach that could be clinically compatible and give us the possibility to discriminate and localize the polymer in the brain.

The question we here aimed at addressing included:

- Are we able to detect with MRI the collagen hydrogel scaffold after *in-situ* polymerization?
- Is MRI sensible enough to detect scaffold's physical changes?
- Are we able to follow-up collagen hydrogel scaffold degradation over time using MRI?
- Is collagen hydrogel safe enough to be used *in vivo*? Could we at least determine if the collagen hydrogel, even a clinical grade type, would lead to any significant/detectable immune reaction and rejection?

6.1 Materials and Methods

6.1.1 Collagen-based hydrogel preparation

Collagen-based hydrogel was prepared following Dowd's group directions (Moriarty et al., 2018a, 2017). All the materials are kept in ice during the preparation of hydrogel, as well as the tube containing the material to be injected.

Briefly for a preparation of 1 ml of hydrogel, 400 µl of bovine collagen type I (5mg/ml - Vorinia Biomaterials) were neutralized to PH 7 with 1M of NaOH, and then added to a 200 µl of 1x phosphate buffer saline (PBS) (Sigma-Aldrich) containing either 0.5 mg/ml, 1 mg/ml, 2 mg/ml, or 4 mg/ml of poly(ethylene glycol) ether tetrasuccinimidyl glutarate (4s- StarPEG) (Jumken-LAB, USA). As empty scaffolds were generated, 400 µl of 10x PBS (Sigma-Aldrich) were also added to the mix.

The particularity of this specific collagen hydrogel is the ability to be liquid at 4°C, and polymerize *in-situ* starting from 37°C.

6.1.2 Phantom preparation

A phantom based on 2% UltraPure Agarose (Invitrogen, Carlsbad, CA, USA) diluted in water was used for *in vitro* developments. Once well mixed, the solution was poured in 15 ml tubes and cooled down at room temperature.

For the crosslinking test, 5mg/ml of collagen was mixed with different crosslinker's concentrations (0.5, 1, 2 and 4 mg/ml). 1 ml of the prepared collagen hydrogel was then placed into a 1 ml plastic syringe and made it polyumerize at 37°C for 30 minutes before MRI detection.

For the volume test, 3, 4, 6 and 10 µl of 5 mg/ml of collagen were mixed with 4mg/ml of crosslinker and then injected into the cold agarose gel with a 0.5-10 µl pipette (Eppendorf Research Plus).

6.1.3 Animals and Stereotactic injection

All surgical procedures were approved by the local ethics committee and registered with the French Research Ministry (committee #44, approval #12-100 and APAFIS#1372-2015080415269690v2).

Sprague-Dawley rats (7 weeks old) sourced by Janvier France were kept in the housing facility with a 12:12 hour light/dark cycle, 21° C regular temperature, 50% humidity and *ad libitum* access to food and water as for European Community (Directive 2010-63/EEC) and French (Code Rural R214/87-130) regulations.

All surgical procedures were completed with animals under 4% isoflurane anaesthesia, followed by local injection of xylazine (5 mg/kg). Once deeply anesthetised, animals were placed in the stereotactic frame and a single injection in the striatum was done with the following coordinates: Tooth bar: -3.3mm; Anterio-Posterior (basing on bregma): + 0.5 mm; Lateral (basing on bregma): ± 3 mm; Ventral (basing on dura): - 4.3 mm.

For *in vivo* preliminary study to evaluate MRI's sensibility to detect collagen hydrogel 3 µl of prepared and ice cooled collagen-based hydrogel and 1x Dubecco's Phosphate Buffer Saline (DPBS, Gibco) were co-injected one in each hemisphere with an automatic pump (CMA-4004) at speed of 0.75 µl/min, with a 34-gauge blunt-tipped needle connected by a polyethylene catheter to a 10 µl Hamilton syringe. The catheter containing the liquid collagen-based hydrogel and connected to the Hamilton syringe was surrounded by another catheter with cold running water, as part of our in-house developed cooling system (described in details below).

Instead, for the characterization of the collagen scaffold and biocompatibility *in vivo*, 6 µl of either 1x Dubecco's Phosphate Buffer Saline (DPBS, Gibco) or prepared and ice cooled collagen-based hydrogel were injected with an automatic pump (CMA-4004) with a speed of 0.75 µl/min, with a 34-gauge blunt-tipped needle connected by a polyethylene catheter to a 10 µl Hamilton syringe. In this case the cooling system was always used.

At completed infusion the needle was left in place for 2 minutes and then was slowly retracted.

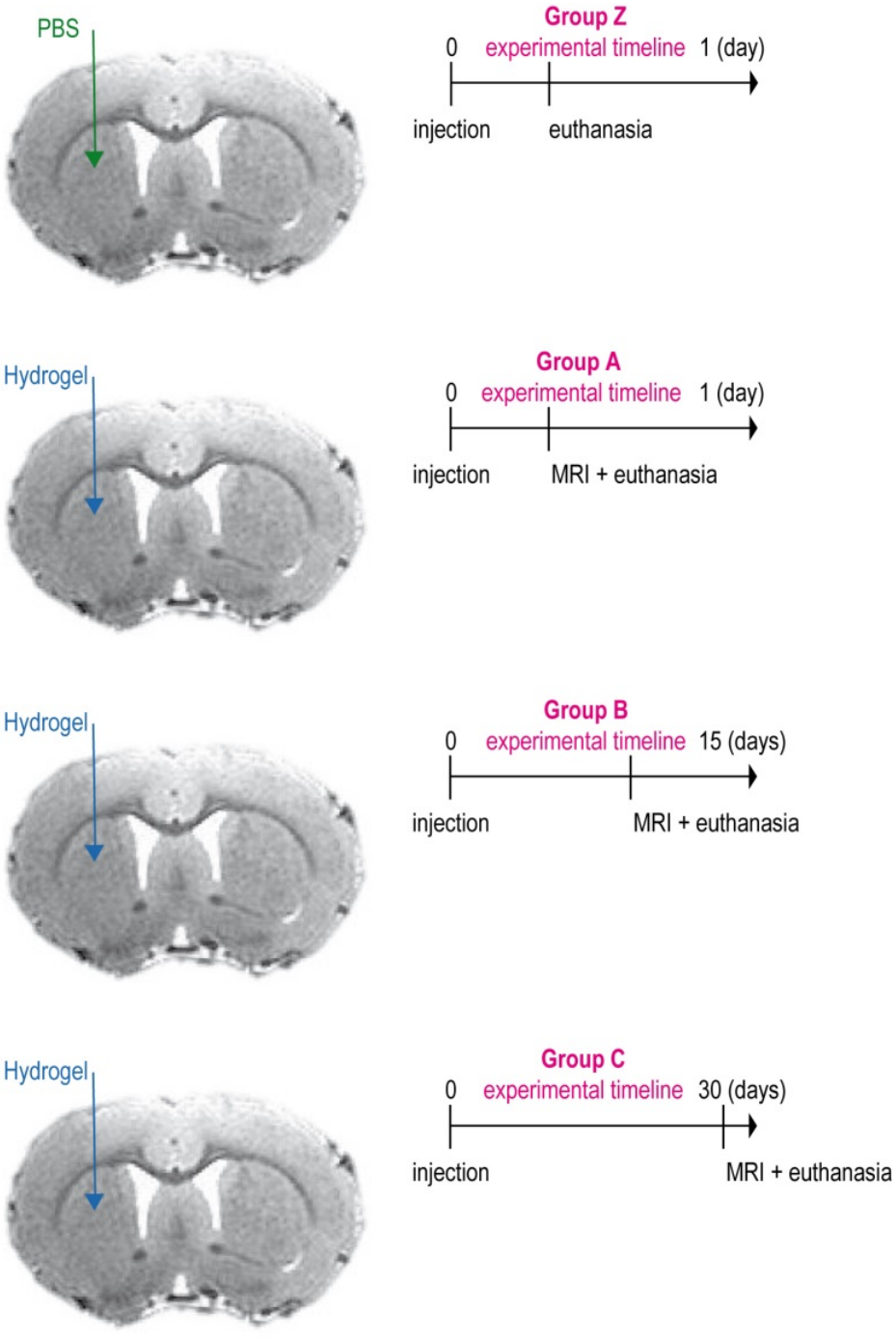

Figure 18: Visual representation of the experimental setup *in vivo*

Animals were randomly divided in 3 groups, representing the time-point of MRI analysis and euthanasia:

1) Group Z: PBS - 1 day post injection timepoint
2) Group A: Hydrogel - 1 day post injection timepoint
3) Group B: Hydrogel - 15 days post injection timepoint
4) Group C: Hydrogel - 30 days post injection timepoint

6.1.4 MRI acquisition and image processing

MRI acquisitions were performed on a horizontal 11.7 T Bruker scanner (Bruker, Ettlingen, Germany). In order to match animal's temperature, phantoms were previously incubated at 37° C for 30 minutes before MRI session. During acquisition, the temperature was continuously monitored and maintained at 37°C with regulated water flow using PC SAM software (Small Animal Instruments, Inc., Stony Brook, NY, USA).

For phantom acquisition, T_2-weighted images (also called anatomical) were acquired using Multi Slices Multi Echoes (MSME) sequence (TR = 10000 ms, TE ranging from 8 to 1000 ms, with a 8-ms step, 4 echoes, in-plane = 250 x 250 μm^2, 3 slices with thickness = 1 mm).

For the *in vivo* study, animals were scanned according to the group of interest; they were anesthetized using 3% isoflurane in a 1:1 gas mixture of air/O2 and positioned in a dedicated stereotaxic frame with mouth and ear bars to prevent from any movements during MRI acquisitions. Animal temperature was monitored with an endorectal probe and maintained at 37°C with regulated water flow and respiratory rate was continuously monitored using PC SAM software (Small Animal Instruments, Inc., Stony Brook, NY, USA) during scanning. The isoflurane level was adjusted around 1% to keep the respiratory rate in the range of 60 to 80 per minute.

T_2-weighted images were acquired using Multi Slices Multi Echoes (MSME) sequence (TR = 1000 ms, TE ranging from 8 to 1000 ms, with a 8-ms step, 8 echoes, in-plane =250 x 250 μm^2, 96 slices with thickness = 0.5 mm).

MRI based hydrogel and striatum volume quantification

Dicom files of the MRI anatomical scans were analysed using 3D Slicer software. The area of interest was delineated, segmented and total volume was calculated.

6.1.5 Tissue processing

Animals immediately after completing MRI scan and still under anaesthesia were quickly intraperitoneally injected with 1 ml/kg of sodium pentobarbital. Subsequently were transcardially perfused with 300 ml of 4% paraformaldehyde (PFA) in phosphate buffer at a rate of 30 ml/min.

After, brains were extracted and placed for 24 h in PFA at 4° C, and then subsequently transferred in 10 % sucrose for 48 hours. After cryoprotection, brains were snap frozen in 2-methylbutane cooled at around -35° C and then placed for long term storage at -80° C.

To acquire pictures of the whole brain during cutting (blockface images), a camera was placed in a stable position on the cryostat (CM3050 S, Leica, Germany) and serial images were taken every 120 µm. To have a better discrimination between brains and background, frozen brains were embedded in Shandon M-1 Embedding Matrix (Thermo Scientific) mixed with 1% FastGreen Dye (Sigma-Aldrich), and cut with coronal sections of 20 µm mounted directly on Superfrost Plus microscope slices (Vandenberghe et al., 2016).

Mounted sections were kept to dry at room temperature for 30 minutes before being placed at -20° C for long term storage.

6.1.6 Immunohistological analysis and quantification

Immunohistochemistry

Sections were removed from freezer and left at room temperature (RT) for 30 minutes. First, they were quickly washed in PBS to remove all traces of embedding medium.

For Masson's trichrome staining (green light variation – RAL Reactif) after washes in PBS, vendor protocol was followed. At the end of coloration, slices are rehydrated in consecutive ethanol baths (50%, 70%, 96%, absolute) and washed in Xylene before coverslip is sealed with Eukitt mounting medium.

For luxol fast blue staining (myelin), after PBS washes, slides were incubated for 1 minute in a 70% ethanol and then for 2 minutes in 96% ethanol. Slides were then incubated overnight in 0.1% luxol fast blue solution dissolved in 96% ethanol at 56° C. The following day, sections were removed from the luxol fast blue solution and washed in 96% ethanol for two minute and then in distilled water for another minute. Sections are then differentiated for 10 seconds in lithium carbonate (0.01% in distilled water) and then immerged in 70% ethanol for 25 seconds. Another round of differentiation is done:

slides are first incubated in distilled water for one minute, and then differentiated for 25 seconds in lithium carbonate with subsequent bath in 70% ethanol for one minute. Before proceeding with counterstaining with crasyl violet, slides are incubated in distilled water for 1 minute to remove all the traces of ethanol. After traditional crasyl violet protocol, slides are mounted using Eukitt mounting medium.

For traditional immunohistochemistry, after initial PBS bath slices are incubated at RT for 30 minutes with 1% hydrogen peroxide (H_2O_2) and then washed three times in PBS. Sections were then blocked at RT in dark for 30 minutes with 4.5% normal goat serum (NGS) in PBS-T (0.2% Triton X-100 in PBS). At the end of this step, without washing, slides were incubated overnight with primary antibody in 3% NGS in PBS-T at 4° C with gentle shaking (WAKO anti-IBA1 rabbit, 1:3000). The following day sections were removed from primary antibody, washed 3 times in PBS, and incubated for 1 hour at RT with specific secondary antibody (Vector Laboratories, Burlingame, 1:1000) in PBS-T. Sections were then washed three times in PBS and incubated for 1 hour at RT with ABC complex solution (Vectastatin, reagents A and B in a ratio of 1:1) in PBS-T (1:250 with reagent A-B mix). Sections were washed again and incubated at RT with DAB solution (Vector) for 30s to 1 minute. After DAB incubation slices were properly washed in PBS and let dry overnight. The next day, sections are rehydrated in consecutive ethanol baths (50%, 70%, 96%, and absolute) and washed in Xylene before sealing with Eukitt mounting medium.

Collagen-based hydrogel volume

Stained sections were digitalised using Zeiss Axioscan.Z1 using its x10 objective.

All the analysis was carried out using Fiji-ImageJ software (quote the URL website of the resource).

In each striatal section, the visible area of stained collagen-based hydrogel was delineated and measured. Basing on the average obtained area the total volume was calculated per animal using the Cavalieri method, similarly to what previously published (Damiano et al., 2013).

Between 10 and 15 brain slices per animal were used.

Microglial area measurement

Stained sections were digitalised using Zeiss Axioscan.Z1 using its x10 or x20 objective.

The occupied area by IBA1+ cells was evaluated using Fiji-ImageJ software: the striatal area of interest was delineated, a specific threshold was applied, and the occupied area was evaluated. Between 8 and 14 brain slices per animal were used.

To quantify the cellular distribution around the implant we delineated the scaffold perimeter using oval selection in Fiji-ImageJ software; we then automatically drew 3 circles ranging respectively 50, 100, and 150 µm from the scaffold's border. At that point a specific threshold was applied and the area occupied by microglial cells (in mm^2) was calculated.

Myelin fibres quantification

Stained sections were digitalised using Zeiss Axioscan.Z1 using its x20 objective.

The occupied area by myelin fibres was evaluated using Fiji-ImageJ software: the injected and non-injected striatum was delineated, and specific threshold was applied. The ratio between injected and non-injected hemisphere for each animal was calculated.

Between 5 and 8 brain slices per animal were used.

Immunofluorescence

Protocol is close to that used in immunohistochemistry; briefly sections were removed from freezer and left at RT for 30 minutes. Subsequently slides were quickly washed in PBS to remove all traces of embedding medium. Sections were then blocked at RT in dark for 30 minutes with 4.5% normal goat serum (NGS) in PBS-T (0.2% Triton X-100 in PBS). At the end of this step, without washing, slides were incubated overnight with CD68 primary antibody (Biorad mouse anti rat CD68, 1:150) in 3% NGS in PBS-T at 4° C with gentle shaking. The following day sections were removed from primary antibody, washed 3 times in PBS, and incubated for 1 hour at RT with specific secondary antibody (Invitrogen Alexa Fluor 594-labeled goat anti-mouse IgG, 1:1000) in PBS-T.

Slides were then washed in PBS and incubated overnight with another primary antibody in 3% NGS in PBS-T at 4° C with gentle shaking (DAKO Polyclonal Rabbit Anti-Glial Fibrillary Acidic Protein – ref: 0334, 1:10000). After overnight incubation sections were removed from primary antibody, washed 3 times in

PBS, and incubated for 1 hour at RT with specific secondary antibody (Invitrogen Alexa Fluor 488-labeled goat anti-rabbit IgG, 1:1000) in PBS-T.

Sections were then washed in PBS, stained for DAPI (5 minutes at RT), washed again in PBS and mounted in a fluorescent mounting medium.

Acquisition was carried out using a laser confocal microscopy (SP8, Leica, Germany), or sections were digitalised using Zeiss Axioscan.Z1 at a magnification of 10x and 20x.

6.1.7 Statistical analysis

Statistical analysis was done by two-tailed, one-way analysis of variance (ANOVA) using GraphPad Prism software (GraphPad Software, San Diego, California, USA) and/or Statistica software (Statsoft Inc., Tulsa, Oklahoma, USA). When needed, LSD post-hoc correction for multiple comparisons was applied.

Paired Student's t-test was performed when possible for pairwise comparisons.

Level of significance annotations are as following: * $p<0.05$; ** $p<0.01$; *** $p<0.001$.

6.2 Results and Discussion

6.2.1 Characterization of collagen-based hydrogel *in vitro*

The first question we addressed in our study was the ability to detect the collagen-based hydrogel implant and its degradation after transplantation using reliable, but at the same time non-invasive tools.

Having in mind the possibility to translate the use of collagen-based hydrogel into humans, MRI was our choice as it represents a simple and non-invasive method to physically locate and detect the collagen scaffold, as well as to follow up its degradation over time.

First, we wanted to elucidate if the composition of the hydrogel would have some influences on the signal detectable by MRI. To answer this questions, different 4s-StarPEG (crosslinker) concentrations (0.5 mg/ml, 1 mg/ml, 2 mg/ml and 4 mg/ml) were mixed with collagen (5 mg/ml) and injected in 2% agarose phantom. Phantoms in clinical imaging are devices created to resemble the real biological system that scientists will need to work with: the phantom has to have almost similar characteristic as structure of interest, (the brain), and it might be imaged to setup the machine performances, test different experimental protocols, and evaluate different analysis methods (Iturralde, 1990). Agarose

was chosen as a substrate to form the phantom as, in addition to be cost-effective and easy to handle, it is considered one of the best material to create brain-resembling structures (Pomfret et al., 2013).
Our results showed that the collagen hydrogel is easily detected by T2 weighted sequence T2 sequence *in vitro* (Fig. 19); the relation time did not change in the different crosslinked gels, showing that the crosslinker itself does not change the behaviour of water molecules inside the hydrogel.

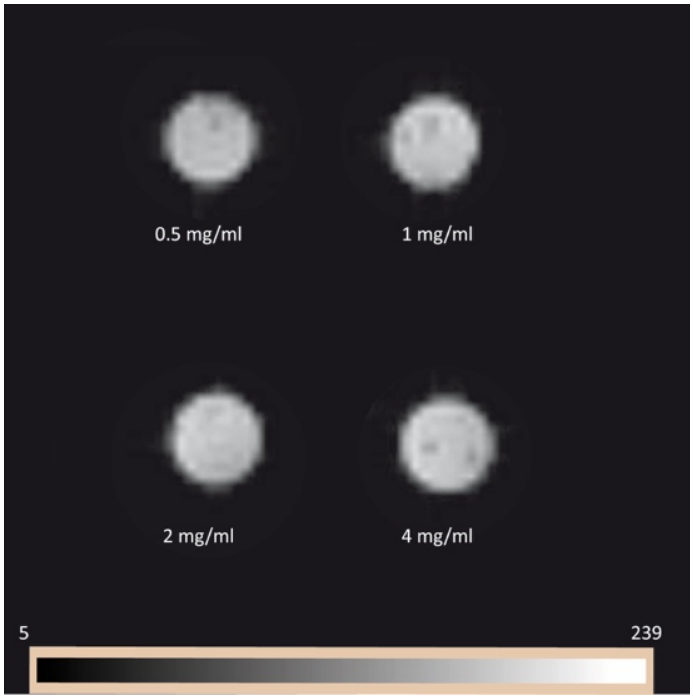

Figure 19: Anatomical scan of the collagen with various crosslinker concentrations.
5 mg/ml of collagen are mixed with different concentrations of crosslinker (0.5 mg/ml, 1 mg/ml, 2 mg/ml and 4 mg/ml) to form a hydrogel and detected using T2 relaxation time sequence with MRI.

After showing that using simple MRI T2 sequences crosslinker concentration does not influence the detection of the biomaterial, we investigated the smallest volume we were able to detect. To do so, 5 mg/ml of collagen was mixed with 4s-StarPEG with a concentration of 4mg/ml: we selected this specific crosslinker concentration as it has been suggested in previous published papers to be non-toxic *in vitro* and *in vivo*, and to give the hydrogel a relatively stable degradation over time (Moriarty et al., 2018a, 2017).
Different concentration (3 µl, 4 µl, 6 µl, and 10 µl) of collagen hydrogel were injected into the phantom. Results showed that even with the lowest amount used (3 µl), we are able to detect a bright dot

consisting of hydrogel **(Fig. 20)**; this proved us that our MRI and sequenced used is sensitive enough to detect signals from objects occupying only few pixels.

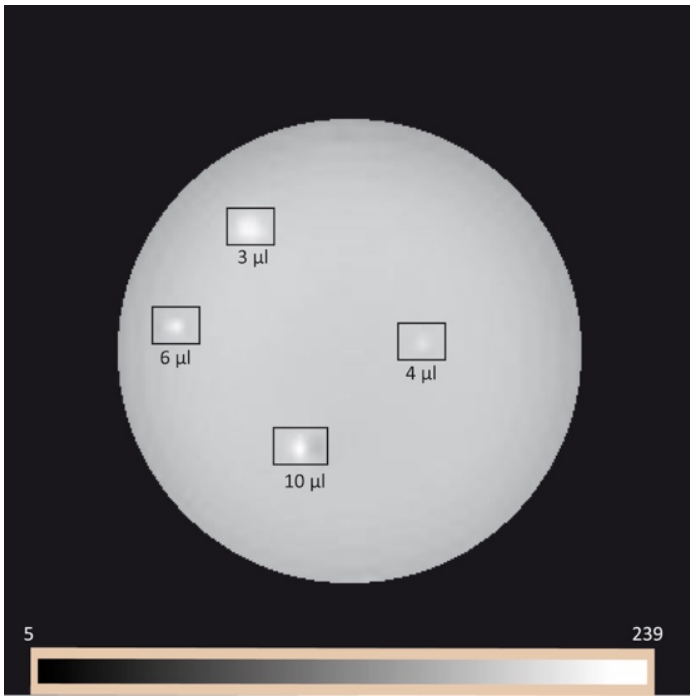

Figure 20: Anatomical scan of various volumes of 5 mg/ml of collagen mixed with 4 mg/ml of crosslinker.

5 mg/ml of collagen are mixed with 4mg/ml of crosslinker to form an hydrogel. Different volumes are injected in an agarose phantom to evaluate the lowest volume detectable by T2 MRI sequence.

6.2.2 Development of a cooling system for temperature-dependent hydrogels

After proving the ability to detect the hydrogel using MRI, we proceed with striatal injection of our collagen hydrogel *in vivo*, in the same conditions as previously described (materials and methods).

A huge obstacle we had to overcome was the unwanted polymerization of the hydrogel during stereotactic injections due to the contact with the ambient air at RT, leading to unprecise and non-reproducible delivery of the hydrogel and clogging of the needle: in fact, due to scaffold's proprieties of being liquid at 4°C and fully polymerized at 37°C, we had to develop a specific cooling system to maintain a stable refrigerated temperature during all the injection procedures. To do so, we developed a cooling system based on Peltier's cell **(Fig. 21 A-B)**. The input signal (the desired temperature) is selected on the main controller via a tactile display **(Fig. 22 A)**, and the signal is sent to the Peltier's driver **(Fig. 22 C)** through a microcontroller unit **(Fig. 22 B)**. Once the signal is read by the Peltier driver,

there is a quick adjustment of the temperature (cooling) of Peltier's cell **(Fig. 22 E)** via PID control until desired temperature is reached. A temperature controller **(Fig. 22 G)** placed between the chamber and the serpentine sends back the real temperature feedback to the controller (**Fig. 22 B, A)**, that consequently adjust the temperature of the cell. Tap water is slowly and continuously pushed into a polyethylene catheter via a 25 ml syringe attached to an automated pump; the tube filled with RT water goes through a serpentine **(Fig. 22 D)** attached to the cooling part of the Peltier's cell **(Fig. 22 E)**, where it is quickly refrigerated to near 2°C. The exiting catheter containing the refrigerated water is then wrapped around the tube and part of the needle where the liquid collagen-hydrogel solution is stored during stereotactic injection **(Fig. 20 B)**. The cooling procedures of the system are accomplished via the thermoelectric effect (transfer of heat from one side of the system to the other): for this reason, to avoid an unsuccessful cooling of the tube in the serpentine, as well as an overheating of the system, a dissipation fan unit **(Fig. 22 F)** was attached to the hot part of the Peltier's cell.

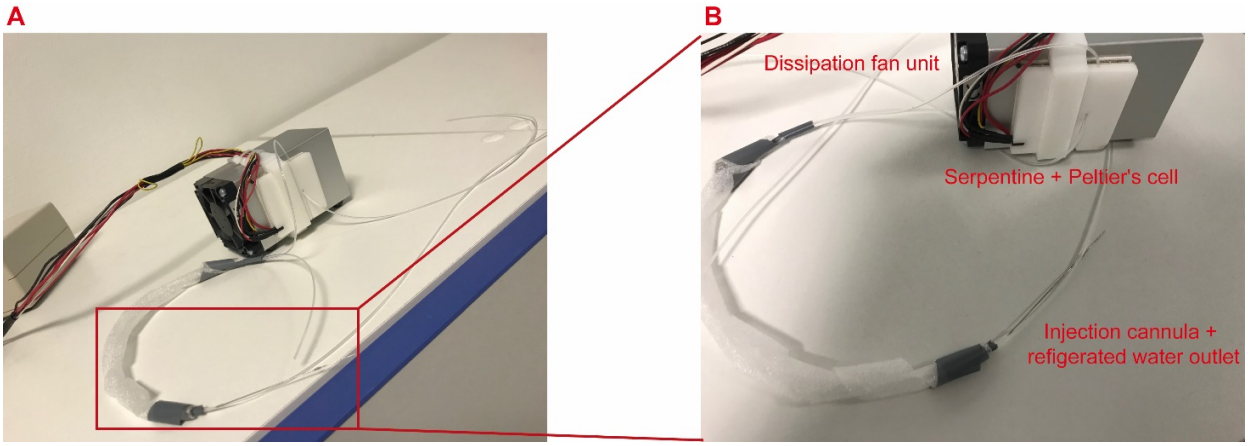

Figure 21: Cooling system for the collagen hydrogel injection.

(A) Picture of the cooling system composed of the Peltier's cell, the refrigerating serpentine, the dissipation fan unit, and the tubes with refrigerated water surrounding the needle used for injection. **(B)** Detail of the tube containing refrigerated water surrounding the tube and the needle where the liquid hydrogel is contained during injection.

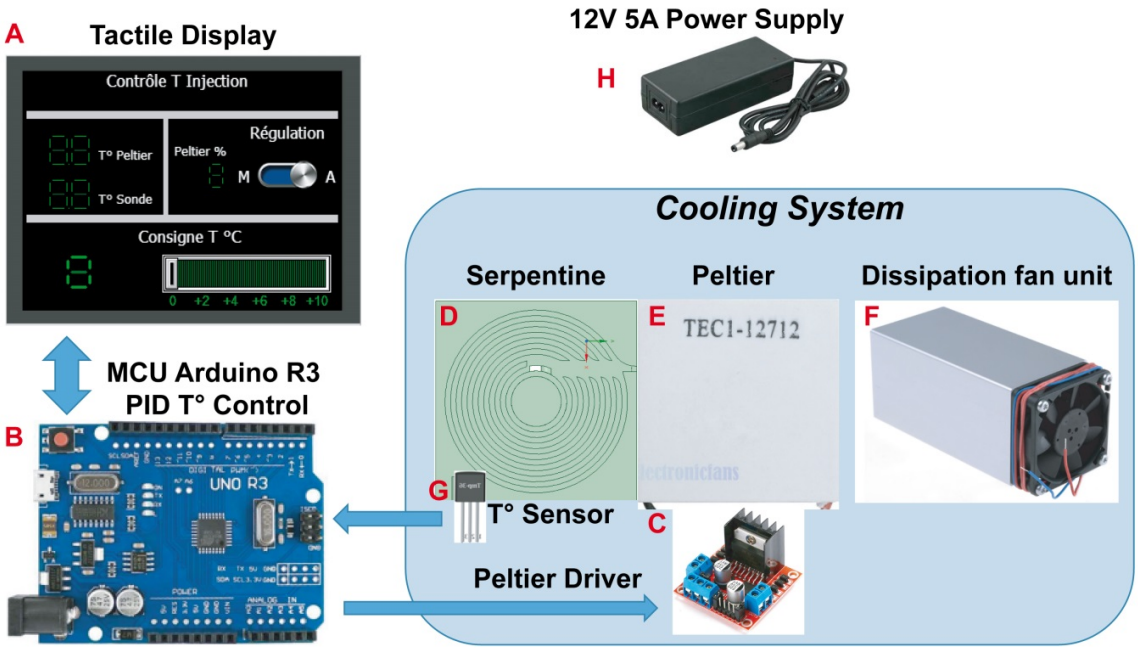

Figure 22: Schematic representation of the cooling system based on Peltier's chamber.

(A) Touch screen display controller. **(B)** Microcontroller unit. **(C)** Peltier driver. **(D)** 3D printed serpentine. **(E)** Peltier unit. **(F)** Dissipation fan unit. **(G)** Temperature sensor placed on Peltier chamber. **(H)** Power supply.

Different preliminary studies *in vivo* **(Fig. 23 A-D)** showed an insufficient reproducibility of the injection protocol when the cooling system was not in place, leading to an unprecise delivery of the scaffold and clogging of the needles. While at 1 day post injection **(Fig. 23 A)** the hydrogel was visible as a small round structure, after 30 days it was undetectable by MRI as it might have been fully reabsorbed by the body **(Fig. 23 B)**. After installation of the refrigerating system, our results showed a greater improvement of the polymer delivery and a clear detection with MRI both at 1 day **(Fig. 23 C)** and 30 days post injection **(Fig. 23 D)**.

These results all together showed the importance and the added value of this cooling system for the control of temperature during *in vivo* injection of a hydrogel sensitive to temperature changes.

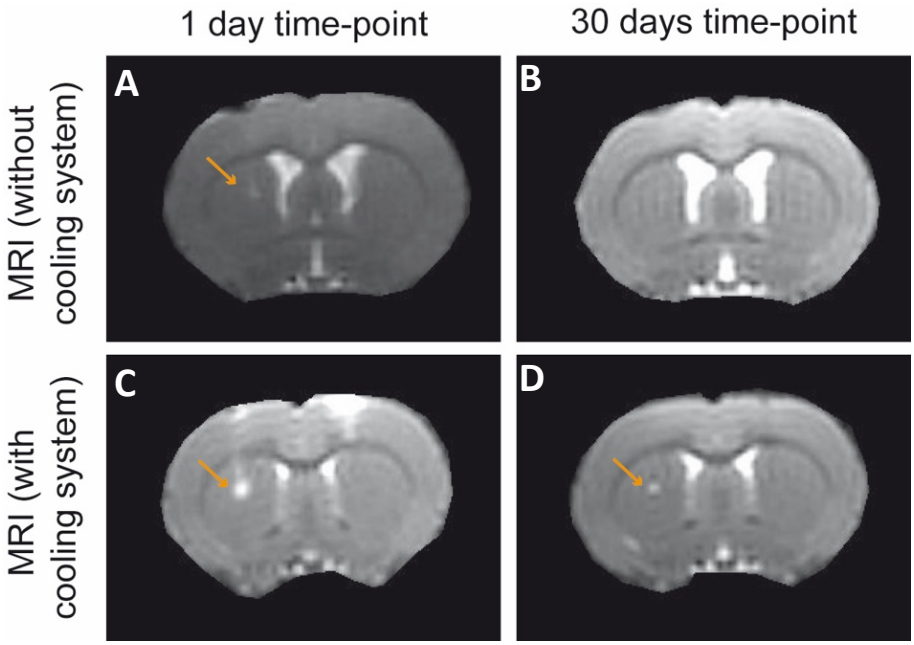

Figure 23: MRI representative images of 3 µl of collagen hydrogel injected in the striatum with or without cooling system.

Injection of collagen hydrogel without a specific cooling system led to an unwanted early polymerization during the injection, and subsequent unprecise volume delivery of the scaffold. Without the cooling system, **(A)** the hydrogel already at day 1 is hardly detectable, while **(B)** at day 30 is undetectable as completely reabsorbed by the body. Using the cooling system, **(C)** at day 1 our scaffold is clearly visible and **(D)** still present at day 30, even if with a reduced area.

Orange arrow: collagen hydrogel

6.2.3 Characterization of collagen-based hydrogel *in vivo*

6.2.3.1 Degradation of the biopolymer

Once we confirmed our ability to fully control the settings of our injection protocol and to have a sensitive detection method, the first aspect of collagen-based hydrogel we wanted to investigate was its degradation time.

Degradation of scaffolds is a complex process that starts quickly after the surgery and it is mediated by different players working synergistically together.

Once the scaffold is implanted, it is quickly surrounded by different types of cells as neutrophils and macrophages that quickly release various molecules, including specific collagen-degrading enzymes (Yahyouche et al., 2011). Collagen degradation is known to occur via collagenases action (Krane, 1982); briefly MMP-1 (matrix metalloproteinsase-1) enzyme cleavages preferentially with α2(I) chain, unwinding the collagen type I triple helix. Subsequently MMP-1 binds with the remaining chains, creating unstable collagen fibres that undergo faster degradation (Chung et al., 2004). How collagen is then completely destroyed is still under discussion: at the moment two different catabolic pathways

are proposed. On the first one, soluble proteases together with membrane bounds work together to degrade the collagen, while in the endocytic pathway it should be destroyed by lysosomal cysteine proteases, after internalization into the cells. (Madsen et al., 2013)

Another structure of the scaffold that influence the degradation time is the crosslinker: as collagen, it also undergo different types of stress when injected, including the surrounding environment and deposition of new tissue and cells around it (Nicodemus and Bryant, 2008).

Degradation time could be controlled and prolonged increasing the crosslinker concentration; from one side this might be a potential solution, giving to scientists the possibility to tune the hydrogels on their demand (Hu et al., 2019; Lin and Anseth, 2009).

It is finally important to mention that some unpublished *in vitro* results showed that degradation of this specific collagen hydrogel occurs much faster when placed in cell media but not PBS or xeno-free cell media, possibly via enzymatic degradation.

On the other hand, this has to be carefully evaluated as high doses of crosslinker might be toxic for the environment, as well as for the living load of the scaffold (e.g. cells).

Our results on hydrogel's degradation **(Fig. 24 A)** time showed that at one day post intrastriatal injection *in vivo*, the collagen-based hydrogel appears as a spherical structure, easily detectable by MRI using anatomical sequence, with a total quantified volume of around 3 mm^3. After 15 days, a great and significant loss of volume is detected (around 94% of original volume), that slowly but progressively continues at 30 days post injection.

To confirm the results obtained by MRI we proceeded with histological evaluation **(Fig. 24 B, 25)**. Our sections were stained for collagen using the Masson's trichrome staining **(Fig 25)**. As visible in green, collagen is detectable in all the three time-points, in shape and location comparable with the MRI data. Volumetric analysis showed coherent results with MRI: a significant decrease is seen in the first 15 days post injection, with a reduction of around 80% when compared with the first time point. Similar to MRI, only a small non-significant decrease in scaffold volume (less than 3%) is seen between 15- and 30-days post injection.

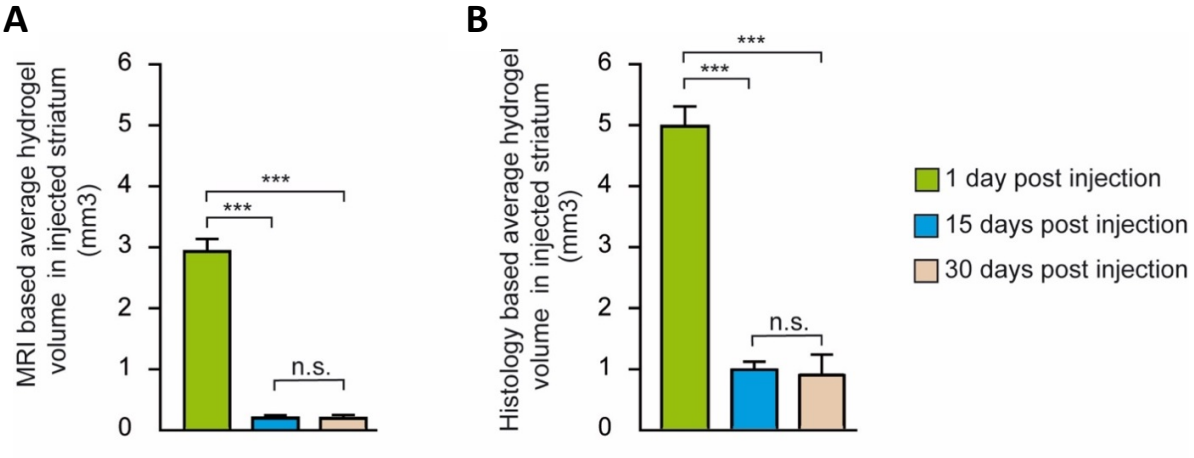

Figure 24: MRI-based (anatomical scan) and histological-based (Masson's trichrome staining) volume quantification of the detectable collagen hydrogel at the time point of interested.

Volume of the implanted hydrogel has been quantified at 1, 15 and 30 days post injection using **(A)** MRI anatomical scans and **(B)** post-mortem histological quantification using the Masson's trichrome staining.

One-way ANOVA was used for between-group comparison and Bonferroni post hoc correction for multiple comparison was applied. *n*=4 to 6/group for MRI and *n*=6/group for post mortem study.

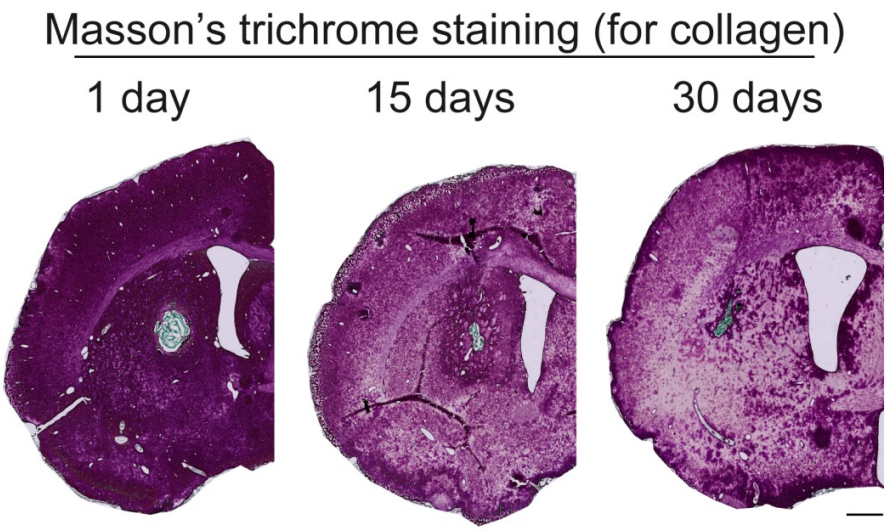

Figure 25: Representative images of the Masson's trichrome staining of the injected hemisphere after intrastriatal injection of 6 µl of collagen hydrogel at 1, 15 and 30 days post injection.

Masson's trichrome staining was performed in striatal sections to easily discriminate the polymerized collagen hydrogel. As visible in green, a fast degradation of the hydrogel occurs within the first two weeks, slowing down at 15 and 30 days post injection
Green: collagen, Pink to Red: cytoplasm. Scale bar: 1 mm

Differences in the volume quantification between MRI data and histological analysis should be attributed to the partial volume effect (PVE) in cross-sectional MRI imaging (González Ballester et al., 2002; Kneeland et al., 1986; Simmons et al., 1994).

We also wanted to evaluate if the hydrogel's polymerization *in-situ* had some negative impact on the striatal anatomy (e.g. striatal enlargement or deformation). Volumetric striatal assessment was based on MRI anatomical scans: our results showed no detectable striatal morphological changes between the injected and non-injected hemisphere in all the analysed time-points **(Fig. 26)**. Our rats' striatal volume quantification is in accordance with previous published data (Andersson et al., 2002).

Interestingly, even not significant, a little striatal dilatation is visible when compared with the ipsilateral non-injected hemisphere; this is in the range of the injected volume, and, as visible, it decreases over time following the hydrogel's degradation.

We believe that the elastic proprieties of the striatal structures are able to cope with such little injection and this partial dilation is neither destructive nor detrimental for the animal.

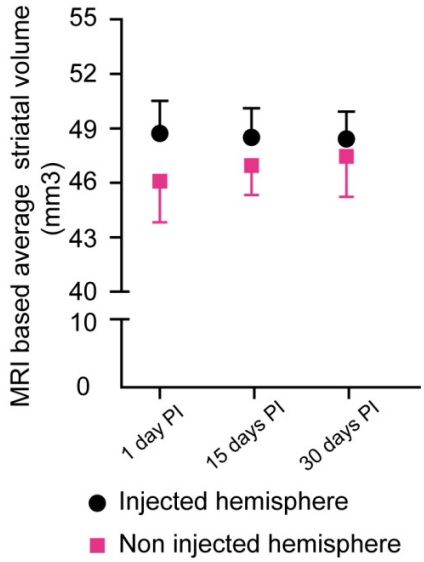

Figure 26: Injected and non-injected striatal volumetric quantification.

To identify possible striatal enlargement or compression due hydrogel's transplantation, MRI-based volumetric analysis of the injected and non-injected striatal area was performed. No detectable changes are visible in the injected hemisphere and total volume is coherent with what found in other studies.

Two-way ANOVA with time post-injection and site of injection (injected or non- injected hemisphere)as variables.

n=4 to 6/group

6.2.3.2 Early microglial response to transplanted hydrogel

Collagen-based scaffolds are known to be well tolerated by the host organism, to produce extremely low immune response and transplant rejection, and they can be easily used as a vehicle to deliver cells, active molecules and therapeutic. Both components of our biomaterial, PEG and collagen, have been extensively studied and tested for direct application. Studies done on primate (Bjugstad et al., 2008) and rats (Bjugstad et al., 2010) showed no adverse consequences of PEG-based hydrogel after striatal and frontal cortex implantation at all the evaluated time points. In addition, numerous clinical trials are evaluating the safety of collagen, and the use of collagen-scaffolds to treat different diseases, including spinal cord injury, infertility, brain injury, periodontitis, articular cartilage defects, urinary bladder dysfunctions, (https://clinicaltrials.gov/ct2/home - keyword: *collagen scaffold*) and bone defects (Zeng et al., 2018).

Microglia are specialised tissue dependant macrophages of the brain constantly patrolling the CNS and protecting it in case of injuries, pathogen invasions, brain tumours and neurodegeneration (Casano and Peri, 2015). A feature of microglial cells is their ability to be rapidly activated upon a minimal pathological change in the CNS: for this reason they are considered the first line of defence against any potential deleterious stimulus (Kreutzberg, 1996). Microglial cells, in physiological conditions, exist in a resting ramified shape with long processes extended in the proximal area (Franco-Bocanegra et al., 2019); in response to environmental signals of danger, they increase their proliferation rate, quickly migrate to the site of the injury and change their morphology into a more rod-like cell, with hypertrophic processes. If needed, another level of activation takes place in where microglial cells enter the phagocytic state, with amoeboid shape, abundant cytoplasm and almost no processes (Gehrmann, 1996). In addition, due to the disruption of BBB and temporary leakage, or in case of extreme need, microglial cells may also receive additional support from peripheral macrophages (Khaing et al., 2014). Both microglia and macrophages under physiological conditions are able to undergo a M1 classical or M2 alternative activation. The M1 state is the pro-inflammatory (and neurotoxic) phase, where microglial and macrophages actively clear the lesioned area and remove all the possible dangerous material; once this acute inflammatory status is resolved, they enter in the M2 phase. The M2 state is considered to be anti-inflammatory, and cells release growth factors as GDNF and BDNF (Batchelor et al., 1999), anti-inflammatory cytokines and neurotrophic factors (Yin et al., 2017), that together promote cellular repair, cellular differentiation, scar formation and vascularization

(Krzyszczyk et al., 2018). In chronic inflammatory conditions, instead, macrophages and microglial cells remain in the activated M1 pro inflammatory phase, leading to a reduced or failing wound healing (Hesketh et al., 2017).

While *in vitro* these states are easily distinguishable, *in vivo* the situation is much more complicated (Yin et al., 2017) and the shift between M1 and M2 phenotype is directly influenced by the stimuli surrounding the lesion (Kopper and Gensel, 2018), producing an overlapping of expressed genes and specific markers (Li and Barres, 2018). In studies done on spinal cord injury, it has been shown that microglial cells migrated in the lesioned area 24 hours after injury, while infiltrating macrophages arrived in a second time, but remained in the area for longer time, up to 42 days (Greenhalgh and David, 2014).

The first information we wanted to obtain was the degree of inflammation caused by intrastriatal injection of bovine-derived collagen hydrogel. Even if biocompatible and safe for transplantation, we expected that the biomaterial, together with surgical procedures and anaesthesia, would cause a small but possibly transitional inflammatory response.

To answer these questions, we evaluated the striatal area occupied by IBA1+ cells 24 hours after striatal injection of either 6 µl of DPBS or collagen hydrogel. DPBS is routinely administered as a control during stereotactic injections due to its low toxicity and reduced immune proprieties. As visible (Fig. 27 B), the hydrogel group had a small but significant increase in microglial activation when compared with the PBS group at the same time point. Such result is not surprising since we were fully aware that, even if well tolerated, a bovine-derived collagen hydrogel would trigger some response of the immune system, especially localized around the site of injection (discussed below).

What generally distinguish microglial cells from all the other cells in the brain, is their fast response and shift from resting-ramified to an activated state, upon that disruption of brain's homeostasis (Kopper and Gensel, 2018). Interestingly, in both the PBS and collagen-hydrogel group, the majority of microglial cells, even when located in the proximity of the scaffold, seemed to have a traditional resting ramified morphology (Fig. 27 A) - a typical sign of non-activated microglia (Ohsawa and Kohsaka, 2009). At the same time, at this time point we did not notice major changes in the cellular body nor any retraction or hypertrophy of the cellular processes.

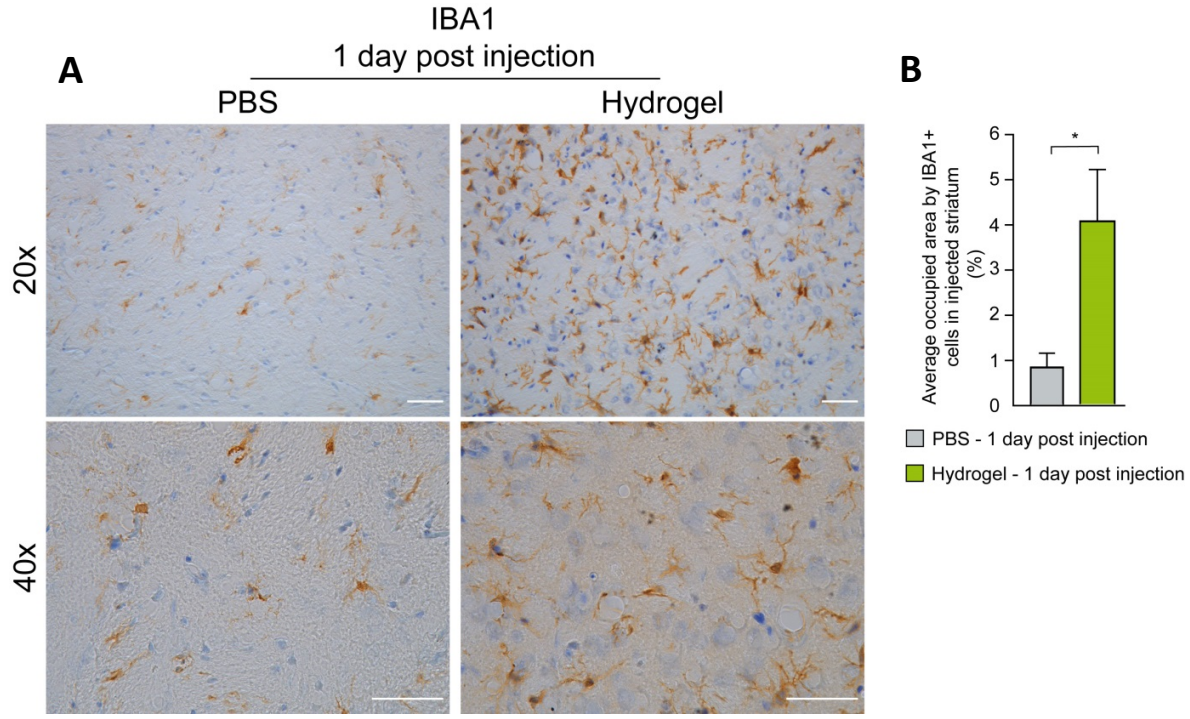

Figure 27: IBA1 histological evaluation of the effect of intrastriatal injection of 6 µl of DPBS or collagen hydrogel at 1-day timepoint in the striatum.

(A) Representative striatal IBA1 staining for sections of the two evaluated groups. **(B)** Striatal area occupied by IBA1+ cells were evaluated in relation to the striatal area and expressed as percentage.

Unpaired Student t-test was used for comparison between the PBS-injected and hydrogel-injected group.

n=4/DPBS and *n*=6/hydrogel. Scale bar: 50 µm

This seems to be coherent with the proposed idea that application of collagen has a beneficial role in mitigation of inflammation *in vivo*: Chen and colleagues showed that in a rodent model of surgical brain injury, application of collagen-glycosaminoglycan matrix led to significant reduction of IBA1+ and ED1+ cells, and changes in the levels of tissue proteins detected by ELISA (increase of *Il-10* and *GMCSF* and decrease in *NF-kB*, *TNF-α* and *Il-6),* when compared with sham or lesioned animals without collagen treatment (Chen et al., 2019). Another study using an injectable hydrogel in mice models of spinal cord injury showed a reduced inflammation, when compared with control animals (Gupta et al., 2006).

Taken together these results suggest that an immune response is activated within the first 24 hours in the hydrogel injected group when compared to PBS. Such immune response is likely to be transitory and not to persist as a chronic inflammatory condition as the cells migrating toward the injury's site did not appear to have a pro-inflammatory phenotype.

6.2.3.3 Microglial response to transplanted hydrogel over time

To better understand the possible development of inflammation over time, following the hydrogel degradation, we analysed the striatal area occupied by microglial cells 1 day, 15 days and 30 days after stereotactic intrastriatal injection of 6 µl of collagen-hydrogel.

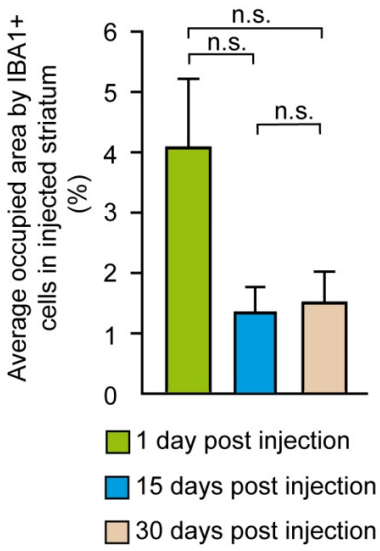

Figure 28: IBA1 histological evaluation of the effect of intrastriatal injection of 6 µl of collagen hydrogel at 1, 15 and 30-day timepoint in the striatum.

Striatal area occupied by IBA1+ cells were evaluated in relation to the striatal area and expressed as percentage.

One-way ANOVA was used for between-group comparison and Bonferroni post hoc correction for multiple comparison was applied.

n=6/group

Our results did not show any significant differences in the striatal area occupied by IBA1+ cells in all the three analysed time-points **(Fig. 28)**. Although not significant, higher levels of microglial cells were visible in the hydrogel-injected hemisphere 24 hours post injection, when compared with 15- and 30-days post injection.

Observing our sections in high magnification **(Fig. 29)**, we noticed an interesting transition in IBA1+ cells organization and morphology, in particular in the area surrounding the implanted hydrogel: at one day post injection, in fact, the IBA1+ cells presented the traditional morphology of resting ramified microglia, with the projections extended in the surrounding area. At 15 days post scaffold's transplantation, while some cells still presented the traditional ramified morphology, some other showed a more rounded cellular body, together with retracted processes. Interestingly, at 30 days post injection, the majority of cells surrounding the hydrogel scaffold presented a traditional macrophages-

like shape, with an amoeboid cellular body and very small cellular processes; in addition, at this time point, we noticed an abundance of cells that were able to infiltrate into the hydrogel scaffold.

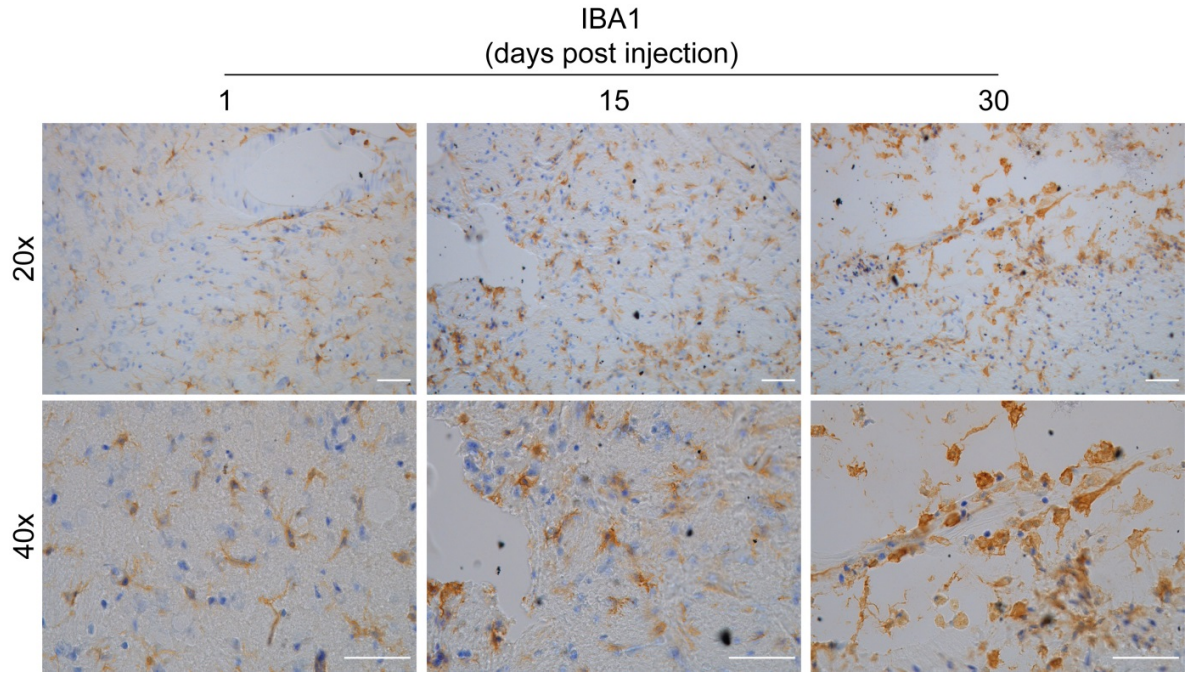

Figure 29: Representative IBA1 expression after intrastriatal injection of 6 µl of collagen hydrogel at 1, 15 and 30 day timepoint in the striatum.

Representative striatal IBA1 staining for sections of the three evaluated groups. Pictures are taken always in the close proximity of the border of the implanted hydrogel. Scale bar: 50 µm

6.2.3.4 Microglial response to transplanted hydrogel is localized in the surrounding of the scaffold

To have an insight on IBA1+ cells disposition and physical localization, we evaluated the cellular density in the area at 50, 100 and 150 µm from the scaffold's border **(Fig. 30 A)**.

Evaluation of cellular density at 1-day post injection showed no statistical differences within the proximal (50 µm), medial (100 µm) and distal (150 µm) areas **(Fig. 30 B)**. While from one side the elevated cellular density might be explained as a generalized inflammatory response in the striatum, on the other it seems to follow the pattern of an organized event as microglial activation and migration toward the site of injury.

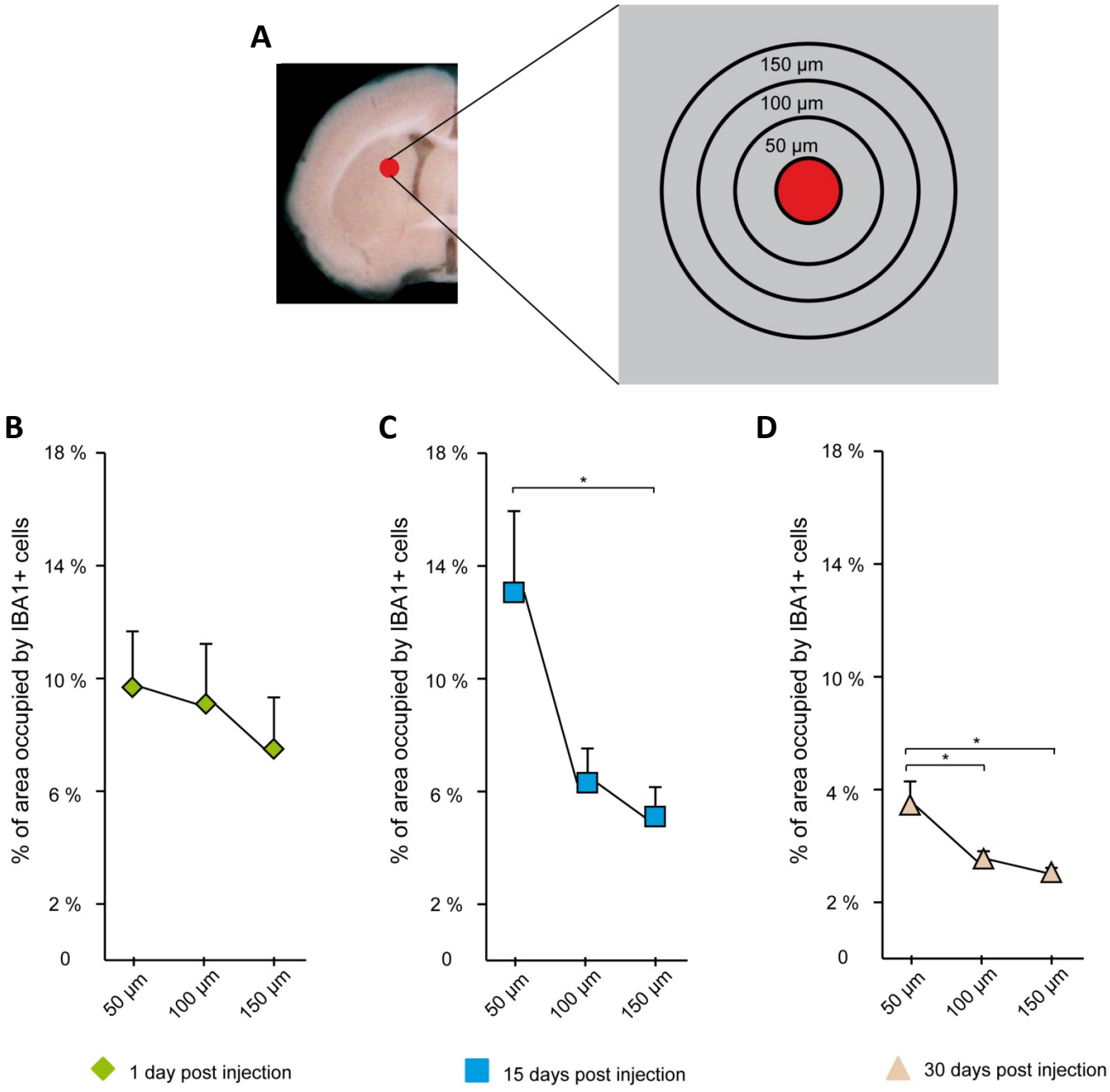

Figure 30: Schematic representation of the microglial disposition analysis and plotted results.

(A) Three concentric circles were created at a distance of 50, 100 and 150 µm from the border of the hydrogel (in red), and the area occupied by IBA1+ cells was evaluated.

Plotted results of the microglial disposition analysis at **(B)** 50 µm, **(C)** 100 µm and **(D)** 150 µm from the border of the polymerized hydrogel scaffold.

One-way ANOVA was used for between-distances comparison and Bonferroni post hoc correction for multiple comparisons was applied. *n*=6/group.

On the time point of 15 and 30 days, we detected a significant concentration of IBA1 + cells in the proximity of the scaffold when compared with the medial and distal areas. The high density of cells in the proximal area at 15 days post injection could be attributed to the peak of inflammation and major phagocytic activity of microglia and macrophages. At 30 days, even if the situation seemed to be almost back to the normality, still a significant increase was visible in the proximal area surrounding the scaffold.

The patterns of cellular organization around the scaffold, and the general immune response to the biomaterial transplantation, made us confident that the inflammatory reaction was only transitory and localized in the area of the implant, and did not develop into a chronic inflammatory state.

The idea of an acute but beneficial inflammation has been proposed in a recent paper by Zhang and colleagues (Zhang et al., 2018). Even if not in the brain, the authors studied the immune response of mice injected subcutaneously with a bovine sourced crosslinked collagen sponge at different time points. Evaluating the cellular population of the major organs controlling the immune response, the authors detected only a slight increase of splenic cells proliferation shortly after collagen sponge transplantation. At the same time, the authors detected, starting from day 7, an increase in TNF-α immunohistochemistry around the implant site, as well as infiltration of inflammatory cells into the collagen sponge (Zhang et al., 2018).

6.2.3.5 Microglia and macrophages play together in collagen-hydrogel's degradation

To better differentiate between microglial cells and macrophages surrounding the implanted hydrogel, we double stained our sections with IBA1 and CD68 (Cluster of Differentiation 68). While IBA1 is widely used to staining microglial cells in the resting phase (Hendrickx et al., 2017), CD68 is a pan-macrophage marker also expressed in advanced activated microglia (Ramprasad et al., 1996).

Macrophages are myeloid cells that are able to encapsulate and degrade different types of harmful agents, including cellular debrides, necrotic tissues, toxic molecules and pathogens (Yin et al., 2017). Together with microglia and astrocytes, are key players in the process of wound healing; such process is very similar to the one occurring in other tissues (e.g. skin), and can be divided in inflammation, proliferation and remodelling (Krzyszczyk et al., 2018).

Using double immunofluorescent staining, we noticed that in the area surrounding the implanted collagen hydrogel of all the three timepoints, the majority of the cells were $IBA1^{+}/CD68^{+}$, showing a clear and fast transformation of microglial cells into an activated phagocytic status; interestingly other

phenotypes as IBA1^{-}/CD68^{+} (recruited macrophages from the periphery) or IBA1^{+}/CD68^{-} (microglial cells in the resting state) were not that abundant, but in some cases were visible **(Fig. 31 A, B)**. The fast transformation of resting microglia into an activated phagocytic state has to be ascribed to the placement of an external protein-based scaffold in rats' striatum. Even if with low immunogenic effect, in fact, we believe that injection of bovine-derived collagen into the brain of other species, would likely to carry some immunological response by the host.

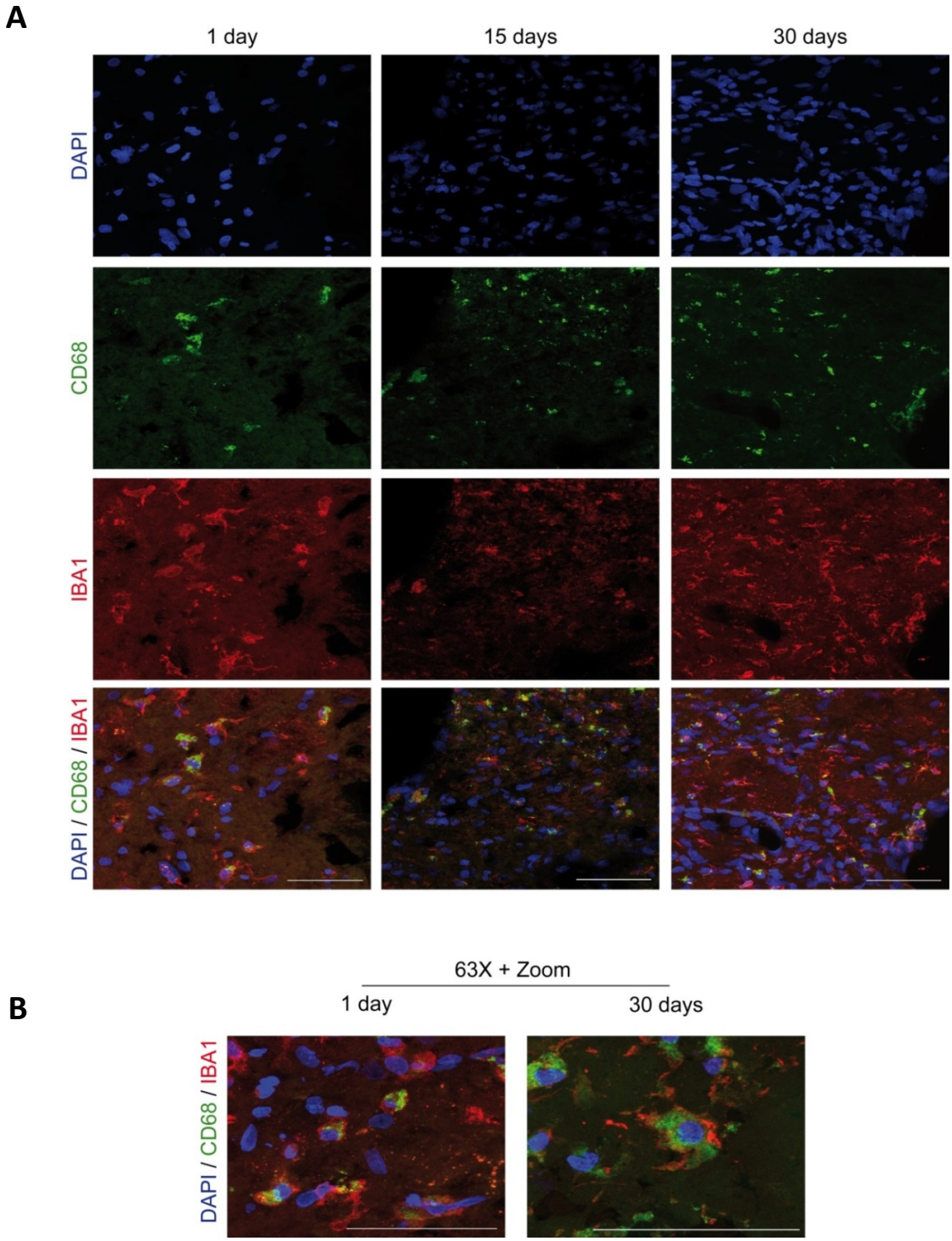

Figure 31: Representative striatal CD68 and IBA1 expression in the three evaluated groups.

Confocal Z-stack pictures were taken in the area surrounding the collagen hydrogel at 1, 15 and 30 days post injection. **(A)** Representative pictures with a magnification 63X. **(B)** Example of co-localization of IBA1 and CD68 makers at 1 and 30 days post injection. In addition to 63X magnification, an addition zoom was used to focus on few specific cells.

Blue: DAPI, Green: CD68, Red: IBA1. Scale bar: 50 µm

Interestingly, in the PBS injected group, we did not detect any $CD68^+$ cell, meaning almost no infiltration of macrophages and no advanced microglial activation into a macrophage status.

At 30 days post injection, we detected a much clearer organizations, with cells that were both $IBA1^+/CD68^-$ and $IBA1^-/CD68^+$. While it is expected to see the $IBA1^-/CD68^+$ population as infiltrating macrophages arrive after microglial activation, it is interesting to see that some microglial cells started already to lose their activated phagocytic phenotype, and seemed to be in the process of returning into a more resting state. This macrophage-microglia relationship seems to be coherent with a recent report by Greenhalgh and colleagues where was shown the important natural regulatory role of infiltrating macrophages over microglial activity. The authors showed that both in human cells and in mice, once macrophages were able to infiltrate in the lesion site, had the ability to suppress the phagocytic activity of microglia and prevent deleterious long term and chronic propagation of the microglia-related inflammation (Greenhalgh et al., 2018).

6.2.3.6 Hydrogel's transplantation did not create any striatal long-term lesion

To confirm that the implanted hydrogel did not create any serious brain injury (as advanced axonal damage), we quantified the amount of myelin fibres in the striatum.

Myelin evaluation is routinely employed as a marker for secondary tissue damage.

Myelin is a multilayer of proteins and fatty acid generated by oligodendrocytes around the axons of the CNS; it plays a crucial role in the correct transmission of electrical impulses along nerve cells, in the regulation of ion and water homeostasis and in the metabolic support to neurons and glial cells (Stadelmann et al., 2019). Disturbance of myelin is widely described in different diseases including spinal cord injuries (SCI), traumatic brain injuries (TBI) and multiple sclerosis (MS).

Traumatic brain injury and diffuse axonal damage are well known to create a reduction in myelin levels. A study done on hockey players showed reduced levels in the myelin water fraction (MRI value used to quantify myelin) following mild traumatic brain injury, and these levels were restored to the subject-specific pre-injury levels within 2 months post injury (Wright et al., 2016). Higher levels in the myelin water fraction were also detected in contact sport players (rugby and football) when compared with a cohort on non-contact sport players. Interestingly, in this study the levels of myelin water fraction were still increased 3 months post-injury when compared with the control cohort, but it is important to mention that patient-specific baseline pre-injury data were not available (Spader et al., 2019). The

authors explained such increase as a “manifestation of exuberant remyelination following an initial decrease in myelin water fraction” (Spader et al., 2019).

Another study done using MRI on human subject following mild traumatic brain injury showed a decrease in fractional anisotropy values, that are interpreted as reduce myelin levels (Kraus et al., 2007). Interestingly, the authors stated that while all type of brain injuries might create axonal damage, only moderate to severe traumatic brain injuries showed an irreversible myelin damage (Kraus et al., 2007).

Myelin quantification **(Fig. 32)** and microscopic observation **(Fig. 33)** achieved via Luxol Fast Blue immunohistochemistry showed a significant decrease in the myelin ratio between the injected and non-injected hemisphere at 1 day post injection when compared with the 30 days post injection. The same significance was visible when comparing the PBS injected group with the hydrogel 30 days post injection. Such results suggest that a demyelination process occurs in the striatum quickly after surgical procedures, but such effect should be seen as a consequence of the stereotactic injection, more than as a consequence of the polymer transplantation and polymerization. In addition, it is also interesting to notice that the remyelination process is not impaired by possible inflammation or permanent lesions caused by the hydrogel, and such process seems to be progressive starting already few days after transplantation, and continuing over the weeks.

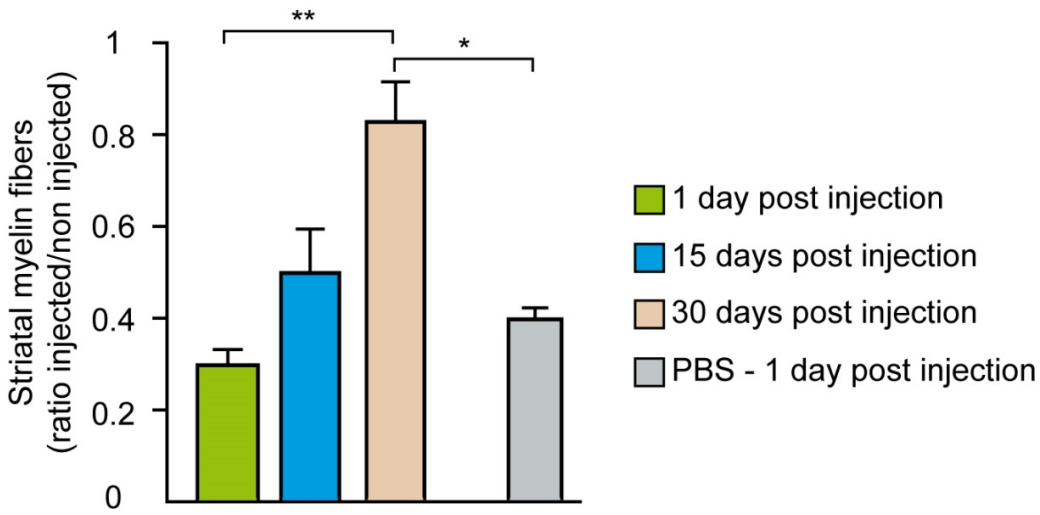

Figure 32: Myelin fibres histological evaluation after intrastriatal injection of 6 µl of collagen hydrogel at 1, 15 and 30-days post injection or after injection of DPBS at 1-day post injection.

Striatal area occupied by myelin fibres was evaluated in relation to the striatal area and expressed as the ratio between the injected and non-injected hemisphere for each animal.

One-way ANOVA was used for between-group comparison and Bonferroni post hoc correction for multiple comparisons was applied.

n=6/hydrogel and *n*=4/DPBS

Interestingly, also the PBS group showed a significant decrease in myelin levels 12 hours injection; this show that general reduction of myelin in our groups has to be ascribed more to the surgical procedures, disruption of BBB and damage to the axons produced by insertion of needle into the brain that to a deleterious effect of transplanted biomaterial. These results are in accordance with what obtained in other labs using a model of mild traumatic brain injury in mice (Mierzwa et al., 2015).

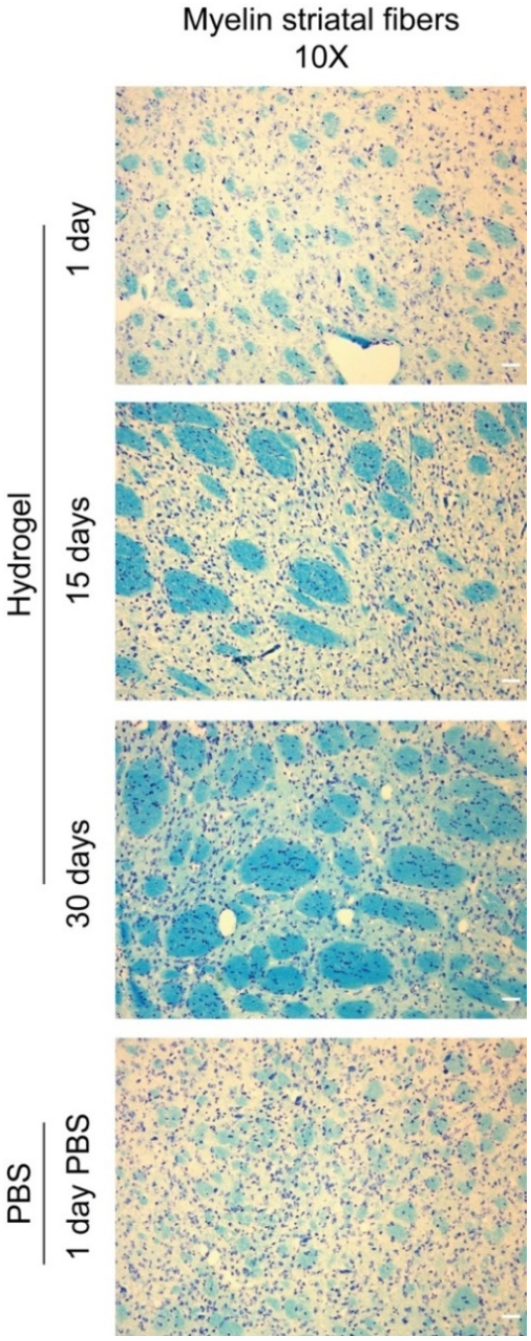

Figure 33: Representative histology of striatal myelin fibres after intrastriatal injection of 6 µl of collagen hydrogel at 1, 15 and 30-days post injection or after injection of DPBS at 1-day post injection.

Striatal sections of all the analysed timepoints were stained for myelin using Luxol Fast Blue. While a significant loss of myelin fibres is visible at 1 and 15 days post injection, a recovery (remyelination) is seen at 30 days. Interestingly, also the injection of DPBS produced a partial loss of myelin in the injected hemisphere.

Light/Dark blue: Myelin, Purple: Nissl bodies. Scale bar: 50 µm.

6.3 Conclusions

In this study we tested the possibility to use a bovine-derived *in-situ* polymerizing collagen hydrogel as a delivery system for cells and molecules. The advantage of our biopolymer is its ability to be liquid at 4°C and to quickly polymerize *in-situ* at 37°C, making it suitable for direct and sterile application in the brain.

While preparation of the hydrogel is relatively simple, fast and inexpensive, some technical expedients have to be considered, especially in regard of temperature control. Unwanted polymerization during injection (possibly due to the movement of liquid collagen in the needle, as well as the exchange of heat between brain and needle), was in fact an issue we had to overcome developing a specific cooling system for our syringes. We here showed that once we had full control on the injection's temperature, we were able to successfully delivery our biopolymer in the rat striatum in a reliable and reproducible manner. We also showed that polymerized collagen-based hydrogel can be detected non-invasively using simple MRI scans that are already routinely used in clinics (anatomical sequences); interestingly we were able to detect it also after 30 days, when reabsorption of the polymer was advanced. In this regard, we also quantified hydrogel's lifetime using live imaging and histopathological techniques, showing that a fast degradation of the polymer occurs within 15 days post transplantation, but that it is still partially in place (and detectable) even at 30 days.

Injection and polymerization of the hydrogel in the striatum did not create any detectable damage in the striatum, as expansion or compression of structure. A decrease in myelin fibres and a subsequent remyelination was visible post-surgery, but this should be attributed more to the surgical procedures than to the hydrogel itself.

In this work we also investigated the immune response caused by injection of a collagen hydrogel in striatum of rats: our results showed that, indeed, an increase of microglial cells activity is detectable in all the hydrogel's groups, but this inflammatory condition is mostly localized in the proximity of the scaffold, and does not seem to be spread in the whole striatal area. It is also interesting to notice that the implanted hydrogel is quickly surrounded by microglial/macrophage cells, and that some of them are infiltrating into the hydrogel at the late time point. Surrounding of the scaffold with consequent increased phagocytic activity of microglia and macrophages could be directly linked with the scaffold's degradation, as described elsewhere (Marchant et al., 1984).

To sum-up, we showed that the use of collagen hydrogel as a delivery system into the brain is of great interest for modern therapies, in particular for the one focusing on cells replacement. This hydrogel could be used to protect the transplanted cells during the surgical procedures, as well as in the first days after transplantation, where the risk of graft rejection and poor survival of the transplant due to immune response is higher. To enhance the cellular survival and reduce the immune response, this hydrogel could be also loaded with active molecules (e.g. GDNF, BDNF, IL-10) or pharmacological treatment of interest.

Different groups already showed the feasibility of using this specific collagen hydrogel for cellular replacement in neurodegenerative diseases as Parkinson's disease, showing *in vitro* and *in vivo* a well-tolerated response to the biomaterial, no transplant rejection, increased survival of cells, as well as increase in functional efficacy (Hoban et al., 2013b; Moriarty et al., 2017; Newland et al., 2013).

7. Final discussion and future studies

In this work we showed that finding an effective and long-lasting treatment for Parkinson's disease is a priority for the patients and their families, as well as for scientific community and the global healthcare system. The available treatments (L-Dopa and rehabilitation) are mostly focused on reducing the symptoms, and are mostly effective during the early onset phase of the disease; for the advanced case of PD at the moment the only solution with acceptable results is the deep brain stimulation, but it has to be carefully considered in each single case due to possible surgical and post-surgical complications.

As stated in this work the way to find a therapy for PD is still long and filled with obstacle; the main problem, in fact, is the lack of a reliable animal model that mimics all the typical features of the disease, as well as the long developmental time of it. In order to partially overcome this problem, we established a mild-progressive neurodegenerative rat model of PD based on the overexpression of two of the most important protein - α-syn and LRRK2.

At to achieve a strong degeneration of DA neurons in a reasonable timeframe seems very challenging with this model, we believe that it could be used in the future as a model of the early-PD phase, and could be of interest for testing therapeutics and cells replacement approaches.

Within all the possible experimental approaches, cells transplantation and cellular replacement seem to be the most promising approach, even if at the moment too many variables have to be taken in account: these include the type of cells and preparation, the route and type of injection, the dose, the time before transplantation, the patient response, as well as a dose of unknown.

The use of a collagen hydrogel scaffold to protect cells during transplantation and in the first hours after grafting could be a solution to the poor results obtained until now by cellular grafting. In addition, the use of a hydrogel would protect the cells by the attack of immune system and provide them with a cellular niche where they could start to grow and proliferate. Looking at this direction, we showed that an *in-situ* polymerizing collagen hydrogel can be safely injected into the striatum of rats, where is able to remain up to 30 days post injection. If needed, the length of polymer's biodegradability could be increased by increasing the crosslinker concentration, but it is also important to mention that high levels of crosslinker could be toxic for the environment. Furthermore, there is correlation between crosslinker concentration and the stiffness of the hydrogel: in fact, to have optimal results and low

toxicity or damage, the mechanical proprieties of the scaffold should resemble the ones of the organ of interest.

While the preparation of this biomaterial is relatively simple, the need of a cooling system to maintain the liquid polymer refrigerated is mandatory, at least in situation where the injection protocol requires small needle's diameter: for this reason, we had to develop a cooling system that is able to control temperature parameters and make our transplantation protocol extremely reliable.

We also showed that the transplanted hydrogel can be detected and followed-up during its degradation by non-invasive imaging methods as MRI, making it suitable for future clinical applications. In our samples, injection of the polymer did not lead to any traumatic brain injury or deleterious tissue-damage; we indeed showed that even if a localized inflammatory response is detectable, it is likely to be only transitory and not deleterious for the brain, especially if compared to injection of naked autologous or non-autologous cells. To overcome the possible inflammatory response and make the scaffold totally suitable for transplantation, it could be loaded with anti-inflammatory neurotrophic factors (e.g. GDNF), interleukins (e.g. IL-10) or neuropeptides (e.g. NPY) as is routinely done in other labs.

The application of *in-situ* polymerizing collagen hydrogel is not limited to simple injections: in fact, due to the thermic proprieties (polymerization at 37° C) it could be also used to reconstruct specific cellular pathways. In such regard, we already started to develop and test an injection protocol to reconstruct the nigrostriatal pathway, which is well known to be impaired in PD. Our idea is to employ this specific *in-situ* polymerizing hydrogel loaded with cells to create a long tube between SNpc and ST that would allow cells to reinnervate the SNpc and project their axon to the ST. Such idea is not new, as many research groups tried it with externally pre-formed hydrogel, but to our knowledge we are the first group trying to achieve it *in-situ*.

8. Supplementary material

8.1 Article: The unlikely partnership between LRRK2 and α-syn in Parkinson's disease (EJN, 2018)

Noemie Cresto[1*], Camille Gardier[1*], Francesco Gubinelli[1], Marie-Claude Gaillard[1], Geraldine Liot[1], Andrew B. West[2 x], Emmanuel Brouillet[1 x]

1 - Neurodegenerative Diseases Laboratory, UMR9199, CEA, CNRS, Université Paris Sud, Université Paris-Saclay, and MIRCen (Molecular Imaging Research Centre), Institut François Jacob, DRF, CEA, Fontenay-aux-Roses, France
2- Center for Neurodegeneration and Experimental Therapeutics, University of Alabama at Birmingham, Birmingham, Alabama, United States 35294

[x] Corresponding authors information:
email: abwest@uab.edu, address: 1719 6th ave s., Birmingham, AL 35294 USA, Ph: 205 996 7697
email: emmanuel.brouillet@cea.fr, address: 18 route du panorama, 92260 Fontenay-aux-Roses, France, Ph: 33 146 549 62

List of Abbreviation:

AAV Adeno-associated virus
ADPD Autosomal dominant Parkinson's disease
ALP Autophagy-lysosome pathway
ANK Ankyrin
APP Amyloid precursor protein
ARM Armadillo
Atg Autophagy related protein
ATP Adenosine Triphosphate
BAC Bacterial artificial chromosome
BAD Bcl-2-associated death promoter
Bcl-2 B-cells lymphoma 2
CaMKII Calcium/calmodulin-dependent protein kinase II
CI – CIV Complex I – Complex IV of mitochondrial respiratory chain
CMA Chaperone-mediated autophagy
CNS Central nervous system
COR C-terminal of Roc
DA Dopamine
DAT Dopamine transporter
Drp1 Dynamid related protein 1
ERK Extracellular signal-regulated-kinase
Fis1 Mitochondrial fission protein 1
GAD G proteins activated by nucleotide-dependent dimerization
GDAP1 Ganglioside-induced differentiation-associated protein 1
GLP1R Glucagon-like peptide-1 receptor
GWAS Genome-wide association
HEK Human embryonic kidney (cell line)
HSC70 Heath shock cognate protein
IBA1 Ionized calcium-binding adapter molecule 1
IBD Inflammatory bowel disease
IFN-γ Interferon gamma
IL-1β Interleukin-1 beta
IL-6 Interleukin 6
iNOS Inducible nitrite oxide synthase
iPD Idiopathic Parkinson's disease
iPS Induced pluripotent stem cells
JNK c-Jun N-terminal kinase
kD kilo-dalton

KI Knock-in
KO Knock out
L-dopa Levodopa
LAMP2 Lysosome-associated membrane protein 2
LB Lewy bodies
LC3-II LC3-phosphatidylethanolamine conjugate
LN Lewy neurites
LPS Lipopolysaccharides
LRR Leucine-rich repeats
LRRK2 Leucine-rich repeat kinase 2
MAPK Mitogen-activated protein kinase
MHC-II Major histocompatibility complex II
Mnf1 – Mnf2 Mitochondrial nucleoid factor 1 – 2
MPTP 1-methyl-4-phenyl-1,2,3,6-tetrahydropyridine
mRNA Messenger RiboNucleic Acid
mTOR Mammalian target of rapamycin
MyD88 Myeloid differentiation primary response 88
NF-kB Nuclear factor kappa B
NFAT Nuclear factor of activated T-cells
NHPs Non-human primates
NO Nitrite oxide
OPA1 mitochondrial dynamin like GTPase
PARK8 Old name for LRRK2
PD Parkinson's disease
PET Positron emission tomography
PFFs Pre-formed fibrils
PrP Prion protein
pSer Phosphorylated Serine
Roc Ras-of-complex
Ser Serine
SH-SY5Y Homo sapiens bone marrow neuroblast cell line
shRNA Short hairpin RNA
siRNA Small interfering RNA
SNc Substantia nigra pars compacta
SNCA alpha synuclein (gene)
SNP Single nucleotide polymorphism
SOD1 Superoxide dismutase 1
TDP43 TAR DNA-binding protein 43
Tg Transgenic
TH Thyrosine hydroxylase
TLR4 Tool-like-receptor 4
TNF-α Tumor necrosis factor alpha
TOM20 Translocase of Outer Mitochondrial Membrane 20
tTa Tetracycline trans activator
Tyr Tyrosine
UPS Ubiquitin-proteasome system
vMAT Vesicle dopamine transporter
WD40 Beta transducing repeat
WT Wild type
α-syn α-synuclei

Abstract
Our understanding of the mechanisms underlying Parkinson's disease, the once archetypical non-genetic neurogenerative disorder, has dramatically increased with the identification of α-synuclein and LRRK2 pathogenic mutations. While α-synuclein protein composes the aggregates that can spread through much of the brain in disease, LRRK2 encodes a multi-domain dual-enzyme distinct from any other protein linked to neurodegeneration. In this review, we discuss emergent datasets from multiple model systems that suggests these unlikely partners do interact in important ways in disease, both within cells that express both LRRK2 and α-synuclein as well as through more indirect pathways that might involve neuroinflammation. Although the link between LRRK2 and disease can be understood in part

through LRRK2 kinase activity (phospho-transferase activity), α-synuclein toxicity is multi-layered and plausibly interacts with LRRK2 kinase activity in several ways. We discuss common protein interactors like 14-3-3s that may regulate α-synuclein and LRRK2 in disease. Finally, we examine cellular pathways and outcomes common to both mutant α-synuclein expression and LRRK2 activity and points of intersection. Understanding the interplay between these two unlikely partners in disease may provide new therapeutic avenues for PD.

1. Introduction to LRRK2 and α-Syn in PD

Parkinson's disease (PD) is a neurodegenerative disorder affecting approximately seven million people worldwide (Cacabelos, 2017). Early symptoms of disease often include REM sleep disorder, gastroinsteninal disorders (e.g., constipation), and hyposmia. Later, characteristic movement-related symptoms often include shaking (resting tremor), rigidity, and slowness of movement (bradykinesia). The neuropathological hallmarks of PD are a progressive loss of dopaminergic (DA) neurons in the substantia nigra*pars compacta* (SNc) and the presence of neuronal aggregates composed mainly of α-synuclein protein (α-syn) (Lewy Bodies, LB) and dystrophic Lewy Neurites (LN) in some surviving neurons (H. Braak & Braak, 2000; Gibb, Scott, & Lees, 1991). Numerous theories exist for the causes of α-syn aggregation and preferential sensitivity of DA neurons, but without treatments that intervene in these processes, pathogenic mechanisms underlying PD remain unclear. Currently, there is no treatment capable of slowing the disease progression and although several therapies such as dopaminergic treatment and deep brain stimulation provide temporary remittance of several movement-related symptoms, the progression of the disease and therefore the aggravation of the neurodegeneration cannot be stopped.

PD is mainly a sporadic neurodegenerative disorder but a proportion of patients have demonstrated genetic origins. Rare mutations in the *α-synuclein* (*SNCA*) and *Leucine-Rich Repeat Kinase 2* (LRRK2) genes can cause autosomal dominant (AD) PD. Recently, genome-wide association studies have identified common genetic variants in both *SNCA* and *LRRK2* in susceptibility to sporadic PD, further supporting the importance of these two genes in the pathogenesis of PD (Nalls *et al.,* 2014; Satake *et al.,*2009). The overlap between clinical phenotypes associated with mutations in *SNCA* or *LRRK2* suggest these two proteins/genes concurrently play a role in sporadic and genetic PD. A number of questions are thus raised: Does α-syn and LRRK2 interactsynergistically in disease susceptibility? Following, does LRRK2 influence the occurrence and triggering of α-syn pathology? Through which molecular and cellular mechanisms do these two proteins interact in PD, and are they involved in both susceptibilityas well as progression? Alternatively, does α-syn play a more permissive role in mutant LRRK2 neurotoxicity?

Beyond improving our understanding of PD pathogenesis, clarifying the interplay between α-syn and LRRK2 may help to determine whether LRRK2 could constitute a relevant therapeutic target to slow down PD progression in patients without rare LRRK2 mutations. Indeed, major research efforts have been conducted in the past decade to design and test novel LRRK2 inhibitors with hopes they will benefit a large proportion of PD patients. Potentially supporting this notion, preliminary results in animal modelsof PD suggest that targeting LRRK2 could be beneficial in both familial and sporadic PD. Thus, the interaction between α-syn and LRRK2 might be central not only in terms of pathogenesis but also in understanding how to best devise effective therapeutic strategies. Here we briefly review both *in vitro* and *in vivo* studies in model systems that may shed light on the relationship between α-syn and LRRK2 in PD.

2. α-Syn and prion-like propagation

In 1997, Polymeropoulos *et al.* identified the α-syn A53T missense mutation as the first genetic lesion causative for an aggressive form of familial PD (Polymeropoulos *et al.,* 1997). α- is a presynaptic protein highly abundant in the brain with suspected roles in vesicle trafficking, membrane dynamics, and synaptic maintenance (reviewed in Bendor, Logan, and Edwards 2013). α-Syn has also been shown to localize to mitochondria and to be degraded in-part via chaperone-mediated autophagy (detailed in the paragraphs below on mitochondria and autophagy). The clear majority of α-syn studies focus on its dysfunction in PD pathology because of its capacity to aggregate and form LBs and LNs. Duplications, triplications and rare mutations (A53T (Polymeropoulos *et al.,* 1997); A30P (Krüger *et al.,* 1998); E46K (Zarranz *et al.,* 2004)) in the *SNCA* gene have been found in several families with dominantly inherited PD. They are associated with early-onset forms of PD with an amplification of the α-synaggregation process (Chartier-Harlin *et al.,* 2004; Singleton *et al.,* 2003). However, while it is generally accepted that aggregation of α-syn leads to neurotoxicity, the underlying mechanisms are still debated. It is possible that α-syn assemblies (aggregates, oligomers, lewy bodies) trigger toxic mechanisms through a gain of function (e.g. novel detrimental interaction with membranes or proteins) or a toxic loss of function of α-syn as a result of the sequestration of α-syn into aggregates. Indeed, multiple studies have shown a toxic effect of α-syn knock out (Tarasova *et al.,* 2018; Benskey *et al.,* 2018; Cali *et al.,* 2012; Gorbatyuk *et al.,* 2010) while others showed that α-syn KO protected against MPTP-induced neurotixicity (Dauer *et al.,* 2002). α-syn is a member of the synuclein protein family together with bêta and gamma-synuclein in mammals. The α-syn protein is composed of three regions: the first one is an amphipathic region (N-term: residues 1-60) containing apolipoprotein lipid-binding motifs and where PD mutations reside. Secondly, α-syn contains a "non-bêta amyloid" component region (NAC region: residues 61-95) which

gives it its potential to form bêta-sheets inherent to protein fibrils (aggregation). The last one is a C-terminal region (residues 96-140) that harbors important post-translational modifications of α-syn including phospho-Ser129. Three post-translational modifications were identified and validated *in vivo* with phosphorylated residues detected on Ser87, Ser129 and Tyr125. In particular, post-mortem biochemical and immunohistological studies showed that in PD brains α-syn is highly phosphorylated on Ser129 in inclusions. This phosphorylation is also found in pre-LB stages suggesting that it is strongly associated to disease progression (Saito *et al.*, 2003). The pharmacological modulation of this phosphorylation may be a relevant strategy for slowing PD progression, although several studies show α-syn related toxicity is enhanced when the Ser129 residue is mutated to an unphosphorylatable alanine residue (da Silveira *et al.,* 2009; Gorbatyuk *et al.*, 2008; Khodr, Pedapati, Han, & Bohn, 2012). Some kinase interactors have been identified that can modulate Ser129 phosphorylation including polo-like kinases, casein kinases, and G-protein receptor coupled kinase (Inglis *et al.* 2009; Ishii *et al.,* 2007; Pronin *et al.,* 2000). LRRK2, a serine/threonine protein kinase, has also been evaluated as a protein kinase for α-syn. Results suggest that LRRK2 is unlikely to directly phosphorylate Ser129 (Lin *et al.,* 2009; Herzig *et al.,* 2012). The instrumental role of Ser129 phosphorylation on α-syn is unclear and an increase of phosphor-Ser129 might not be toxic *per se*. Studies using kinase interactors of α-syn to produce hyper-phosphorylation at Ser129 have shown opposite effects(accelerated neurodegeneration vs mitigated toxicity) in the rat midbrain (Sato *et al*., 2011; Oueslati *et al*., 2013). Also, Buck and collaborators showed that phosphorylation of α-syn at Ser129 was not enough to trigger neurodegeneration, further questioning the role of phosphor-Ser129 in the pathogenesis of PD (Buck *et al*., 2015).

The pathological mechanisms underlying α-syn mediated degeneration of DA neurons has been linked to the very high concentrations of α-syn inherent to A9 DA neurons (that can serve as substrates for α-syn inclusions). SNc DA neurons also have relatively high metabolic demands and lowered oxidative capacity and long extremely branched axonal fibers that lack myelin (Braak and Del Tredici 2004; Post, Lieberman, and Mosharov 2018). Experimental evidence also indicates central roles for mitochondrial damage and associated vulnerabilities, and deregulation of the endolysosomal and autophagic pathways. Some evidence, particularly *in vitro*, clearly demonstrates that α-syn inclusions can be transferred, through some substrate, from one cell to the next (Busquets, Espargaró, Estelrich, & Sabate, 2015; Domert *et al.*, 2016; Kordower, Chu, Hauser, Freeman, & Olanow, 2008). Kordower and collaborators suggested cell-cell transmission of α-syn in 2008. A *post mortem* observation of PD brains transplanted with fetal neurons in the striatum showed that, fourteen years after transplantation, the grafted nigral neurons presented LB-like inclusions that stained positively for α-syn and ubiquitin and had a reduced expression of dopamine transporter. Alternatively, the transplanted cells could have intrinsically formed inclusions *de novo* in the environment of PD-affected nerve terminals in the striatum. Moreover, all healthy grafts of human midbrain transplants do not automatically show signs of α-syn pathology (reviewed in Engelender and Isacson, 2017). Experimentally, cell-to-cell transmission *in vivo* generally involves over-expression of α-syn and exposures to preformed fibrils of α-syn, brain extracts from α-syn transgenic (tg) mice, and total homogenates from post-mortem PD patients. Many experimental results are supportive of the hypothesis of a prion-like propagation of α-syn. α-Syn linked disease is different from prototypical prion disease in that there is no evidence of disease transmissibility in PD and intrinsic susceptibilities inherent to some sub-populations of neurons appears to outweigh the ability of α-syn to successfully transmit in a continuous way across circuits (Abdelmotilib *et al.,* 2017; Desplats *et al.,* 2009; Luk *et al.*, 2012; Mougenot *et al.*, 2012; Paumier*et al.,* 2015; Peelaerts *et al.,* 2015; Recasens & Dehay, 2014) (Reviewed in Surmeier, Obeso, and Halliday 2017b, 2017a).

However, even though there are many experimental studies supporting this prion-like hypothesis, it is important to note that there is a limited number of clinical evidence directly supporting it, and other experimental evidence goes against it. Indeed,Manfredsson and collaborators failed to show any significant spread of α-syn after they inoculated PFFs directly into the colon of rats and NHPs (Manfredsson *et al*., 2018). Most of the studies supporting α-syn spreading theory use overexpression models, or brain extracts from individuals presenting synucleinopathies, and among them, not all confirm this spreading hypothesis. This contrasted point of view is very well reviewed by Endelender and Isacson, who present a "Threshold theory for PD" (Engelenderand Isacson, 2017).

3. LRRK2 and the Kinase-Hypothesis of LRRK2-linked PD

In the mid-1990s, several families were identified that transmit autosomal dominant PD phenotypes identical to sporadic PD, a feature very uncommon for genetic forms of PD (Wszolek and Pfeiffer, 1992). In 2002, Funayama and collaborators performed a genome wide linkage analysis showing linkage to a 13.6 cM interval in 12p11.2-q13.1, dubbed the PARK8 locus. While the haplotype was shared by all the patients, it was also present in some unaffected carriers, suggesting the disease penetration to be incomplete. The authors hypothesized other parameters could affect the development of the disease such as environmental factors or other genetics factors (Funayama *et al.,* 2002).

Mutations in *LRRK2* are the most common genetic "cause" of both familial and sporadic PD, with causation understood as high-odds ratios (e.g., >20) for susceptibility to disease (Clark *et al.,* 2006; Paisán-Ruíz *et al.,* 2004; Ross *et al.,* 2011; Trabzuni *et al.,*2013; Trinh *et*

al., 2014; Zimprich *et al.,* 2004). Kachergus and collaborators identified the G2019S mutation in 2005 (Kachergus *et al.,* 2005), known as the most prevalent pathogenic mutation in LRRK2 that accounts for 5–6% of autosomal-dominant familial cases and 1–2% of *de novo* generic PD cases in some Western populations (Gilks *et al.,* 2005; Healy et al., 2008). The prevalence can be much higher depending on the population: a recent report suggested that as many as 70% of late-onset PD patients seen at a neurology clinic in Morocco were positive for G2019S (Bouhouche *et al.,* 2017). However, in far-east Asian populations, the frequency of pathogenic LRRK2 mutations is extremely low (Tan *et al.,* 2005; Tan *et al.,* 2007; Wu *et al.,* 2012; Zabetian *et al.,* 2009). True to the initial description of LRRK2-linked families, patients harboring the G2019S mutation are clinically indistinguishable from sporadic PD cases, including the presence of typical LBs in the majority of cases (Biskup & West, 2009; Yahalom *et al.,* 2014). The mechanisms underlying LRRK2's neurotoxicity remain unclear as it is a protein that does not itself form the proteinaceous inclusions typical of genetically linked proteins in neurodegeneration (like tau, APP, TDP43, SOD1, etc.). Rather, the *LRRK2* gene encodes a large 2527 AA multidomain protein with pathogenic mutations clustered among the central tri-domain region that forms the catalytic core (Cookson, 2010; Mata, Wedemeyer, Farrer, Taylor, & Gallo, 2006). LRRK2 is part of the ROCO protein family identified first in single-celled organisms and contains the tandem Ras-of-complex proteins (Roc) GTPase and C-terminal of Roc (COR) domains. LRRK2 may homodimerize through its COR domain and may function in a dimeric form as a GAD (G proteins activated by nucleotide-dependent dimerization) in which both ROC domains are brought close together and participate in the catalytic activity of their counterpart within the dimer (Civiero *et al.,* 2012). In addition to its GTPase domain, LRRK2 is composed of a kinase domain, with a characteristic activation loop (P-loop) with a DYG-APE motif altered to DYS-APE with the G2019S mutation. Other domains in LRRK2 include multiple protein–protein interaction regions [ankyrin (ANK), armadillo (ARM), and leucine-rich repeats (LRR) and WD40]. The number and conservation of protein-protein interaction domains suggest LRRK2 functions as a scaffolding protein contributing to the formation of multiprotein complexes that may functioin trafficking and signaling.

In vitro evidence and limited *in vivo* evidence suggest pathogenic LRRK2 mutations, like G2019S, enhance kinase activities associated with autophosphorylation and Rab-substrate phosphorylation (Alessi & Sammler, 2018; West *et al.,* 2005, 2007), and LRRK2-linked neurotoxicity originates from this increased activity (Greggio *et al.,* 2006; Lee *et al.,* 2010; Smith *et al.,* 2006; West *et al.,* 2007). Based on these observations, pharmaceutical companies have developed compounds targeting the kinase activity of LRRK2 in order to block the increased kinase activity associated with LRRK2 mutations. So-called first-generation LRRK2 kinase inhibitors like staurosporine, sunitinib, CZC 54252, TAE684 and LRRK2-IN-1 have a good potential to inhibit the kinase activity of LRRK2 (Deng *et al.,* 2011). However, they are not specific for LRRK2 and inhibit other critical kinases, together with poor drug properties, making them difficult to use for modeling or functional studies. Second generation compounds included more selectivity and better *in vivo* potential, although the inhibition of LRRK2 in the brain was limited (Saez-Atienzar *et al.,* 2014; Choi *et al.,* 2012; Estrada *et al.,* 2014) (reviewed in Taymans and Greggio 2016; West 2015, 2017).

Early studies demonstrated LRRK2 is a highly phosphorylated protein in the N-terminal part between the ankyrin and the LRR domains (S910; S935; S955; S973) (West *et al.,* 2007). This cluster, more specifically Ser910 and 935, is responsible for 14-3-3 protein binding (Dzamko *et al.,* 2010; R. J. Nichols *et al.,* 2010). The 14-3-3 proteins are a highly conserved family of proteins found throughout the evolutionary scale and are implicated in many cellular functions, notably, they act to promote cell survival through inhibition of many known pro-apoptotic factors including the mitochondrial Bcl-2 family member BAD and the transcription factor span (Yuan & Yankner, 2000). The 14-3-3 proteins bind to serine/threonine-phosphorylated residues, often functioning as direct regulators of the target proteins to which they bind (Loeffler, Klaver, Coffey, Aasly, & LeWitt, 2017). Seven isoforms are described in mammals. Studies show that 14-3-3 proteins are linked to PDpathology, as 14-3-3 also interacts with α-syn (for more details, see the common interactors paragraph). LRRK2 binding of 14-3-3 leads to a uniform LRRK2 distribution throughout the cytoplasm and may inhibit LRRK2 kinase activity (Lavalley, Slone, Ding, West, & Yacoubian, 2016). Decreased 14-3-3 binding to LRRK2 induced by PD-associated mutations leads to a re-localization of LRRK2 in cytoplasmic pools (Nichols *et al.,* 2010; Rudenko and Cookson 2010). LRRK2 may also be subject to autophosphorylation on a cluster of threonines in the Rab-like ROC GTPase domain (T1343; T1368; T1403; T1404; T1410; T1452; T1491; T1503) and on two isolated serine and threonine residues in the LRR domain (S1292) and in the kinase domain (T2031) (Kamikawaji, Ito, & Iwatsubo, 2009; Sheng *et al.,* 2012; Webber *et al.,* 2011). LRRK2 autophosphorylation appears to act as an enzymatic activator for both the GTPase and the kinase activity. In 2011, Webber and collaborators studied the effect of autophosphorylation on GTPase and on kinase activity in G2019S or in WT context. They showed that autophosphorylation on the T1503 that is localized in the GTPase domain alters both kinase and GTP binding activity, concluding that autophosphorylationin the GTPase domain induces functional and conformational changes that enhance the dimerization and leads to upregulation of kinase activity. In 2012, Sheng and collaborators validated *in vivo* S1292 as a critical autophosphorylation site (Sheng *et al.,*2012). Familial PD mutations (N1437H, R1441G, R1441C, G2019S and I2020T) all induced significant increases in phospho-S1292 levels compared to WT-LRRK2 in cellular models, and when the S1292 residue was mutated to a non-phosphorylatablealanine residue, the toxicity associated

with LRRK2 kinase activity was ablated. Taken together, these data suggest that LRRK2 kinase activity links pathogenic mutations with neurotoxicity.

4. Rationale for a meaningful interaction between LRRK2 and α-synuclein in PD

4.1 Evidence from humans

4.1.1 Clinical phenotypes

Several *LRRK2* mutations from a number of different families in different countries have been described and since they are relatively rare compared to sporadic (i.e., idiopathic or iPD) disease in most populations, comparisons that lack clinic bias are difficult to formulate. However, clinic bias tends to skew genetic forms of disease phenotypically away from sporadic disease and with LRRK2, clinical characteristics of the symptomatic carriers are very similar to one another (Adams *et al.,*2005; Hasegawa *et al.,* 2009; Huang *et al.,* 2007; Hulihan *et al.,* 2008; Khan *et al.,* 2005; Lin *et al.,* 2008; Nichols *et al.,* 2005). Presently, there is no single clinical phenotype or scale that might predict a LRRK2 mutation carrier from typical late-onset PD. Curiously, no major difference seems to exist between homozygous patients and the ones who are heterozygous, although the number of homozygous LRRK2 mutation carriers yet described is very small, consistent with the frequency of the most common LRRK2 mutation G2019S at less than 0.1% in the Caucasian population (where it is most frequent).

LRRK2 mutations do not cause early-onset disease; the age of onset in susceptible carriers is relatively similar for iPD and LRRK2 mutation carriers (~55-65 years old). Motor symptoms of LRRK2 carriers include resting tremor, rigidity, akinesia, postural instability, and gait difficulty, which are reminiscent of those seen in iPD. Unilateral onset is often seen in LRRK2 mutation carriers as it is in iPD. As expected, LRRK2 carriers with PD are responsive to L-dopa treatment. Further, PET imaging studies of the dopaminergic system indicate alterations in symptomatic LRRK2 carriers that are typical of iPD, especially the reduction in ^{18}F-dopa accumulation in striatal DA projections, and reduced binding of ^{11}C-tetrabenazine to the vesicle dopamine transporter (vMAT) and reduced binding of the ^{11}C-methylphenidate to the dopamine transporter (DAT). The relative preservation of the DA projections in the caudate nucleus as compared to the putamen seen in iPD has been also observed in LRRK2 mutation carriers (reviewed in Biskup and West 2009).

Subtle differences have been described regarding the effect of LRRK2 mutations on the timing and progression of certain symptoms in different populations of carriers. However, a prospective longitudinal follow up of a cohort (n=122) of LRRK2 variant carriers over more than five years indicated that the onset and symptoms were not different from iPD (Oosterveld *et al.,* 2015). However, the progression of the disease after onset might be slightly accelerated in LRRK2 carriers when compared to non-carriers (Oosterveld *et al.,* 2015). Finally, some studies highlighted the possibility of differences in the prevalence and timing of onset of non-motor symptoms (REM sleep disorder, cognitive deficits), especially in PD with dementia (Goldwurm *et al.,* 2006; Sun *et al.,* 2016). In summary, the striking clinical overlap between LRRK2 mutation carriers with PD and PD without LRRK2 mutations suggests common disease mechanisms.

4.1.2 LRRK2 and α-syn in Lewy bodies and Lewy neurites.

Two years after the discovery of *LRRK2* as a gene responsible for autosomal dominant forms of PD, Zimprich and collaborators speculated that LRRK2 kinase activity may be responsible for the phosphorylation of α-syn and that this effect may trigger its accumulation and aggregation (Zimprich *et al.,* 2004). The authors found typical LB-dominant pathology, comparable to sporadic PD patients, in LRRK2 mutation carriers. These observations suggested that LRRK2, as a kinase, and α-syn, as a kinase substrate, could physically interact. Later, Giasson and collaborators studied via immunohistochemistry three individuals with the G2019S LRRK2 mutation and concluded LRRK2 protein was not found in LBs or in LNs, in contrast to typical α-syn pathology in these cases. However, studies including larger numbers of LRRK2 mutation carriers revealed that a proportion of cases, up to 1/3 of G2019S carriers of both non-Ashkenazi Jewish and European non-Ashkenazi Jewish descent were negative for Lewy bodies (Kalia *et al.,* 2015). Although the total number of brains evaluated remains low, the number without Lewy bodies is high compared to typical late-onset disease brains evaluated from patients clinically diagnosed with PD.

There are several possibilities to interpret G2019S-LRRK2 carrier brains clinically diagnosed with PD that lack Lewy bodies. First, in the presence of the G2019S LRRK2 mutation, LBs may be more toxic than usual and cells that harbor them may not survive through late stages of disease. Second, the G2019S LRRK2 mutation favors smaller less-phosphorylated α-syn inclusions or abnormal oligomers that are more difficult to detect than typical eosinophilic inclusions, and this drives disease in those patients. Third, the proportion of G2019S-LRRK2 carriers negative for LBs may experience disease onset and progression without the contribution of α-syn. For example, some LRRK2 mutation carriers have been described with Tau tangle pathology. Unfortunately, there is typically insufficient clinical data associated with most tissues available to test whether disease characteristics and progression might be different inLRRK2 carriers with and with α-syn LB burden. A PET tracer that might label α-syn inclusions in life would effectively solve the riddle and such tracers are

under active development. In the meantime, better clinical phenotyping within brain donation centers supported by LRRK2 mutation carriers seems vital to better understanding pathology linked to LRRK2.

4.1.3 SNCA genetic variants in modifying PD susceptibility in LRRK2 carriers.

Genome-wide association (GWAS) studies indicate that variants in *SNCA* and *LRRK2*, independent from rare pathogenic missense mutations, are among the top genetic risk factors for PD susceptibility (Nalls *et al.,* 2014; Satake *et al.,* 2009; Simón-Sánchez *et al.,* 2009). Studies focused on gene-gene interactions effects of *SNCA* and *LRRK2* found no significant evidence of an interaction between the two genes, although power is still limited due to low individual effect sizes of the linked variants (Biernacka *et al.,* 2011). Botta-Orfila and collaborators genotyped the *SNCA* polymorphism rs356219 in 84 Spanish LRRK2-associated PD patients carrying the G2019S mutation (Botta-Orfila *et al.,*2012). This single nucleotide polymorphism (SNP) is known to regulate *SNCA* expression in idiopathic PD-affected brain regions, blood, and plasma. Results showed that *LRRK2* mutation carriers carrying one or two *SNCA* rs356219-G alleles presented with an earlier PD onset than patients carrying the *SNCA* rs356219-A homozygote (55.37+/-1.54 vs 64.19+/-2.8 years respectively) (Botta-Orfila *et al.,* 2012). A similar study was performed in iPD patients, and the authors found that this SNP also influenced the age of onset (Cardo *et al.,* 2012). Tese initial studies suggest that *SNCA* genetic variants could be a modifier of age of onset but not necessarily disease susceptibility (Botta-Orfila *et al.,* 2012). Thus, these observations indirectly suggest that α-syn may play a permissive role in *LRRK2* mutation carriers in disease.

4.2 Evidence of α-syn and LRRK2 interaction in animal models

In 2009, Lin et al reported results from triple-transgenic mice with inducible A53T-α-syn and LRRK2 (WT or G2019S) under the *CaMKII* promoter-controlled tetracycline trans activator (tTA) (*CaMKII-tTA*), or on a LRRK2 knockout background, to examine the role of LRRK2 in the progression of neuropathological alterations and phenotypes associated with mutant α-syn. This heroic effort first determined the number of neurons that remained in the striatum of *A53T/LRRK2WT* and *A53T/G2019S* mice after months of expression; while the difference was not statistically significant in comparisons between WT-LRRK2 or G2019S-LRRK2 expression, a trend towards a decrease in the number of neurons in the A53T/G2019S striatum was reported. More convincingly, the inhibition of LRRK2 expression dramatically ameliorated α-syn-induced neuropathology almost to the level of doxycycline-induced silencing of transgenic mutant α-syn expression. Furthermore the number of neurons at 12 months of age in the striatum of mice was significantly higher in the A53T/LRRK2$^{-/-}$ mice compared to A53T/LRRK2$^{+/+}$ mice. Moreover, no significant increase of astrocytosis, microgliosis, or somatic accumulation of α-syn was detected in these mice. These experimentshighlighted the potential link between WT-LRRK2 expression and α-syn protein in neurodegeneration observed in PD, with a more speculative role for G2019S-LRRK2 in exacerbating α-syn neurotoxicity (Lin *et al.,* 2009).

Further testing the link between G2019S-LRRK2 and α-syn neurotoxicity, in 2012 Herzig and collaborators reported tg mice that expressed human LRRK2 (WT or G2019S) with mice that expressed human α-syn (A53T or WT) under the same neuron-specific promoter (Thy1 promoter) (A53T/G2019S; A53T/WT; WT/G2019S) (Herzig *et al.,* 2012). This strain of A53T-α-syn mice (van der Putten *et al.,* 2000) were known to develop motor coordination deficits in the rotarod test at 40 days of age and severe motor deficits, hypokinesia and weight loss at 6 months of age, although they lack the overt neurodegeneration that occurs in the Lin et al study. The G2019S-LRRK2 tg mice showed no obvious brain pathology at 19 months of age, with no further decline of motor performance in double tg mice (Herzig *et al.,* 2012). In 2017, Xiong and collaborators went back to the CamKII-induction approach to obtain a high expression level of G2019S-LRRK2 in the adult mouse forebrain, and consistent with Lin et al, these animals showed a nominal increase in α-syn aggregation, especially in the cortex (Xiong *et al.,* 2017). They obtained similar results in tg mice with a selective overexpression of G2019S-LRRK2 in the SNc, where they showed a degeneration of DA neurons and the aggregation of endogenous mouse α-syn (Xiong *et al.,* 2018). Potentially consistent, A53T-α-syn transgenic mice directed from the PrP promoter (Lee *et al.,* 2002)(see also: Giasson *et al.,* 2002), when crossed with G2019S-LRRK2 mice expressing mutant LRRK2 under the control of the CMVe-PDGFb promoter, demonstrated mild enhancement of phosphorylated inclusions but did not worsen survival rates or other phenotypes (Ramonet *et al.,* 2011; Daher *et al.,* 2012).

Outside of traditional transgenic mice, the acute induction of α-syn overexpression via viral vector or injection of preformed α-syn fibrils also suggests a role for LRRK2 in α-syn neurotoxicity. BAC-mediated expression of G2019S-LRRK2 in rats causes a very mild motor impairment with no dopaminergic cell loss even at 12 months of age (Lee and Cannon 2015; Walker *et al.,* 2014). However, injection of an AAV coding for α-syn (Daher *et al.,* 2015) in the SNc of these G2019S-LRRK2 rats induces a loss of TH-positive neurons that appears slightly more pronounced as compared to that seen in WT-LRRK2 rats. A larger effect was described in LRRK2 knockout rats that may be protected from viral-vector mediated α-syn-induced dopaminergic neurodegeneration (delivered by an AAV) (Daher *et al.,* 2014).

In summary, the effects of the G2019S LRRK2 mutation on α-syn neurotoxicity and aggregation is mixed, with either mild or no effects reported in rodent studies. In contrast, phenotypes are generally more robust in the amelioration of α-syn phenotypes in LRRK2 knockout rats and mice. For transgenic LRRK2 expression, it is important to note that except in Lin's study, the co-expression of both proteins (α-syn and LRRK2) in the same anatomical region and in the same neurons is not precisely validated thereby introducing a potential confounder to interpretation. In a recent study in primary hippocampal neurons, G2019S-LRRK2 expression mildly increases α-syn fibril induced inclusions but the effects of LRRK2 inhibition are much larger in reducing α-syninclusion maturation (L. A. Volpicelli-Daley *et al.,* 2016). Thus it remains possible that, at least in part, G2019S-LRRK2 expression may mediate a cell autonomous (albeit subtle) mechanism in the aggregation of α-syn in neurons. More the convincingly interactions appear from LRRK2 inhibition or knockdown which implies a general effect of LRRK2 interacting with α-syn in PD, outside of pathogenic mutations.

4.3 Molecular mechanisms to explain the interaction of LRRK2 and α-syn in PD

An important interaction between LRRK2 and α-syn may plausibly occur within cells that express both proteins at the same time (i.e., cell-autonomous), or through the interaction of cells important in disease that express one protein or the other (i.e., non-cell-autonomous). For example, in neurons, LRRK2 might modulate total α-syn levels (synthesis or degradation levels), levels of a post-translational modification in α-syn, modulate α-syn aggregation through changing interactions with α-syn interacting proteins, or change the subcellular compartments where α-syn normally resides. Within cells that express both LRRK2 and α-syn, understanding their interaction may shed light on how key organelles regulate survival, for example through mitochondria or endolysosome function. Alternatively, LRRK2 and α-syn might be functionally linked through mechanisms involving cell-cell interactions. For example, cells of the innate immune system involved in neuroinflammation that carry high levels of LRRK2 (mutated or with particular polymorphisms) could have increased sensitivity to the presence of aggregated α-syn in the brain. The complexity of the potential functional interaction between a-syn and LRRK2 may also involve different types of glial cells that act on one another in neuroinflammatory processes, namely astrocytes and microglial cells (Liddelow *et al.,* 2017).

Neuron-neuron interaction might also play a role in the apparent spread of abnormal α-syn from one susceptible brain area to the next. Whether the cellular mechanisms dictating α-syn interaction with LRRK2 are cell-autonomous or non-cell-autonomous or some combination, therapeutic targeting of LRRK2, for better or worse, is almost exclusively focused on inhibiting LRRK2 kinase activity. In the second part of this review, we shall emphasize the different directions of research that provide yet imperfect but promising answers.

4.4 LRRK2 activity in α-syn expression and aggregation

As the endogenous levels of α-syn phosphorylation are low in the unaggregated state, the phosphorylation state of α-syn, notably on Serine 129, is an excellent readout of the aggregation of α-syn. In recent studies, G2019S-LRRK2 KI mice or G2019S-LRRK2 expressing rats exhibited significantly higher levels of pSer129 α-syn in the striatum compared to WT controls (Longo *et al.,* 2017; L. A. Volpicelli-Daley *et al.,* 2016). LRRK2 could affect the subcellular localization of α-syn, notably its membrane association, promoting the aggregation by increasing the cytosolic pool of α-syn. ThroughG2019S-LRRK2 upregulation of total levels of α-syn, the net effect may also be an increase in the aggregation-prone cytosolic pool. In SH-SY5Y cells studied byKondo and collaborators (Kondo, Obitsu, and Teshima 2011), the aggregation capacity of α-syn was evaluated in the presence or absence of G2019S-LRRK2. Cell viability decreases when the cells are co-transfected with α-syn and G2019S-LRRK2 but also with WT-LRRK2 whereas viability remains unchanged in presence of each protein alone. In differentiated cells, α-syn-containing vesicles are not produced when the cells are transfected with α-syn alone. In contrast, the co-transfection of α-syn with G2019S-LRRK2 induces the formation of aggregates and vesicles. Most of the α-syn aggregates co-localize with the mitochondrial outer-membrane marker TOM20 in cells co-transfected with α-syn and G2019S-LRRK2 but not with the WT form of LRRK2. In 2014, Skibinski and collaborators demonstrated that the neurotoxicity caused by G2019S-LRRK2 could be mitigated through knockdown of α-syn (Skibinski, Nakamura, Cookson, & Finkbeiner, 2014). More recently, a study in primary cortical neurons from homozygous G2019S-LRRK2 KI mice shows that expression of G2019S-LRRK2 induced the accumulation of endogenous, detergent-insoluble α-syn, and that this effect can be reversed through pharmacological inhibition of LRRK2 kinase activity (Schapansky *et al.,* 2018). Altogether, these observations indicate that LRRK2 can accelerate aggregation of α-syn, and possibly the localization of the aggregates, but the precise mechanisms have yet to be fully elucidated.

4.5 LRRK2 mediation of α-syn cell-to-cell propagation

It is now generally established that α-syn can propagate via the synapse in model systems *in vitro*, particularly those that use triple-chamber systems. In 2011, Volpicelli-Daley and colleagues observed this cell-to-cell transmission in chambered cultured neurons with bath-application of pre-formed α-syn fibrils (Volpicelli-Daley *et al.,* 2011). Kondo and collaborators also studied the cell-to-ctransmission of α-syn through evaluating exocytosis of α-syn in the media and the internalization in neighboringneuroblastoma cells (Kondo *et*

al., 2011). In this system, G2019S-LRRK2 significantly enhances α-syn release into the conditioned media. Interestingly the phosphorylation state of α-syn is not different in the cells co-transfected compared to cells transfected with α-syn alone, suggesting that LRRK2 can influence the propagation mechanism but not the phosphorylation state of α-syn (Kondo *et al.,* 2011). These preliminary observations warrant further investigations into LRRK2 mediation of cell-to-cell transmission of abnormal α-syn.

4.6 Impact of LRRK2 on α-syn-induced neuroinflammation

Evidence of on-going neuroinflammation in affected brain regions in PD first come from analysis of brain tissue for reactive microglia and analyses of pro-inflammatory cytokines like Interferon gamma, (IFN-γ), TNF-α, Interleukin-6 (IL-6), and Interleukin-1β, (IL-1β) (Hunt *et al.,* 1999; Mogi *et al.,* 1994; McGeer, Itagaki, and McGeer 1988; Mogi *et al.,* 1996). In addition, GWAS studies point to polymorphisms in loci with genes related to immunity (e.g. MHC-II genes). Neuroinflammation can be seen as adefense reaction that involves both the adaptative and innate immune systems, occurring in the central nervous system (CNS) after an event that perturbates "normal" homeostasis (reviewed in Gelders *et al.,* 2018; Xanthos and Sandkühler, 2014). It is widely accepted that neuroinflammation occurs in many different acute and chronic neurological disorders. Whether it is only a consequence of neurodegeneration or is also actually a key active player favoring or opposing neurodegeneration is unknown. Presenting extensively the *pros* and *cons* of these different hypotheses on the role of neuroinflammation in degenerative diseases is out of the scoop of the present review. Comprehensive overview of this aspect of PD pathogenesis can be found extremely well-reviewed elsewhere (e.g. Skaper *et al.*, 2018). In brief, number of experimental observations in animal models and neuropathological findings in post-mortem tissue from PD patients support the view that neuroinflammation modulates neurodegeneration. For example, in the acute model of PD in animals using the mitochondrial toxin MPTP, signs of neuroinflammation, including activated microglial cells, appear in the substantia nigra pars compacta (SNpc) before actual loss of dopaminergic cells (Liberatore *et al.,* 1999).Similar findings have been recently reported in a model using intrastriatal injection of pre-formed α-syn fibrils (Duffy *et al.*, 2018) and in a model of α-syn overexpression using AAV injection into the SN. In these synuclein related models, the presence of reactive microglia cells and proinflammatory molecules precedes neurodegeneration of dopaminergic neurons. Blockage/inhibition of signaling pathways linked to neuroinflammation reduces the loss of dopaminergic cells induced by MPTP (e.g. Wu *et al.,* 2002; Maatouk *et al.,* 2018). In models of PD using overexpression of α-syn, cellular pathways that trigger activation of microglial cells (such as Toll-like Receptors) favor neurodegeneration (Wong and Krainc, 2017). In line with this, it has been recently showed that the inhibition of the microglia-induced activation of astrocytes using agonists of the Glucagon-like peptide-1 receptor (GLP1R) into their neurotoxic phenotype protect against α-syn toxicity in mouse models (Yun *et al.*, 2018). However, all facets of neuroinflammation are not detrimental and to some extent, there are molecular components and signaling pathways linked to the regulation of immune and glial cells that play a protective role in PD models. For example, the partial ablation of microglial cells increases the vulnerability to MPTP in mice (Yang *et al.*, 2018). The overexpression of α-syn produces changes in activated microglial cells leading not only to the production of pro-inflammatory molecules (e.g. iNOS and IL1-beta) but also anti-inflammatory molecules (e.g. Heme oxygenase-1) (Lastres-Becker *et al.*, 2012).

LRRK2 is expressed not only in neurons in the brain but also in some subsets of immune cells that include myeloid cells (Isolectin B4 positive, CD68 positive) in pathological conditions (Moehle *et al.,* 2012; Daher *et al.,* 2014). In the periphery, LRRK2 is found to be expressed in monocytes with much lower expression in T cells involved in the adaptive immune system, suggesting a role for LRRK2 in the innate immune system (Thévenet, Gobert, van Huijsduijnen, Wiessner, & Sagot, 2011). GWAS studies show LRRK2 variants implicated in the heritability of Crohn's disease, a type of inflammatory bowel disease (IBD) that may affect any part of the gastrointestinal tract (Barrett, Hansoul, Nicolae, & Cho, 2008), as well as mycobacterium infection (Zhang *et al.,* 2009; Marcinek *et al.,* 2013; Wang *et al.,* 2015). Following, studies by Gardet and Hakami both suggest important roles for LRRK2 in the maturation of myeloid cells that offer host protection from infection (Gardet *et al.,* 2010; Hakimi *et al.,* 2011). Thissuggests that LRRK2 plays a role in innate immune responses not only in the nervous system but also in the periphery. The exact role of LRRK2 in the inflammatory response has not been characterized but these and other recent studies converge towards the observation that LRRK2 kinase inhibition or LRRK2 knockdown attenuates pro-inflammatory signaling *in vitro* and *in vivo* (B. Kim *et al.,* 2012; Ma *et al.,* 2015; Puccini *et al.,* 2015; Russo *et al.,* 2015).

The role of mutated LRRK2 in inflammatory processes has been recently shown. Kozina and colleagues demonstrated that in transgenic mice overexpressing mutant LRRK2, intraperitoneal injection of LPS is able to trigger a long-term inflammation associated with neurodegeneration of DA neurons in the SNpc, which is not the case in mice overexpressing the human wild type LRRK2 or wild type mice (Kozina *et al.*, 2018). This change produced by mutant LRRK2 is not directly linked to activation of innate brain cells but may be linked to a type II interferon immune response in peripheral cells. However, this does not rule out the possible role of LRRK2 in the regulation of brain immune cells, in particular microglia.

Microglial cells are resident innate immune cells and professional phagocytes of the brain, as well as the first line of defense against pathogens. In neurodegenerative disorders there are roles in clearing aggregated proteins and the clearance of dead cells and other

debris. Microglia can switch from a resting state (ramified phenotype) into an activated state (ameboid phenotype) through signaling molecules that mediate activation (e.g., MAPK subtypes p38, JNK and ERK). A failure in the appropriate and proportional activation process of microglia can have dramatic consequences. Excessive activation can lead to an abundant secretion of inflammatory mediators and reactive oxygen species that are cytotoxic to neurons. LPS (lipopolysaccharide) treatment, *in vitro* or *in vivo*, is known to induce a TLR4-mediated inflammatory response and microglial activation. In primary microglial cells, LPS exposure can induce the switch between the resting phenotype to the activated phenotype with an extension of processes into the environment and eventually a retraction into an amoeboid morphology. In cultured microglial cells isolated from tg mice overexpressing R1441G-LRRK2 or WT littermates, LPS treatment induces an increase in LRRK2 protein expression that is not reflected at the mRNA level, suggesting that LPS-treatment can impact the turn-over of LRRK2 (Gillardon, Schmid, & Draheim, 2012; Moehle *et al.,* 2012). In addition, R1441G-LRRK2 expression increases expression and secretion of proinflammatorycytokines (TNF) compared to WT microglia in culture (Gillardon *et al.,* 2012).RRK2 inhibitors, LRRK2-IN-1 and sunitinib, were found to attenuate the release and transcriptional induction of TNF and reduce phospho-p38 protein levels. Similarly, knockdown of LRRK2 by a lentivirus coding for an shRNA targeting LRRK2 has the same effect, except for the phosphorylation of p38 that remains unchanged by LRRK2 shRNA. More interestingly, in the presence of LRRK2 inhibitors or LRRK2 shRNA, the LPS treatment fails to induce the switch between the resting phenotype to the activated phenotype (Moehle *et al.,* 2012). The knockdown of LRRK2 in the microglial cell line BV-2 by lentiviral vectors encoding a shRNA significantly reduces the secretion of TNFα and IL-6 with an increase of NO production as compared to control conditions. Treatment with LPS in these knockdown cells induces a decrease in the level of the phosphorylated form of p38 and induces a significant reduction of nuclear factor kappa B (NF-kB) transcriptional activity while JNK and ERK are unaffected (B. Kim *et al.,* 2012). LRRK2 enhances the association of NFAT1 with proteins that seem to block the NFAT transport to the nucleus and thus inhibits the transcription of immune response genes (Liu *et al.,* 2011). Microglia isolated from LRRK2 KO mice have an increased α-syn uptake and clearance when treated with recombinant α-syn, compared to WT mice microglia (Maekawa *et al.,* 2016). In these studies, primary microglia and cell lines in culture adopt a macrophage-like phenotype on a transcriptional and functional level, necessitating studies *in vivo* with a preserved dynamic innate immune system (Butovsky *et al.,* 2014).

In LRRK2 knockout rats as well as LRRK2 knockout mice, LPS and Tat-induced neuroinflammation (respectively) are dramatically dulled compared to WT rodents (Daher *et al.,* 2014; Puccini *et al.,* 2015). The absence of LRRK2 protects from neurodegeneration induced by an AAV coding for α-syn (Daher *et al.,* 2014). Like LPS, injections of viral vectors coding α-syn are known to induce microglial activation. In this study, the number of CD68-positive cells recruited in response to α-synexpression is reduced in LRRK2 KO rats compared to WT rats. The morphology of IBA1-positive cells shift to the amoeboid (activated) phenotype in WT rats injected with α-syn that was not observed in LRRK2 KO rats also injected with α-syn. In addition, treatment with PF-06447475 attenuates the neuroinflammation in G2019S-LRRK2-BAC Tg rats when compared to untreated animals and to non-Tg rats expressing WT rat LRRK2 after the injection of AAV-α-syn (Daher *et al.,* 2015). Overall it seems likely that LRRK2 modulates the inflammatory response induced by α-syn. It could be imagined that G2019S-LRRK2 could increase the neuroinflammation induced by α-syn, therefore aggravating the deleterious effects of this neuroinflammation. Selective LRRK2 mutant expression or knockdown within cells of the immune system has not yet been described, limiting interpretations of mechanisms.

Many studies have correlated α-syn aggregates with activated microglia, MHC-II expression, and neuroinflammation. Studies in human post-mortem PD brain show that MHC-II detection of microglia performs as well as phosphorylated α-syn in staging brains in PD pathology (Imamura *et al.,* 2003). α-Syn fibrils, perhaps all fibrillized amyloid proteins, are substrates of TLR2 expressed in cells of the innate immune system, and can activate MyD88 pathways similar to TLR4 agonists (e.g., LPS). α-Syn fibrils and aggregates may bind to and activate both TLR2 and TLR4 (Codolo *et al.,* 2013; Daniele *et al.,* 2015; Gustot *et al.,* 2015; C. Kim *et al.,* 2013). The implication is that abnormal α-syn activates an immune response that may be potentiated by mutant LRRK2 expression. Alternatively, LRRK2 activity may initiate an abnormal immune response that causes α-syn to aggregate ineurons, with the immune response further potentiated in perpetuity with α-syn aggregates interacting with toll-like receptors. Future studies can dissect these possibilities.

4.7 LRRK2, α-syn, and 14-3-3s

Among all the pathways plausibly affected by α-syn and LRRK2, one possibility is that a common protein interactor could weave together the two proteins in a cell in response to specific stimuli. The 14-3-3 chaperone-like protein family is known to interact robustly with both α-syn and LRRK2, as well as becomes entrapped in LBs in PD (Berg, Holzmann, and Riess 2003; Kawamoto *et al.,* 2002; Nichols *et al.,* 2010). In 2002, Xu and collaborators showed that 14-3-3 proteins interact with α-syn in a 54-83-kD complex (Xu *et al.,* 2002). 14-3-3 sequestration in LBs, plausibly mediated by an interaction with α-syn, may cause loss of 14-3-3 function and lowered anti-apoptotic activity and lead to toxicity and cell death. Moreover, expression of 14-3-3 theta is significantly decreased in tg mice overexpressing human WT-α-syn under the platelet-derived growth factor beta promoter (Yacoubian *et al.,* 2008). In dopaminergic cells, the level of

tyrosine hydroxylase can be modulated both with α-syn and 14-3-3expression. 14-3-3 proteins are known to interact with phosphorylated TH to enhance its activity and to promote dopamine synthesis. α-Syn in turn may bind to unphosphorylated TH to reduce its activity (for more details see Review from Berg, Holzmann, and Riess 2003). This is a compelling exampe of how 14-3-3 and α-syn binding to each other may manipulate cell phenotypes associated with a rate-limited enzyme (TH) critical for neuronal phenotypes.

As with α-syn and LRRK2, 14-3-3 proteins themselves are subject to phosphorylation. In 2015, Slone and collaborators found that modulation of 14-3-3 phosphorylation reduced their neuroprotective potential (Slone, Lavalley, McFerrin, Wang, & Yacoubian, 2015). 14-3-3 binding to LRRK2 is mediated by the LRRK2 Ser910 and 935 phosphorylation sites (Gloeckner *et al.,* 2010; Nichols *et al.,* 2010; West *et al.,* 2007). Oxidative stress may promote dephosphorylation of LRRK2 causing a loss of 14-3-3 binding to LRRK2 (Mamais *et al.,* 2014). Disruption of 14-3-3 binding to LRRK2 alters LRRK2 localization in the cell and potentially affects LRRK2 kinase activity and membrane-related functions, such as exosome release (Dzamko *et al.,* 2010; Mamais *et al.,* 2014). 14-3-3 binding to LRRK2 could prevent the dephosphorylation of LRRK2 and may stabilize LRRK2 structure. In 2017, Civiero and collaborators showed *in vitro* that the serine/threonine kinase PAK6 bound and phosphorylated 14-3-3gamma at its Ser59residue, thus promoting 14-3-3gamma/LRRK2 complex dissociation. In neurons, the activation of this kinase rescues G2019S-LRRK2 neurotoxicity (Civiero *et al.,* 2017). Other recent work concluded that 14-3-3 binding to LRRK2 could control LRRK2 kinase activity (Lavalley *et al.,* 2016). 14-3-3 binding to LRRK2 preventes LRRK2 kinase activity and autophosphorylation, whereas a loss of 14-3-3 expression and binding result in hyper-activated LRRK2 and exacerbate LRRK2 neurotoxicity. In a cell autonomous manner, α-syn-mediated sequestration of 14-3-3 proteins may hyper-activate LRRK2 kinase activity, encourage pro-apoptotic pathways, and reduce levels of dopamine synthesis needed for proper basal ganglia function.

4.8 α-syn, LRRK2, and Mitochondria

Mitochondria have been a favorite organelle for study in PD-related research stemming back to post-mortem descriptions of a complex I deficiency in the striatum (Mizuno *et al.,* 1989) and in the SNc (Schapira *et al.,* 1990) of PD patients. Mitochondrial complex I inhibitors (for example rotenone or MPTP) can also induce parkinsonism in exposed people as well as in rodents (Langston and Ballard 1983; Schapira 2008). Mutations in the genes encoding PARKIN, DJ-1 and PINK1 cause autosomal recessive forms of PD, and these proteins are all involved in mitochondrial quality control (reviewed in Dawson, Ko, and Dawson 2010). In rodents, endogenous as well as exogenously administered α-syn (WT or A53T) localizes in-part to mitochondria (Chinta, Mallajosyula, Rane, & Andersen, 2010; Li *et al.,* 2007; Martin *et al.,* 2006; Nakamura *et al.,* 2008; Subramaniam, Vergnes, Franich, Reue, & Chesselet, 2014; Ling Zhang *et al.,* 2008). α-Syn may directly interact with TOM20 (translocase of the outer mitochondrial membrane) and inhibit mitochondrial protein import (Di Maio *et al.,* 2016). Moreover, partial homology to mitochondrial targeting sequence was found in the N-term portion of α-syn. α-Syn binding to mitochondrial membranes appears particularly high in the striatum, in the SNc and in the cortex of PD brains, regions highly affected in PD pathology (Devi, Raghavendran, Prabhu, Avadhani, & Anandatheerthavarada, 2008). α-Syn import to mitochondria may depend on intracellular pH (Cole, DiEuliis, Leo, Mitchell, & Nussbaum, 2008) and on mitochondrial membrane potential and the ATP pool (Devi *et al.,* 2008). *In vitro*, about 10% of total LRRK2 protein localizes to a mitochondrial enriched protein fraction (West *et al.,* 2005), although a lower percentage is probably associated with the outer mitochondrial membrane without significant levels detected inside mitochondria (Biskup *et al.,* 2006).

Studies in model systems with increased or abnormal α-syn expression, or mutant LRRK2, have demonstrated compromised mitochondrial function such as decreased mitochondrial membrane potential and ATP production and increased oxidative stress(Butler *et al.,* 2012; Mortiboys *et al.,* 2015; Papkovskaia *et al.,* 2012; Parihar *et al.,* 2008; Su and Qi 2013; Wang *et al.,* 2012; Melo *et al.,* 2016; Erustes *et al.,* 2017; Martinez *et al.,* 2018; Martin *et al.,* 2006; Mortiboys *et al.,* 2010; Sarafian *et al.,* 2013). While α-syn null mice are protected against MPTP toxicity, and tg mice overexpressing human α-syn may be more sensitive to MPTP-induced toxicity (Dauer *et al.,* 2002; Klivenyi *et al.,* 2006; Song, Shults, Sisk, Rockenstein, & Masliah, 2004), LRRK2 knockout mice do not appear protected from MPTP (Andres-Mateos *et al.,* 2009). However, mice over-expressing G2019S-LRRK2 appear more sensitive to MPTP (Karuppagounder *et al.,* 2015). Thus, at least through MPTP, both α-syn and LRRK2 appear to have a functional role in mitochondria-dysfunction that can cause neurodegeneration.

While the mechanism of how LRRK2 interacts with mitochondria is speculative at this time, several studies may shed light on α-syn interaction with mitochondria. α-Syn KO mice present with reductions of mitochondria respiration and linked CI/III activity (Ellis *et al.,* 2005), and tg mice expressing α-syn A53T in DA neurons present an age-related mitochondrial CI inhibition (Chinta *et al.,* 2010). Devi and collaborators have identified in 2008 a large decrease in CI activity associated with abnormal α-syn, both in human fetal primary cortical neuronal cultures overexpressing α-syn and in mitochondria isolated from the ST and SN of autopsy brain hemispheres from PD subjects (Devi *et al.,* 2008) and these results have been reproduced in other *in vitro* models (Loeb, Yakunin, Saada, & Sharon, 2010;

Reeve *et al.,* 2015). Mitochondria isolated from Wistar rats exposed to different concentrations of recombinant human α-syn also show a dose-dependent decrease in CI activity (Liu *et al.,* 2009).

Potentially corroborating these results, Tg mice expressing A53T-α-syn display dysmorphic mitochondria (Martin *et al.,* 2006). Double tg mice α-syn/parkin KO have marked alterations ofitochondrial architecture, especially in the SN and cortex (Stichel *et al.,* 2007). Similarly, tg A53T mice show changes in mitochondrial morphology and decreased mitochondrial interconnectivity (Xie & Chung, 2012) and even fragmented mitochondria that appear before DA neuron loss (Chen, Xie, Turkson, & Zhuang, 2015).*In vitro*, α-syn knock down increases the number of cells presenting elongated mitochondria (Kamp *et al.,* 2010) and overexpression of both WT and A53T-α-syn induced the fragmentation of mitochondria (Butler *et al.,* 2012; Devoto *et al.,* 2017; Guardia-Laguarta *et al.,* 2014; Martinez *et al.,* 2018) that precedes any disturbance in mitochondrial function and cell death (Nakamura *et al.,* 2011). This effect of α-syn on mitochondrial fragmentation was also shown in DA neurons derived from patients with the A53T mutation (Ryan *et al.,* 2018). Moreover, this α-syn-dependent mitochondrial fragmentation requires a direct interaction with the outer mitochondrial membrane in iPS overexpressing α-syn (Devoto *et al.,* 2017). In primary mouse cortical cultures, astrocytes internalize α-syn oligomers causing mitochondrial fragmentation after a 24h exposure (Lindström *et al.,* 2017). In particular, Grassi and collaborators recently identified a conformationally distinct phosphorylated α-syn species (resulting from the incomplete degradation of fibrillar α-syn) that associates with mitochondria to induce mitochondrial dysfunction (Grassi *et al.,* 2018). More precisely, significant reductions of Mnf1 and 2 proteins were observed in tg A53T mice with no changes in Drp1 or OPA1 (Xie and Chung 2012). Drp1 mostly locates in the cytoplasm, but is stimulated after fission stimuli to migrate to the mitochondria. In Drp1 KO mice, the overexpression of WT-α-syn still induces significant fragmentation of mitochondria, even though it is still less importat than in the WT mice, implying that α-syn-induced mitochondrial fragmentation might go through an effect on Drp1, but that it would not be the only mechanism (Nakamura *et al.,* 2011). Thus, these findings suggest that the fragmentation of mitochondria caused by α-syn aggregation and expression decreases mitochondrial fusion, rather than an increase in fission.

LRRK2 may interact with Drp1 to enhance Drp1 mitochondrial translocation, and the blockage of Drp1 inhibits mitochondrial fragmentation and dysfunction (Niu, Yu, Wang, & Xu, 2012; Su & Qi, 2013; X. Wang *et al.,* 2012). G2019S-LRRK2 might phosphorylate Drp1 leading to mitochondrial fragmentation (Su & Qi, 2013). Through this pathway, LRRK2 kinase activity could activate Drp1 and enhance its localization to mitochondria, therefore tipping the balance in favor of mitochondrial fission. Supporting this hypothesis, LRRK2 (and not its dead kinase mutant) enhances ROS production, which is known to lead to increased fission (Niu *et al.,* 2012). However, Saez-Atienzar and collaborators observed the opposite effects: in their *in vitro* study, it was the pharmacological inhibition of LRRK2 that led to a Drp-1-dependent increase in mitochondrial fission (Saez-Atienzar *et al.,* 2014). Similarly, there is no conclusion as to the effect of LRRK2 expression or activity on mitochondrial morphology. In a tgfly model, the expression of G2019S-LRRK2 is associated with mitochondrial deformity (Mortiboys *et al.,* 2015). *In vitro*, in cell lines, the expression of WT-LRRK2, and even more that of G2019S or R1441C-LRRK2 induces mitochondrial fragmentation (Su & Qi, 2013; X. Wang *et al.,* 2012). Interestingly, this effect seems to be kinase-dependent, which is consistent with the fact that the G2019S mutant has more pronounced effects on mitochondria (Su & Qi, 2013; X. Wang *et al.,* 2012). However, two other studies demonstrated the opposite results in fibroblasts derived from PD patients carrying the G2019S mutation, one observing an increased mitochondrial fragmentation, pointing towards a misbalance in favor of mitochondrial fission (Niu *et al.,* 2012), and the other enhanced mitochondrial elongation and interconnectivity, pointing towards a misbalance in favor of mitochondrial fusion (Mortiboys *et al.,* 2010). Further, the direct effect of LRRK2 on mitochondrial respiration is not clear. In HEK cells, the expression of WT-LRRK2, and to a further degree G2019S, decrease both CI and CIV activities (Su & Qi, 2013). In other model systems, tg flies expressing G2019S, G2385R, or I2020T-LRRK2 are more sensitive to rotenone-induced toxicity (Ng *et al.,*2009; Venderova *et al.,* 2009), and in *C. elegans*, WT-LRRK2 but not G2019S-LRRK2 expression protects against rotenone-induced toxicity (Saha *et al.,* 2009).

Taken together, these studies may imply that LRRK2 and α-syn can have a direct effect on the mitochondrial respiratory chain, leading to mitochondrial dysfunction and altered energy production. However, second hypothesis that links LRRK2 and α-syn with the disruption of the equilibrium between mitochondrial fission and fusion also seems plausible. All the data showing an effect of α-syn and LRRK2 on the toxicity of complex I inhibitors point towards a potential effect of α-syn and LRRK2 on mitochondrial respiratory chain, more precisely on CI activity. These complex I defects can lead to oxidative stress, a decrease in ATP production or in mitochondrial respiration (Devi *et al.,* 2008; Loeb *et al.,* 2010; Reeve *et al.,* 2015). All of these events ending up inmitochondrial dysfunction could therefore be a relevant explanation for the mitochondrial deficits induced by α-syn and LRRK2. As mitochondrial homeostasis is a finely regulated process with a precise equilibrium between fission (involving the proteins Drp1 (Dynamin-related protein 1), Fis1 and GDAP1) and fusion (involving the proteins Mfn 1 and 2 and OPA1), mitochondrial fragmentation can reflect an increase in mitochondrial fission or a decrease in mitochondrial fusion. Overall, these results suggest that α-syn and LRRK2 have the potential for a common effect on two major aspects of mitochondrial homeostasis: the energy production and the dynamics of mitochondria. However, there is a tight relationship between the structure and the energy function of the mitochondrial network, and an alteration of one aspect has repercussions on the other. It is

therefore difficult to know which effect comes first, but newer model systems with conditional manipulation of LRRK2 and α-syn may shed light onto the relationship between these proteins, mitochondrial respiratory chain function and fusion and fission events.

4.9 α-syn, LRRK2 and Autophagy

Proteins can be removed by the ubiquitin-proteasome system (UPS) as well as the autophagy-lysosome pathway (ALP), and both have been extensively evaluated with respect to LRRK2 and α-syn in PD models. α-Syn degradation via the UPS was observed and UPS dysfunction was predicted to lead to α-syn accumulation in early studies (Bennett *et al.,* 1999; McNaught *et al.,* 2002; Tofaris, Layfield, & Spillantini, 2001; Webb, Ravikumar, Atkins, Skepper, & Rubinsztein, 2003). However, other groups failed to show an involvement of the proteasome machinery in this process (Ancolio, Alves Da Costa, Uéda, & Checler, 2000; Rideout, Larsen, Sulzer, & Stefanis, 2001; Rideout & Stefanis, 2002; Vogiatzi, Xilouri, Vekrellis, & Stefanis, 2008) suggesting another pathway to α-syn degradation such as ALP (Petroi *et al.,* 2012). Given the close overlap between LRRK2 and α-syn in other pathways we describe here, LRRK2 function may shed light on this controversy.

Autophagy clears cytoplasmic components through three distinct pathways depending of the way substrates reach the lysosomal lumen and the types of substrates supported: chaperone-mediated autophagy (CMA), macroautophagy, and microautophagy (Ana Maria Cuervo, 2004; Levine & Klionsky, 2004). In contrast, the UPS mainly drives short-lived protein degradation, typically via polyubiquitin chains, whereas autophagy is responsible for long-lived proteins, larger protein aggregates, and cytoplasmic organelles (Zhang *et al.,* 2012). CMA involves chaperone proteins (especially hsc0) which bind target proteins containing a KFERQ peptide motif. These chaperones address the proteins to lysosomes where they interact with the lysosomal receptor, LAMP2a, the rate-limiting step in CMA (A. M. Cuervo & Dice, 1996; Majeski & Fred Dice, 2004; A. Massey, Kiffin, & Cuervo, 2004). At the membrane, LAMP2a multimerizes to allow substrate translocation inside the lysosome with the help of lys-hsc70, an intraluminal chaperone (Agarraberes, Terlecky, and Dice 1997; Cuervo, Dice, and Knecht 1997). Macroautophagy involves the creation of a double membrane structure, named phagophore, engulfing proteins and organelles. Closure completion of the phagophore forms the autophagosome which will fuse with lysosomes to generate the autolysosome, where substrates are degraded. Mitophagy is a subtype of macroautophagy which leads to dysfunctional mitochondria degradation. (Shintani & Klionsky, 2004). The molecular machinery participating in macroautophagy is composed of different type of proteins, including Atg proteins, and Beclin. Microautophagy involves the engulfment and internalization (pinocytosis) of small quantities of cytosol components directly by lysosomes (A. Massey *et al.,* 2004; Müller *et al.,* 2000). In PD brains, autophagic characteristics were shown through immunohistochemistry (Anglade, Vyas, Hirsch, & Agid, 1997) and impairment of autophagy (defective clearance of autophagosomes and lysosomal depletion) was observed in PD patient brains (Dehay *et al.,* 2010). Additionally, LAMP2a and HSC70 protein levels in the SNc of PD patient brains were decreased (Alvarez-Erviti *et al.,* 2010).

The potential degradation of α-syn by CMA is suggested since the protein contains a CMA recognition motif (95-VKKDQ-99) (Cuervo *et al.,* 2004; Dice 1990). First evidence confirming this hypothesis was depicted incubating α-syn with isolated liver lysosomes showing its degradation in a CMA-dependent manner (Cuervo *et al.,* 2004). Evidence of α-syn degradation by CMA is also demonstrated in cell lines and neurons using lysosomal inhibitors which lead to α-syn accumulation (Lee *et al.,* 2004; Paxinou *et al.,* 2001; Webb *et al.,* 2003). In 2004, Cuervo and collaborators also demonstrated that the mutant forms of α-syn (A53T and A30P) can bind to lysosome membranes but can not be engulfed and degraded efficiently by lysosomes. In fact, mutant α-syn interacts more strongly with LAMP2a, blocking CMA (Cuervo *et al.,* 2004). In different cell lines and in primary neuronal cells, mutant α-syn interaction with LAMP2a and impairment of CMA is also demonstrated (Vogiatzi *et al.,* 2008). More recently, decreasing LAMP2a expression through a strategy of shRNA-AAV injections in rat brain results in intracellular accumulation of α-syn and autophagic vacuoles (Xilouri *et al.,* 2016). Additionally, when the recognition motif 95-VDKKQ-99 is mutated, CMA is dysfunctional and compensatory mechanisms occur with the activation of macroautophagy (Vogiatzi *et al.,* 2008; Xilouri, Vogiatzi, Vekrellis, Park, & Stefanis, 2009). In cell culture, LAMP2a silencing blocks CMA but upregulates macroautophagy and sensitizes cells to oxidative stress suggesting also a compensatory mechanism (Massey *et al.,* 2006). α-Syn overexpression inhibits macroautophagy through blockade of autophagosome formation. However, cells expressing α-syn in contact with preformed α-syn aggregates leads to the formation of autophagosomes but their clearance is blocked (Tanik, Schultheiss, Volpicelli-Daley, Brunden, & Lee, 2013). In Atg7 knock out mice, macroautophagy impairment leads to ubiquitinated proteins, α-syn and p62 increased (Ahmed *et al.,* 2012). In another model of Atg7 knock out targeting TH positive cells, accumulation of α-syn in dopaminergic neurons, especially midbrain dopaminergic dendrites which exhibit numerous varicosities containing massive ubiquitinated inclusions, was identified (Friedman *et al.,* 2012). Mechanistically, α-syn compromises autophagy via Rab1a inhibition and causes mislocalization of the autophagy protein Atg9. Atg9 is implicated in the initiation of autophagosome formation (Winslow *et al.,* 2010). Additional experiments are needed in order to decipher the molecular mechanisms implicated in macroautophagy in α-syn toxicity.

While fewer studies have explored LRRK2 function in the UPS and ALP, LRRK2 contains several CMA targeting motifs suggesting its possible degradation by CMA. The role of LRRK2 in CMA has been partially elucidated in a study from Orenstein in 2013. In this study, LRRK2 is degraded by CMA as knock down of LAMP2a increases intracellular levels of LRRK2. Degradation of LRRK2 reaches 50% of normal levels in LAMP2a knock downs whereas G2019S-LRRK2 is limited suggesting impairment of CMA through mutant LRRK2 activity (Orenstein *et al.,* 2013). Degradation of LRRK2 through macroautophagy is supported through experiments in Atg5 KO and Atg7 KO mice showing accumulation of LRRK2 in cells and tissue (Friedman *et al.,* 2012). Moreover, a fraction of LRRK2 is localized to membranes (Berger, Smith, & Lavoie, 2010; Biskup *et al.,* 2006) and more specifically to autophagic vacuoles, amphisomes, and autolysosomes and lysosomes (Alegre-Abarrategui *et al.,* 2009; Mark W. Dodson, Zhang, Jiang, Chen, & Guo, 2012; Higashi *et al.,* 2009; Orenstein *et al.,* 2013). However, contradictory results were obtained on the role of LRRK2 in macroautophagy. On the one hand, several groups observe a positive regulation of autophagy by LRRK2.Saha and collaborators demonstrate that expression of human LRRK2 or dead kinase LRRK2 in C. elegans increases autophagy (Saha *et al.,* 2015). In macrophages and microglial cells, LRRK2 knockdown significantly decreases the autophagic capacity (reduction of LC3 conversion), and LRRK2 inhibitors (GSK2578215A or LRRK2-IN-1) block protein aggregate clearance (Schapansky, Nardozzi, Felizia, & LaVoie, 2014). In 2010, Tong and collaborators showed that LRRK2 KO mice present accumulation of lipofuscin granules and p62 protein and a decrease of LC3-II conversion in renal tubule cells of aged mice (Tong *et al.,* 2010), suggesting slowdown of autophagy in those cells. In flies, knockout of the LRRK2 ortholog dLRRK leads to an impairment of autophagy with enlarged early endosomes, accumulation of autophagosomes which involves a modulation of Rab9 activity (Dodson *et al.,* 2014). On the other hand, knock down of LRRK2 by siRNA produces an induction of autophagy suggesting LRRK2 act as a negative regulator of autophagy (Alegre-Abarrategui *et al.,* 2009). In astrocytes, inhibition of LRRK2 stimulates macroautophagy in an mTor independent manner that requires Beclin (Manzoni *et al.,* 2016). Bravo-San Pedro et collaborators observed an increase of autophagy induction (increase of LC3, LAMP2, Beclin1 and decrease p62) in G2019S-LRRK2 skin fibroblasts from PD patients via a MAPK/ERK dependent pathway resulting in a highest sensitization to cell death (Bravo-San Pedro *et al.,* 2013). As usual, the apparent discrepancies between these different studies may originate from different experimental conditions and cell types used, but as yet there is no clear consensus of LRRK2 effect on ALP.

To go deeper in our understanding of the possible link between α-syn, LRRK2 and ALP, an interesting point is the role of Rab proteins and particularly Rab7. In fact, as mentioned above, Rab7 interacts with LRRK2 and plays a role in autophagosome and lysosome trafficking, positioning, and fusion events. Rab7 promotes clearance of α-syn aggregates (Dinter *et al.,* 2016). Rab7 is also a key regulator of late endosome maturation and autophagosome-lysosome fusion (Jager, 2004). Therefore, it is conceivable that the link between LRRK2 and α-syn in producing autophagy defects would be through Rab-dependent action, for example Rab7, at the membrane of autophagosomes. This modulation could interfere with trafficking of autophagosomes, which need to reach the soma to fuse with lysosomes to have an efficient autophagy.

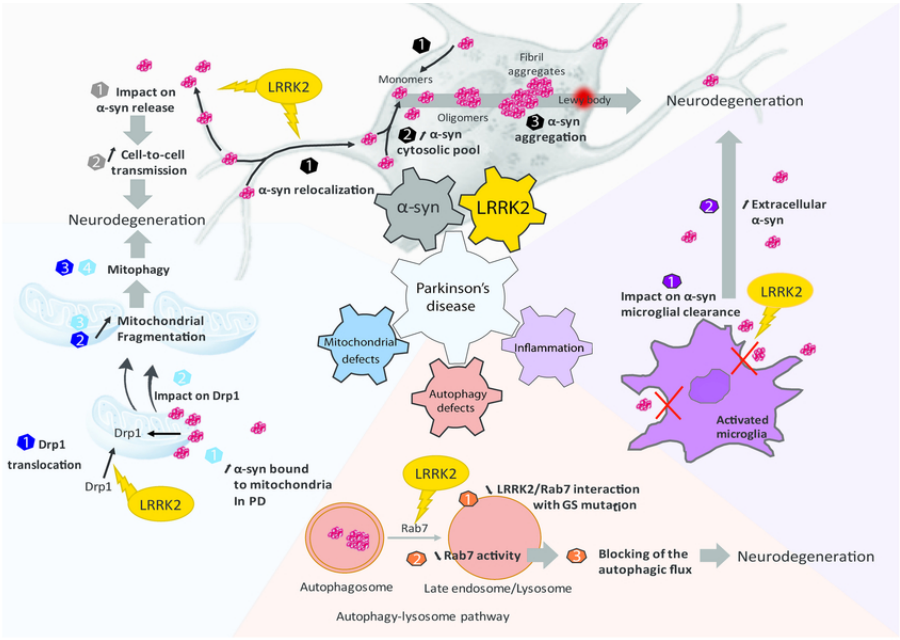

Figure 1: **Cellular dysfunction and neurodegeneration through several distinct but non-mutually exclusive mechanisms.** LRRK2 could have an impact on α-syn release (grey numbers) as well as on its relocalization (black numbers) leading to a cell-cell transmission of the pathology and to an increase of the aggregation through an excess of α-syn in the cytosolic pool (grey part). Three mechanisms seem to be impacted: the mitochondrial biology (blue part), the autophagic system (orange part) and the inflammation (violet part). Both LRRK2 and α-syn are known to play a role in mitochondrial biology through Drp1 (blue number) in favor of a mitochondrial fragmentation leading to mitophagy and cell death. Inside the cell, α-syn aggregates are mainly degraded by the autophagic-lysosomal pathway, which is one of the major protein breakdown systems (orange part). LRRK2 was found to decrease the activity of Rab7, which is implicated in the maturation of the autophagosome and thus blocking the degradation of the α-syn aggregates. Outside the cell, α-syn aggregates are captured by microglia to be degraded. One hypothesis is that LRRK2 could alter the machinery of phagocytosis leading to an accumulation of extracellular aggregates.

5. Conclusion and future directions

A compelling and growing body of evidence points towards a functional interaction between α-syn and LRRK2. Intriguingly, in many studies, larger effects are observed by knocking down LRRK2 expression or activity compared to over-expressing mutated LRRK2, giving hope that LRRK2-targeting therapeutics may offer benefit to all PD patients rather than just those that have LRRK2 mutations. Yet, the underlying mechanisms that dictate LRRK2 and α-syn interaction in PD are not clear. Based on our current understanding of both proteins in disease, cell autonomous and non-cell autonomous pathways are likely relevant in linking the proteins together in pathogenesis and disease progression. When expressed in the same cell, in disease, α-syn and LRRK2 likely interact in response to mitochondria disruption, in autophagy pathways in the endolysosomal system, as well as in normal interactions with common protein partners like 14-3-3 that maintain homeostasis of a number of systems. While α-syn expression in the brain is highly restricted to neurons, LRRK2 is also expressed in the immune system, particularly in cells known to respond to amyloid forms of α-syn, and LRRK2 appears to exacerbate damaging pro-inflammatory responses caused by α-syn. Considering current knowledge, none of the mechanisms we discussed in this review appear to be more prominent than the others. These interactions will all take time and more advanced model systems and experiments to fully resolve. In the meantime, therapeutic targeting of both LRRK2 and α-syn, if our understanding of these proteins in disease is at least partially correct, should provide the best opportunities to intervene in the disease process.

Acknowledgements: NC is a recipient of a PhD fellowship from Association France Parkinson (2016). CG is a recipient of the PhD fellowship from the French Ministry of Research. FG is funded by the European Union Horizon 2020 Programme (H2020-MSCA-ITN-2015) under the Marie Skłodowska-Curie Innovative Training Network and Grant Agreement No. 676408. EB is supported by "Fondation de France, Parkinson committee" grants (AAP 2010, Engt 00016819 and AAP 2014, Engt 2014-0052580) and the national "Translational Research Infrastructure for Biotherapies in Neurosciences" (NeurATRIS, "Investissement d'Avenir", ANR-11-INBS-0011). ABW is supported by NIH grants R01 NS064934, U01 NS097028, and R33 NS097643.

Authors' contributions: N.C. wrote the first draft of the review with E.B. with a focus on PD characteristics and pathogenesis. She also contributed to the drawing of figure 1. C.G. LG. and M-C G. focused on the detailed autophagy and mitochondrial mechanisms potentially involved in PD and the synergy between a-syn and LRRK2. F.G. edited the text and the figure. He took in charge the management of references to double-check for scientific relevance. A.B.W. and E.B. supervised the writing of the manuscript and edited the text.

Conflict of interests: The authors of the present review declare to have no conflict of interest.

References

Abdelmotilib, H., Maltbie, T., Delic, V., Liu, Z., Hu, X., Fraser, K.B., Moehle, M.S., Stoyka, L., Anabtawi, N., Krendelchtchikova, V., Volpicelli-Daley, L.A. & West, A. (2017) α-Synuclein fibril-induced inclusion spread in rats and mice correlates with dopaminergic Neurodegeneration. Neurobiol Dis, 105, 84–98.

Adams, J.R., Van Netten, H., Schulzer, M., Mak, E., Mckenzie, J., Strongosky, A., Sossi, V., Ruth, T.J., Lee, C.S., Farrer, M., Gasser, T., Uitti, R.J., Calne, D.B., Wszolek, Z.K. & Stoessl, A.J. (2005) PET in LRRK2 mutations: Comparison to sporadic Parkinson's disease and evidence for presymptomatic compensation. Brain, 128, 2777–2785.

Agarraberes, F. A., Terlecky, S. R., & Dice, J. F. (1997) An intralysosomal hsp70 is required for a selective pathway of lysosomal protein degradation. J Cell Biol, 137, 825–834.

Ahmed, I., Liang, Y., Schools, S., Dawson, V. L., Dawson, T. M., & Savitt, J. M. (2012) Development and Characterization of a New Parkinson's Disease Model Resulting from Impaired Autophagy. *J Neurosci*, 32, 16503–16509.

Alegre-Abarrategui, J., Christian, H., Lufino, M. M. P., Mutihac, R., Venda, L. L., Ansorge, O., & Wade-Martins, R. (2009) LRRK2 regulates autophagic activity and localizes to specific membrane microdomains in a novel human genomic reporter cellular model. *Hum Mol Genet*, 18, 4022–4034.

Alessi, D. R., & Sammler, E. (2018) LRRK2 kinase in Parkinson's disease. *Science*, 360, 36–37.

Alvarez-Erviti, L., Rodriguez-Oroz, M. C., Cooper, J. M., Caballero, C., Ferrer, I., Obeso, J. A., & Schapira, A. H. V. (2010) Chaperone-mediated autophagy markers in Parkinson disease brains. *Arch Neurol*, 67, 1464–1472.

Ancolio, K., Alves Da Costa, C., Uéda, K., & Checler, F. (2000) α-Synuclein and the Parkinson's disease-related mutant Ala53Thr-α-synuclein do not undergo proteasomal degradation in HEK293 and neuronal cells. *Neurosci Lett*, 285, 79–82.

Andres-Mateos, E., Mejias, R., Sasaki, M., Li, X., Lin, B.M., Biskup, S., Zhang, L., Banerjee, R., Thomas, B., Yang, L., Liu, G., Beal, M.F., Huso, D.L., Dawson, T.M. & Dawson, V.L. (2009) Unexpected lack of hypersensitivity in LRRK2 knock-out mice to MPTP (1-methyl-4-phenyl-1,2,3,6-tetrahydropyridine). *J Neurosci*, 29, 15846–15850.

Anglade, P., Vyas, S., Hirsch, E. C., & Agid, Y. (1997) Apoptosis in dopaminergic neurons of the human substantia nigra during normal aging. *Histol Histopathol*, 12, 603–610.

Barrett, J., Hansoul, S., Nicolae, D., & Cho, J. (2008) Genome-wide association defines more than 30 distinct susceptibility loci for Crohn's disease. *Nat Genet*, 40, 955–962.

Bendor, J. T., Logan, T. P., & Edwards, R. H. (2013) The Function of a-Synuclein. *Neuron*, 79, 1044–1066.

Bennett, M. C., Bishop, J. F., Leng, Y., Chock, P. B., Chase, T. N., & Mouradian, M. M. (1999) Degradation of alpha-synuclein by proteasome. *J Biol Chem*, 274, 33855–33858.

Benskey, M. J., Sellnow, R. C, Sandoval, I. M., Sortwell, C. E., Lipton, J. W. & Manfredsson, F. P. (2018) Silencing Alpha Synuclein in Mature Nigral Neurons Results in Rapid Neuroinflammation and Subsequent Toxicity. *Front Mol Neurosci*, 11, 1–21.

Berg, D., Holzmann, C., & Riess, O. (2003) 14-3-3 Proteins in the Nervous System. *Nat Rev Neurosci*, 4, 752–762.

Berger, Z., Smith, K. A., & Lavoie, M. J. (2010) Membrane localization of LRRK2 is associated with increased formation of the highly active LRRK2 dimer and changes in its phosphorylation. *Biochemistry*, 49, 5511–5523.

Biernacka, J. M., Armasu, S. M., Cunningham, J. M., Eric Ahlskog, J., Chung, S. J., & Maraganore, D. M. (2011) Do interactions between SNCA, MAPT, and LRRK2 genes contribute to Parkinson's disease susceptibility? *Parkinsonism Relat Dis*, 17, 730–736.

Biskup, S., Moore, D.J., Celsi, F., Higashi, S., West, A.B., Andrabi, S.A., Kurkinen, K., Yu, S.W., Savitt, J.M., Waldvogel, H.J., Faull, R.L.M., Emson, P.C., Torp, R., Ottersen, O.P., Dawson, T.M. & Dawson, V.L. (2006) Localization of LRRK2 to membranous and vesicular structures in mammalian brain. *Ann Neurol*, 60, 557–569.

Biskup, S., & West, A. B. (2009) Zeroing in on LRRK2-Linked Pathogenic Mechanisms in Parkinson's Disease. *Biochim Biophys Acta*, 7, 625-633.

Biskup, S., Moore, D.J., Celsi, F., Higashi, S., West, A.B., Andrabi, S.A., Kurkinen, K., Yu, S.W., Savitt, J.M., Waldvogel, H.J., Faull, R.L.M., Emson, P.C., Torp, R., Ottersen, O.P., Dawson, T.M. & Dawson, V.L. (2012) Age at onset in LRRK2-associated PD is modified by SNCA variants. *J Mol Neurosci*, 48, 245–247.

Bouhouche, A., Tibar, H., Haj, R.B.E., El Bayad, K., Razine, R., Tazrout, S., Skalli, A., Bouslam, N., Elouardi, L., Benomar, A., Yahyaoui, M. & Regragui, W (2017) LRRK2 G2019S Mutation: Prevalence and Clinical Features in Moroccans with Parkinson's Disease. *Parkinson Dis*.

Braak, H., & Braak, E. (2000) Pathoanatomy of Parkinson's disease. *J Neurol*, 247, II3-II10.

Braak, H., & Del Tredici, K. (2004) Poor and protracted myelination as a contributory factor to neurodegenerative disorders. *Neurobiol Aging*, 25, 19–23.

Bravo-San Pedro, J.M., Niso-Santano, M., Gómez-Sánchez, R., Pizarro-Estrella, E., Aiastui-Pujana, A., Gorostidi, A., Climent, V., López De Maturana, R., Sanchez-Pernaute, R., López De Munain, A., Fuentes, J.M. & González-Polo, R.A. (2013) The LRRK2 G2019S mutant exacerbates basal autophagy through activation of the MEK/ERK pathway. *Cell Mol Life Sci*, 70, 121–136.

Buck, K., Landeck, N., Ulusoy, A., Majbour, N. K., El-Agnaf, O. M. & Kirik, D. (2015) Ser129 Phosphorylation of Endogenous α-Synuclein Induced by Overexpression of Polo-like Kinases 2 and 3 in Nigral Dopamine Neurons Is Not Detrimental to Their Survival and Function. *Neurobiol Dis*, 78, 100–114.

Busquets, M. A., Espargaró, A., Estelrich, J., & Sabate, R. (2015) Could α -synuclein amyloid-like aggregates trigger a prionic neuronal invasion? *Biomed Res Int*.

Butler, E. K., Voigt, A., Lutz, A. K., Toegel, J. P., Gerhardt, E., Karsten, P., Falkenburger, B., Reinartz, A., Winklhofer, K. F. & Schulz, J. B. (2012) The mitochondrial chaperone protein TRAP1 mitigates alpha-synuclein toxicity. *Plos Genet*, 8.

Butovsky, O., Jedrychowski, M.P., Moore, C.S., Cialic, R., Lanser, A.J., Gabriely, G., Koeglsperger, T., Dake, B., Wu, P.M., Doykan, C.E., Fanek, Z., Liu, L., Chen, Z., Rothstein, J.D., Ransohoff, R.M., Gygi, S.P., Antel, J.P. & Weiner, H.L. (2014)Identification of a unique TGF-β-dependent molecular and functional signature in microglia. *Nat Neurosci*, 17, 131–143.

Cacabelos, R. (2017) Parkinson's disease: From pathogenesis to pharmacogenomics. *Int J Mol Scices*, 18.

Calì, T., Ottolini, D., Negro, A. & Brini, M. (2012) A-Synuclein Controls Mitochondrial Calcium Homeostasis By Enhancing Endoplasmic Reticulum-Mitochondria Interactions. *J Biol Chem*, 287, 17914–29.

Cardo, L.F., Coto, E., De Mena, L., Ribacoba, R., Lorenzo-Betancor, O., Pastor, P., Samaranch, Ll., Mata, I.F., Díaz, M., Moris, G., Menéndez, M., Corao, A.I. & Alvarez, V. (2012) A search for SNCA 3′ UTR variants identified SNP rs356165 as a determinant of disease risk and onset age in Parkinson's disease. *J Mol Neurosci*, 47, 425–430.

Chartier-Harlin, M.C., Kachergus, J., Roumier, C., Mouroux, V., Douay, X., Lincoln, S., Levecque, C., Larvor, L., Andrieux, J., Hulihan, M., Waucquier, N., Defebvre, L., Amouyel, P., Farrer, M. & Destee, A. (2004) alpha-Synuclein locus duplication as a cause of familial Parkinson's disease. *Lancet*, 364, 1167–1169.

Chen, L., Xie, Z., Turkson, S., & Zhuang, X. (2015) Neurobiol Dis A53T Human alpha-Synuclein Overexpression in Transgenic Mice Induces Pervasive Mitochondria Macroautophagy Defects Preceding Dopamine Neuron Degeneration. *J Neurosci*, 35, 890–905.

Chinta, S. J., Mallajosyula, J. K., Rane, A., & Andersen, J. K. (2010) Mitochondrial alpha-synuclein accumulation impairs complex I function in dopaminergic neurons and results in increased mitophagy in vivo. *Neurosci Lett*, 486, 235–239.

Choi, H. G., Zhang, J., Deng, X., Hatcher, J. M., Patricelli, M. P., Zhao, Z., Alessi, Dario R. & Gray, N. S. (2012) Brain penetrant LRRK2 inhibitor. *Acs Med Chem Lett*, 3, 658–662.

Civiero, L., Vancraenenbroeck, R., Belluzzi, E., Beilina, A., Lobbestael, E., Reyniers, L., Gao, F., Micetic, I., de Maeyer, M., Bubacco, L., Baekelandt, V., Cookson, M.R., Greggio, E. & Taymans, J.M. (2012) Biochemical Characterization of Highly Purified Leucine-Rich Repeat Kinases 1 and 2 Demonstrates Formation of Homodimers. *PLoS ONE*, 7.

Civiero, L., Cogo, S., Kiekens, A., Morganti, C., Tessari, I., Lobbestael, E., Baekelandt, V., Taymans, J.-M., Chartier-Harlin, M.-C., Franchin, C., Arrigoni, G., Lewis, P.A., Piccoli, G., Bubacco, L., Cookson, M.R., Pinton, P. & Greggio, E. (2017) PAK6 Phosphorylates 14-3-3γ to Regulate Steady State Phosphorylation of LRRK2. *Font Mol Neurosci*, 10, 417.

Clark, L.N., Wang, Y., Karlins, E., Saito, L., Mejia-Santana, H., Harris, J., Louis, E.D., Cote, L.J., Andrews, H., Fahn, S., Waters, C., Ford, B., Frucht, S., Ottman, R. & Marder, K. (2006) Frequency of LRRK2 mutations in early- and late-onset Parkinson disease. *Neurology*, 67, 1786–1791.

Codolo, G., Plotegher, N., Pozzobon, T., Brucale, M., Tessari, I., Bubacco, L., & de Bernard, M. (2013) Triggering of Inflammasome by Aggregated α-Synuclein, an Inflammatory Response in Synucleinopathies. *PLoS ONE*, 8.

Cole, N. B., DiEuliis, D., Leo, P., Mitchell, D. C., & Nussbaum, R. L. (2008) Mitochondrial translocation of alpha-synuclein is promoted by intracellular acidification. *Exp Cell Res*, 314, 2076–2089.

Cookson, M. R. (2010) The role of leucine-rich repeat kinase 2 (LRRK2) in Parkinson's disease. *Nat Rev Neurosci,* 11, 791–7.

Cuervo, A. M., & Dice, J. F. (1996) A Receptor for the Selective Uptake and Degradation of Proteins by Lysosomes. *Science*, 273 501–503.

Cuervo, A. M., Dice, J. F., & Knecht, E. (1997) A population of rat liver lysosomes responsible for the selective uptake and degradation of cytosolic proteins. *J Biol Chem*, 272, 5606–5615.

Cuervo, A. M. (2004) Autophagy: In sickness and in health. *Trends Cell Biol*, 14, 70–7.

Cuervo, A. M., Stefanis, L., Fredenburg, R., Lansbury, P. T., & Sulzer, D. (2004) Impaired degradation of mutant alpha-synuclein by chaperone-mediated autophagy. *Science*, 305, 1292–1295.

Da Silveira, S. A., Schneider, B. L., Cifuentes-Diaz, C., Sage, D., Abbas-Terki, T., Iwatsubo, T., Unser, M. & Aebischer, P. (2009) Phosphorylation does not prompt, nor prevent, the formation of α-synuclein toxic species in a rat model of Parkinson's disease. *Hum Mol Genet*, 18, 872–887.

Daher, J.P.L., Pletnikova, O., Biskup, S., Musso, A., Gellhaar, S., Galter, D., Troncoso, J.C., Lee, M.K., Dawson, T.M., Dawson, V.L. & Moore, D.J. (2012) Neurodegenerative phenotypes in an A53T α-synuclein transgenic mouse model are independent of LRRK2. *Hum Mol Genet*, 21, 2420–2431.

Daher, J. P. L., Volpicelli-Daley, L. A., Blackburn, J. P., Moehle, M. S., & West, A. B. (2014) Abrogation of alpha-synuclein-mediated dopaminergic neurodegeneration in LRRK2-deficient rats. *P Natl A Sci USA*, 111, 9289–9294.

Daher, J.P.L., Abdelmotilib, H.A., Hu, X., Volpicelli-Daley, L.A., Moehle, M.S., Fraser, K.B., Needle, E., Chen, Y., Steyn, S.J., Galatsis, P., Hirst, W.D. & West, A.B. (2015) Leucine-rich repeat kinase 2 (LRRK2) pharmacological inhibition abates α-synuclein gene-induced neurodegeneration. *J Biol Chem*, 290, 19433–19444.

Daniele, S. G., Béraud, D., Davenport, C., Cheng, K., Yin, H., & Maguire-Zeiss, K. A. (2015) Activation of MyD88-dependent TLR1/2 signaling by misfolded α-synuclein, a protein linked to neurodegenerative disorders. *Sci Signal*, 8.

Dauer, W., Kholodilov, N., Vila, M., Trillat, A.-C., Goodchild, R., Larsen, K. E., Staal, R., Tieu, K., Schmitz, Y., Yuan, C. A., Rocha, M., Jackson-Lewis, V., Hersch, S., Sulzer, D., Przedborski, S., Burke, R. & Hen, R. (2002) Resistance of alpha -synuclein null mice to the parkinsonian neurotoxin MPTP. *P Natl A Sci USA*, 99, 14524–14529.

Dawson, T. M., Ko, H. S., & Dawson, V. L. (2010) Genetic animal models of Parkinson's disease. *Neuron*, 66, 646–661.

Dehay, B., Bove, J., Rodriguez-Muela, N., Perier, C., Recasens, A., Boya, P., & Vila, M. (2010) Pathogenic Lysosomal Depletion in Parkinson's Disease. *J Neurosci*, 30, 12535–12544.

Deng, X., Dzamko, N., Prescott, A., Davies, P., Liu, Q., Yang, Q., Lee, J.D., Patricelli, M.P., Nomanbhoy, T.K., Alessi, D.R. & Gray, N.S. (2011) Characterization of a selective inhibitor of the Parkinson's disease kinase LRRK2. *Nat Chem Biol*, 7, 203–205.

Desplats, P., Lee, H.-J., Bae, E.-J., Patrick, C., Rockenstein, E., Crews, L., Spencer, B., Masliah, E. & Lee, S.-J. (2009) Inclusion formation and neuronal cell death through neuron-to-neuron transmission of alpha-synuclein. *P Natl A Sci*, 106, 13010–13015.

Devi, L., Raghavendran, V., Prabhu, B. M., Avadhani, N. G., & Anandatheerthavarada, H. K. (2008) Mitochondrial import and accumulation of α-synuclein impair complex I in human dopaminergic neuronal cultures and Parkinson disease brain. *J Biol Chem*, 283, 9089–9100.

Devoto, V.M.P., Dimopoulos, N., Alloatti, M., Pardi, M.B., Saez, T.M., Otero, M.G., Cromberg, L.E., Marín-Burgin, A., Scassa, M.E., Stokin, G.B., Schinder, A.F., Sevlever, G. & Falzone, T.L. (2017) αsynuclein control of mitochondrial homeostasis in human-derived neurons is disrupted by mutations associated with Parkinson's disease. *Sci Rep*, 7.

Di Maio, R., Barrett, P.J., Hoffman, E.K., Barrett, C.W., Zharikov, A., Borah, A., Hu, X., McCoy, J., Chu, C.T., Burton, E.A., Hastings, T.G. & Greenamyre, J.T. (2016) α-synuclein binds to TOM20 and inhibits mitochondrial protein import in Parkinson's disease. *Sci Transl Med*, 8.

Dinter, E., Saridaki, T., Nippold, M., Plum, S., Diederichs, L., Komnig, D., Fensky, L., May, C., Marcus, K., Voigt, A., Schulz, J.B. & Falkenburger, B.H. (2016) Rab7 induces clearance of α-synuclein aggregates. *J Neurochem*, 758–774.

Dodson, M. W., Zhang, T., Jiang, C., Chen, S., & Guo, M. (2012) Roles of the Drosophila LRRK2 homolog in Rab7-dependent lysosomal positioning. *Hum Mol Genet*, 21, 1350–1363.

Dodson, M. W., Leung, L. K., Lone, M., Lizzio, M. A., & Guo, M. (2014) Novel ethyl methanesulfonate (EMS)-induced null alleles of the Drosophila homolog of LRRK2 reveal a crucial role in endolysosomal functions and autophagy in vivo. *Dis Mol Mech*, 7, 1351–1363.

Domert, J., Sackmann, C., Agholme, L., Bergstrï¿½m, J., Ingelsson, M., Hallbeck, M., & Severinsson, E. (2016) Aggregated alpha-synuclein transfer efficiently between cultured human neuron- like cells and localize to lysosomes. *PLoS ONE*, 11.

Duffy, M. F., Collier, T. J., Patterson, J. R., Kemp, C. J., Luk, K. C., Tansey, M. G., Paumier, K. L., Kanaan, N. M., Fischer, L. D., Polinski, N. K., Barth, O. L., Howe, J. W., Vaikath, N. N., Majbour, N. K., El-Agnaf, O. M. A. & Sortwell, C. E. (2018) Lewy body-like alpha-synuclein inclusions trigger reactive microgliosis prior to nigral degeneration. *J Neuroinflamm,* 15, 1–18.

Dzamko, N., Deak, M., Hentati, F., Reith, A. D., Prescott, A. R., Alessi, D. R., & Nichols, R. J. (2010) Inhibition of LRRK2 kinase activity leads to dephosphorylation of Ser 910 /Ser 935 , disruption of 14-3-3 binding and altered cytoplasmic localization. *Biochem J*, 430, 405–413.

Ellis, C. E., Murphy, E. J., Mitchell, D. C., Golovko, M. Y., Scaglia, F., Gwendolyn, C., Nussbaum, R. L. & Barcelo, G. C. (2005) Mitochondrial Lipid Abnormality and Electron Transport Chain Impairment in Mice Lacking α -Synuclein Mitochondrial Lipid Abnormality and Electron Transport Chain Impairment in Mice Lacking alpha-Synuclein. *Mol Cell Biol*, 25, 10190–10201.

Dinter, E., Saridaki, T., Nippold, M., Plum, S., Diederichs, L., Komnig, D., Fensky, L., May, C., Marcus, K., Voigt, A., Schulz, J.B. & Falkenburger, B.H. (2017) Overexpression of alpha-synuclein in an astrocyte cell line promotes autophagy inhibition and apoptosis. *J Neurosci Research*, 96,160-171.

Engelender, S. & Isacson, O. (2017) The Threshold Theory for Parkinson's Disease. *Trends Neurosci*, 40.

Estrada, A.A., Chan, B.K., Baker-Glenn, C., Beresford, A., Burdick, D.J., Chambers, M., Chen, H., Dominguez, S.L., Dotson, J., Drummond, J., Flagella, M., Fuji, R., Gill, A., Halladay, J., Harris, S.F., Heffron, T.P., Kleinheinz, T., Lee, D.W., Pichon, C.E.L., Liu, X., Lyssikatos, J.P., Medhurst, A.D., Moffat, J.G., Nash, K., Scearce-Levie, K., Sheng, Z., Shore, D.G., Wong, S., Zhang, S., Zhang, X., Zhu, H. & Sweeney, Z.K. (2014) Discovery of highly potent, selective, and brain-penetrant aminopyrazole Leucine-rich repeat kinase 2 (LRRK2) small molecule inhibitors. *J Med Chemy*, 57, 921–936.

Fred Dice, J. (1990) Peptide sequences that target cytosolic proteins for lysosomal proteolysis. *Trends Biochem Sci*, 15, 305–309.

Friedman, L. G., Lachenmayer, M. L., Wang, J., He, L., Poulose, S. M., Komatsu, M., Holstein, G. R. &Yue, Z. (2012) Disrupted Autophagy Leads to Dopaminergic Axon and Dendrite Degeneration and Promotes Presynaptic Accumulation of -Synuclein and LRRK2 in the Brain. *J Neurosci*, 32, 7585–7593.

Funayama, M., Hasegawa, K., Kowa, H., Saito, M., Tsuji, S., & Obata, F. (2002) A new locus for Parkinson's Disease (PARK8) maps to chromosome 12p11.2-q13.1. *Ann Neurol*, 51, 296–301.

Gardet, A., Benita, Y., Li, C., Sands, B. E., Ballester, I., Stevens, C., Korzenik, J. R., Rioux, J. D. *et al*. (2010) LRRK2 Is Involved in the IFN-γ Response and Host Response to Pathogens. *J Immunol*, 185, 5577–5585.

Gelders, G., Baekelandt, V. & Van Der Perren, A. (2018) Linking Neuroinflammation and Neurodegeneration in Parkinson's Disease. *J Immunol Res*.

Giasson, B. I., Duda, J. E., Quinn, S. M., Zhang, B., Trojanowski, J. Q., & Lee, V. M. Y. (2002) Neuronal α-synucleinopathy with severe movement disorder in mice expressing A53T human α-synuclein. *Neuron*, 34, 521–533.

Gibb, W. R. G., Scott, T., & Lees, A. J. (1991) Neuronal inclusions of Parkinson's disease. *Movement Disord*, 6, 2–11.

Gilks, W.P., Abou-Sleiman, P.M., Gandhi, S., Jain, S., Singleton, A., Lees, A.J., Shaw, K., Bhatia, K.P., Bonifati, V., Quinn, N.P., Lynch, J., Healy, D.G., Holton, J.L., Revesz, T. & Wood, N.W. (2005) A common LRRK2 mutation in idiopathic Parkinson's disease. *Lancet*, 365, 415–416.

Gillardon, F., Schmid, R., & Draheim, H. (2012) Parkinson's disease-linked leucine-rich repeat kinase 2(R1441G) mutation increases proinflammatory cytokine release from activated primary microglial cells and resultant neurotoxicity. *Neuroscience*, 208, 41–48.

Gloeckner, C. J., Boldt, K., Von Zweydorf, F., Helm, S., Wiesent, L., Sarioglu, H., & Ueffing, M. (2010) Phosphopeptide analysis reveals two discrete clusters of phosphorylation in the N-terminus and the Roc domain of the Parkinson-disease associated protein kinase LRRK2. *J Proteome Res*, 9, 1738–1745.

Goldwurm, S., Zini, M., Di Fonzo, A., De Gaspari, D., Siri, C., Simons, E.J., van Doeselaar, M., Tesei, S., Antonini, A., Canesi, M., Zecchinelli, A., Mariani, C., Meucci, N., Sacilotto, G., Cilia, R., Isaias, I.U., Bonetti, A., Sironi, F., Ricca, S., Oostra, B.A., Bonifati, V. & Pezzoli, G. (2006) LRRK2 G2019S mutation and Parkinson's disease: A clinical, neuropsychological and neuropsychiatric study in a large Italian sample. *Parkinsonism Relat Dis*, 12, 410–419.

Gorbatyuk, O. S., Li, S., Sullivan, L. F., Chen, W., Kondrikova, G., Manfredsson, F. P., Mandel, R. J. & Muzyczka, N. (2008) The phosphorylation state of Ser-129 in human alpha-synuclein determines neurodegeneration in a rat model of Parkinson disease. *P Natl A Sci USA*, 105, 763–768.

Gorbatyuk, O. S., Li, S., Nash, K., Gorbatyuk, M., Lewin, A. S., Sullivan, L. F., Mandel, R. J., Chen, W., Meyers, C., Manfredsson, F. P. & Muzyczka N. (2010) In Vivo RNAi-Mediated α-Synuclein Silencing Induces Nigrostriatal Degeneration. *Mol Ther*, 18, 1450–57.

Grassi, D., Howard, S., Zhou, M., Diaz-Perez, N., Urban, N.T., Guerrero-Given, D., Kamasawa, N., Volpicelli-Daley, L.A., LoGrasso, P. & Lasmézas, C.I. (2018) Identification of a highly neurotoxic α-synuclein species inducing mitochondrial damage and mitophagy in Parkinson's disease. *P Natl A Sci*.

Greggio, E., Jain, S., Kingsbury, A., Bandopadhyay, R., Lewis, P., Kaganovich, A., van der Brug, M.P., Beilina, A., Blackinton, J., Thomas, K.J., Ahmad, R., Miller, D.W., Kesavapany, S., Singleton, A., Lees, A., Harvey, R.J., Harvey, K. & Cookson, M.R.(2006) Kinase activity is required for the toxic effects of mutant LRRK2/dardarin. *Neurobiol Dis*, 23, 329–341.

Guardia-Laguarta, C., Area-Gomez, E., Rüb, C., Liu, Y., Magrané, J., Becker, D., Voos, W., Schon, E. & Przedborski, S. (2014) α-Synuclein Is Localized to Mitochondria-Associated ER Membranes. *J Neurosci*, 34, 249–259.

Gustot, A., Gallea, J. I., Sarroukh, R., Celej, M. S., Ruysschaert, J.-M., & Raussens, V. (2015). Amyloid fibrils are the molecular trigger of inflammation in Parkinson's disease. *Biochem J*, 471, 323–333.

Hakimi, M., Selvanantham, T., Swinton, E., Padmore, R.F., Tong, Y., Kabbach, G., Venderova, K., Girardin, S.E., Bulman, D.E., Scherzer, C.R., Lavoie, M.J., Gris, D., Park, D.S., Angel, J.B., Shen, J., Philpott, D.J. & Schlossmacher, M.G. (2011) Parkinson's disease-linked LRRK2 is expressed in circulating and tissue immune cells and upregulated following recognition of microbial structures. *J Neural Transm*, 118, 795–808.

Hasegawa, K., Stoessl, A. J., Yokoyama, T., Kowa, H., Wszolek, Z. K., & Yagishita, S. (2009) Familial parkinsonism: Study of original Sagamihara PARK8 (I2020T) kindred with variable clinicopathologic outcomes. *Parkinsonism Relat Dis*, 15, 300–306.

Healy, D.G., Falchi, M., O'Sullivan, S.S., Bonifati, V., Durr, A., Bressman, S., Brice, A., Aasly, J., Zabetian, C.P., Goldwurm, S., Ferreira, J.J., Tolosa, E., Kay, D.M., Klein, C., Williams, D.R., Marras, C., Lang, A.E., Wszolek, Z.K., Berciano, J., Schapira, A.H., Lynch, T., Bhatia, K.P., Gasser, T., Lees, A.J. & Wood, N.W. (2008) Phenotype, genotype, and worldwide genetic penetrance of LRRK2-associated Parkinson's disease: a case-control study. *Lancet Neurol*, 7, 583–590.

Herzig, M. C., Bidinosti, M., Schweizer, T., Hafner, T., Stemmelen, C., Weiss, A., Danner, S., Vidotto, N. *et al.* (2012) High LRRK2 levels fail to induce or exacerbate neuronal alpha-synucleinopathy in mouse brain. *PloS One*, 7.

Higashi, S., Moore, D. J., Yamamoto, R., Minegishi, M., Sato, K., Togo, T., Katsuse, O., Uchikado, H. *et al*. (2009) Abnormal localization of leucine-rich repeat kinase 2 to the endosomal-lysosomal compartment in lewy body disease. *J Neuropath Exp Neur*, 68, 994–1005.

Huang, Y., Halliday, G.M., Vandebona, H., Mellick, G.D., Mastaglia, F., Stevens, J., Kwok, J., Garlepp, M., Silburn, P.A., Horne, M.K., Kotschet, K., Venn, A., Rowe, D.B., Rubio, J.P. & Sue, C.M. (2007) Prevalence and clinical features of common LRRK2 mutations in Australians with Parkinson's disease. *Movement Disord*, 22, 982–989.

Hulihan, M.M., Ishihara-Paul, L., Kachergus, J., Warren, L., Amouri, R., Elango, R., Prinjha, R.K., Upmanyu, R., Kefi, M., Zouari, M., Sassi, S.B., Yahmed, S.B., El Euch-Fayeche, G., Matthews, P.M., Middleton, L.T., Gibson, R.A., Hentati, F. & Farrer, M.J. (2008) LRRK2 Gly2019Ser penetrance in Arab-Berber patients from Tunisia: a case-control genetic study. *Lancet Neurol*, 7, 591–594.

Hunot, S., Dugas, N., Faucheux, B., Hartmann, A., Tardieu, M., Debré, P., Agid, Y., Dugas, B. & Hirsch, E.C. (1999) FcepsilonRII/CD23 is expressed in Parkinson's disease and induces, in vitro, production of nitric oxide and tumor necrosis factor-alpha in glial cells. *J Neurosci*, 19, 3440–3447.

Imamura, K., Hishikawa, N., Sawada, M., Nagatsu, T., Yoshida, M., & Hashizume, Y. (2003) Distribution of major histocompatibility complex class II-positive microglia and cytokine profile of Parkinson's disease brains. *Acta Neuropathol*, 106, 518–526.

Inglis, K.J., Chereau, D., Brigham, E.F., Chiou, S.S., Sch??bel, S., Frigon, N.L., Yu, M., Caccavello, R.J., Nelson, S., Motter, R., Wright, S., Chian, D., Santiago, P., Soriano, F., Ramos, C., Powell, K., Goldstein, J.M., Babcock, M., Yednock, T., Bard, F., Basi, G.S., Sham, H., Chilcote, T.J., McConlogue, L., Griswold-Prenner, I. & Anderson, J.P. (2009) Polo-like kinase 2 (PLK2) phosphorylates alpha-synuclein at serine 129 in central nervous system. *J Biol Chem*, 284, 2598–2602.

Ishii, A., Nonaka, T., Taniguchi, S., Saito, T., Arai, T., Mann, D., Iwatsubo, T., Hisanaga, S.-I., Goedert, M. & Hasegawa, M. (2007) Casein kinase 2 is the major enzyme in brain that phosphorylates Ser129 of human alpha-synuclein: Implication for alpha-synucleinopathies. *FEBS Lett*, 581, 4711–4717.

Jager, S. (2004) Role for Rab7 in maturation of late autophagic vacuoles. *J Cell Sci*, 117, 4837–4848.

Kachergus, J., Mata, I.F., Hulihan, M., Taylor, J.P., Lincoln, S., Aasly, J., Gibson, J.M., Ross, O.A., Lynch, T., Wiley, J., Payami, H., Nutt, J., Maraganore, D.M., Czyzewski, K., Styczynska, M., Wszolek, Z.K., Farrer, M.J. & Toft, M. (2005) Identification of a novel LRRK2 mutation linked to autosomal dominant parkinsonism: evidence of a common founder across European populations. *Am J Hum Genet*, 76, 672–680.

Kalia, L.V., Lang, A.E., Hazrati, L.N., Fujioka, S., Wszolek, Z.K., Dickson, D.W., Ross, O.A., Van Deerlin, V.M., Trojanowski, J.Q., Hurtig, H.I., Alcalay, R.N., Marder, K.S., Clark, L.N., Gaig, C., Tolosa, E., Ruiz-Martínez, J., Marti-Masso, J.F., Ferrer, I., López De Munain, A., Goldman, S.M., Schüle, B., Langston, J.W., Aasly, J.O., Giordana, M.T., Bonifati, V., Puschmann, A., Canesi, M., Pezzoli, G., Maues De Paula, A., Hasegawa, K., Duyckaerts, C., Brice, A., Stoessl, A.J. & Marras, C. (2015)Clinical correlations with lewy body pathology in LRRK2-related Parkinson disease. *JAMA Neurol*, 72, 100–105.

Kamikawaji, S., Ito, G., & Iwatsubo, T. (2009) Identification of the autophosphorylation sites of LRRK2. *Biochemistry*, 48, 10963–10975.

Kamp, F., Exner, N., Lutz, A. K., Wender, N., Hegermann, J., Brunner, B., Nuscher, B., Bartels, T., Giese, A., Beyer, K., Eimer, S., Winklhofer, K. F. & Haass, C. (2010) Inhibition of mitochondrial fusion by α-synuclein is rescued by PINK1, Parkin and DJ-1. *EMBO J*, 29, 3571–3589.

Karuppagounder, S. S., Xiong, Y., Lee, Y., Lawless, M. C., Kim, D., Nordquist, E., Martin, I., Ge, P. Brahmachari, S., Jhaldiyal, A., Kumar, M., Andrabi, S. A., Dawson, T. M. & Dawson, V. L. (2015) LRRK2 G2019S transgenic mice display increased susceptibility to 1-methyl-4-phenyl-1,2,3,6-tetrahydropyridine (MPTP)-mediated neurotoxicity. *J Chem Neuroanat*, 2, 4–11.

Kawamoto, Y., Akiguchi, I., Nakamura, S., Honjyo, Y., Shibasaki, H., & Budka, H. (2002) 14-3-3 Proteins in Lewy bodies in Parkinson disease and diffuse Lewy body disease brains. *J Neuropath Exp Neur*, 61, 245–253.

Khan, N.L., Jain, S., Lynch, J.M., Pavese, N., Abou-Sleiman, P., Holton, J.L., Healy, D.G., Gilks, W.P., Sweeney, M.G., Ganguly, M., Gibbons, V., Gandhi, S., Vaughan, J., Eunson, L.H., Katzenschlager, R., Gayton, J., Lennox, G., Revesz, T., Nicholl, D., Bhatia, K.P., Quinn, N., Brooks, D., Lees, A.J., Davis, M.B., Piccini, P., Singleton, A.B. & Wood, N.W. (2005) Mutations in the gene LRRK2 encoding dardarin (PARK8) cause familial Parkinson's disease: Clinical, pathological, olfactory and functional imaging and genetic data. *Brain*, 128, 2786–2796.

Khodr, C. E., Pedapati, J., Han, Y., & Bohn, M. C. (2012) Inclusion of a portion of the native SNCA 3'UTR reduces toxicity of human S129A SNCA on striatal-projecting dopamine neurons in rat substantia Nigra. *Dev Neurobiol*, 72, 906–917.

Kim, B., Yang, M.S., Choi, D., Kim, J.H., Kim, H.S., Seol, W., Choi, S., Jou, I., Kim, E.Y. & Joe, E. H. (2012) Impaired inflammatory responses in murine lrrk2-knockdown brain microglia. *PLoS ONE*, 7.

Kim, C., Ho, D.H., Suk, J.E., You, S., Michael, S., Kang, J., Lee, Sung Joong, Masliah, E., Hwang, D., Lee, H.J. & Lee, S. J. (2013) Neuron-released oligomeric α-synuclein is an endogenous agonist of TLR2 for paracrine activation of microglia. *Nat Commun*, 4.

Klivenyi, P., Siwek, D., Gardian, G., Yang, L., Starkov, A., Cleren, C., Ferrante, R. J., Kowall, N. W. Abeliovich, A. & Beal, M. F. (2006) Mice lacking alpha-synuclein are resistant to mitochondrial toxins. *Neurobiol Dis*, 21, 541–548.

Kondo, K., Obitsu, S., & Teshima, R. (2011) α-Synuclein aggregation and transmission are enhanced by leucine-rich repeat kinase 2 in human neuroblastoma SH-SY5Y cells. *Biol Pharm Bull*, 34, 1078–1083.

Kordower, J. H., Chu, Y., Hauser, R. A., Freeman, T. B., & Olanow, C. W. (2008) Lewy body-like pathology in long-term embryonic nigral transplants in Parkinson's disease. *Nat Med*, 14, 504–506.

Kozina, E., Shankar, S., Yun, J., Yuchen, D., Zhijun, M., Haiyan, T., Kiran, K., Timothy, S., Junmin, P. & Richard, J. S. (2018) Mutant LRRK2 Mediates Peripheral and Central Immune Responses Leading to Neurodegeneration in Vivo. *Brain*. 141, 1753–1769.

Krüger, R., Kuhn, W., Müller, T., Woitalla, D., Graeber, M., Kösel, S., Przuntek, H., Epplen, J.T., Schols, L. & Riess, O (1998) AlaSOPro mutation in the gene encoding α-synuclein in Parkinson's disease. *Nat Genet*, 18, 106–108.

Langston, J. W., & Ballard, P. A. (1983) Parkinson's disease in a chemist working with 1-methyl-4-phenyl-1,2,5,6-tetrahydropyridine. *New Engl J Med*, 309, 310.

Lastres-Becker, I., Ulusoy, A., Innamorato, N. G., Sahin, G., Rábano, A., Kirik, D. & Cuadrado, A. (2012) α-synuclein expression and Nrf2 deficiency cooperate to aggravate protein aggregation, neuronal death and inflammation in early-stage Parkinson's disease. *Hum Mol Genet*, 21, 3173–3192.

Lavalley, N. J., Slone, S. R., Ding, H., West, A. B., & Yacoubian, T. A. (2016) 14-3-3 Proteins regulate mutant LRRK2 kinase activity and neurite shortening. *Hum Mol Genet*, 25, 109–122.

Lee, M.K., Stirling, W., Xu, Y., Xu, X., Qui, D., Mandir, A.S., Dawson, T.M., Copeland, N.G., Jenkins, N.A. & Price, D.L. (2002) Human alpha-synuclein-harboring familial Parkinson's disease-linked Ala-53 Thr mutation causes neurodegenerative disease with -synuclein aggregation in transgenic mice. *P Natl A Sci*, 99, 8968–8973.

Lee, H.-J., Khoshaghideh, F., Patel, S., & Lee, S.-J. (2004) Clearance of alpha-synuclein oligomeric intermediates via the lysosomal degradation pathway. *J Neurosci*, 24, 1888–1896.

Lee, B.D., Shin, J.H., Vankampen, J., Petrucelli, L., West, A.B., Ko, H.S., Lee, Y.I., Maguire-Zeiss, K.A., Bowers, W.J., Federoff, H.J., Dawson, V.L. & Dawson, T.M. (2010) Inhibitors of leucine-rich repeat kinase-2 protect against models of Parkinson's disease. *Nat Med,* 16, 998–1000.

Lee, J.-W., & Cannon, J. R. (2015) LRRK2 mutations and neurotoxicant susceptibility. *Exp Biol Med*, 240, 752–9.

Levine, B., & Klionsky, D. J. (2004) Development by self-digestion: Molecular mechanisms and biological functions of autophagy. *Dev Cell*, 6.

Li, W.-W., Yang, R., Guo, J.-C., Ren, H.-M., Zha, X.-L., Cheng, J.-S., & Cai, D.-F. (2007) Localization of alpha-synuclein to mitochondria within midbrain of mice. *Neuroreport*, 18, 1543–1546.

Liberatore, G. T., Jackson-Lewis, V., Vukosavic, S., Mandir, A. S., Vila, M., McAuliffe, W. G., Dawson, V. L., Dawson, T. M. & Przedborski, S. (1999) Inducible Nitric Oxide Synthase Stimulates Dopaminergic Neurodegeneration in the MPTP Model of Parkinson Disease. *Nat Med*, 5, 1403–9.

Liddelow, S. A., Guttenplan, K. A., Clarke, L. E., Bennett, F. C., Bohlen, C. J., Schirmer, L., Bennett, M. L., Münch, A. E., Chung, W. S., Peterson, T. C., Wilton, D. K., Frouin, A., Napier, B. A., Panicker, N., Kumar, M., Buckwalter, M. S., Rowitch, D. H., Dawson, V. L., Dawson, T. M., Stevens, B. & Barres, B. A. (2017) Neurotoxic reactive astrocytes are induced by activated microglia. *Nature*, 541, 481–487.

Lin, C. H., Tzen, K. Y., Yu, C. Y., Tai, C. H., Farrer, M. J., & Wu, R. M. (2008) LRRK2 mutation in familial Parkinson's disease in a Taiwanese population: Clinical, PET, and functional studies. *J Biomed Sci*, 15, 661–667.

Lin, X., Parisiadou, L., Gu, X.L., Wang, L., Shim, H., Sun, L., Xie, C., Long, C.X., Yang, W.J., Ding, J., Chen, Z.Z., Gallant, P.E., Tao-Cheng, J.H., Rudow, G., Troncoso, J.C., Liu, Z., Li, Z. & Cai, H. (2009) Leucine-Rich Repeat Kinase 2 Regulates the Progression of Neuropathology Induced by Parkinson's-Disease-Related Mutant α-synuclein. *Neuron*, 64, 807–827.

Lindström, V., Gustafsson, G., Sanders, L.H., Howlett, E.H., Sigvardson, J., Kasrayan, A., Ingelsson, M., Bergström, J. & Erlandsson, A. (2017) Extensive uptake of α-synuclein oligomers in astrocytes results in sustained intracellular deposits and mitochondrial damage. *Mol Cell Neurosci*, 82, 143–156.

Liu, G., Zhang, C., Yin, J., Li, X., Cheng, F., Li, Y., Yang, H., Uéda, K. Chan, P. & Yu, S. (2009) α-Synuclein is differentially expressed in mitochondria from different rat brain regions and dose-dependently down-regulates complex I activity. *Neurosci Lett*, 454, 187–192.

Liu, Z., Hamamichi, S., Lee, B.D., Yang, D., Ray, A., Caldwell, G.A., Caldwell, K.A., Dawson, T.M., Smith, W.W. & Dawson, V.L. (2011) Inhibitors of LRRK2 kinase attenuate neurodegeneration and Parkinson-like phenotypes in Caenorhabditis elegans and Drosophila Paarkinson's disease models. *Hum Mol Genet*, 20, 3933–3942.

Loeb, V., Yakunin, E., Saada, A., & Sharon, R. (2010) The transgenic overexpression of alph-synuclein and not its related pathology associates with complex I inhibition. *J Biol Chem*, 285, 7334–7343.

Loeffler, D. A., Klaver, A. C., Coffey, M. P., Aasly, J. O., & LeWitt, P. A. (2017) Increased Oxidative Stress Markers in Cerebrospinal Fluid from Healthy Subjects with Parkinson's Disease-Associated LRRK2 Gene Mutations. *Front Aging Neurosci*, 9.

Longo, F., Mercatelli, D., Novello, S., Arcuri, L., Brugnoli, A., Vincenzi, F., Russo, I., Berti, G., Mabrouk, O.S., Kennedy, R.T., Shimshek, D.R., Varani, K., Bubacco, L., Greggio, E. & Morari, M. (2017) Age-dependent dopamine transporter dysfunction and Serine129 phospho-α-synuclein overload in G2019S LRRK2 mice. *Acta Neuropathol Communications*, 5, 22.

Luk, K. C., Kehm, V., Carroll, J., Zhang, B., O'Brien, P., Trojanowski, J. Q., & Lee, V. M. Y. (2012) Pathological α-synuclein transmission initiates Parkinson-like neurodegeneration in nontransgenic mice. *Science*, 338, 949–953.

Ma, B., Xu, L., Pan, X., Sun, L., Ding, J., Xie, C., Koliatsos, V. E. & Cai, H. (2015) LRRK2 modulates microglial activity through regulation of chemokine (C-X3-C) receptor 1 -mediated signalling pathways. *Hum Mol Genet*, 25, 3515–3523.

Maatouk, L., Yi, C., Carrillo-de Sauvage, M.-A., Compagnion, A.-C., Hunot, S., Ezan, P., Hirsch, E. C., Koulakoff, A., Pfrieger, F. W., Tronche, F., Leybaert, L., Giaume, C., Vyas, S. (2018) Glucocorticoid receptor in astrocytes regulates midbrain dopamine neurodegeneration through connexin hemichannel activity. *Cell Death Differ*.

Maekawa, T., Sasaoka, T., Azuma, S., Ichikawa, T., Melrose, H. L., Farrer, M. J., & Obata, F. (2016) Leucine-rich repeat kinase 2 (LRRK2) regulates α-synuclein clearance in microglia. *BMC Neurosci*, 17.

Majeski, A. E., & Fred Dice, J. (2004) Mechanisms of chaperone-mediated autophagy. *Int J Biochem Cell Biol*, 36, 2435-44.

Mamais, A., Chia, R., Beilina, A., Hauser, D. N., Hall, C., Lewis, P. A., Cookson, M. R. & Bandopadhyay, R. (2014) Arsenite stress down-regulates phosphorylation and 14-3-3 binding of leucine-rich repeat kinase 2 (LRRK2), promoting self-association and cellular redistribution. *J Biol Chem*, 289, 21386–21400.

Manfredsson, F. P., Luk, K. C., Benskey, M. J., Gezer, A., Garcia, J., Kuhn, N. C., Sandoval, I. M., Patterson, J. R., O'Mara, A., Yonkers, R. & Kordower, J. H. (2018) Induction of Alpha-Synuclein Pathology in the Enteric Nervous System of the Rat and Non-Human Primate Results in Gastrointestinal Dysmotility and Transient CNS Pathology. *Neurobiol Dis,* 112, 106–18.

Manzoni, C., Mamais, A., Roosen, D. A., Dihanich, S., Soutar, M. P. M., Plun-Favreau, H., Bandopadhyay, R., Hardy, J. *et al.* (2016) MTOR independent regulation of macroautophagy by Leucine Rich Repeat Kinase 2 via Beclin-1. *Sci Rep*, 6.

Marcinek, P., Jha, A.N., Shinde, V., Sundaramoorthy, A., Rajkumar, R., Suryadevara, N.C., Neela, S.K., van Tong, H., Balachander, V., Valluri, V.L., Thangaraj, K. & Velavan, T.P., (2013) LRRK2 and RIPK2 Variants in the NOD 2-Mediated Signaling Pathway Are Associated with Susceptibility to Mycobacterium leprae in Indian Populations. *PLoS ONE*, 8.

Martin, L. J., Pan, Y., Price, A. C., Sterling, W., Copeland, N. G., Jenkins, N. A., Price, D. L. & Lee, M. K. (2006) Parkinson's Disease α-synuclein transgenic mice develop neuronal mitochondrial degeneration and cell death. *J Neurosci*, 26, 41–50.

Martinez, J. H., Alaimo, A., Gorojod, R. M., Porte Alcon, S., Fuentes, F., Coluccio Leskow, F., & Kotler, M. L. (2018) Drp-1 dependent mitochondrial fragmentation and protective autophagy in dopaminergic SH-SY5Y cells overexpressing alpha-synuclein. *Mol Cell Neurosci*, 88, 107–117.

Massey, A., Kiffin, R., & Cuervo, A. M. (2004) Pathophysiology of chaperone-mediated autophagy. *Int J Biochem Cell B*.

Massey, A. C., Kaushik, S., Sovak, G., Kiffin, R., & Cuervo, A. M. (2006). Consequences of the selective blockage of chaperone-mediated autophagy. *P Natl A Sci USA*, 103, 5805–5810.

Mata, I. F., Wedemeyer, W. J., Farrer, M. J., Taylor, J. P., & Gallo, K. A. (2006) LRRK2 in Parkinson's disease: protein domains and functional insights. *Trends Neurosci*, 29, 286-93.

McGeer, P. L., Itagaki, S., & McGeer, E. G. (1988) Expression of the histocompatibility glycoprotein HLA-DR in neurological disease. *Acta Neuropathol*, 76, 550–557.

McNaught, K. S. P., Mytilin, C., JnoBaptiste, R., Yabut, J., Shashidharan, P., Jenner, P., & Olanow, C. W. (2002) Impairment of the ubiquitin-proteasome system causes dopaminergic cell death and inclusion body formation in ventral mesencephalic cultures. *J Neurochem*, 81, 301–306.

Melo, T. Q., van Zomeren, K. C., Ferrari, M. F. R., Boddeke, H. W. G. M., & Copray, J. C. V. M. (2016) Impairment of mitochondria dynamics by human A53T α-synuclein and rescue by NAP (davunetide) in a cell model for Parkinson's disease. *Exp Brain Res*, 235, 731-742.

Mizuno, Y., Ohta, S., Tanaka, M., Takamiya, S., Suzuki, K., Sato, T., Oya, H., Ozawa, T & Kagawa, Y. (1989) Deficiencies in Complex I subunits of the respiratory chain in Parkinson's disease. *Biochem Bioph Res Co*, 163, 1450–1455.

Moehle, M. S., Webber, P. J., Tse, T., Sukar, N., Standaert, D. G., DeSilva, T. M., Cowell, R. M. & West, A. B. (2012) LRRK2 Inhibition Attenuates Microglial Inflammatory Responses. *J Neurosci*, 32, 1602–1611.

Mogi, M., Harada, M., Riederer, P., Narabayashi, H., Fujita, K., & Nagatsu, T. (1994) Tumor necrosis factor-alpha (TNF-alpha) increases both in the brain and in the cerebrospinal fluid from parkinsonian patients. *Neurosci Lett*, 165, 208–210.

Mogi, M., Harada, M., Narabayashi, H., Inagaki, H., Minami, M., & Nagatsu, T. (1996) Interleukin (IL)-1β, IL-2, IL-4, IL-6 and transforming growth factor-α levels are elevated in ventricular cerebrospinal fluid in juvenile parkinsonism and Parkinson's disease. *Neurosci Lett*, 211, 13–16.

Mortiboys, H., Johansen, K. K., Aasly, J. O., & Bandmann, O. (2010) Mitochondrial impairment in patients with Parkinson disease with the G2019S mutation in LRRK2. *Neurology*, 75, 2017–2020.

Mortiboys, H., Furmston, R., Bronstad, G., Aasly, J., Elliott, C., & Bandmann, O. (2015) UDCA exerts beneficial effect on mitochondrial dysfunction in LRRK2 G2019S carriers and in vivo. *Neurology*, 85, 846–852.

Mougenot, A. L., Nicot, S., Bencsik, A., Morignat, E., Verchère, J., Lakhdar, L., Legastelois, S. & Baron, T. (2012). Prion-like acceleration of a synucleinopathy in a transgenic mouse model. *Neurobiol Aging*, 33, 2225–2228.

Müller, O., Sattler, T., Flötenmeyer, M., Schwarz, H., Plattner, H., & Mayer, A. (2000) Autophagic tubes: Vacuolar invaginations involved in lateral membrane sorting and inverse vesicle budding. *J Cell Biol*, 151, 519–528.

Nakamura, K., Nemani, V. M., Wallender, E. K., Kaehlcke, K., Ott, M., & Edwards, R. H. (2008) Optical reporters for the conformation of alpha-synuclein reveal a specific interaction with mitochondria. *J Neurosci*, 28, 12305–12317.

Nakamura, K., Nemani, V. M., Azarbal, F., Skibinski, G., Levy, J. M., Egami, K., Munishkina, L., Zhang, J., Gardner, B., Wakabayashi, J., Sesaki, H., Cheng, Y., Finkbeiner, S., Nussbaum, R. L., Masliah, E. & Edwards, R. H. (2011) Direct membrane association drives mitochondrial fission by the Parkinson disease-associated protein α-synuclein. *J Biol Chem*, 286, 20710–20726.

Nalls, M. A., Pankratz, N., Lill, C. M., Do, C. B., Hernandez, D. G., Saad, M., DeStefano, A. L., Kara, E., Bras, J., Sharma, J., Schulte, J., Keller, M. F., Arepalli, S., Letson, C., Edsall, C., Stefansson, H., Liu, X., Pliner, H., Lee, J. H., Cheng, R., Ikram, M. A., Ioannidis, J. P. A., Hadjigeorgiou, G. M., Joshua C., Martinez, M., Perlmutter, J. S., Goate, A., Marder, K., Fiske, B., Sutherland, M., Xiromerisiou, G., Myers, R. H., Clark, L. N., Stefansson, K., Hardy, J. A., Heutink, P., Chen, H., Wood, N. W., Houlden, H., Payami, H., Brice, A., Scott, W. K., Gasser, T.,

Bertram, L., Eriksson, N., Foroud, T. & Singleton, A. B. (2014) Large-scale meta-analysis of genome-wide association data identifies six new risk loci for Parkinson's disease. *Nat Genet*, 46, 989–993.

Ng, C.-H., Mok, S. Z. S., Koh, C., Ouyang, X., Fivaz, M. L., Tan, E.-K., Dawson, V. L., Dawson, T. M., Yu, F. & Lim, K.-L. (2009) Parkin protects against LRRK2 G2019S mutant-induced dopaminergic neurodegeneration in Drosophila. *J Neurosci*, 29, 11257–11262.

Nichols, W. C., Pankratz, N., Hernandez, D., Paisán-Ruíz, C., Jain, S., Halter, C. A., Michaels, V. E., Reed, T., Rudolph, A., Shults, C. W., Singleton, A. & Foroud, T. (2005) Genetic screening for a single common LRRK2 mutation in familial Parkinson's disease. *Lancet*, 365, 410–412.

Nichols, R. J., Dzamko, N., Morrice, N. A., Campbell, D. G., Deak, M., Ordureau, A., Macartney, T., Tong, Y., Shen, J., Prescott, A. R. & Alessi, D. R. (2010) 14-3-3 binding to LRRK2 is disrupted by multiple Parkinson's disease-associated mutations and regulates cytoplasmic localization. *Biochem J*, 430, 393–404.

Niu, J., Yu, M., Wang, C., & Xu, Z. (2012) Leucine-rich repeat kinase 2 disturbs mitochondrial dynamics via dynamin-like protein. *J Neurochem*, 122, 650–658.

Oosterveld, L. P., Allen, J. C., Ng, E. Y. L., Seah, S. H., Tay, K. Y., Au, W. L., Tan, E. K. & Tan, L. C. S. (2015) Greater motor progression in patients with Parkinson disease who carry LRRK2 risk variants. *Neurology*, 85, 1039–1042.

Orenstein, S. J., Kuo, S. H., Tasset, I., Arias, E., Koga, H., Fernandez-Carasa, I., Cortes, E., Honig, L. S., Dauer, W., Consiglio, A., Raya, A., Sulzer, D. & Cuervo, A. M. (2013) Interplay of LRRK2 with chaperone-mediated autophagy. *Nat Neurosci*, 16, 394–406.

Oueslati, A., Schneider, B. L., Aebischer, P. & Lashuel, H. A. (2013) Polo-like Kinase 2 Regulates Selective Autophagic alpha-Synuclein Clearance and Suppresses Its Toxicity in Vivo. *P Natl A Sci USA*, 110, E3945–54.

Paisán-Ruíz, C., Jain, S., Evans, E. W., Gilks, W. P., Simón, J., Van Der Brug, M., De Munain, A. L., Aparicio, S., Gil, A. M., Khan, N., Johnson, J., Martinez, J. R., Nicholl, D., Carrera, I. M., Peňa, A. S., De Silva, R., Lees, A., Martí-Massó, J. F., Pérez-Tur, J., Wood, N. W. & Singleton, A. B. (2004) Cloning of the gene containing mutations that cause PARK8-linked Parkinson's disease. *Neuron*, 44, 595–600.

Papkovskaia, T. D., Chau, K. Y., Inesta-vaquera, F., Papkovsky, D. B., Healy, D. G., Nishio, K., Staddon, J., Duchen, M. R., Hardy, J., Schapira, A. H. V. & Cooper, J. M. (2012) G2019s leucine-rich repeat kinase 2 causes uncoupling protein-mediated mitochondrial depolarization. *Hum Mol Genet*, 21, 4201–4213.

Parihar, M. S., Parihar, A., Fujita, M., Hashimoto, M., & Ghafourifar, P. (2008) Mitochondrial association of alpha-synuclein causes oxidative stress. *Cell Mol Life Sci*, 65, 1272–1284.

Paumier, K. L., Luk, K. C., Manfredsson, F. P., Kanaan, N. M., Lipton, J. W., Collier, T. J., Steece-Collier, K., Kemp, C. J., Celano, S., Schulz, E., Sandoval, I. M., Fleming, S., Dirr, E., Polinski, N. K., Trojanowski, J. Q., Lee, V. M. & Sortwell, C. E. (2015)Intrastriatal injection of pre-formed mouse α-synuclein fibrils into rats triggers α-synuclein pathology and bilateral nigrostriatal degeneration. *Neurobiol Dis*, 82, 185–199.

Paxinou, E., Chen, Q., Weisse, M., Giasson, B. I., Norris, E. H., Rueter, S. M., Trojanowski, J. Q., Lee, V. M. & Ischiropoulos, H. (2001) Induction of alpha-synuclein aggregation by intracellular nitrative insult. *J Neurosci,* 21, 8053–8061.

Peelaerts, W., Bousset, L., Van Der Perren, A., Moskalyuk, A., Pulizzi, R., Giugliano, M., Van Den Haute, C., Melki, R. & Baekelandt, V. (2015) α-Synuclein strains cause distinct synucleinopathies after local and systemic administration. *Nature*, 522, 340–344.

Petroi, D., Popova, B., Taheri-Talesh, N., Irniger, S., Shahpasandzadeh, H., Zweckstetters, M., Outeiro, T. F. & Braus, G. H. (2012) Aggregate clearance of alpha-synuclein in Saccharomyces cerevisiae depends more on autophagosome and vacuole function than on the proteasome. *J Biol Chem*, 287, 27567–27579.

Polymeropoulos, M. H., Lavedan, C., Leroy, E., Ide, S. E., Dehejia, A., Dutra, A., Pike, B., Root, H., Rubenstein, J., Boyer, R., Stenroos, E. S., Chandrasekharappa, S., Athanassiadou, A., Papapetropoulos, T., Johnson, W. G., Lazzarini, A. M., Duvoisin, R. C., Di Iorio, G., Golbe, L. I. & Nussbaum, R. L. (1997) Mutation in the α-synuclein gene identified in families with Parkinson's disease. *Science*, 276, 2045–2047.

Post, M. R., Lieberman, O. J., & Mosharov, E. V. (2018) Can interactions between α-synuclein, dopamine and calcium explain selective neurodegeneration in Parkinson's disease? *Font Neurosci*, 12, 1–11.

Pronin, a N., Morris, a J., Surguchov, a, & Benovic, J. L. (2000) Synucleins are a novel class of substrates for G protein-coupled receptor kinases. *J Biol Chem*, 275, 26515–26522.

Puccini, J. M., Marker, D. F., Fitzgerald, T., Barbieri, J., Kim, C. S., Miller-Rhodes, P., Lu, S. M., Dewhurst, S.& Gelbard, H. A. (2015) Leucine-Rich Repeat Kinase 2 Modulates Neuroinflammation and Neurotoxicity in Models of Human Immunodeficiency Virus 1-Associated Neurocognitive Disorders. *J Neurosci*, 35, 5271–5283.

Qing, H., Wong, W., McGeer, E. G., & McGeer, P. L. (2009) Lrrk2 phosphorylates alpha synuclein at serine 129: Parkinson disease implications. *Biochem Bioph Res Co*, 387, 149–152.

Ramonet, D., Daher, J. P. L., Lin, B. M., Stafa, K., Kim, J., Banerjee, R., Westerlund, M., Pletnikova, O., Glauser, L., Yang, L., Liu, Y., Swing, D. A., Beal, M. F., Troncoso, J. C., McCaffery, J. M., Jenkins, N. A., Copeland, N. G., Galter, D., Thomas, B., Lee, M. K., Dawson, T. M., Dawson, V. L. & Moore, D. J. (2011) Dopaminergic Neuronal loss, Reduced Neurite Complexity and Autophagic Abnormalities in Transgenic Mice Expressing G2019S Mutant LRRK2. *PLoS ONE*, 6, 13–19.

Recasens, A., & Dehay, B. (2014) Alpha-synuclein spreading in Parkinson's disease. *Front Neuroanat*, 8.

Reeve, A. K., Ludtmann, M. H. R., Angelova, P. R., Simcox, E. M., Horrocks, M. H., Klenerman, D., Gandhi, S., Turnbull, D. M. & Abramov, A. Y. (2015) Aggregated α-synuclein and complex I deficiency: exploration of their relationship in differentiated neurons. *Cell Death Dis*, 6, e1820.

Rideout, H. J., Larsen, K. E., Sulzer, D., & Stefanis, L. (2001) Proteasomal inhibition leads to formation of ubiquitin/alpha-synuclein-immunoreactive inclusions in PC12 cells. *J Neurochem*, 78, 899–908.

Rideout, H. J., & Stefanis, L. (2002) Proteasomal inhibition-induced inclusion formation and death in cortical neurons require transcription and ubiquitination. *Mol Cell Neurosci*, 21, 223–238.

Ross, O. A., Soto-Ortolaza, A. I., Heckman, M. G., Aasly, J. O., Abahuni, N., Annesi, G., Bacon, J. A., Bardien, S., Bozi, M., Brice, A., Brighina, L., Van Broeckhoven, C., Carr, J., Chartier-Harlin, M. C., Dardiotis, E., Dickson, D. W., Diehl, N. N., Elbaz, A., Ferrarese, C., Ferraris, A., Fiske, B., Gibson, J. M., Gibson, R., Hadjigeorgiou, G. M., Hattori, N., Ioannidis, J. P.A., Jasinska-Myga, B., Jeon, B. S., Kim, Y. J., Klein, C., Kruger, R., Kyratzi, E., Lesage, S., Lin, C. H., Lynch, T., Maraganore, D. M., Mellick, G. D., Mutez, E., Nilsson, C., Opala, G., Park, S. S., Puschmann, A., Quattrone, A., Sharma, M., Silburn, P. A., Sohn, Y. H., Stefanis, L., Tadic, V., Theuns, J., Tomiyama, H., Uitti, R. J., Valente, E. M., van de Loo, S., Vassilatis, D. K., Vilariño-Güell, C., White, L. R., Wirdefeldt, K., Wszolek, Z. K., Wu, R. M. & Farrer, M. J. (2011) Association of LRRK2 exonic variants with susceptibility to Parkinson's disease: A case-control study. *Lancet Neurol*, 10, 898–908.

Rudenko, I. N., & Cookson, M. R. (2010) 14-3-3 proteins are promising LRRK2 interactors. *Biochem J*, 430, e5–e6.

Russo, I., Berti, G., Plotegher, N., Bernardo, G., Filograna, R., Bubacco, L., & Greggio, E. (2015) Leucine-rich repeat kinase 2 positively regulates inflammation and down-regulates NF- κB p50 signaling in cultured microglia cells. *J Neuroinflamm,* 9, 1–13.

Ryan, T., Bamm, V. V., Stykel, M. G., Coackley, C. L., Humphries, K. M., Jamieson-Williams, R., Ambasudhan, R., Mosser, D. D., Lipton, S. A., Harauz, G. & Ryan, S. D. (2018) Cardiolipin exposure on the outer mitochondrial membrane modulates α-synuclein. *Nat Commun*, 9.

Saez-Atienzar, S., Bonet-Ponce, L., Blesa, J. R., Romero, F. J., Murphy, M. P., Jordan, J., & Galindo, M. F. (2014) The LRRK2 inhibitor GSK2578215A induces protective autophagy in SH-SY5Y cells: involvement of Drp-1-mediated mitochondrial fission and mitochondrial-derived ROS signaling. *Cell Death Dis*, 5, e1368.

Saha, S., Guillily, M. D., Ferree, A., Lanceta, J., Chan, D., Ghosh, J., Hsu, C. H., Segal, L., Raghavan, K., Matsumoto, K., Hisamoto, N., Kuwahara, T., Iwatsubo, T., Moore, L., Goldstein, L., Cookson, M. & Wolozin, B. (2009) LRRK2 modulates vulnerability to mitochondrial dysfunction in Caenorhabditis elegans. *J Neurosci*, 29, 9210–9218.

Saha, S., Ash, P. E. a., Gowda, V., Liu, L., Shirihai, O., & Wolozin, B. (2015) Mutations in LRRK2 potentiate age-related impairment of autophagic flux. *Mol Neurodegener*, 10, 26.

Saito, Y., Kawashima, A., Ruberu, N. N., Fujiwara, H., Koyama, S., Sawabe, M., Arai, T., Nagura, H., Yamanouchi, H., Hasegawa, M., Iwatsubo, T. & Murayama, S. (2003) Accumulation of phosphorylated alpha-synuclein in aging human brain. *J Neuropath Exp Neur*, 62, 644–654.

Sarafian, T. A., Ryan, C. M., Souda, P., Masliah, E., Kar, U. K., Vinters, H. V., Mathern, G. W., Faull, K. F., Whitelegge, J. P. & Watson, J. B. (2013) Impairment of Mitochondria in Adult Mouse Brain Overexpressing Predominantly Full-Length, N-Terminally Acetylated Human alpha-Synuclein. *PLoS ONE*, 8.

Satake, W., Nakabayashi, Y., Mizuta, I., Hirota, Y., Ito, C., Kubo, M., Kawaguchi, T., Tsunoda, T., Watanabe, M., Takeda, A., Tomiyama, H., Nakashima, K., Hasegawa, K., Obata, F., Yoshikawa, T., Kawakami, H., Sakoda, S., Yamamoto, M., Hattori, N., Murata, M., Nakamura, Y. & Toda, T. (2009) Genome-wide association study identifies common variants at four loci as genetic risk factors for Parkinson's disease. *Nat Genet*, 41, 1303–1307.

Sato, H., Arawaka, S., Hara, S., Fukushima, S., Koga, K., Koyama, S. & Kato, T. (2011) Authentically Phosphorylated alpha-Synuclein at Ser129 Accelerates Neurodegeneration in a Rat Model of Familial Parkinson's Disease. *J Neurosci*, 31, 16884–94.

Schapansky, J., Nardozzi, J. D., Felizia, F., & LaVoie, M. J. (2014) Membrane recruitment of endogenous LRRK2 precedes its potent regulation of autophagy. *Hum Mol Genet*, 23, 4201–4214.

Schapansky, J., Khasnavis, S., DeAndrade, M. P., Nardozzi, J. D., Falkson, S. R., Boyd, J. D., Sanderson, J. B., Bartels, T., Melrose, H. L. & LaVoie, M. J. (2018) Familial knockin mutation of LRRK2 causes lysosomal dysfunction and accumulation of endogenous insoluble α-synuclein in neurons. *Neurobiol Dis*, 111, 26–35.

Schapira, A. H., Cooper, J. M., Dexter, D., Clark, J. B., Jenner, P., & Marsden, C. D. (1990) Mitochondrial complex I deficiency in Parkinson's disease. *J Neurochem*, 54, 823–827.

Schapira, A. H. (2008). Mitochondria in the aetiology and pathogenesis of Parkinson's disease. *Lancet Neurol*, 7, 97–109.

Sheng, Z., Zhang, S., Bustos, D., Kleinheinz, T., Le Pichon, C. E., Dominguez, S. L., Solanoy, H. O., Drummond, J., Zhang, X., Ding, X., Cai, F., Song, Q., Li, X., Yue, Z., van der Brug, M. P., Burdick, D. J., Gunzner-Toste, J., Chen, H., Liu, X., Estrada, A. A., Sweeney, Z. K., Scearce-Levie, K., Moffat, J. G., Kirkpatrick, D. S. & Zhu, H. (2012) Ser1292 Autophosphorylation Is an Indicator of LRRK2 Kinase Activity and Contributes to the Cellular Effects of PD Mutations. *Sci Transl Med*, 4, 164ra161-164ra161.

Shintani, T., & Klionsky, D. J. (2004) Autophagy in health and disease: A double-edged sword. *Science*, 306, 990-5.

Simón-Sánchez, J., Schulte, C., Bras, J. M., Sharma, M., Gibbs, J. R., Berg, D., Paisan-Ruiz, C., Lichtner, P., Scholz, S W., Hernandez, D. G., Krüger, R., Federoff, M., Klein, C., Goate, A., Perlmutter, J., Bonin, M., Nalls, M. A., Illig, T., Gieger, C., Houlden, H., Steffens, M., Okun, M. S., Racette, B. A., Cookson, M. R., Foote, K. D., Fernandez, K. H., Traynor, B. J., Schreiber, S., Arepalli, S., Zonozi, R., Gwinn, K., Van Der Brug, M., Lopez, G., Chanock, S. J., Schatzkin, A., Park, Y., Hollenbeck, A., Gao, J., Huang, X., Wood, N. W., Lorenz, D., Deuschl, G., Chen, H., Riess, O., Hardy, J. A. & Gasser, T. (2009) Genome-wide association study reveals genetic risk underlying Parkinson's disease. *Nat Genet*, 41, 1308–1312.

Singleton, A. B., Farrer, M., Johnson, J., Singleton, A., Hague, S., Kachergus, J., Hulihan, M., Peuralinna, T., Dutra, A., Nussbaum, R., Lincoln, S., Crawley, A., Hanson, M., Maraganore, D., Adler, C., Cookson, M. R., Muenter, M., Baptista, M., Miller, D., Blancato, J., Hardy, J. & Gwinn-Hardy, K. (2003) α-Synuclein Locus Triplication Causes Parkinson's Disease. *Science*, 302, 841.

Skaper, S. D., Facci, L., Zusso, M., & Giusti, P. (2018) An Inflammation-Centric View of Neurological Disease: Beyond the Neuron. *Front Cell Neurosci*, 12, 1–26.

Skibinski, G., Nakamura, K., Cookson, M. R., & Finkbeiner, S. (2014) Mutant LRRK2 toxicity in neurons depends on LRRK2 levels and synuclein but not kinase activity or inclusion bodies. *J Neurosci*, 34, 418–433.

Slone, S. R., Lavalley, N., McFerrin, M., Wang, B., & Yacoubian, T. A. (2015) Increased 14-3-3 phosphorylation observed in Parkinson's disease reduces neuroprotective potential of 14-3-3 proteins. *Neurobiol Dis*, 79, 1–13.

Smith, W. W., Pei, Z., Jiang, H., Dawson, V. L., Dawson, T. M., & Ross, C. A. (2006) Kinase activity of mutant LRRK2 mediates neuronal toxicity. *Nat Neurosci*, 9, 1231–1233.

Song, D. D., Shults, C. W., Sisk, A., Rockenstein, E., & Masliah, E. (2004) Enhanced substantia nigra mitochondrial pathology in human alpha-synuclein transgenic mice after treatment with MPTP. *Exp Neurol*, 186, 158–172.

Stichel, C. C., Zhu, X. R., Bader, V., Linnartz, B., Schmidt, S., & Lübbert, H. (2007) Mono- and double-mutant mouse models of Parkinson's disease display severe mitochondrial damage. *Hum Mol Genet*, 16, 2377–2393.

Su, Y. C., & Qi, X. (2013) Inhibition of excessive mitochondrial fission reduced aberrant autophagy and neuronal damage caused by LRRK2 G2019S mutation. *Hum Mol Genet*, 22, 4545–4561.

Subramaniam, S. R., Vergnes, L., Franich, N. R., Reue, K., & Chesselet, M. F. (2014) Region specific mitochondrial impairment in mice with widespread overexpression of alpha-synuclein. *Neurobiol Dis*, 70, 204–213.

Sun, Q., Wang, T., Jiang, T., Huang, P., Li, D., Wang, Y., Xiao, Q., Liu, J. & Chen, S. (2016) Effect of a Leucine-rich Repeat Kinase 2 Variant on Motor and Non-motor Symptoms in Chinese Parkinson's Disease Patients. *Aging Dis*, 7, 230–236.

Surmeier, D. J., Obeso, J. A., & Halliday, G. M. (2017a) Parkinson's Disease Is Not Simply a Prion Disorder. *J Neurosci*, 37, 9799–9807.

Surmeier, D. J., Obeso, J. A., & Halliday, G. M. (2017b) Selective neuronal vulnerability in Parkinson disease. *Nat Rev Neurosci*, 18, 101–113.

Tan, E.K., Shen, H., Tan, L.C.S., Farrer, M., Yew, K., Chua, E., Jamora, R.D., Puvan, K., Puong, K.Y., Zhao, Y., Pavanni, R., Wong, M.C., Yih, Y., Skipper, L. & Liu, J.J. (2005) The G2019S LRRK2 mutation is uncommon in an Asian cohort of Parkinson's disease patients. *Neurosci Lett*, 384, 327–329.

Tan, E.K., Zhao, Y., Tan, L., Lim, H.Q., Lee, J., Yuen, Y., Pavanni, R., Wong, M.C., Fook-Chong, S. & Liu, J.J. (2007) Analysis of LRRK2 Gly2385Arg genetic variant in non-Chinese Asians. *Movement Disord*, 22, 1816–1818.

Tanik, S. A., Schultheiss, C. E., Volpicelli-Daley, L. A., Brunden, K. R., & Lee, V. M. Y. (2013) Lewy body-like alpha-synuclein aggregates resist degradation and impair macroautophagy. *J Biol Chem*, 288, 15194–15210.

Tarasova, T. V., Lytkina, O. A., Goloborshcheva, V. V., Skuratovskaya, L. N., Antohin, A. I., Ovchinnikov, R. K. & Kukharsky, M. S. (2018) Genetic Inactivation of Alpha-Synuclein Affects Embryonic Development of Dopaminergic Neurons of the Substantia Nigra, but Not the Ventral Tegmental Area, in Mouse Brain. *PeerJ*.

Taymans, J.-M., & Greggio, E. (2016) LRRK2 Kinase Inhibition as a Therapeutic Strategy for Parkinson's Disease, Where Do We Stand? *Current Neuropharmacology*, 14, 214–225.

Thévenet, J., Gobert, R., van Huijsduijnen, R. H., Wiessner, C., & Sagot, Y. J. (2011) Regulation of LRRK2 expression points to a functional role in human monocyte maturation. *PLoS ONE*, 6.

Tofaris, G. K., Layfield, R., & Spillantini, M. G. (2001) α-Synuclein metabolism and aggregation is linked to ubiquitin-independent degradation by the proteasome. *FEBS Lett*, 509, 22–26.

Tong, Y., Yamaguchi, H., Giaime, E., Boyle, S., Kopan, R., Kelleher, R. J., & Shen, J. (2010) Loss of leucine-rich repeat kinase 2 causes impairment of protein degradation pathways, accumulation of -synuclein, and apoptotic cell death in aged mice. *P Natl A Sci*, 107, 9879–9884.

Trabzuni, D., Ryten, M., Emmett, W., Ramasamy, A., Lackner, K.J., Zeller, T., Walker, R., Smith, C., Lewis, P.A., Mamais, A., de Silva, R., Vandrovcova, J., Hernandez, D., Nalls, M.A., Sharma, M., Garnier, S., Lesage, S., Simon-Sanchez, J., Gasser, T., Heutink, P., Brice, A., Singleton, A., Cai, H., Schadt, E., Wood, N.W., Bandopadhyay, R., Weale, M.E., Hardy, J. & Plagnol, V. (2013) Fine-Mapping, Gene Expression and Splicing Analysis of the Disease Associated LRRK2 Locus. *PLoS ONE*, 8.

Trinh, J., Amouri, R., Duda, J.E., Morley, J.F., Read, M., Donald, A., Vilariño-Güell, C., Thompson, C., Szu Tu, C., Gustavsson, E.K., Ben Sassi, S., Hentati, E., Zouari, M., Farhat, E., Nabli, F., Hentati, F. & Farrer, M.J. (2014) A comparative study of Parkinson's disease and leucine-rich repeat kinase 2 p.G2019S parkinsonism. *Neurobiol Aging*, 35, 1125–1131.

Van der Putten, H., Wiederhold, K.H., Probst, A., Barbieri, S., Mistl, C., Danner, S., Kauffmann, S., Hofele, K., Spooren, W., Ruegg, M.A., Lin, S., Caroni, P., Sommer, B., Tolnay, M. & Bilbe, G. (2000) Neuropathology in mice expressing human α-synuclein. *J Neurosci*, 20, 6021–6029.

Venderova, K., Kabbach, G., Abdel-Messih, E., Zhang, Y., Parks, R. J., Imai, Y., Gehrke, S., Ngsee, J., Lavoie, M. J., Slack, R. S., Rao, Y., Zhang, Z., Lu, B., Haque, M. E. & Park, D. S. (2009) Leucine-rich repeat kinase 2 interacts with Parkin, DJ-1 and PINK-1 in a Drosophila melanogaster model of Parkinson's disease. *Hum Mol Genet*, 18, 4390–4404.

Vogiatzi, T., Xilouri, M., Vekrellis, K., & Stefanis, L. (2008) Wild type alpha-synuclein is degraded by chaperone-mediated autophagy and macroautophagy in neuronal cells. *J Biol Chem*, 283, 23542–23556.

Volpicelli-Daley, L.A., Luk, K.C., Patel, T.P., Tanik, S.A., Riddle, D.M., Stieber, A., Meaney, D.F., Trojanowski, J.Q. & Lee, V.M.Y. (2011) Exogenous α-Synuclein Fibrils Induce Lewy Body Pathology Leading to Synaptic Dysfunction and Neuron Death. *Neuron*, 72, 57–71.

Volpicelli-Daley, L.A., Abdelmotilib, H., Liu, Z., Stoyka, L., Daher, J.P.L., Milnerwood, A.J., Unni, V.K., Hirst, W.D., Yue, Z., Zhao, H.T., Fraser, K., Kennedy, R.E. & West, A.B. (2016) G2019S-LRRK2 Expression Augments -Synuclein Sequestration into Inclusions in Neurons. *J Neurosci*, 36, 7415–7427.

Walker, M.D., Volta, M., Cataldi, S., Dinelle, K., Beccano-Kelly, D., Munsie, L., Kornelsen, R., Mah, C., Chou, P., Co, K., Khinda, J., Mroczek, M., Bergeron, S., Yu, K., Cao, L.P. in., Funk, N., Ott, T., Galter, D., Riess, O., Biskup, S., Milnerwood, A.J., Stoessl, A.J., Farrer, M.J. & Sossi, V. (2014) Behavioral deficits and striatal DA signaling in LRRK2 p.G2019S transgenic rats: a multimodal investigation including PET neuroimaging. *J Parkinson Dis*, 4, 483–498.

Wang, X., Yan, M. H., Fujioka, H., Liu, J., Wilson-delfosse, A., Chen, S. G., Perry, G., Casadesus, G. & Zhu, X. (2012) LRRK2 regulates mitochondrial dynamics and function through direct interaction with DLP1. *Hum Mol Genet*, 21, 1931–1944.

Wang, D., Xu, L., Lv, L., Su, L.Y., Fan, Y., Zhang, D.F., Bi, R., Yu, D., Zhang, W., Li, X.A., Li, Y.Y. & Yao, Y.G. (2015) Association of the LRRK2 genetic polymorphisms with leprosy in Han Chinese from Southwest China. *Genes Immun*, 16, 112–119.

Webb, J. L., Ravikumar, B., Atkins, J., Skepper, J. N., & Rubinsztein, D. C. (2003) α-synuclein Is Degraded by Both Autophagy and the Proteasome. *J Biol Chem*, 278, 25009–25013.

Webber, P. J., Smith, A. D., Sen, S., Renfrow, M. B., Mobley, J. A., & West, A. B. (2011) Autophosphorylation in the leucine-rich repeat kinase 2 (LRRK2) GTPase domain modifies kinase and GTP-binding activities. *Journal of Molecular Biology*, 412, 94–110.

West, A. B., Moore, D. J., Biskup, S., Bugayenko, A., Smith, W. W., Ross, C. a, Dawson, V. L. & Dawson, T. M. (2005) Parkinson's disease-associated mutations in leucine-rich repeat kinase 2 augment kinase activity. *P Natl A Sci USA*, 102, 16842–16847.

West, A.B., Moore, D.J., Choi, C., Andrabi, S.A., Li, X., Dikeman, D., Biskup, S., Zhang, Z., Lim, K.L., Dawson, V.L. & Dawson, T.M. (2007) Parkinson's disease-associated mutations in LRRK2 link enhanced GTP-binding and kinase activities to neuronal toxicity. *Hum Mol Genet*, 16, 223–232

West, A. B. (2015) Ten years and counting: Moving leucine-rich repeat kinase 2 inhibitors to the clinic. *Movement Disord*, 30, 180–189.

West, A. B. (2017) Achieving neuroprotection with LRRK2 kinase inhibitors in Parkinson disease. *Exp Neurol*, 298, 236–245.

Winslow, A.R., Chen, C.W., Corrochano, S., Acevedo-Arozena, A., Gordon, D.E., Peden, A.A., Lichtenberg, M., Menzies, F.M., Ravikumar, B., Imarisio, S., Brown, S., O'Kane, C.J. & Rubinsztein, D.C. (2010) α-Synuclein impairs macroautophagy: Implications for Parkinson's disease. *J Cell Biol*, 190, 1023–1037.

Wong, Y. C., & Krainc, D. (2017) α-synuclein toxicity in neurodegeneration: Mechanism and therapeutic strategies. *Nat Med*, 23, 1–13.

Wszolek, Z. K. & Pfeiffer, R. F. (1992) Genetic considerations in movement disorders. *Curr Opin Neurol Neurosurg*, 5, 324–330.

Wu, D. C., Jackson-Lewis, V.,Vila, M., Tieu, K., Teismann, P., Vadseth, C., Choi, D-K., Ischiropoulos, H. & Przedborski, S. (2002) Blockade of Microglial Activation Is Neuroprotective in the 1-Methyl-4-Phenyl-1,2,3,6-Tetrahydropyridine Mouse Model of Parkinson Disease. *J Neurosci*, 22,1763–71.

Wu, Y.R., Tan, L.C., Fu, X., Chen, C.M., Au, W.L., Chen, L., Chen, Y.C., Prakash, K.M., Zheng, Y., Lee-Chen, G.J., Zhao, Y., Zeng, J.S., Tan, E.K.& Pei, Z. (2012) LRRK2 A419V is not associated with Parkinson's disease in different Chinese populations. *PLoS ONE*, 7.

Xanthos, D. N., & Sandkühler, J. (2014) Neurogenic neuroinflammation: Inflammatory CNS reactions in response to neuronal activity. *Nat Rev Neurosci*, 15, 43–53.

Xie, W., & Chung, K. K. K. (2012) Alpha-synuclein impairs normal dynamics of mitochondria in cell and animal models of Parkinson's disease. *J Neurochem*, 122, 404–414.

Xilouri, M., Vogiatzi, T., Vekrellis, K., Park, D., & Stefanis, L. (2009) Abberant α-synuclein confers toxicity to neurons in part through inhibition of chaperone-mediated autophagy. *PLoS ONE*, 4.

Xilouri, M., Brekk, O. R., Polissidis, A., Chrysanthou-Piterou, M., Kloukina, I., & Stefanis, L. (2016) Impairment of chaperone-mediated autophagy induces dopaminergic neurodegeneration in rats. *Autophagy*, 12, 2230–2247.

Xiong, Y., Neifert, S., Karuppagounder, S.S., Stankowski, J.N., Lee, B.D., Grima, J.C., Chen, G., Ko, H.S., Lee, Y., Swing, D., Tessarollo, L., Dawson, T.M. & Dawson, V.L. (2017). Overexpression of Parkinson's Disease-Associated Mutation LRRK2 G2019S in Mouse Forebrain Induces Behavioral Deficits and α-Synuclein Pathology. *Eneuro*, 4, 1–10.

Xiong, Y., Neifert, S., Karuppagounder, S. S., Liu, Q., Stankowski, J. N., Lee, B. D., Ko, Han SeokLee, YunjongGrima, J. C., Mao, X., Jiang, H., Kang, S. U., Swing, D. A., Iacovitti, L., Tessarollo, L., Dawson, T. M. & Dawson, V. L. (2018) Robust kinase- and age-dependent dopaminergic and norepinephrine neurodegeneration in LRRK2 G2019S transgenic mice. *P Natl A Sci*, 115, 201712648.

Xu, J., Kao, S.-Y., Lee, F. J. S., Song, W., Jin, L.-W., & Yankner, B. A. (2002) Dopamine-dependent neurotoxicity of alpha-synuclein: a mechanism for selective neurodegeneration in Parkinson disease. *Nat Med*, 8, 600–606.

Yacoubian, T. A., Cantuti-Castelvetri, I., Bouzou, B., Asteris, G., McLean, P. J., Hyman, B. T., & Standaert, D. G. (2008) Transcriptional dysregulation in a transgenic model of Parkinson disease. *Neurobiol Dis*, 29, 515–528.

Yahalom, G., Orlev, Y., Cohen, O. S., Kozlova, E., Friedman, E., Inzelberg, R., & Hassin-Baer, S. (2014) Motor progression of Parkinson's disease with the leucine-rich repeat kinase 2 G2019S mutation. *Movement Disord*, 29, 1057–1060.

Yang, X., Ren, H., Wood, K., Li, M., Qiu, S., Shi, F.-D., Ma, C. & Liu, Q. (2018) Depletion of microglia augments the dopaminergic neurotoxicity of MPTP. *FASEB J.*, 32, 3336–3345.

Yuan, J., & Yankner, B. A. (2000) Apoptosis in the nervous system. *Nature*, 407, 402–9.

Yun, S. P., Kam, T., Panicker, N., Kim, S., Oh, Y., Park, J., Kwon, S-H., Park, Y. J., Karuppagounder, S. S., Park, H., Kim, S., Oh, N., Kim, N. A., Lee, S., Brahmachari, S., Mao, X., Lee, J. H., Kumar, M., An, D., Kang, S-U., Lee, Y., Lee, K. C., Na, D. H., Kim, D., Lee, S. H., Roschke, V. V., Liddelow, S. A., Mari, Z., Barres, B. A., Dawson, V. L. & Lee, S. (2018) Block of A1 astrocyte conversion by microglia is neuroprotective in models of Parkinson's disease. *Nat Med*, 24, 931–938.

Zabetian, C.P., Yamamoto, M., Lopez, A.N., Ujike, H., Mata, I.F., Izumi, Y., Kaji, R., Maruyama, H., Morino, H., Oda, M., Hutter, C.M., Edwards, K.L., Schellenberg, G.D., Tsuang, D.W., Yearout, D., Larson, E.B. & Kawakami, H. (2009) LRRK2 mutations and risk variants in Japanese patients with Parkinson's disease. *Movement Disord*, 24, 1034–1041.

Zarranz, J.J., Alegre, J., Gómez-Esteban, J.C., Lezcano, E., Ros, R., Ampuero, I., Vidal, L., Hoenicka, J., Rodriguez, O., Atarés, B., Llorens, V., Gomez Tortosa, E., Del Ser, T., Muñoz, D.G. & De Yebenes, J.G. (2004) The New Mutation, E46K, of α-Synuclein Causes Parkinson and Lewy Body Dementia. *Ann Neurol*, 55, 164–173.

Zhang, L., Zhang, C., Zhu, Y., Cai, Q., Chan, P., Uéda, K., Yu, S. & Yang, H. (2008) Semi-quantitative analysis of α-synuclein in subcellular pools of rat brain neurons: An immunogold electron microscopic study using a C-terminal specific monoclonal antibody. *Brain Res*, 1244, 40–52.

Zhang, F.-R., Huang, W., Chen, S.-M., Sun, L.-D., Liu, H., Li, Y., Cui, Y., Yan, X.-X., Yang, H.-T., Yang, R.-D., Chu, T.-S., Zhang, C., Zhang, L., Han, J.-W., Yu, G.-Q., Quan, C., Yu, Y.-X., Zhang, Z., Shi, B.-Q., Zhang, L.-H., Cheng, H., Wang, C.-Y., Lin, Y., Zheng, H.-F., Fu, X.-A., Zuo, X.-B., Wang, Q., Long, H., Sun, Y.-P., Cheng, Y.-L., Tian, H.-Q., Zhou, F.-S., Liu, H.-X., Lu, W.-S., He, S.-M., Du, W.-L., Shen, M., Jin, Q.-Y., Wang, Y., Low, H.-Q., Erwin, T., Yang, N.-H., Li, J.-Y., Zhao, X., Jiao, Y.-L., Mao, L.-G., Yin, G., Jiang, Z.-X., Wang, X.-D., Yu, J.-P., Hu, Z.-H., Gong, C.-H., Liu, Y.-Q., Liu, R.-Y., Wang, D.-M., Wei, D., Liu, J.-X., Cao, W.-K., Cao, H.-Z., Li, Y.-P., Yan, W.-G., Wei, S.-Y., Wang, K.-J., Hibberd, M.L., Yang, S., Zhang, X.-J. & Liu, J.-J. (2009) Genomewide association study of leprosy. *New Engl J Med*, 361, 2609–2618.

Zhang, L., Dong, Y., Xu, X., & Xu, Z. (2012) The role of autophagy in Parkinson's disease. *Neural Regen Res*, 7, 141–145.

Zimprich, A., Biskup, S., Leitner, P., Lichtner, P., Farrer, M., Lincoln, S., Kachergus, J., Hulihan, M., Uitti, R.J., Calne, D.B., Stoessl, A.J., Pfeiffer, R.F., Patenge, N., Carbajal, I.C., Vieregge, P., Asmus, F., Müller-Myhsok, B., Dickson, D.W., Meitinger, T., Strom, T.M., Wszolek, Z.K. & Gasser, T. (2004) Mutations in LRRK2 cause autosomal-dominant parkinsonism with pleomorphic pathology. *Neuron*, 44, 601–607

8.2 Article: The C-terminal domain of LRRK2 with the G2019S mutation is sufficient to produce neurodegeneration of dopaminergic neurons in vivo (Neurobiol Dis., 2019)

Noémie Cresto [1,2], Marie-Claude Gaillard [1,2], Camille Gardier[1,2], Francesco Gubinelli[1,2], Elsa Diguet [1,2,3], Déborah Bellet [1,2], Laurine Legroux [1,2], Julien Mitja [1,2], Gwenaëlle Auregan [1,2], Martine Guillermier [1,2], Charlène Josephine [1,2], Caroline Jan [1,2], Noëlle Dufour [1,2], Alain Joliot [4], Philippe Hantraye [1,2], Gilles Bonvento [1,2], Nicole Déglon [1,5,6], Alexis-Pierre Bemelmans [1,2], Karine Cambon [1,2], Géraldine Liot [1,2], Emmanuel Brouillet [1,2] §

1 - CEA, DRF, Institut de Biologie Françoise Jacob, Molecular Imaging Research Center (MIRCen), F-92265 Fontenay-aux-Roses, France
2 - CNRS, CEA, Paris-Sud Univ., Univ. Paris-Saclay, Neurodegenerative Diseases Laboratory (UMR9199), F-92265, Fontenay-aux-Roses, France
3 - Institut de Recherche SERVIER, Neuropsychiatry Department, 125 chemin de ronde, 78290 Croissy sur Seine, France
4 - Homeoprotein and Plasticity, Center for Interdisciplinary Research in Biology (CIRB), College de France, CNRS, INSERM, PSL Research University, Paris, France.
5 - Lausanne University Medical School (CHUV), Department of Clinical Neurosciences (DNC), Laboratory of Cellular and Molecular Neurotherapies (LNCM), Lausanne, Switzerland
6 - Lausanne University Medical School (CHUV), Neuroscience Research Center (CRN), Laboratory of Cellular and Molecular Neurotherapies (LNCM), Lausanne, Switzerland

§, Correspondence: emmanuel.brouillet@cea.fr

Highlights

New LVs and AAVs were developed to study the effects of a C-terminal fragment of LRRK2 containing the kinase domain
ΔLRRK2^{G2019S} produces molecular and cellular effects that are kinase activity-dependent
In vivo, ΔLRRK2^{G2019S} leads to DA neurodegeneration when using AAV-mediated gene transfer

Abbreviations:

ΔLRRK2 ROC-COR-kinase plus the WD40 domain
AAV adeno-associated virus
ANK Ankyrin
ANOVA analysis of variance
ARM Armadillo
ATP Adenosine triphosphate
BSA Bovine serum albumin
BCA bicinchoninic acid assay
CamKII Calmodulin-kinase II
COR C-terminal of ROC
DA Dopaminergic
DAB Diaminobenzidine
DLU Density light unit
DK double-mutant G2019S/D1994A dead kinase
GFP Green fluorescent protein
GS G2019S mutation
GWAS Genome-wide association studies
HA Hemagglutinin tag
K Kinase domain of LRRK2
KB1 Kinase buffer 1 (20 mM HEPES; 150 mM NaCl, 5 mM
EGTA; 20 mM □-glycerophosphate)
KB2 Kinase buffer 2 (10 mM ATP; 20 mM MgCl2)
LB Lysis buffer (50 mM Tris, pH 8.0, 150 mM NaCl, 1 mM EDTA, 0.5% Triton X-100, 1% NP40, protease inhibitors)
LRR Leucin-rich repeats
LRRK2 Leucin-rich repeats kinase 2
LV Lentivirus

MBP Myelin basic protein
PAGE Poly-Acrylamide Gel Electrophoresis
PBS Phosphate buffer saline
PBS-T Phosphate Buffer Saline with 0.2% Triton X-100
PD Parkinson's disease
RCK Kinase domain plus the ROC-COR domain
ROC Ras-of-complex protein
SDS Sodium-dodecyl-Sulfate
SNc Substantia nigra *pars compacta*
SNPs single-nucleotide polymorphisms
TBS Tris Buffer Saline
TBS-T Tris Buffer Saline with 0.1% Tween-20
TH Tyrosine hydroxylase
WT Wild-type

Abstract

The G2019S substitution in the kinase domain of LRRK2 (LRRK2^{G2019S}) is the most prevalent mutation associated with Parkinson's disease (PD). Neurotoxic effects of LRRK2^{G2019S} are thought to result from an increase in its kinase activity as compared to wild type LRRK2. However, it is unclear whether the kinase domain of LRRK2^{G2019S} is sufficient to trigger degeneration or if the full length protein is required. To address this question, we generated constructs corresponding to the C-terminal domain of LRRK2 (ΔLRRK2). A kinase activity that was increased by G2019→S substitution could be detected in ΔLRRK2. However biochemical experiments suggested it did not bind or phosphorylate the substrate RAB10, in contrast to full length LRRK2. The overexpression of ΔLRRK2^{G2019S} in the rat striatum using lentiviral vectors (LVs) offered a straightforward and simple way to investigate its effects in neurons *in vivo*. Results from a RT-qPCR array analysis indicated that ΔLRRK2^{G2019S} led to significant mRNA expression changes consistent with a kinase-dependent mechanism. We next asked whether ΔLRRK2 could be sufficient to trigger neurodegeneration in the substantia nigra *pars compacta* (SNc) in adult rats. Six months after infection of the substantia nigra pars compacta (SNc) with LV-ΔLRRK2^{WT} or LV-ΔLRRK2^{G2019S}, the number of DA neurons was unchanged. To examine whether higher levels of ΔLRRK2^{G2019S} could trigger degeneration we cloned ΔLRRK2 in AAV2/9 construct. As expected, AAV2/9 injected in the SNc led to neuronal expression of ΔLRRK2^{WT} and ΔLRRK2^{G2019S} at much higher levels than those obtained with LVs. Six months after injection, unbiased stereology showed that AAV-ΔLRRK2^{G2019S} produced a significant ~30% loss of neurons positive for tyrosine hydroxylase- and for the vesicular dopamine transporter whereas AAV-ΔLRRK2^{WT} did not. These findings show that overexpression of the C-terminal part of LRRK2 containing the mutant kinase domain is sufficient to trigger degeneration of DA neurons, through cell-autonomous mechanisms, possibly independent of RAB10.

Introduction

Parkinson's disease (PD) is a neurodegenerative disorder affecting approximately seven million people worldwide. It is characterised by motor symptoms (rigidity, bradykinesia, resting tremors, gait instability) and a large spectrum of non-motor symptoms (e.g. dysosmia, sleep disorder, dementia) (Poewe, 2008; Rodriguez-Oroz et al., 2009). The neuropathological hallmarks of PD are a progressive loss of dopaminergic (DA) neurons in the substantia nigra *pars compacta* (SNc) and the presence of neuronal inclusions (Lewy bodies) and dystrophic neurites containing aggregated α-synuclein protein (Braak and Braak, 2000). The cause of DA neuron degeneration is poorly understood. PD is mostly sporadic, but a genetic origin can be found in about 10% of cases. Several genes are known to be associated with familial (or *de novo* genetic) forms of PD (Lesage and Brice, 2009).

Mutations in the *LRRK2* (Leucine-Rich Repeat Kinase 2) gene are the most common genetic cause of both familial and sporadic PD (Paisán-Ruíz et al., 2004). Genome-wide association studies (GWAS) have also identified single-nucleotide polymorphisms (SNPs) at the *LRRK2* locus significantly associated with an increase or a decrease in the risk of developing PD, consistent with a key role for LRRK2 in PD pathogenesis (Nalls et al., 2014; Satake et al., 2009). It has also recently been shown that LRRK2 was activated (increased autophosphorylation and increased phosphorylation of its substrate RAB10) in the SNc of sporadic PD patients (Di Maio et al., 2018). The most prevalent pathogenic mutation of LRRK2 is the G2019S substitution (Gilks et al., 2005; Healy et al., 2008).

The mechanisms underlying the neurotoxicity of the G2019S mutant LRRK2 protein (LRRK2^{G2019S}) are unknown (Cresto et al., 2018). *LRRK2* gene encodes a large 2527-amino acid multidomain protein. The pathogenic mutations of *LRRK2* are clustered in the central region encoding the three domains forming the catalytic (kinase) core of the protein (Cookson, 2010; Mata et al., 2006). The G2019S mutation affects an amino acid located in this kinase domain. LRRK2 belongs to the ROCO protein family, and bears the tandem Ras-of-complex proteins (Roc), GTPase and C-terminal of Roc (COR) domains characteristic of this family. LRRK2 also has regions involved in protein-protein interactions [ankyrin (ANK), armadillo (ARM), leucine-rich repeats (LRR)] at its N-terminal and a WD40 domain at its C-terminal, suggesting a possible function as a scaffolding protein. The G2019S mutation increases LRRK2 kinase activity (both auto-phosphorylation and the phosphorylation of substrates) and there is compelling evidence to suggest that the neurotoxicity of LRRK2^{G2019S} is linked to an increase in the kinase activity of this protein (Lee et al., 2010a; West et al., 2007). Recent results obtained in transgenic mice expressing LRRK2 in non-dopaminergic neurons show that full length LRRK2^{G2019S} is no longer neurotoxic when its kinase domain is inactivated (e.g. D1994E mutation), which demonstrates that the activity of the kinase domain is crucial for toxicity (Xiong et al., 2017). In support of this, a number of studies showed that pharmacological inhibitors of the kinase can produce neuroprotection against mutant LRRK2 (for a

review see Cresto et al, 2019). However, it is unclear whether the kinase domain of LRRK2^{G2019S} is sufficient to trigger degeneration or if the full length protein is required. Several reports indicated that truncated fragments of LRRK2 can produce cellular changes that depend on the activity of the kinase domain, indicating that the entire protein may not be required to trigger some of LRRK2 signalling/biological functions (Aufschnaiter et al., 2018; Pereira et al., 2014; Sheng et al., 2010). This question is not purely theoretical. It may have practical implications. Especially, apart from existing compounds that produce LRRK2 kinase inhibition, other types of strategies (peptide, aptamers etc…) selectively impeaching the interaction of the kinase domain with its substrates (without interfering with non-kinase-dependent LRRK2 functions associated with the N-terminal domain for example) may also be of interest.
The role of the LRRK2 kinase domain in dopaminergic (DA) neurons has rarely been studied *in vivo*. Transgenic and knock-in genetic models expressing LRRK2^{G2019S} have been developed in rodents. These animals display very progressive motor deficits, subtle defects in striatal DA release, but little or no DA neuron loss, even at two years of age (Beccano-Kelly et al., 2014; Lee et al., 2015; Ramonet et al., 2011; Yue et al., 2015). This is likely due to the low expression of LRRK2 in DA neurons is these models. Double transgenic mice expressing high levels of LRRK2 under the control of the CamKII and Tet promoters show progressive degeneration of neurons in the cortex and striatum (Lin et al., 2009), whereas the SNc is spared since CamKII induces minimal expression in DA cells. Of major interest, a recent report showed that expression of LRRK2^{G2019S} under the control of the TH promoter leads to robust degeneration of DA neurons and a severe behavioural phenotype (Xiong et al., 2018). These results suggest that high levels of LRRK2^{G2019S} expression are required to trigger cell death in the SNc. In support of this hypothesis, intrastriatal injection of an HSV amplicon (HSV) and an adenovirus (Adeno) encoding LRRK2^{G2019S} in the mouse and rat striatum respectively, produces a partial but relatively rapid degeneration of DA neurons (Dusonchet et al., 2011; Lee et al., 2010a). It was also shown recently that overexpression of LRRK2^{G2019S} in SNc after injection of canine-Adeno viral vectors (CAV2) in the striatum leads to partial degeneration of dopaminergic neurons in the SNc in the primate *microcebus murinus* (Mestre-Francés et al., 2018). Although these vectors do not transduce DA neurons alone (striatal neurons and astrocytes are transduced as well), these new studies demonstrate that local brain infection with viral vectors might be a versatile approach to study mutant LRRK2 pathophysiology *in vivo* in different animal species.
Here, we investigated whether an increase in the kinase activity of LRRK2^{G2019S} selectively in DA neurons could lead to cell-autonomous neurodegeneration. We addressed this question *in vivo,* in the context of the DA neurons of the SNc in rats. We used lentiviral vectors (LVs) and adeno-associated viruses (AAV2/9), which can overexpress transgenes selectively in neurons. In this study, we generated lentiviral vectors (LVs) encoding the C-terminal part [1326-2527 a.a., called hereafter "ΔLRRK2"] of the wild-type (ΔLRRK2^{WT}), G2019S mutant (ΔLRRK2^{G2019S}) or double-mutant G2019S/D1994A dead kinase (ΔLRRK2^{DK}) forms of LRRK2. Since our results showed that LV-mediated overexpression of ΔLRRK2 produced no significant toxicity in dopaminergic neurons *in vivo*, we generated AAV2/9 encoding ΔLRRK2 fragments and tested the potential neurotoxic effects of these AAVs after their stereotaxic injection into the SNc of adult rats. Effects of vectors coding ΔLRRK2 were mainly evaluated using behavioural motor tests and histological evaluation of the nigro-striatal pathway (See Supplementary Fig. S1 for general design of *in vivo* experiments in rats).

Materials and methods

Viral construction and production

Lentivirus. DNA sequences encoding GFP and the C-terminal part of human LRRK2 (kinase,K; ROC-COR-kinase, RCK; RCK plus the WD40 domain, called hereafter "ΔLRRK2") were synthesised and inserted into the self-inactivated vector (SIN) backbone containing the WPRE element (W) and the murine ubiquitous phosphoglycerate kinase 1 promoter (PGK). We generated lentivirus vectors LV-GFP, and LV-ΔLRRK2 coding for the WT form or G2019S forms of the fragments. Viral particles were produced as described elsewhere (Hottinger et al., 2000). All the SIN vectors were pseudotyped with VSVg glycoprotein G. Briefly, the viral particles were produced in HEK-293T cells by a four plasmid transient transfection system (Naldini et al., 1996). The supernatant was collected 48 hours later and filtered, and the particle content of the viral batches was determined by ELISA for the p24 antigen (Gentaur, Paris, France). High-titre stocks were obtained by ultracentrifugation. The pellet was re-suspended in 1% BSA in PBS, frozen and stored at −80°C. LV-ΔLRRK2 vectors were used at a concentration of 100 ng/µl p24.
Adeno-associated viral vector (AAV). Plasmid constructs were packaged into AAV2/9 capsids as described previously (Berger et al., 2015). Briefly, viral particles were produced by co-transfection of HEK-293T cells with (1) an adenovirus helper plasmid (pXX6-80), (2) an AAV and expressed as viral genomes per ml of concentrated stocks (Vg/ml) (Aurnhammer et al., 2012).

Cell studies

Human embryonic kidney 293T cells (HEK293T) were grown at 37°C in Dulbecco's modified Eagle's medium supplemented with 10% bovine calf serums, under an atmosphere containing 5% CO_2 . For the study of recombinant ΔLRRK2, cultured cells were seeded on wells and transfected by calcium phosphate transfection methods with the different forms of ΔLRRK2 vectors. For RAB10 immunoprecipitation studies with the ΔLRRK2 fragments, a stable HEK 293T cell line was generated using lentivirus infection. The ΔLRRK2 cell lines (LacZ, WT, GS, DK) were maintained as the parental HEK described just above.

Biochemical analysis

Western blotting. Overall levels of fragment expression were determined by lysing cells in modified RIPA buffer (without SDS): 50 mM Tris, pH 8.0, 150 mM NaCl, 1 mM EDTA, 0.5% Triton X-100, 1% NP40 and protease inhibitor cocktail (Roche). Cell lysates were centrifuged at 13,000 x g for 20 min at 4°C. The supernatant was collected, and dispensed into aliquots, which were stored at -80°C to prevent degradation. A fraction was retained for the determination of total protein concentration with a BCA kit (Pierce). Equal amounts of total

protein extract were subjected to SDS–PAGE in 4 to 12% Bis–Tris gels (NuPAGE Novex Bis-Tris midi gel; 15 or 26 wells, Invitrogen) and the bands were transferred to nitrocellulose membranes. The membranes were blocked (5% milk in TBS–0.1% Tween-20) and incubated overnight with primary antibodies against actin (1:5000, rabbit, Sigma), and, for the detection of transgenes, with antibodies against HA (1:3000, mouse, Covance). The membranes were washed three times, with 0.1% Tween-20 in TBS (TBS-T), for 10 min each. For chemo-luminescence-based detection, membranes were labelled for 1h with secondary IgG-HRP antibodies raised against the corresponding primary antibodies. The membranes were washed three times with TBS-T and incubated with ECL chemo-luminescence reagent (Clarity Western ECL substrate; Bio-Rad), according to the supplier's instructions. Peroxidase activity was detected with the Fusion TX7 camera system (Fisher Scientific). Signals were normalized against the actin signal, by densitometry analysis with ImageJ software. For fluorescence-based detection, membranes were labelled for 1h with secondary IgG-coupled with fluorescents dyes (Li-cor Biosciences, Germany). The fluorescent signal was then visualized using Odyssey CLx Imager (Li-cor Biosciences, Germany) and analysis performed using Image Studio software (Li-cor Biosciences, Germany).

Immunoprecipitation of LRRK2-HA fragments.
Lysates of transfected HEK cells were used for the immunoprecipitation protocol. In total, 750 µg protein, as determined with the BCA kit, was mixed in 500 µl of lysis buffer (LB) and a 1:150 dilution of HA antibody was added. The mixture was incubated overnight at 4°C, with 360° rotation, to allow the protein-antigen complex to form. The next day, 20 µl of magnetic beads coated with protein A/G (Dynabeads NOVEX, Life Technologies) were washed three times in LB. The tube containing the beads was placed on a magnet, causing the beads to migrate to the side of the tube facing the magnet, thereby facilitating supernatant removal. The protein-antigen complex was added to the beads, and the mixture was incubated at room temperature for 2 hours to allow the bead-Ab-Ag complex to form. The supernatant was removed and the beads were washed three times in LB.

Immunoprecipitation of RAB10
Lysates of HEK stable cells for ΔLRRK2 or calcium phosphate transfected HEK cells for full length LRRK2 were obtained using a lysis buffer (LB; 50mM Tris pH8.0, 150mM NaCl, 1% NP-40, 1mM PMSF, 1% protease inhibitor cocktail and 1% phosphatase inhibitor cocktail). Lysate was centrifuged at 15000 g for 10 minutes at 4°C and supernatant was collected to perform a total protein assay (BCA kit). Magnetic beads coated with protein A/G (Dynabeads NOVEX, Life Technologies) were incubated with 2 µl (= 1µg) of RAB10 antibody during 1h at 4°C. Next, 30 µl of this complex RAB10 Antibody/magnetic beads was incubated with 500 µg of total proteins in 500 µl of lysis buffer during 2 hours at 4°C on rotation. After 3 washes with the lysis buffer, proteins were denaturated with Laemmli buffer and submitted to SDS-PAGE in 4-20% Tris-Glycine gels (Bio-Rad). Detection of corresponding western blots was performed with: anti RAB10 Ab (Abcam), anti-phosho-RAB10 T73 (Abcam), anti-HA (Covance), anti-Actin (Sigma), anti-tubulin (Sigma). The secondary antibody used for detection of Rab10 and Phospho-RAB10 was the Clean-Blot IP Detection Reagent-HRP (Thermo Fisher).

Kinase activity assay
The lysate buffer (LB) was removed and the beads-Ab-Ag complex was resuspended in 30 µl of kinase buffer (KB1: 20 mM HEPES; 150 mM NaCl, 5 mM EGTA; 20 mM beta-glycerophosphate). The mixture was split into two samples (10 µl and 20 µl), one for estimation of the amount of protein (non-radioactive fraction) and the other for a phosphorylation activity assay with MBP. For measurements of phosphorylation activity, we added 5 µl of KB2 (10 mM ATP, 20 mM $MgCl_2$) and 5µCi ^{32}P-ATP (1 mCi, BLU502Z001MC, PerkinElmer) to activate the reaction, and the mixture was then incubated at 30°C for 30 min with gentle agitation. The denaturation buffer was added and the mixture was heated at 90°C for 5 minutes to complete the denaturation process. The beads were isolated with the magnet, the supernatant was loaded in 4 to 12% Bis-Tris gels. For the non-radioactive fraction, we performed western blotting as described above, in the section on "biochemical analyses". The radioactive blot was dried onto Whatman filter paper for two hours. The dried-down gel was then placed against a phosphor screen. Two hours of incubation were sufficient for the detection of radiolabelled phosphorylated proteins. The phosphor screen was scanned with a Cyclone Plus machine (Perkin Elmer) and the number of DLU (density light unit) was determined with the software provided.

Stereotaxic injection
Adult male Sprague-Dawley rats (Charles River Laboratories) weighing ~250 g were housed under a 12 h light/12 h dark cycle, with *ad libitum* access to food and water, in accordance with European Community (Directive 2010-63/EEC) and French (Code Rural R214/87-130) regulations. Experimental procedures were approved by the local ethics committee and registered with the French Research Ministry (committee #44, approval #12-100 and APAFIS#1372-2015080415269690v2). For stereotaxic injections, the animals were deeply anaesthetised with 4% isoflurane followed by a mixture of ketamine (75 mg/kg) and xylazine (5 mg/kg), and placed in a stereotaxic frame. Recombinant lentiviruses and adeno-associated viral vectors were injected bilaterally into the substantia nigra, at the following stereotaxic co-ordinates: +3.4 mm anterior to the interaural zero and ±2.0 mm lateral to bregma, at a depth of -7.8 mm relative to the skull, with the tooth bar set at -3.3 mm (Supplementary Fig. 1, B and F). For striatal injections of lentiviral vectors, the following coordinates were used: +0.86 mm anterior to the interaural zero and ±4.0 mm lateral to bregma, at a depth of -4.5 mm relative to the skull, with the tooth bar set at -3.3 mm. We injected 2 µl of virus (200 ng for lentiviruses and $5x10^{10}$ viral particles for AAV into each site), with a 34-gauge blunt-tipped needle linked to a 10 µl Hamilton syringe by a polyethylene catheter, at a rate of 0.25 µl/min, with an automatic pump (CMA-4004). The needle was left in place for five minutes and was then slowly withdrawn.

Behavioural analysis

The Catwalk method (Noldus information Technology, Wageningen, the Netherlands) is an automated and computerised gait-analysis technique for the objective quantification of multiple static and dynamic gait parameters. The following gait parameters were calculated: intensity of the paw print intensity, print length, print width, print area (surface area of the complete print), stand, swing (duration for which there was no contact with the glass plate in a step cycle), swing speed (speed of the paw during swing), stand index, stride length (the distance between successive placements of the same paw), and angle. All rats were trained to cross the runway in a consistent manner, during at least three training sessions per day, before the experiment was begun. Analysis was performed on a minimum of three normal step sequence patterns in each uninterrupted run.

Tissue processing

For all procedures, rats were first deeply anaesthetised by isoflurane inhalation followed by the intraperitoneal injection of a lethal dose of sodium pentobarbital.

For immunohistochemistry, rats were transcardially perfused with 300 ml of 4% paraformaldehyde in phosphate buffer at a rate of 30 ml/min. After perfusion, the brain of each rat was removed quickly and immersed in ice-cold 4% paraformaldehyde for at least 24 h, before transfer to 15% sucrose for 24 hours and then 30% sucrose the next day, for cryoprotection. The brains were then cut into 40 µm sections on a freezing microtome (CM1900, Leica, Germany). Serial sections of the striatum and midbrain were stored in antifreeze solution (30% sucrose, 30% ethylene glycol in PBS) until use.

Immunohistological analysis and quantification

Immunohistochemistry. The sections were removed from the antifreeze solution and washed in PBS. Endogenous peroxidase activity was quashed by transferring these sections to 1% H_2O_2 for 30 minutes at room temperature (RT) and washing them three times with PBS, for 10 min each. The sections were then blocked by incubation with 4.5% normal goat serum for 30 min in PBS-T (0.2% Triton X-100 in PBS) and they were then incubated overnight with primary antibody in 3% normal goat serum in PBS-T, at 4°C, with gentle shaking (anti-tyrosine hydroxylase (TH) antibody: MAB318 clone LNC1, 1:3000; anti-hemagglutinin tag (HA), Covance clone 11, 1:1000). The next day, these sections were removed from the primary antibody solution, washed three times and incubated for 1 hour at room temperature with the appropriate biotinylated secondary antibody in PBS-T (Vector Laboratories, Burlingame, CA, USA, 1:1000). The sections were then washed and incubated with ABC complex solution in PBS-T (1:250, reagents A and B combined in a 1:1 ratio, Vector Laboratories) for 1 h. The sections were then incubated with DAB for 30 s to 1 min and mounted on slides, in Eukitt mounting medium.

Cells counting. Optical fractionators sampling was carried out on a Zeiss microscope AxioPlan. Midbrain dopaminergic neurons were outlined on the basis of TH immunolabelling, with reference to a coronal atlas of the rat brain (Paxinos and Watson, 6th edition). For the lentiviral-mediated transduction of DA neurons, TH-positive cells in vicinity of the injection site were counted and the number of positive neurons per section was calculated with Mercator Software (Explora Nova, France). We placed 100 × 100 µm grids in a systematic random manner, 80 × 80 µm apart, with a 3 µm offset from the surface of the section. Quantification was performed on five serial sections spaced by 200 µm, from the anterior to the middle of the SNc, corresponding to the infection volume. For the AAV-mediated transduction of DA neurons, TH-positive cells were evaluated by unbiased stereology in the entire SNc. The same parameters were used as described above.

Immunofluorescence. The procedure used was similar to that for immunohistochemistry, but without the incubation in 1% H_2O_2. The primary antibodies used for the immunofluorescence procedure were directed against TH (AB152 1:1000, EMD Millipore, US) and HA (Covance clone11, 1:1000). On the first day, sections were incubated with the primary antibody against TH overnight at 4°C. The next day, they were incubated with a fluorescent secondary antibody: Alexa Fluor 594-labeled goat anti-rabbit IgG (1:1000, Life Technologies) for 1 hour at RT. The sections were then washed and incubated overnight at 4°C with another primary antibody directed against HA. Finally, they were incubated with a second fluorescent secondary antibody, Alexa Fluor 488-labeled goat anti-mouse IgG (1:1000, Life Technologies) for 1 hour at room temperature. The sections were stained with DAPI, washed and mounted in a fluorescence mounting medium. Images were acquired with a laser confocal microscope (SP8, Leica, Germany) or an epifluorescence microscopy (DM8000, Leica, Germany).

Measurement of transduction volumes after lentiviral injection in the substantia nigra. Transduction volume was evaluated by epifluorescence microscopy. Serial sections were taken from each animal: five to six sections 400 µm apart, covering the entire SNc. The SNc was segmented on the basis of TH staining, analysed in the red channel, and the area was measured. TH segmentation was analysed in the green channel, corresponding to HA staining, and the zone of positive green staining within the TH area was segmented and measured. The transduction volume was calculated from the percentage of transduction measured for each section.

Real-time quantitative PCR

The transcriptomic analysis was performed on rat striatum, to ensure that it was performed on a relatively homogeneous population of transduced neurons. Rats were infected with the different LVs coding for ΔLRRK2 and LV-GFP. The striatal region displaying fluorescence was dissected out with a circular punch (1.5 mm in diameter) from 1 mm-thick fresh coronal brain sections visualised under a fluorescence binocular microscope (Leica). The punch samples were crushed and stored in Trizol solution (Life Technologies) at -80°C before processing. Total RNA was treated with DNase RQ1 and reverse-transcribed with the SuperScript™ III reverse transcriptase (VILO

kit, Life Technologies). The rat Huntington's disease RT^2 profiler PCR array (Qiagen) was used to evaluate gene expression directly and to assess potential involvement in striatal disease. cDNAs were generated in accordance with the array manufacturer's instructions. The list of the 88 mRNA analysed can be found at https://www.qiagen.com/be/shop/genes-and-pathways/complete-biology-list/huntingtons-disease/. A statistical analysis was performed to identify genes upregulated or downregulated in the GS group relative to the WT or dead kinase (DK) group. The expression of the genes identified with the RT^2 profiler PCR array were checked in SYBR Green-based real-time quantitative RT-PCR assays performed in triplicate with the *Taq* Platinum enzyme (SYBR Green qPCR kit, Invitrogen) on a Master cycler Realplex system (Eppendorf) with different primers designed and validated in house (Supplementary Table 1).

Statistical analysis

Data were analysed by two-tailed, one-way analysis of variance (ANOVA) performed with Statistica software (Statsoft Inc., Tulsa, Oklahoma, USA) and, when appropriate, Bonferroni post hoc correction for multiple comparisons was applied. Unpaired Student's T-tests were performed for pairwise comparisons. For the analysis of gene array, results (n=6/group) showed that data distribution was not normal so that non-parametric tests were used. When Kruskal-Wallis test showed significance, Mann-Whitney *post hoc* test was applied for comparison between groups. The annotations used to indicate the level of significance are as follows: *p<0.05; **p<0.01; ***p<0.001.

Results

Functional and biochemical characterisation of ΔLRRK2

The expression of the different fragments was first evaluated *in vitro* after the transfection of HEK293T cells with expression vectors encoding the K, RCK or RCKWD40 (ΔLRRK2) [1326-2527 a.a.] fragments of LRRK2, with or without the G2019S mutation (Fig. 1, A). We added an HA tag to the C-terminus of all constructs. RT-qPCR analysis after transfection showed that mRNA coding for K, RCK and ΔLRRK2 were not expressed at statistically different levels, although the larger fragment ΔLRRK2 tended to be less expressed compared to the smaller fragments (Fig. 1, B). After protein extraction in buffer with non-ionic detergents (NP40 and Triton X100), western blot analysis based on detection of the HA tag showed that the fragments migrated at their expected molecular weights: 30 kDa for K, 100 kDa for RCK and ~143 kDa for ΔLRRK2, demonstrating an absence of abnormal cleavage or instability (Fig. 1, C). The detection and the quantification of protein levels were done with the HA tag. Only for the K fragment, a small but significant difference was seen between the expression of the G2019S form when compared to the WT form (Fig. 1, D). RCK and RCKWD40 (ΔLRRK2) forms tended to be much less expressed than the smaller fragment K but no significant differences were seen between RCK^{WT} and RCK^{G2019S} or ΔLRRK2^{WT} and ΔLRRK2^{G2019S}. To better focus on the comparison between ΔLRRK2^{WT} and ΔLRRK2^{G2019S}, we repeated the transfection experiment, protein extraction and quantification of western blot for this long fragment (Fig. 1, E). No difference of expression was detected between ΔLRRK2^{WT} and ΔLRRK2^{G2019S} (Fig. 1, F).

We next asked whether the kinase activity of ΔLRRK2 could be detected. For this purpose a kinase activity assay with ^{32}P-γ-ATP in the presence of the pan-kinase substrate myelin basic protein (MBP) was performed (Galvan et al., 2018). The higher level of kinase activity observed with LRRK2^{G2019S} compared to wild-type LRRK2 is thought to be a key molecular aspect of its neurotoxicity (Lee et al., 2010b; West et al., 2007). This increase in kinase activity is dependent on adjacent functional domains: the presence of the ROC domain facilitates LRRK2 kinase activity and synergistically enhances G2019S-induced kinase activity (Lewis et al., 2007; Smith et al., 2006; Webber et al., 2011). For these reasons, we assessed the biochemical activity of ΔLRRK2 in comparison with two other "shorter" fragments containing the kinase domain. The three recombinant fragments containing the G2019S substitution (kinase, K^{G2019S}; ROC-COR-kinase, RCK^{G2019S}; RCK-WD40^{G2019S} i.e. ΔLRRK2^{G2019S}) were purified by HA-mediated immunoprecipitation after the transfection of HEK cells. In this radioactive assay with ^{32}P-γ-ATP, the radioactivity of the different kinase fragments was assessed after immunoprecipitation and separation by SDS-PAGE. Only ΔLRRK2^{G2019S} displayed detectable autophosphorylation similar to that reported in previous studies for the (1326-2527 aa) ΔLRRK2 (Shogo Kamikawaji et al., 2016). The K^{G2019S} and RCK^{G2019S} fragments displayed no detectable autophosphorylation in our assay. An analysis of ^{32}P incorporation into the MBP substrate was performed to determine the phosphorylation activity of the different fragments. In parallel, the levels of immune-precipitated recombinant fragments were evaluated by western blotting with an antibody directed against the HA tag (see Fig. 2, non-radioactive fraction). K^{G2019S} and RCK^{G2019S} had similar low levels of kinase activity (Fig. 2, A-C). Conversely, ΔLRRK2^{G2019S} had much higher level of phosphorylation activity than the smaller fragments. We then compared the catalytic activity of ΔLRRK2^{G2019S} with that of the corresponding wild-type form, ΔLRRK2^{WT}. MBP phosphorylation levels were higher with ΔLRRK2^{G2019S} than with ΔLRRK2^{WT}, suggesting that the G2019S substitution had indeed increased the kinase activity of this long C-terminal fragment of LRRK2 (Fig. 2, D-E).

We also studied RAB10 phosphorylation in presence of the different forms of ΔLRRK2 in HEK cells infected with lentivirus to produce stable cell lines or in HEK transfected with the full length LRRK2. Results were congruent with the literature. Only the overexpression of full length LRRK2^{WT} and LRRK2^{G2019S} produced an increase in phospho-RAB10 while total levels of (non-phosphorylated) RAB10 remained unchanged (Supplementary Fig. S2, A, B). In our hands, the double dead mutant LRRK2^{DK} produced no increase in phospho-RAB10, but the expression levels of this double mutant was found to be always low, possibly as a result of its abolished autophosphorylation which should accelerate its degradation as reported for LRRK2 (Lobbestael et al., 2016). We next used RAB10 as bait in co-immunoprecipitation experiments to investigate whether full length LRRK2 could be pulled down with RAB10. Results showed that both full length LRRK2^{WT} and LRRK2^{G2019S} could be detected in the immunoprecipitate (Supplementary Fig. S2A, C).

Similar experiments using HEK cells were carried out in parallel with ΔLRRK2^{WT} and ΔLRRK2^{G2019S} to determine whether these fragments could interact with RAB10 (Supplementary Fig. S2B, D). Results showed no detectable change in RAB10 phosphorylation in presence of

ΔLRRK2 fragments. ΔLRRK2 fragments were not detected in the immunoprecipitate, indicating no major interaction with RAB10 (Supplementary Fig. S2B, D).

The preliminary biochemical characterization thus suggested that ΔLRRK2 displays a kinase activity. It also indicated that the molecular "switch" induced by G2019S mutation was preserved in the ΔLRRK2 constructs, as previously reported for the LRRK2 protein (Jaleel et al., 2007). However, ΔLRRK2 fragments do not phosphorylate the substrate of full length LRRK2, RAB10, consistent with the reported importance of the serines (S910 and S935) in the N-terminus of LRRK2 for its interaction with RAB10 and other RAB proteins (Liu et al., 2018; Steger et al., 2017).

Transcriptomic analysis of LRRK2 fragments in vivo

We investigated whether the overproduction of LRRK2 fragments had a biological effect in neurons *in vivo*. We used a straightforward and simple approach in order to target a homogeneous population of transduced neurons (which could not be done easily in the SNc to obtain a sufficient amount of neurons) and after resection of the transduced region perform a mRNA expression analysis. We chose the striatum, a region which does not degenerate in LRRK2^{G2019S} carriers, but is naturally enriched in LRRK2 (Brochier et al., 2008; Higashi et al., 2007). In these experiments, we aimed to assess the effect of LV-ΔLRRK2^{G2019S} relative to that of LVs encoding GFP, ΔLRRK2^{WT} and ΔLRRK2$^{G2019S/D1994A}$, the kinase-dead form of ΔLRRK2. The mutation D1994A is known to abolish kinase activity and was therefore used as a negative control for kinase activity (Smith et al., 2006). For the selective collection of transduced striatal tissue, we co-injected in rats LVs encoding ΔLRRK2 (100 ng p24/µl) with LV-GFP (50 ng p24/µl) (Fig. S3). Six weeks later, we measured the expression levels of 84 striatal genes using a commercial RT-qPCR array (see Materials and methods) (Fig. 3). RT-qPCR was also performed to compare the mRNA levels for the three ΔLRRK2 transgenes and we found no significant difference between the three transgenes (Fig. 3, A). The statistical analysis of expression profiles for the 84 genes showed that overexpression of ΔLRRK2^{G2019S} resulted in significant changes in the expression of eight genes, when compared to ΔLRRK2^{WT} and ΔLRRK2$^{G2019S/D1994A}$ (Fig. 3, C-E). This suggested that an increase in kinase activity was required for this effect in neurons *in vivo*. The changes in expression for these genes were confirmed with a different RT-qPCR method (data not shown, primers used for RT-qPCR in Supplementary Table S1). Consistent with the lack of obvious toxicity *in vivo,* no difference was observed in the expression of genes directly related to apoptosis mechanisms (Akt, Bax, and Casp3) (Fig. 3, B). ΔLRRK2^{G2019S} overexpression induced changes in mRNA levels for genes directly related to neurotransmission/cell signalling: *Tac1* (preprotachykinin/substance P), *Grin2a* (NMDA receptor subunit A), *Cnr1* (cannabinoid receptor 1), *RGS4* (regulator of G protein signalling 4) and *HPCA* (hippocalcin) were significantly downregulated in the ΔLRRK2^{G2019S} group relative to the other three groups (Fig. 3, C-D). The levels of *Snap25* (synaptosomal-associated protein 25) and *Rph3a* (rabphilin 3a) mRNA were significantly lower following transduction with a LV encoding ΔLRRK2^{G2019S} than after transduction with LVs encoding the WT and dead-kinase forms of the ΔLRRK2 fragment (Fig. 3, D). For one gene, encoding *Bbox1* (gamma-butyrobetaine dioxygenase, the enzyme responsible for L-carnitine synthesis) mRNA levels in the ΔLRRK2^{G2019S} group were more than three times those in the other groups (Fig. 3, E). These results therefore indicate that overexpression of ΔLRRK2^{G2019S} can produce perturbations in neurons *in vivo*.

Characterisation of LVs-induced transduction in the rat substantia nigra

LVs with the VSV-G envelope and coding for proteins under the control of PGK promoter are known to almost exclusively express transgenes in neuronal cells in the brain (Francelle et al., 2015; Galvan et al., 2018). We checked with LV-GFP that it was also the case in the SNc in rats. Double immunofluorescence studies showed no expression in astrocytes or microglial cells (Supplementary Fig. S4). At low magnification, after infection with LV-ΔLRRK2, the HA tag was detected in a large proportion of cells reminiscent of neurons in the SNc (Fig. 4, A). Confocal analysis showed that, close to the injection site, about 90% of TH–positive (DA) neurons labelled with an antibody directed against tyrosine hydroxylase (TH) were transduced and displayed strong HA-positive immunofluorescence signal in the cytoplasm and dendrites (Fig. 4, B). The pattern and intensity of fluorescence were similar for both ΔLRRK2 forms (Fig. 4 A, B). As for LV-GFP, transduction of cell types other than neurons has never been observed with LV-ΔLRRK2. Quantification of the volume of SNc transduced after infection with the different LVs coding for ΔLRRK2 showed that approximately 30% of the SNc was transduced (mostly its anterior part) and no significant differences were seen between LV-ΔLRRK2^{G2019S} and LV-ΔLRRK2^{WT} (Fig. 5, A-D).

In vivo experiments with LVs to study the potential toxic effects of LRRK2 fragments

We evaluated the potential toxicity of LV-ΔLRRK2^{WT} or LV-ΔLRRK2^{G2019S}. LVs were injected into the SNc of WT rats (200 ng per site). We injected LVs encoding the WT form of ΔLRRK2 into the left hemisphere, and LVs encoding the G2019S form, which we thought might be toxic, into the right hemisphere. In addition, a control group received injections of vehicle (PBS/BSA) and a LV encoding GFP. Pilot experiments with lentiviral vector and AAVs (not shown) indicated no obvious degeneration in the SNC and no behavioral (motor) abnormalities at 10 and 15 weeks post-infection respectively. We reasoned that degeneration could occur very progressively, so we chose a 25 weeks (6 months) time point. Rats were subjected to the Catwalk® test 25 weeks after injection, for the detection of motor deficits and three days later, the rats were euthanatized for histological evaluation.

We hypothesised that asymmetric abnormalities would be detected when the animals were crossing the elevated board, if the fragments harbouring the G2019S substitution resulted in a dysfunction of DA neurons after LV infection. We evaluated nine different gait parameters (Supplementary Fig. S5), including maximal contact area, mean stride length and mean swing speed, which have been reported to be altered in rat models of motor deficits (Vandeputte et al., 2010; Zhou et al., 2015). We analysed the right limb, corresponding to the left SNc infected with LVs encoding the WT form of ΔLRRK2, and the left front limb, corresponding to the right SNc infected with LVs encoding the G2019S form, separately. No significant asymmetry was observed 25 weeks after injection, for any of the

parameters studied (Supplementary Fig. S5). Overall, the nine parameters studied did not differ between the rats infected with LRRK2 fragments and the rats receiving injections of PBS/BSA and LV-GFP.
We then investigated the integrity of the nigrostriatal pathway, by counting the dopaminergic neurons, which displayed TH staining, in the injected part of the SNc (Fig. 6, A and B). Low-magnification observations revealed no marked loss of TH-positive cells, even in the vicinity of the injection site (Fig. 6, A). As mentioned above, only a fraction (~30% on average) of the SNc cells was transduced, and these cells were close to the injection site, due to the limited diffusion of LVs. Thus, we assumed that the total loss would be limited (20-30% at most) and "diluted", making it difficult or impossible to detect this loss by determining the total number of TH-positive cells in the entire rostro-caudal extension of the SNc. We therefore counted TH-positive cells close to the injection site (-4.0 to -4.8 mm rostro-caudal from bregma) and determined relative densities. The apparent density of TH-positive cells in this part of the SNc did not differ significantly between wild-type and G2019S ΔLRRK2, or between these fragments and the control (GFP) (Fig. 6, B). In conclusion, no significant differences were observed between the groups expressing ΔLRRK2^{WT} and ΔLRRK2^{G2019S}.

Comparison between AAVs and lentiviral transduction
We hypothesized that the lack of neurotoxicity observed with lentiviral-mediated transduction of DA neurons could be due to the low level of transgene expression in comparison with what could be observed with AAVs. We compared the transduction efficacy of lentiviruses and AAVs encoding for the GFP protein at 1 month after stereotaxic injection. Results showed that the transduction by AAVs was higher than that obtained with LVs by approximately 10 fold (Fig. 7, A, B). Moreover, the transduction of cells by the AAV2/9-GFP was continuous throughout the SNc, which was not the case for the LV-GFP (Fig. 7, C).
As described for the LVs experiments, we carried out immunofluorescence analyses after infection with AAV-GFP to assess the transduction of neurons in the SNc as compared to other cell types. Results showed that GFP expression was almost exclusively seen in neurons (Supplementary Fig. S4).

Characterisation of AAVs-induced transduction in the rat substantia nigra
Next, AAV2/9 vectors encoding either ΔLRRK2^{WT} or ΔLRRK2^{G2019S} under the PGK promoter and with a HA tag were injected into the SNc of adult rats. AAV preparations (batches) were diluted to similar concentrations (5x10^{10} viral particles/µl) and 2 µl of the final preparation was injected to determine the distribution of the wild-type and mutant ΔLRRK2 fragments in the SNc. Histological evaluations showed that all transduced cells expressing ΔLRRK2 (WT or G2019S) had a neuronal phenotype. Apart from neurons, no other transduced cell types were observed. Immunofluorescence detected by confocal microscopy of the HA tag was localized in the cytoplasm, with some punctate structures at 10 weeks P.I. (Fig. 8, A, B). Using immunohistochemical detection of ΔLRRK2-HA and bright field microscopy, the neuronal staining appeared mainly diffuse in the cytoplasm without major punctate staining and dendrites could also be observed (Fig. 9, A-P). Similar levels of expression were observed between AAV-ΔLRRK2^{WT} and AAV-ΔLRRK2^{G2019S}.

In vivo experiments with AAVs, to study the potential toxic effects of ΔLRRK2^{G2019S}
We evaluated the potential toxicity of AAV-ΔLRRK2^{WT} or AAV-ΔLRRK2^{G2019S} to dopaminergic neurons *in vivo* after their injection into the SNc. In this case, AAVs were injected bilaterally into the SNc. A control group received injections of vehicle (PBS pluronic acid). We evaluated nine different gait parameters in the CatWalk test. No significant changes were observed 25 weeks after injection, for any of the parameters studied. Overall, the nine parameters studied did not differ between the rats infected with LRRK2 fragments and the rats who received injections of vehicle (Supplementary Fig. S6). Rats were also subjected to the open field test to evaluate the spontaneous locomotion activity. No significant motor alteration was detected in this test (data not shown).
We then investigated the integrity of the nigrostriatal pathway, by counting the dopaminergic neurons, which displayed TH staining, in the SNc (Fig. 10, A). In the case of AAVs, because of their good diffusion in the entire SNc, we counted TH-positive cells by unbiased stereology. The number of TH-positive cells, 25 weeks after infection, differed significantly between rats infected with AAV-ΔLRRK2^{WT} and AAV-ΔLRRK2^{G2019S} (Fig. 10, A). The number of neurons was similar between the PBS group and the ΔLRRK2^{WT} with approximately 10,000 neurons counted. We observed a 30 % decrease of TH positive neurons in the group injected with ΔLRRK2^{G2019S} as compared to the two others groups. Since apparent TH loss could be linked to a selective down regulation of the protein, we also counted by stereology the number of cells positive for the vesicular monoamine transporter (VMAT). A statistically significant loss of VMAT positive cells was also found (Fig. 10, B).
In conclusion, neuronal overexpression of ΔLRRK2 with the G2019S missense mutation but not its WT form induced neurodegeneration of the nigro-striatal pathway six months after the injection of the AAVs.

Discussion
The toxicity of the mutant LRRK2 is thought to be related to an increase in the activity of its kinase domain. This hypothesis is particularly well supported for the G2019S substitution. In this study, we used lentiviral and adeno-associated viral vectors to express the C-terminal part of LRRK2 harbouring the G2019S mutation in the DA neurons of the rat SNc. Biochemical experiments demonstrated that the largest fragment with the G2019S substitution studied here (ΔLRRK2^{G2019S}) was "biochemically" active *in vitro* and induced changes in cells when overproduced *in vivo* in neurons. While quantitative histological studies indicated that the overexpression of ΔLRRK2^{G2019S} via LVs did not result in a loss of TH-positive DA neurons, results with AAVs showed that ΔLRRK2^{G2019S} induced a 30 % loss of DA neurons.

A biochemical comparison of the three different types of C-terminal fragments of LRRK2 performed before the insertion of these fragments into lentiviral vectors showed that K (the kinase domain only) and RCK (the kinase domain and the ROC-COR domain) harbouring the G2019S substitution had relatively low levels of phosphorylation activity, at least in our experimental conditions *in vitro*. ΔLRRK2^{WT}, the largest fragment, containing the kinase, ROC-COR and WD40 domains, had relatively high levels of phosphorylation activity, which was significantly increased by the presence of the G2019S substitution. The higher kinase activity of the ΔLRRK2 fragment than of the shorter fragments is consistent with the previous demonstration of a requirement of the ROC-COR domain for the G2019S mutation to cause an increase in the kinase activity of the full-length LRRK2 (Jaleel et al., 2007) and the amplification of this effect by the WD40 domain (Jorgensen et al., 2009). An intramolecular mechanism involving the GTPase domain seems to play a key role in regulating the catalytic activity of LRRK2 (Taymans et al., 2011; Xiong et al., 2010).
Our biochemical analyses to investigate whether ΔLRRK2^{G2019S} could phosphorylate the LRRK2 substrate RAB10 showed, in agreement with previous studies, that the N-terminus part of LRRK2 is required for the physical interaction between the two proteins. Even when the N-terminal part of LRRK2 is partly modified by simple amino acid substitution to block phosphorylation of S910 and S935, the binding to RAB10 is disrupted and the kinase is no longer able to phosphorylate RAB10 (Steger et al., 2017). As further discussed below, ΔLRRK2 (WT or G2019S forms) is not expected to behave as the full length protein.
We then investigated whether the ΔLRRK2^{G2019S} fragment could induce a biological effect when expressed in neurons *in vivo*. Before assessing the potential toxic effects produced by ΔLRRK2^{G2019S} in the SNc neurons, a phenomenon that we assumed to require several months to be detected, we used a simple RT-qPCR array to determine whether ΔLRRK2^{G2019S} modified gene expression in neurons *in vivo* within a couple of weeks. This experiment was performed in the striatum since almost every neuron can be transduced around the site of injection in this brain region as previously shown (Francelle et al., 2015; Galvan et al., 2018), which would have been very difficult to achieve in the SNc. We found that ΔLRRK2^{G2019S} significantly modified the expression of neuronal genes with respect to the pattern of expression observed with the WT form and the catalytically inactive fragment ΔLRRK2$^{G2019S/D1994A}$. In contrast, the effects of ΔLRRK2^{G2019S} were observed in the absence of hallmarks of neurodegeneration (no changes in caspase, Bim and Bcl2 mRNA levels, and no obvious cell loss). The genes with expression patterns modified by ΔLRRK2^{G2019S} (and not ΔLRRK2$^{G2019S/D1994A}$) were all related to signalling/exocytosis and synaptic transmission. The ΔLRRK2^{G2019S}-induced reduction of neuronal genes – such as the SNAP25 gene coding for a synaptic protein and TAC1 which encodes preprotachykinin the precursor of Substance P – suggests that the LRRK2 mutation may induce an early alteration of the expression of genes related to synaptic functions in a kinase-dependent manner. Interestingly, a reduction in SNAP25 has been also reported in the brain of Lemurs infected with CAV2 to overexpress full length LRRK2^{G2019S} (Mestre-Francés et al., 2018). Reduced levels of Substance P have been reported in the SNc and in the putamen in the brains of PD patients who had not received L-DOPA therapy (Tenovuo et al., 1984). The changes in gene expression we observed are intriguing and their precise consequences remain to be determined. This finding is consistent with the key role played by LRRK2 in the regulation of synaptic mechanisms (Parisiadou et al., 2014; Piccoli et al., 2011).
At the time point considered for behavioural and histological evaluation (25 weeks after infection), rats overexpressing ΔLRRK2^{G2019S} by LVs, displayed no major signs of neurotoxicity in the dopaminergic pathway *in vivo*. Counts of DA neurons in the SNc revealed no tendency towards neuronal loss in rats expressing ΔLRRK2^{G2019S}. In contrast, rats overexpressing ΔLRRK2^{G2019S} through the injection of an AAV vector displayed a 30 % neuronal loss as seen using not only TH immunochemistry but also immunochemistry of the dopaminergic marker VMAT, the vesicular transporter. We showed that at one month post-injection the protein expression level induced by AAVs was approximately 10 fold higher than that induced by LVs. These results suggested that in addition to the mutation, the level of ΔLRRK2^{G2019S} expression in the few weeks after injection was crucial to trigger a toxic effect. However, ΔLRRK2^{WT} did not produce toxicity, indicating that the G2019S-induced molecular change in the kinase domain (possibly related to an increase in the activity of its kinase) and not only a higher level of expression is required to trigger neurodegeneration in DA neurons.
However, whereas it is probable that cell perturbations in DA neurons after expression of ΔLRRK2^{G2019S} may induce a kind of dysfunction, it did not lead to manifest motor dysfunctions. In rats expressing ΔLRRK2^{G2019S}, the chronic dysfunction of a relatively low proportion of the DA neurons in the SNc (~30%) may be compensated to hide major motor deficits. The nigrostriatal pathway is very “plastic” and capable of major compensatory mechanisms. For example, PD symptoms appear when more than 70% of the DA levels in the striatum are lost.

Our data are consistent with published results, including those from studies on G2019S knock-in mice where one copy of LRRK2 is expressed (Yue et al., 2015) and BAC-transgenic rats overexpressing LRRK2^{G2019S} which have approximately 8 copies of the human gene (Lee et al., 2015). In these genetic models, no major loss of dopaminergic cells and no major motor deficits were observed, even in aged animals. This lack of effect may be due to the low level of LRRK2^{G2019S} expression, close to endogenous levels, in these transgenic animals. In our experiments, the LRRK2 transgenes were much more strongly expressed after AAV transduction (about 25-50 copies per cell) (Ruiz and Déglon, 2012). Our results are, therefore, more directly comparable with those of three groups that generated viral models of LRRK2 overexpression based on the use of adeno- or herpes simplex viruses (Ad and HSV, respectively) encoding the full-length LRRK2 protein (Dusonchet et al., 2011; Lee et al., 2010; Mestre-Francés et al., 2018). In these models, LRRK2^{G2019S} overexpression led to the partial degeneration of DA neurons in the SNc. These studies used viral vectors that underwent retrograde transport (which is not the case for the LVs and AAVs vectors used here), which means that neurons were transduced along with other cells in the striatum. It remains unclear whether the DA neuron degeneration induced by LRRK2^{G2019S} in the adenovirus, HSV and CAV2 models results purely from cell-autonomous mechanisms. The medium-sized striatal GABAergic neurons, and neighbouring glial cells are probably also infected after striatal injections of adenovirus and HSV vectors. The neurodegeneration of SNc neurons in these two models may involve changes in

both DA neurons and striatal cells. In our study, ΔLRRK2^{G2019S} was overexpressed only in DA neurons and we found a comparable DA neuron loss.

The LRRK2 fragments studied here are unlikely to be able to mimic all aspects of the biology of the full-length LRRK2, because they cannot interact with partners of the N-terminal domain of LRRK2. Our biochemical data confirmed that RAB10 is a substrate of full length LRRK2. This is coherent with recent work showing that in the SN DA neurons of both idiopathic PD patients and rat models (rotenone-based model and human α-synuclein overexpression in the SNc via AAV2) there is an increase of LRRK2 kinase activity. This event might lead to phosphorylation of RAB10 substrate, followed by impairment of lysosomal and mitochondrial functions (Di Maio et al., 2018). Here we showed that ΔLRRK2^{G2019S} and ΔLRRK2^{WT} cannot increase the level of phosphorylation of RAB10, underscoring that ΔLRRK2, despite its phospho-transferase catalytic activity, cannot interact with all partners of the full length LRRK2. Although RAB10 may be a key molecular player in PD, it cannot be excluded that other parallel mechanisms also contribute to mutant LRRK2-related toxicity. Substrates exist that do not require the N-terminus of LRRK2 for interaction with the kinase. Especially, the C-terminal WD40 domain is thought to be a key molecular player for the interaction of LRRK2 with different partners. For example, the WD40 domain allows LRRK2 to bind synaptic vesicles and to phosphorylate synapsin I (Marte et al., 2019; Piccoli et al., 2014). WD40 may also be involved in the interaction of LRRK2 with microtubules (Kett et al., 2012). Thus it is conceivable that ΔLRRK2^{G2019S} may trigger neurodegeneration, despite the absence of the N-terminal domain of LRRK2. ΔLRRK2 fragments provide an interesting tool for the precise evaluation *in vivo*, and more specifically in neurons, of the role of the kinase and neighbouring domains, namely the ROC-COR GTPase domain and the WD40 domain. The requirement of the ROC-COR domain for the G2019S mutation to cause an increase in the kinase activity of the full-length LRRK2 has been shown (Jaleel et al., 2007). An intramolecular mechanism involving the GTPase domain seems to play a key role in regulating the catalytic activity of LRRK2 (Taymans et al., 2011; Xiong et al., 2010). In addition, there is an amplification of this effect by the WD40 domain (Jorgensen et al., 2009). It is tempting to speculate that the differential effects between the wild type and G2019S forms of ΔLRRK2 in our experiments partly result from a change in the activity of the kinase, although this awaits further *in vivo* studies with pharmacological LRRK2 inhibitors and dead kinase mutants to be fully supported.

The ΔLRRK2 constructs are also versatile tools for studying the effects of increases in the kinase activity of LRRK2^{G2019S} in different brain cells. For example, driving ΔLRRK2 expression with the GFAP promoter might be an interesting approach for studying the selective role of LRRK2's (WT and G2019S) kinase domain in astrocytes (Colin et al., 2009). These C-terminal fragments could also be used to investigate the selective role of the physiological kinase activity of LRRK2 in other types of neurons, such as striatal GABAergic neurons, in which levels of LRRK2 expression are naturally higher than in other brain regions.

LRRK2 has also been shown to interact physically or genetically with several other important proteins involved in PD. Potential "functional" interactors of LRRK2 include the □-synuclein protein (Cresto et al., 2019; Lin et al., 2009). The exact role of the kinase domain in this important interaction should be further studied. The use of truncated LRRK2 proteins such as ΔLRRK2 we used in the present study, in comparison with the full length LRRK2, could be of interest to address the existence of this functional LRRK2/□-synuclein interaction specifically in DA neurons or other cell types.

Conclusion

In conclusion, we present a novel molecular tool for studying the effects of the C-terminal part of LRRK2 in neurons, *in vivo*. Our results indicate that a selectively high expression in DA neurons of ΔLRRK2^{G2019S} is sufficient to induce DA neuronal loss within an experiment time frame of 6 months. These results suggest that both the expression level and the G2019S substitution-induced increase in kinase activity of the overexpressed LRRK2 fragment may be key factors to trigger cell death pathways in animal models.

Figures

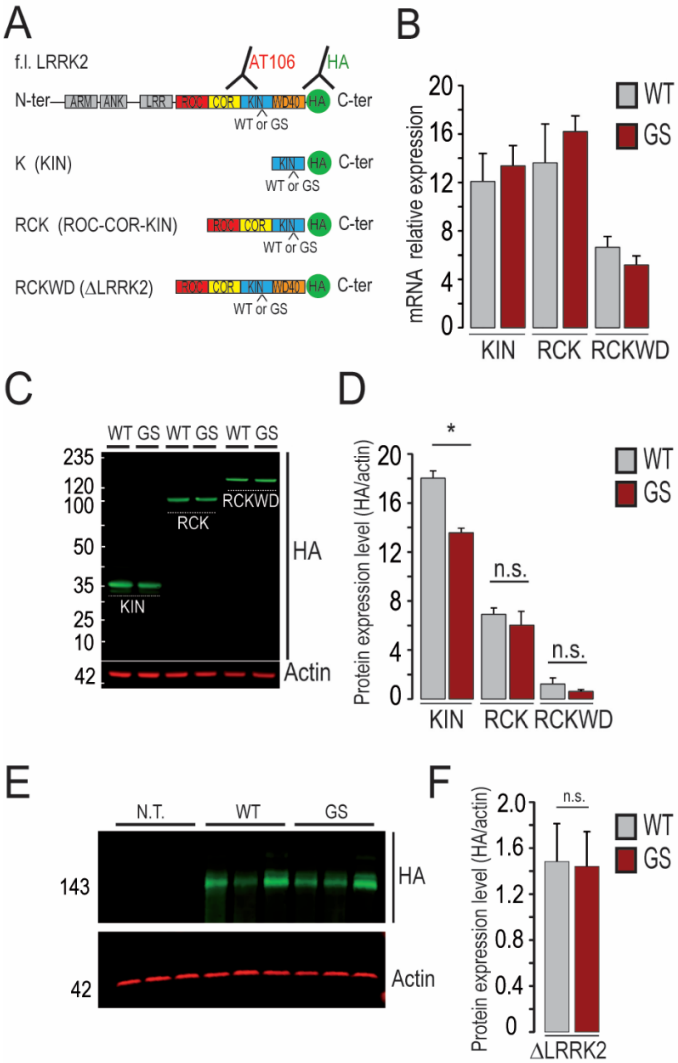

Figure 1: Characterization of the expression of LRRK2 constructs *in vitro* in cell lines. (A) Plasmids coding for the full length (FL), kinase domain (K), the ROC/COR GTPase domain (RCK), and the RCK with the WD40 domain (RCKWD40, i.e. ΔLRRK2) with the addition of a hemagglutinin tag (HA) were synthetized in the WT or G2019S forms. (B) Quantitative analysis of the results from RT-qPCR on mRNA extracts after transfection of HEK293T cells with plasmids coding the different forms shown in A. (C) Western blot analysis after SDS-PAGE showed that the six different fragments migrated at their expected molecular weights when detected with the anti-HA antibody. (D) Quantification of the western blots shown in C. (E) Western blot analysis after SDS-PAGE of protein extracts obtained from three independent transfections with plasmids coding either WT or GS forms of ΔLRRK2. (F) Quantification of the western blots shown in E. *, $p<0.05$; n=3, Student's *t* test for paired comparison.

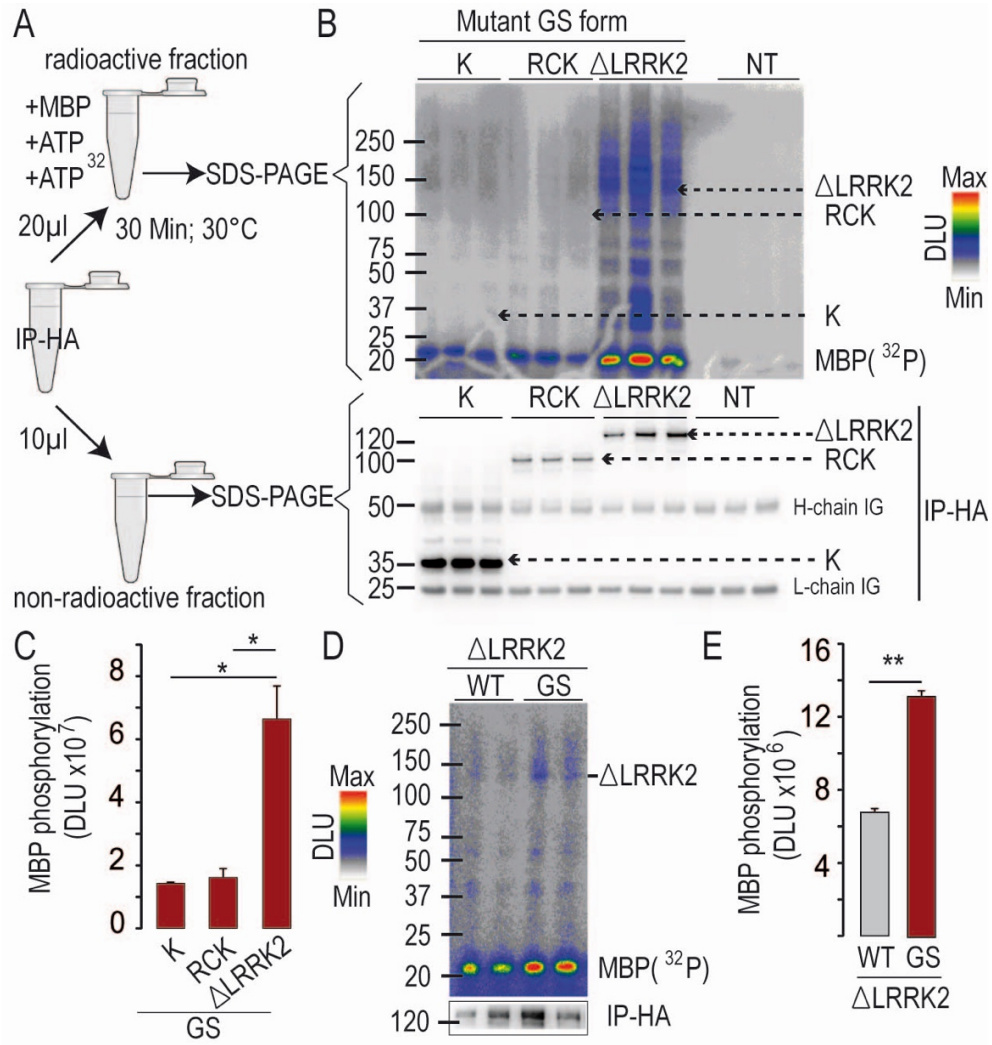

Figure 2: **Biochemical characterization of the C-terminal fragments of LRRK2.** Kinase assay: Fragments were purified by HA-mediated immunoprecipitation. A portion of the magnetic beads was used to study the levels of recombinant fragments by western blotting (IP-HA). The rest of the beads were incubated with radioactive ^{32}P-ATP and myelin basic protein (MBP) as a kinase substrate **(A)**. After incubation, K (kinase domain), RCK ROC-COR-kinase) and ΔLRRK2 (ROC-COR-kinase-WD40 domain) and MBP were separated by SDS-PAGE, and ^{32}P-labelled proteins were detected with a PhosphoImager. (B) Representative image showing ^{32}P-incorporation into MBP after incubation with each of the three fragments carrying the G2019S mutation (GS). (D) ^{32}P-incorporation into MBP after incubation in the presence of wild-type (WT) ΔLRRK2, relative to incorporation in the presence of ΔLRRK2 carrying the G2019S (GS) mutation. (C, E). Quantification of ^{32}P-incorporation into MBP. *, p<0.05; One-way ANOVA with Bonferroni post hoc test.**, p<0.01, or Student's t test for paired comparison.

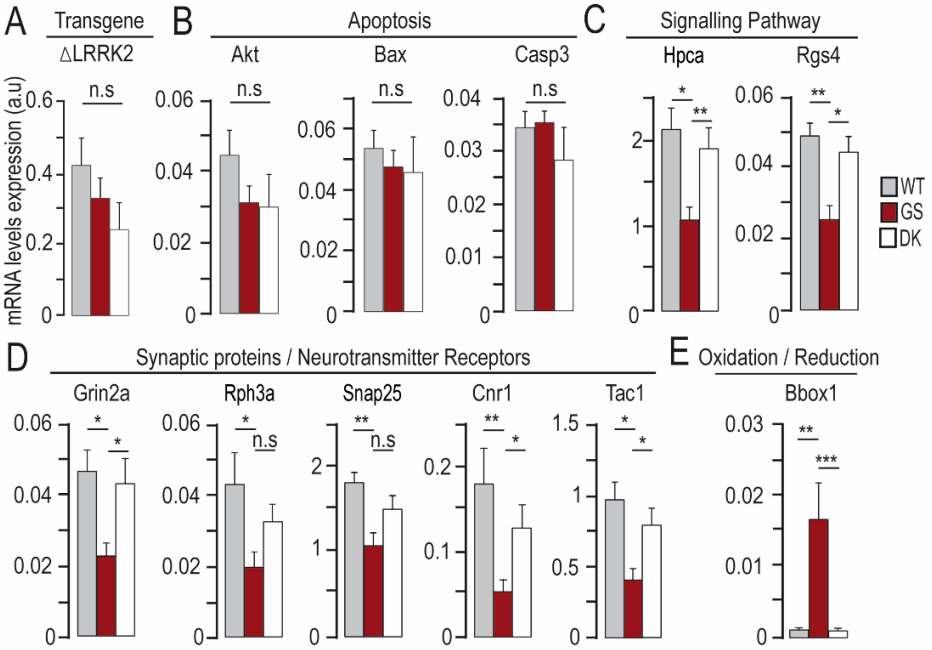

Figure 3: Biological effects of ΔLRRK2 fragments in the striatum assessed using a RT-qPCR array. Rats received intrastriatal co-injections of LV-ΔLRRK2 [WT, G2019S or the dead kinase (DK: G2019S + D1994A) forms (100 ng/µl)] with LV-GFP (50 ng/µl) and the levels of 84 different mRNA species were measured with an RT-qPCR array at 6 weeks post-infection. (A) The levels of mRNA for each LRRK2 fragment (Transgene) were measured by RT-qPCR. (B) No major change in the expression of the apoptosis-related genes on the array was induced by ΔLRRK2^{G2019S} overexpression (Akt, Bax and Casp3). (C-E) Gene products (of the 84 on the array – see the materials and methods section) with a different level of expression in the group injected with LV-ΔLRRK2^{G2019S} than in the other groups, including (C) signalling pathway genes (HPCA, hippocalcin; RGS4, regulator of G protein signalling 4), (D) synaptic proteins and neurotransmission genes (Grin2a, NMDA receptor subunit A; Rph3a, rabphilin 3a; SNAP25, synaptosomal-associated protein 25; Cnr1, cannabinoid receptor 1; Tac1, preprotachykinin/substance P) and (E) oxidation/reduction pathway (Bbox1, gamma-butyrobetaine dioxygenase). *, p<0.05; **, p<0.01; ***, p<0.001, Kruskal-Wallis, ANOVA and Mann-Whitney tests (n=6/group).

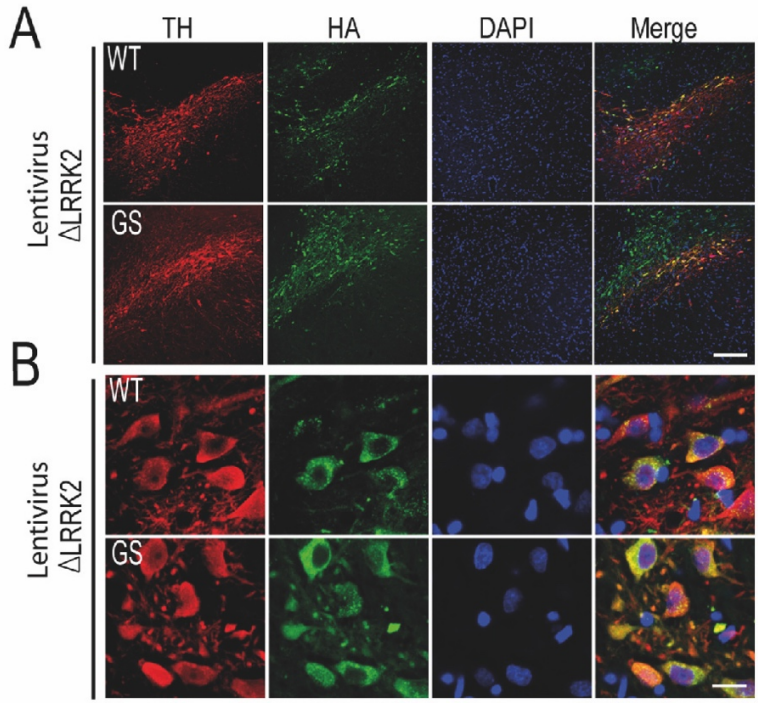

Figure 4: Expression of ΔLRRK2 fragments at the cellular level ten weeks after infection of the SNc with AAV-ΔLRRK2. Double-immunofluorescence labelling and confocal microscopy were used to study ΔLRRK2-HA expression in transduced SNc at 10 weeks post-infection with AAV2/9-ΔLRRK2^{WT} or AAV2/9-ΔLRRK2^{G2019S} (HA-positive, green). Representative images at low (A) or high (B) magnification are shown. Note that dopaminergic cells (TH-positive, red) in SNc co-localize with ΔLRRK2 (HA-positive/TH-positive, green) (B). Scale bars in A and B: 400 µm and 10 µm respectively.

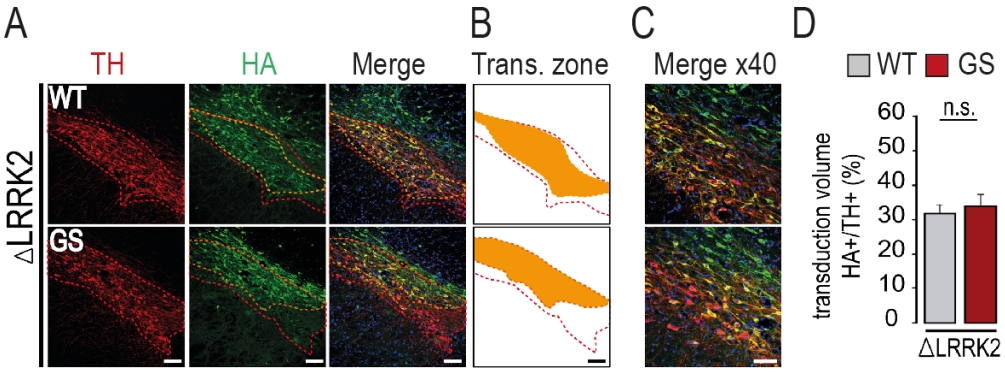

Figure 5: Quantification of the expression of ΔLRRK2 in the SNc ten weeks after LV injection. (A) Double-immunofluorescence labelling and confocal microscopy were used to determine the volume of the SNc (TH-positive, red) at 10 weeks post infection with LV-ΔLRRK2^{WT} or LV-ΔLRRK2^{G2019S} (HA-positive, green). The TH-positive (in red) and HA-positive (in green) zones were delineated and mapped onto the merged acquisition for delimitation of the co-infected area (HA-positive/TH-positive) (B). (C) Higher magnification showing SNc neurons co-expressing TH and LRRK2 fragments. (D) Quantification was performed along the rostro-caudal extension of the total SNc to calculate, using the Cavalieri method, the volume of transduction with regard to the volume of the SNc. *n*=6-7/ group; unpaired Student's *t* test; n.s.: non-significant. Scale bars: 200 µm.

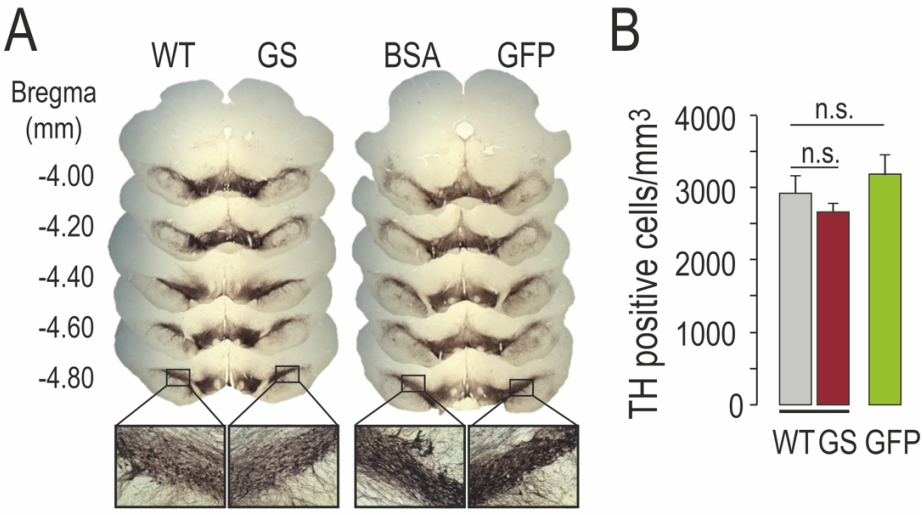

Figure 6: Histological evaluation of the effects of wild-type and G2019S LV-ΔLRRK2 in the SNc, 25 weeks after injection. Lentiviral vectors encoding the ΔLRRK2 fragment or GFP as a control were injected into the SNc. (A) Representative histological sections of the SNc at different antero-posterior levels after immunohistochemical staining of tyrosine hydroxylase (TH). Note that TH immunohistochemistry indicates an absence of major toxicity for ΔLRRK2 in the SNc even when observed at higher magnification (bottom images). (B) The number of TH-positive neurons was counted in the part of the SNc into which the injections were made. Two-way ANOVA was used for between-group comparison; *n*=5/ group.

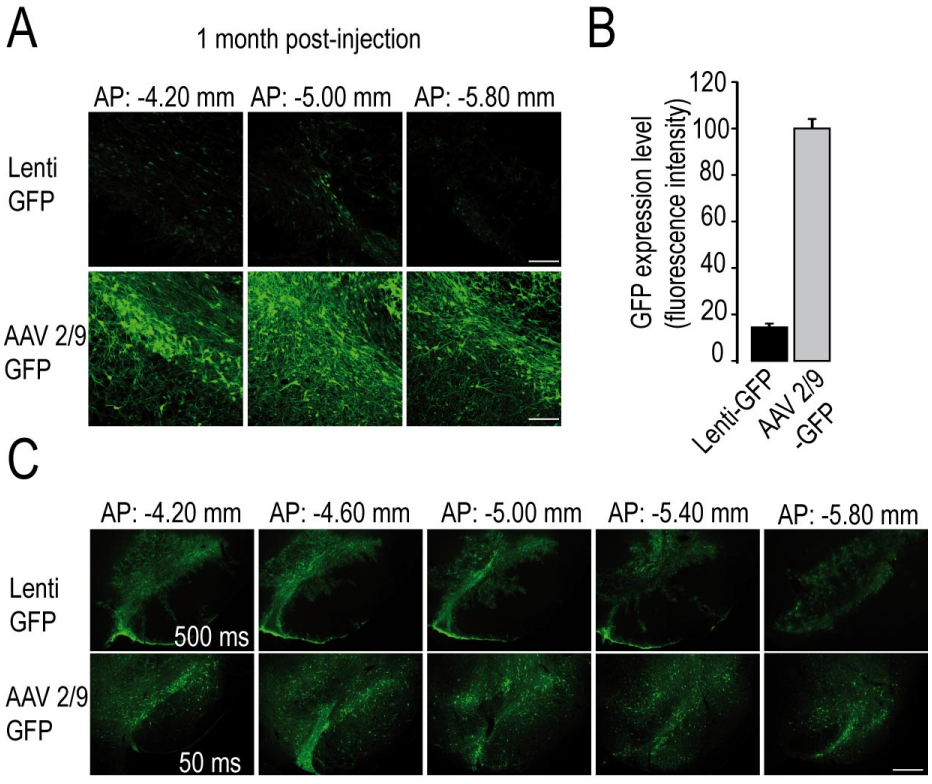

Figure 7: Comparison between AAV and lentiviral transduction. (A) Direct GFP expression was evaluated by confocal microscopy one month post-injection of LVs or AAVs coding for the GFP protein. Acquisitions were made in three different levels of the SNc with the same confocal parameters between LV and AAV. Scale bar: 400 µm. (B) The quantification represents the mean fluorescence intensity. (C) Direct GFP expression was also evaluated by epifluorescence microscopy at low magnification. Note that for the same apparent fluorescence intensity, the time of illumination was 10 fold higher for LV-mediated transduction in comparison with AAV. n= 6 animal/group. AP: antero-posterior from Bregma. Unpaired Student's *t* test for comparison; n.s.: non-significant. Scale bar: 500 µm.

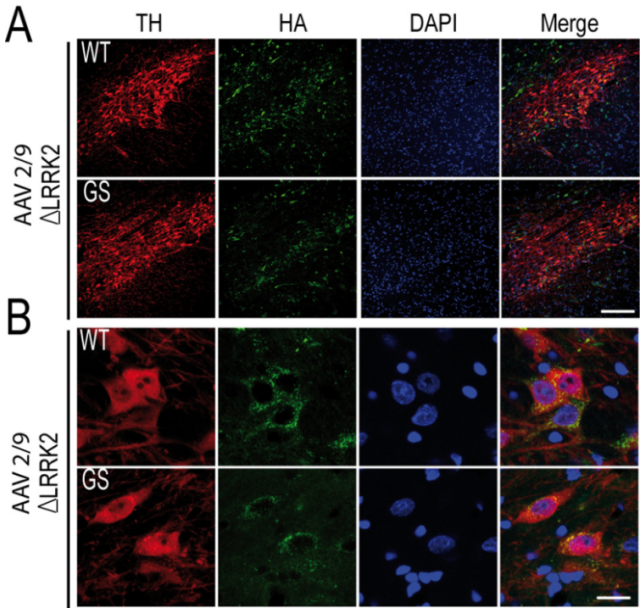

Figure 8: Immunofluorescence analysis of *in vivo* expression of ΔLRRK2 ten weeks after infection with AAV2/9 in the SNc. (A) Double-immunofluorescence labelling and confocal microscopy were used to evaluate the specificity of AAV-ΔLRRK2^{WT} and AAV-ΔLRRK2^{G2019S} for DA neurons in the SNc at 10 weeks P.I.. (B) Higher magnification showing SNc neurons co-expressing TH and ΔLRRK2 fragments. Note that the expression of the HA tag in the SNc is not markedly different in the presence of the G2019S substitution and in the presence of the wild-type (WT) form. Scale bar: 400 µm in A and 10 µm in B.

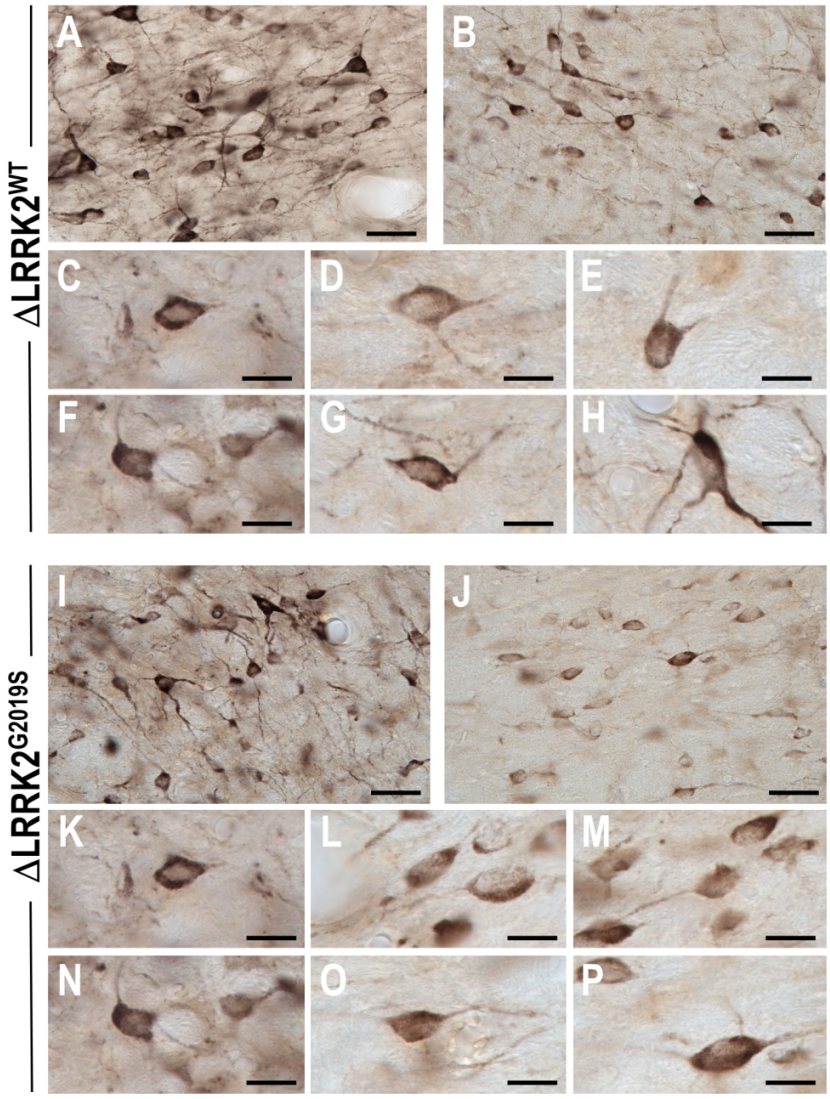

Figure 9: Immunohistochemical analysis of the expression of ΔLRRK2 twenty five weeks after infection with AAV2/9 in the rat SNc.
Photomicrographs of neurons labelled by HA-tagged ΔLRRK2 immunohistochemistry at 25 weeks post-infection in rats injected with either AAV-ΔLRRK2^{WT} (A-H) or AAV-ΔLRRK2^{G2019S} (I-P). Exposition time was set to allow light to go through labelled neurons in order to detect the potential presence of punctuate staining. Some neurons show moderate (A, I) to weak (B, J) staining. Note that the staining is relatively diffuse throughout the cytoplasm. Scale bar: 50 µm in A, B, I, J. and 10 µm in other fields of view.

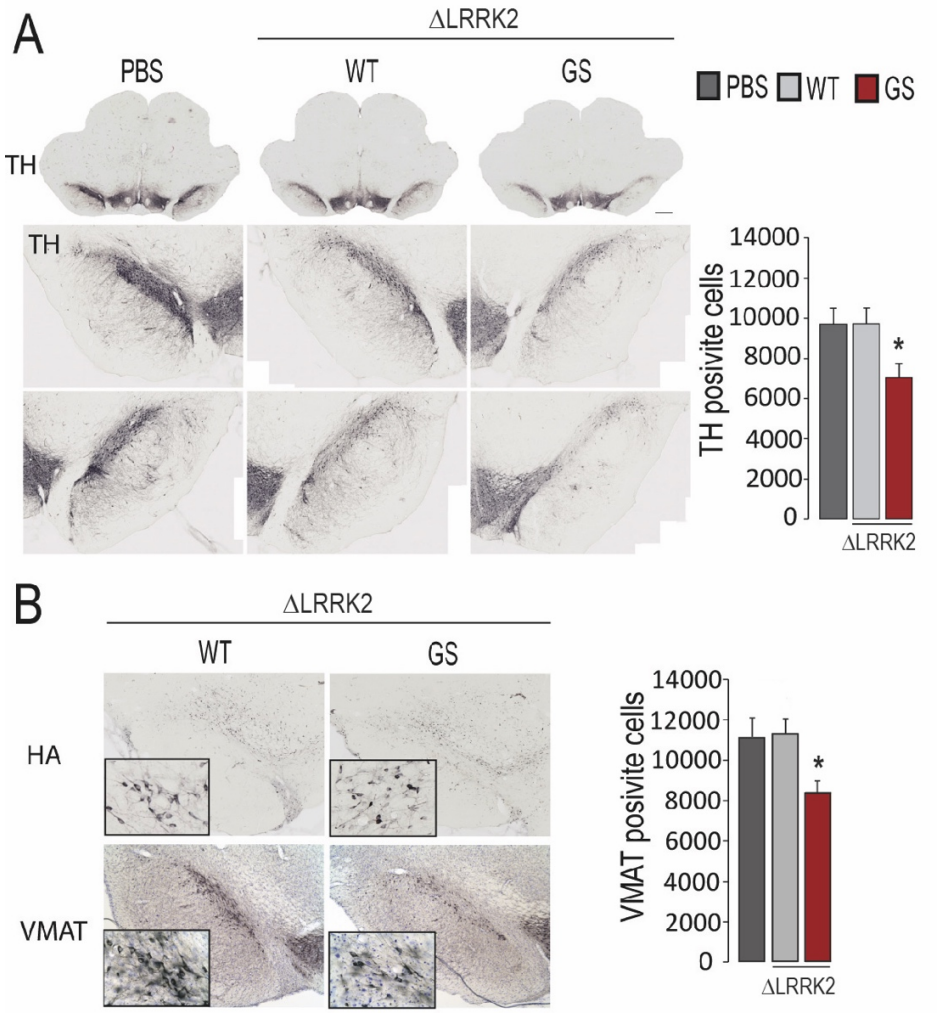

Figure 10: Histological evaluation of the effects of wild-type and G2019S AAV-ΔLRRK2 in the SNc at 25 weeks post-injection. AAVs encoding the ΔLRRK2 fragments or PBS as a control were injected bilaterally into the SNc. (A) Tyrosine hydroxylase (TH) immunohistochemistry was performed in the SNc to evaluate the toxicity. The number of TH-positive neurons was evaluated by stereology in the entire SNc. (B) Vesicular Monoamine Transporter (VMAT2) immunochemistry was performed in the SNc and the number of VMAT-positive neurons was assessed by stereology in the entire SNc. One-way ANOVA was used for between-group comparison and Bonferroni *post hoc* correction for multiple comparisons was applied ; *n*=9/ group; *, p<0.01. Scale bar: 750 µm.

Supplementary figures

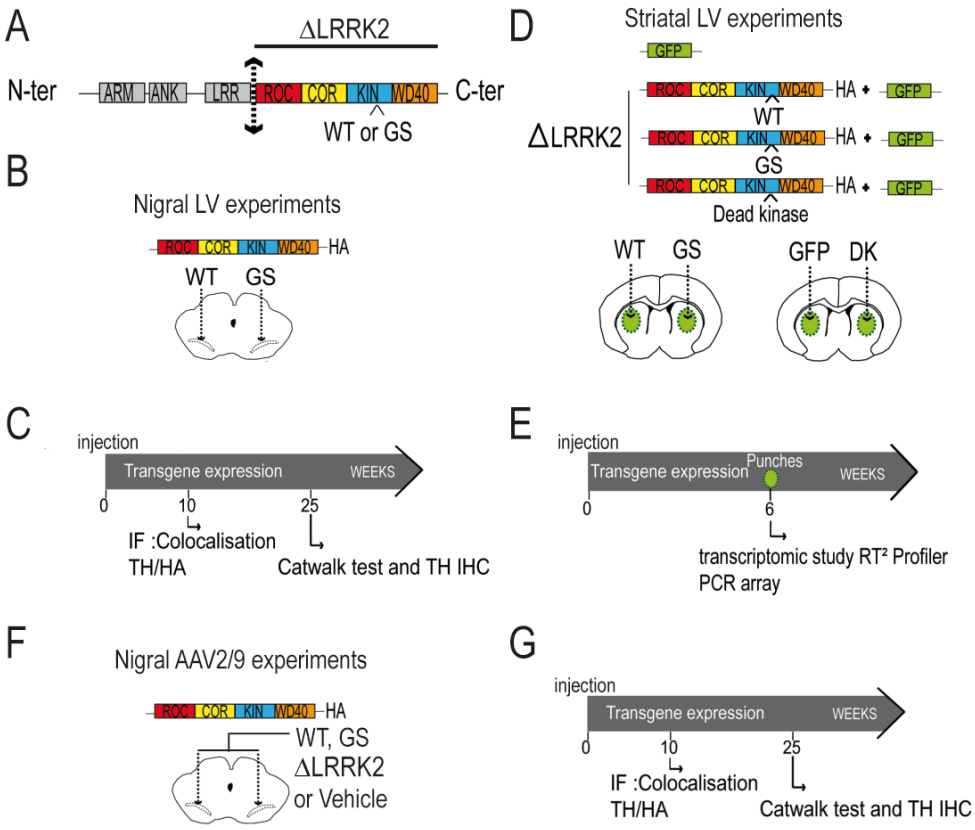

Supplementary Figure S1: Experimental design of *in vivo* experiments in adult rats. (A) The potential toxicity of different LRRK2 fragments containing the kinase domain was studied *in vivo* by generating lentiviruses (LV) and Adeno-Associated Virus (AAV) encoding the C-terminal domains of LRRK2 (ΔLRRK2), either wild-type (WT), or with the G2019S mutation. (B) Adult rats received bilateral stereotaxic injections in the SNc of LVs encoding WT ΔLRRK2 in the left hemisphere, and the G2019S form (GS) in the right hemisphere. As a control, rats received a LV encoding GFP or an injection of BSA. (C) Potential effects of LVs on motor performance and DA neuron survival was assessed. At 10 weeks post-injection (P.I.), the histological evaluation by immunofluorescence focused on the co-localisation of the transgene products with a HA antibody and DA neurons labelled with a tyrosine hydroxylase antibody (TH). At 25 weeks P.I., rats were subjected to a motor test (CatWalk) and *post mortem* histological evaluation. (D) For the striatal experiment aiming at detecting cellular perturbation produced by ΔLRRK2, rats received bilateral injections of LVs encoding ΔLRRK2 into the striatum mixed with LV-GFP. (E) Six weeks after injection, the GFP-positive area in the striatum was dissected out for RT-qPCR array analysis (see Supplementary Fig. S3). (F) Groups of rats received bilateral stereotaxic injections of AAVs in the SNc. AAVs encoded either, $\Delta LRRK2^{WT}$ or $\Delta LRRK2^{G2019S}$. As control, rats received an AAV encoding GFP or an injection of the vehicle (PBS/pluronic acid). (G) Potential effects of AAVs on motor performance and DA neuron survival were studied. At 10 weeks P.I, the histological evaluation by immunohistochemistry and immunofluorescence were carried out. At 25 weeks P.I., rats were subjected to a motor test (CatWalk) and histological evaluation, including unbiased stereological counts of TH and VMAT2 positive neurons in the SNc.

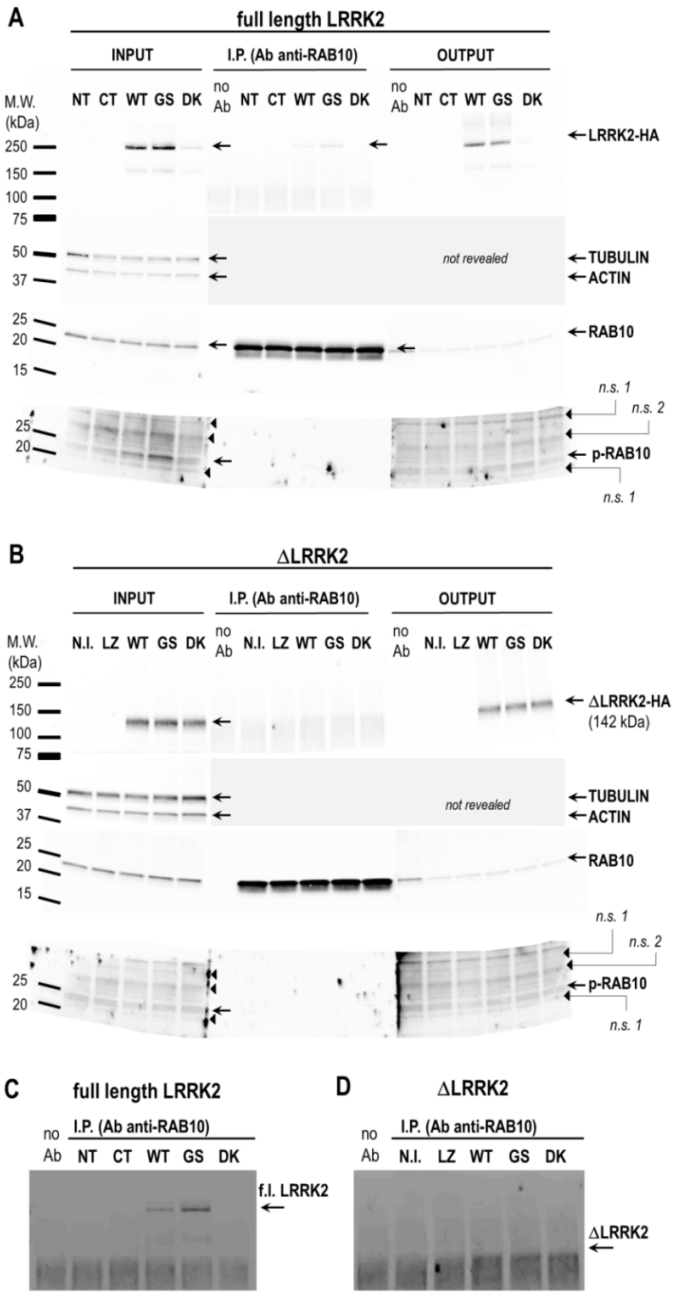

Supplementary Figure S2: Only full length LRRK2 phosphorylates RAB10 at T73 and is co-immuno-precipitated by RAB10. Total protein extracts from HEK293T cells transfected with the full length (A, C) forms of LRRK2 (WT, GS, DK) or from stable HEK293T cells generated by lentiviral infection with ΔLRRK2 (B, D) forms (WT, GS, DK) were submitted to RAB10 immunoprecipitation. Western blot were processed to visualize the level of expression of RAB10, phospho-RAB10 (p-RAB10), LRRK2 (with HA tag) in the input and the immune-precipitated (I.P.) fraction. Actin (42 kDa) and tubulin (52 kDa) were used to visualize the loading homogeneity in the input. Actin and tubulin were not revealed in the I.P. and output fractions. The signal for phospho-RAB10 (Threonine 73) being relatively weak in HEK cells, exposition time had been increased so that non-specific bands (n.s.) can also be seen. (C) and (D) are magnification of images of the HA detection shown in A and B respectively using increased contrast and less luminosity to better illustrate that full length LRRK2 and not ΔLRRK2 could co-immunoprecipitate with RAB10. Abbreviations: NI, Not Infected; NT, Not Transfected; CT, Control ; LZ, LV-LacZ.

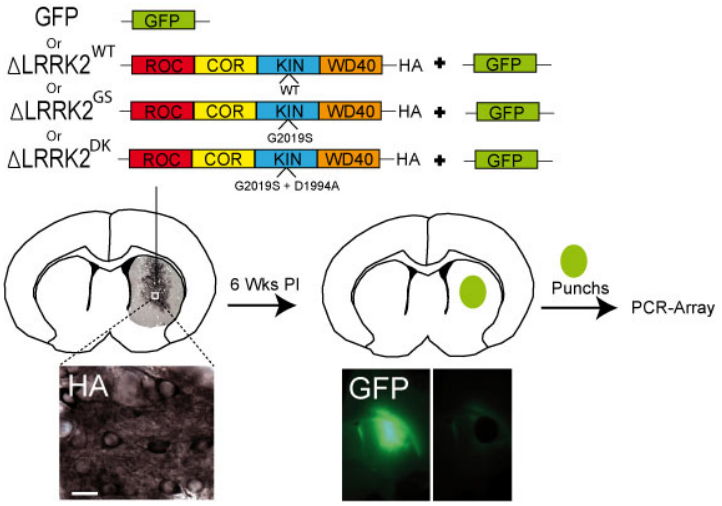

Supplementary Figure S3: Transcriptomic analysis of LRRK2 fragments *in vivo*. LVs-ΔLRRK2 (WT, G2019S or G2019S/D1994A) and LVs-GFP were co-injected in the striatum. The striatal region displaying GFP fluorescence was dissected under a fluorescence binocular microscope (Leica). The punch samples were then processed for RT-qPCR.

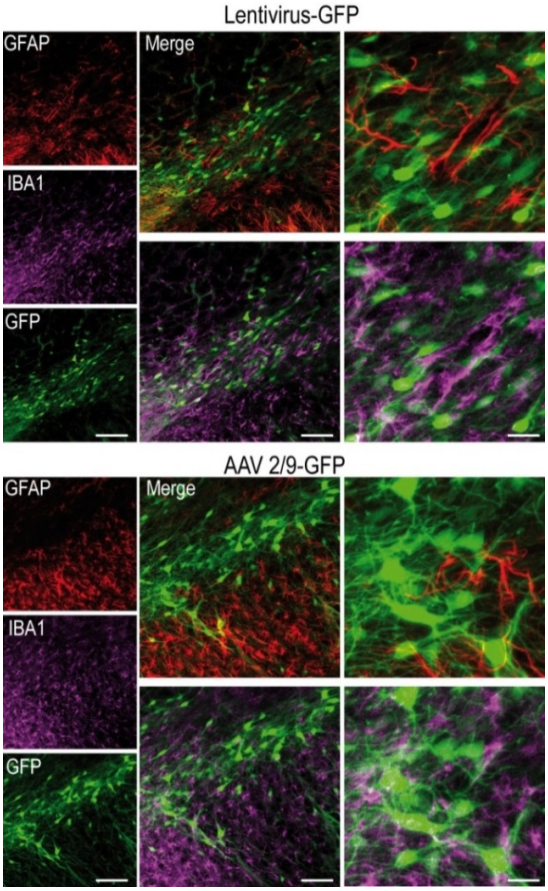

Supplementary Figure S4: Preferential expression of transgenes in neurons after infection with lentiviral vectors and AAV2/9. LV-GFP or AAV-GFP were injected in the SNc. Histological evaluation was performed 4 weeks post-infection. Double immunofluorescence labelling for GFAP (astrocytes) and IBA1 (microglia) was used to evaluate the specificity of LVs and AAVs for neurons compared to other cell types (scale bar = 400µm and 10µm for the magnifications). No expression was seen in astrocytes or microglial cells. Similar results were obtained in groups of 3 animals for each vector.

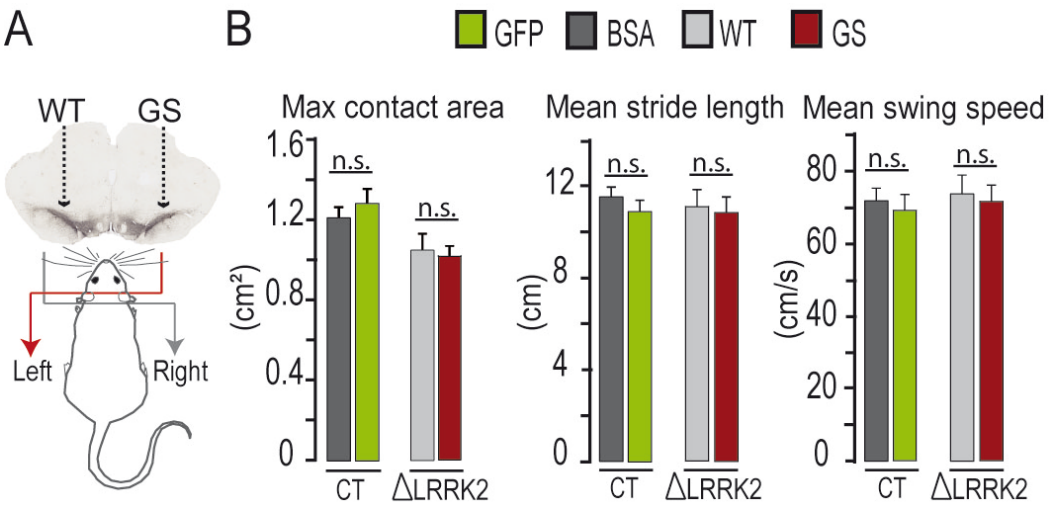

Supplementary Figure S5: Motor performance of rats receiving injections of LV coding for WT or G2019S ΔLRRK2 and GFP in the SNc, measured 25 weeks after injection. The gait of the rats was evaluated in the Catwalk apparatus. We analysed the right forelimb, corresponding to the contralateral SNc infected with a LV encoding wild type (WT) LRRK2 fragments (in light grey), and the left forelimb, corresponding to the right SNc infected with LVs encoding G2019S forms (in red), separately (A). Three parameters are presented: maximal (max) contact area (B), mean stride length (C) and mean swing speed (D). Two-way ANOVA for between-group comparison (*n*=12/group), n.s. (non-significant).

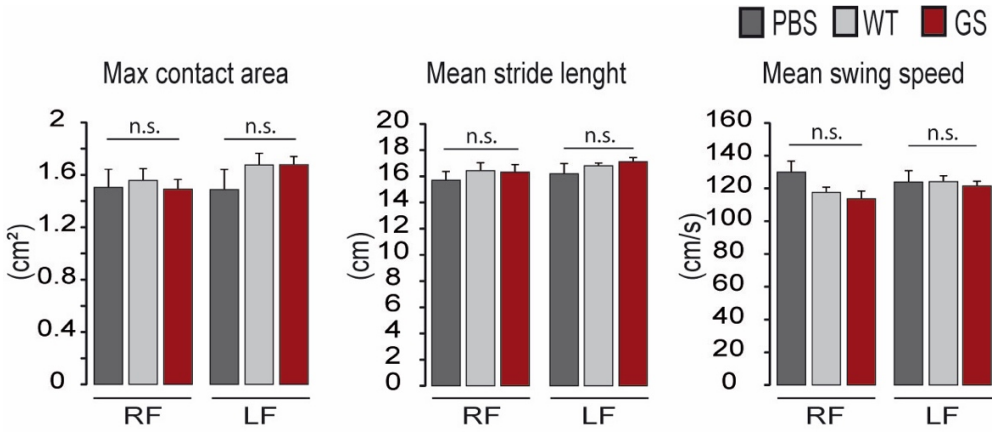

Supplementary Figure S6: Motor performance of rats receiving injections of PBS or AAV coding for WT or G2019S ΔLRRK2 or in the SNc, measured 25 weeks after injection. The gait of the rats was evaluated in the Catwalk apparatus for the three different groups. We analysed the right forelimb (RF) and the left forelimb (LF). Three parameters are presented: maximal (max) contact area, mean stride length and mean swing speed. One-way ANOVA for between-group comparison (*n*=12/group), n.s. (non-significant).

Supplementary Table 1

	Primer sequences
ΔLRRK2	RnWD40-F TCAGCGTTCAGCGATTCTAACAT
	RnWD40-R CTTCTTGTCCCACACCTCTACGA
Hpca	RnHpca_1F CCGGGAGTTCATCATCGCTCT
	RnHpca_2R CCATTGCCGTCCAGGTCGTA
Rgs4	RnRgs4_1F TTCTCTCCTCGCTCCGAATCC
	RnRgs4_2R GCAGAAATCCCAGCCGATGTT
Grin2a	RnGrin2a_1F ACAGGGACCCTAAGTGGCGAC
	RnGrin2a_2R CCAGCAGCACCGCAATG
Rph3a	RnRph3a_1F GGGCTCTGCGTGTGTCGTGT
	RnRph3a_2R ACTGGATGCGGACGGTTGTTG
Snap25	RnSnap25_1F TCCGCAGGGTAACAAACGATG
	RnSnap25_2R TCCGATGATGCCGCTCAC
Cnr1	RnCnr1-1F AGTCACCTTGAGTCTGGCCTAATC
	RnCnr1-2R GTCATTCGAGCCCACGTAGAG
Tac1	RnTac1-1F TCAACTGTTTGCAGAGGAAATCGG
	RnTac1-2R GCTGAGGCTTGGGTCTTCGG
Bbox	RnBbox1-3F TCAGCTTCCACACAGATTACCCA
	RnBbox1-4R GCACACATTAAACCCATCTACGA

Table 1: In house designed primer sequences used for double checking the results of the RT-qPCR analysis. The primers of the "Huntington's Disease" RT^2 Profiler PCR Array (Qiagen) are proprietary. List can be found at https://www.qiagen.com/be/shop/genes-and-pathways/complete-biology-list/huntingtons-disease/

Acknowledgements

This work was funded by rolling grants from the CEA and the CNRS.
The research generating these results received funding from la Fondation de France (AAP 2010-2011 and 2013, Engt 00016819). Noémie Cresto is a recipient of a PhD fellowship from Association France Parkinson (2016). The studies were also funded by European Union Horizon 2020 Programme (H2020-MSCA-ITN-2015) under the Marie Skłodowska-Curie Innovative Training Networks and Grant Agreement No. 676408.
This work benefited from a support from the national "Translational Research Infrastructure for Biotherapies in Neurosciences" (NeurATRIS, "Investissement d'Avenir", ANR-11-INBS-0011).

Conflict of Interest Statement

All authors declare that they have no conflict of interest

References

Aufschnaiter, A., Kohler, V., Walter, C., and Tosal-castano, S. (2018). The Enzymatic Core of the Parkinson ' s Disease-Associated Protein LRRK2 Impairs Mitochondrial Biogenesis in Aging Yeast. Front. Mol. Neurosci. *11*, 1–15.

Aurnhammer, C., Haase, M., Muether, N., Hausl, M., Rauschhuber, C., Huber, I., Nitschko, H., Busch, U., Sing, A., Ehrhardt, A., et al. (2012). Universal real-time PCR for the detection and quantification of adeno-associated virus serotype 2-derived inverted terminal repeat sequences. Hum. Gene Ther. Methods *23*, 18–28.

Beccano-Kelly, D.A., Kuhlmann, N., Tatarnikov, I., Volta, M., Munsie, L.N., Chou, P., Cao, L.-P., Han, H., Tapia, L., Farrer, M.J., et al. (2014). Synaptic function is modulated by LRRK2 and glutamate release is increased in cortical neurons of G2019S LRRK2 knock-in mice. Front. Cell. Neurosci. *8*.

Berger, A., Lorain, S., Joséphine, C., Desrosiers, M., Peccate, C., Voit, T., Garcia, L., Sahel, J.-A., and Bemelmans, A.-P. (2015). Repair of Rhodopsin mRNA by Spliceosome-Mediated RNA Trans-Splicing: A New Approach for Autosomal Dominant Retinitis Pigmentosa. Mol. Ther. *23*, 918–930.

Braak, H., and Braak, E. (2000). Pathoanatomy of Parkinson's disease. J. Neurol. *247*, II3–II10.

Brochier, C., Gaillard, M.-C., Diguet, E., Caudy, N., Dossat, C., Ségurens, B., Wincker, P., Roze, E., Caboche, J., Hantraye, P., et al. (2008). Quantitative gene expression profiling of mouse brain regions reveals differential transcripts conserved in human and affected in disease models. Physiol. Genomics *33*, 170–179.

Colin, A., Faideau, M., Dufour, N., Auregan, G., Hassig, R., Andrieu, T., Brouillet, E., Hantraye, P., Bonvento, G., and Déglon, N. (2009). Engineered lentiviral vector targeting astrocytes In vivo. Glia *57*, 667–679.

Cookson, M.R. (2010). The role of leucine-rich repeat kinase 2 (LRRK2) in Parkinson's disease. Nat. Rev. Neurosci. *11*, 791–797.

Cresto, N., Gardier, C., Gubinelli, F., Gaillard, M.-C., Liot, G., West, A.B., and Brouillet, E. (2019). The Unlikely Partnership Between LRRK2 and α-Synuclein in Parkinson's Disease. Eur. J. Neurosci. *49*, 339-363.

Di Maio, R., Hoffman, E.K., Rocha, E.M., Keeney, M.T., Sanders, L.H., De Miranda, B.R., Zharikov, A., Van Laar, A., Stepan, A.F., Lanz, T.A., et al. (2018). LRRK2 activation in idiopathic Parkinson's disease. Sci. Transl. Med. *10*, eaar5429.

Dusonchet, J., Kochubey, O., Stafa, K., Young, S.M., Zufferey, R., Moore, D.J., Schneider, B.L., and Aebischer, P. (2011). A Rat Model of Progressive Nigral Neurodegeneration Induced by the Parkinson's Disease-Associated G2019S Mutation in LRRK2. J. Neurosci. *31*, 907–912.

Francelle, L., Galvan, L., Gaillard, M.C., Guillermier, M., Houitte, D., Bonvento, G., Petit, F., Jan, C., Dufour, N., Hantraye, P., et al. (2015). Loss of the thyroid hormone-binding protein Crym renders striatal neurons more vulnerable to mutant huntingtin in Huntington's disease. Hum. Mol. Genet. *24*, 1563–1573.

Galvan, L., Francelle, L., Gaillard, M.-C., de Longprez, L., Carrillo-de Sauvage, M.-A., Liot, G., Cambon, K., Stimmer, L., Luccantoni, S., Flament, J., et al. (2018). The striatal kinase DCLK3 produces neuroprotection against mutant huntingtin. Brain *141*, 1434–1454.

Gilks, W.P., Abou-Sleiman, P.M., Gandhi, S., Jain, S., Singleton, A., Lees, A.J., Shaw, K., Bhatia, K.P., Bonifati, V., Quinn, N.P., et al. (2005). A common LRRK2 mutation in idiopathic Parkinson's disease. The Lancet *365*, 415–416.

Healy, D.G., Falchi, M., O'Sullivan, S.S., Bonifati, V., Durr, A., Bressman, S., Brice, A., Aasly, J., Zabetian, C.P., Goldwurm, S., et al. (2008). Phenotype, genotype, and worldwide genetic penetrance of LRRK2-associated Parkinson's disease: a case-control study. Lancet Neurol. *7*, 583–590.

Higashi, S., Moore, D.J., Colebrooke, R.E., Biskup, S., Dawson, V.L., Arai, H., Dawson, T.M., and Emson, P.C. (2007). Expression and localization of Parkinson's disease-associated leucine-rich repeat kinase 2 in the mouse brain. J. Neurochem. *100*, 368–381.

Hottinger, A.F., Azzouz, M., Déglon, N., Aebischer, P., and Zurn, A.D. (2000). Complete and Long-Term Rescue of Lesioned Adult Motoneurons by Lentiviral-Mediated Expression of Glial Cell Line-Derived Neurotrophic Factor in the Facial Nucleus. J. Neurosci. *20*, 5587–5593.

Jaleel, M., Nichols, R.J., Deak, M., Campbell, D.G., Gillardon, F., Knebel, A., and Alessi, D.R. (2007). LRRK2 phosphorylates moesin at threonine-558: characterization of how Parkinson's disease mutants affect kinase activity. Biochem. J. *405*, 307–317.

Jorgensen, N.D., Peng, Y., Ho, C.C.-Y., Rideout, H.J., Petrey, D., Liu, P., and Dauer, W.T. (2009). The WD40 Domain Is Required for LRRK2 Neurotoxicity. PLoS ONE *4*.

Kett, L.R., Boassa, D., Ho, C.C.-Y., Rideout, H.J., Hu, J., Terada, M., Ellisman, M., and Dauer, W.T. (2012). LRRK2 Parkinson disease mutations enhance its microtubule association. Hum. Mol. Genet. *21*, 890–899.

Lee, B.D., Shin, J.-H., VanKampen, J., Petrucelli, L., West, A.B., Ko, H.S., Lee, Y., Maguire-Zeiss, K.A., Bowers, W.J., Federoff, H.J., et al. (2010). Inhibitors of Leucine Rich Repeat Kinase 2 (LRRK2) Protect Against LRRK2-Models of Parkinson's Disease. Nat. Med. *16*, 998–1000.

Lee, J.-W., Tapias, V., Di Maio, R., Greenamyre, J.T., and Cannon, J.R. (2015). Behavioral, neurochemical, and pathologic alterations in bacterial artificial chromosome transgenic G2019S leucine-rich repeated kinase 2 rats. Neurobiol. Aging *36*, 505–518.

Lesage, S., and Brice, A. (2009). Parkinson's disease: from monogenic forms to genetic susceptibility factors. Hum. Mol. Genet. *18*, R48–R59.

Lewis, P.A., Greggio, E., Beilina, A., Jain, S., Baker, A., and Cookson, M.R. (2007). The R1441C mutation of LRRK2 disrupts GTP hydrolysis. Biochem. Biophys. Res. Commun. *357*, 668–671.

Lin, X., Parisiadou, L., Gu, X.-L., Wang, L., Shim, H., Sun, L., Xie, C., Long, C.-X., Yang, W.-J., Ding, J., et al. (2009). Leucine-rich repeat kinase 2 regulates the progression of neuropathology induced by Parkinson's-disease-related mutant alpha-synuclein. Neuron *64*, 807–827.

Liu, Z., Bryant, N., Kumaran, R., Beilina, A., Abeliovich, A., Cookson, M.R., and West, A.B. (2018). LRRK2 phosphorylates membrane-bound Rabs and is activated by GTP-bound Rab7L1 to promote recruitment to the trans-Golgi network. Hum. Mol. Genet. *27*, 385–395.

Lobbestael, E., Civiero, L., Wit, T.D., Taymans, J.-M., Greggio, E., and Baekelandt, V. (2016). Pharmacological LRRK2 kinase inhibition induces LRRK2 protein destabilization and proteasomal degradation. Sci. Rep. *6*, 33897.

Marte, A., Russo, I., Rebosio, C., Valente, P., Belluzzi, E., Pischedda, F., Montani, C., Lavarello, C., Petretto, A., Fedele, E., et al. (2019). Leucine-rich repeat kinase 2 phosphorylation on synapsin I regulates glutamate release at pre-synaptic sites. J. Neurochem.

Mata, I.F., Wedemeyer, W.J., Farrer, M.J., Taylor, J.P., and Gallo, K.A. (2006). LRRK2 in Parkinson's disease: protein domains and functional insights. Trends Neurosci. *29*, 286–293.

Mestre-Francés, N., Serratrice, N., Gennetier, A., Devau, G., Cobo, S., Trouche, S.G., Fontès, P., Zussy, C., De Deurwaerdere, P., Salinas, S., et al. (2018). Exogenous LRRK2G2019S induces parkinsonian-like pathology in a nonhuman primate. JCI Insight *3*.

Naldini, L., Blömer, U., Gage, F.H., Trono, D., and Verma, I.M. (1996). Efficient transfer, integration, and sustained long-term expression of the transgene in adult rat brains injected with a lentiviral vector. Proc. Natl. Acad. Sci. U. S. A. *93*, 11382–11388.

Nalls, M.A., Pankratz, N., Lill, C.M., Do, C.B., Hernandez, D.G., Saad, M., DeStefano, A.L., Kara, E., Bras, J., Sharma, M., et al. (2014). Large-scale meta-analysis of genome-wide association data identifies six new risk loci for Parkinson's disease. Nat. Genet. *46*, 989–993.

Paisán-Ruíz, C., Jain, S., Evans, E.W., Gilks, W.P., Simón, J., van der Brug, M., de Munain, A.L., Aparicio, S., Gil, A.M., Khan, N., et al. (2004). Cloning of the Gene Containing Mutations that Cause PARK8-Linked Parkinson's Disease. Neuron *44*, 595–600.

Parisiadou, L., Yu, J., Sgobio, C., Xie, C., Liu, G., Sun, L., Gu, X.-L., Lin, X., Crowley, N.A., Lovinger, D., et al. (2014). LRRK2 regulates synaptogenesis and dopamine receptor activation through modulation of PKA activity. Nat. Neurosci. *17*, 367–376.

Pereira, C., Miguel Martins, L., and Saraiva, L. (2014). LRRK2, but not pathogenic mutants, protects against H2O 2 stress depending on mitochondrial function and endocytosis in a yeast model. Biochim. Biophys. Acta - Gen. Subj. *1840*, 2025–2031.

Piccoli, G., Condliffe, S.B., Bauer, M., Giesert, F., Boldt, K., Astis, S.D., Meixner, A., Sarioglu, H., Vogt-Weisenhorn, D.M., Wurst, W., et al. (2011). LRRK2 Controls Synaptic Vesicle Storage and Mobilization within the Recycling Pool. J. Neurosci. *31*, 2225–2237.

Piccoli, G., Onofri, F., Cirnaru, M.D., Kaiser, C.J.O., Jagtap, P., Kastenmüller, A., Pischedda, F., Marte, A., von Zweydorf, F., Vogt, A., et al. (2014). Leucine-rich repeat kinase 2 binds to neuronal vesicles through protein interactions mediated by its C-terminal WD40 domain. Mol. Cell. Biol. *34*, 2147–2161.

Poewe, W. (2008). Non-motor symptoms in Parkinson's disease. Eur. J. Neurol. *15*, 14–20.

Ramonet, D., Daher, J.P.L., Lin, B.M., Stafa, K., Kim, J., Banerjee, R., Westerlund, M., Pletnikova, O., Glauser, L., Yang, L., et al. (2011). Dopaminergic Neuronal Loss, Reduced Neurite Complexity and Autophagic Abnormalities in Transgenic Mice Expressing G2019S Mutant LRRK2. PLoS ONE *6*.

Rodriguez-Oroz, M.C., Jahanshahi, M., Krack, P., Litvan, I., Macias, R., Bezard, E., and Obeso, J.A. (2009). Initial clinical manifestations of Parkinson's disease: features and pathophysiological mechanisms. Lancet Neurol. *8*, 1128–1139.

Ruiz, M., and Déglon, N. (2012). Viral-mediated overexpression of mutant huntingtin to model HD in various species. Neurobiol. Dis. *48*, 202–211.

Satake, W., Nakabayashi, Y., Mizuta, I., Hirota, Y., Ito, C., Kubo, M., Kawaguchi, T., Tsunoda, T., Watanabe, M., Takeda, A., et al. (2009). Genome-wide association study identifies common variants at four loci as genetic risk factors for Parkinson's disease. Nat. Genet. *41*, 1303–1307.

Sheng, D., Qu, D., Kwok, K.H.H., Ng, S.S., Lim, A.Y.M., Aw, S.S., Lee, C.W.H., Sung, W.K., Tan, E.K., Lufkin, T., et al. (2010). Deletion of the WD40 Domain of LRRK2 in Zebrafish Causes Parkinsonism-Like Loss of Neurons and Locomotive Defect. PLoS Genet. *6*.

Shogo Kamikawaji, Genta Ito, and Takeshi Iwatsubo (2016). Identification of the Autophosphorylation Sites of LRRK2.

Smith, W.W., Pei, Z., Jiang, H., Dawson, V.L., Dawson, T.M., and Ross, C.A. (2006). Kinase activity of mutant LRRK2 mediates neuronal toxicity. Nat. Neurosci. *9*, 1231–1233.

Steger, M., Diez, F., Dhekne, H.S., Lis, P., Nirujogi, R.S., Karayel, O., Tonelli, F., Martinez, T.N., Lorentzen, E., Pfeffer, S.R., et al. (2017). Systematic proteomic analysis of LRRK2-mediated Rab GTPase phosphorylation establishes a connection to ciliogenesis. ELife *6*.

Taymans, J.-M., Vancraenenbroeck, R., Ollikainen, P., Beilina, A., Lobbestael, E., De Maeyer, M., Baekelandt, V., and Cookson, M.R. (2011). LRRK2 Kinase Activity Is Dependent on LRRK2 GTP Binding Capacity but Independent of LRRK2 GTP Binding. PLoS ONE *6*.

Tenovuo, O., Rinne, U.K., and Viljanen, M.K. (1984). Substance P immunoreactivity in the post-mortem parkinsonian brain. Brain Res. *303*, 113–116.

Vandeputte, C., Taymans, J.-M., Casteels, C., Coun, F., Ni, Y., Van Laere, K., and Baekelandt, V. (2010). Automated quantitative gait analysis in animal models of movement disorders. BMC Neurosci. *11*, 92.

Webber, P.J., Smith, A.D., Sen, S., Renfrow, M.B., Mobley, J.A., and West, A.B. (2011). Autophosphorylation in the Leucine-Rich Repeat Kinase 2 (LRRK2) GTPase Domain Modifies Kinase and GTP-Binding Activities. J. Mol. Biol. *412*, 94–110.

West, A.B., Moore, D.J., Choi, C., Andrabi, S.A., Li, X., Dikeman, D., Biskup, S., Zhang, Z., Lim, K.-L., Dawson, V.L., et al. (2007). Parkinson's disease-associated mutations in LRRK2 link enhanced GTP-binding and kinase activities to neuronal toxicity. Hum. Mol. Genet. *16*, 223–232.

Xiong, Y., Coombes, C.E., Kilaru, A., Li, X., Gitler, A.D., Bowers, W.J., Dawson, V.L., Dawson, T.M., and Moore, D.J. (2010). GTPase Activity Plays a Key Role in the Pathobiology of LRRK2. PLoS Genet. *6*.

Xiong, Y., Neifert, S., Karuppagounder, S.S., Stankowski, J.N., Lee, B.D., Grima, J.C., Chen, G., Ko, H.S., Lee, Y., Swing, D., et al. (2017). Overexpression of Parkinson's Disease-Associated Mutation LRRK2 G2019S in Mouse Forebrain Induces Behavioral Deficits and α-Synuclein Pathology. ENeuro *4*, 1–10.

Xiong, Y., Neifert, S., Karuppagounder, S.S., Liu, Q., Stankowski, J.N., Lee, B.D., Ko, H.S., Lee, Y., Grima, J.C., Mao, X., et al. (2018). Robust kinase- and age-dependent dopaminergic and norepinephrine neurodegeneration in LRRK2 G2019S transgenic mice. Proc. Natl. Acad. Sci. *115*, 201712648.

Yue, M., Hinkle, K.M., Davies, P., Trushina, E., Fiesel, F.C., Christenson, T.A., Schroeder, A.S., Zhang, L., Bowles, E., Behrouz, B., et al. (2015). Progressive dopaminergic alterations and mitochondrial abnormalities in LRRK2 G2019S knock-in mice. Neurobiol. Dis. *78*, 172–195.

Zhou, M., Zhang, W., Chang, J., Wang, J., Zheng, W., Yang, Y., Wen, P., Li, M., and Xiao, H. (2015). Gait analysis in three different 6-hydroxydopamine rat models of Parkinson's disease. Neurosci. Lett. *584*, 184–189.

8.3 Article: Overexpression of the C-terminal fragment of LRRK2 harboring the G2019S substitution in substantia nigra dopaminergic neurons increases the neurotoxicity of mutant A53T α-synuclein in vivo (submitted)

Noémie Cresto [1,2], Francesco Gubinelli [1,2], Camille Gardier [1,2], Marie-Claude Gaillard [1,2], Charlène Josephine [1,2], Gwenaëlle Auregan [1,2], Martine Guillermier [1,2], Suéva Bernier [1,2], Caroline Jan [1,2], Pauline Gipchtein [1,2], Philippe Hantraye [1,2], Gilles Bonvento [1,2], Karine Cambon [1,2], Géraldine Liot [1,2], Alexis-Pierre Bemelmans [1,2], Emmanuel Brouillet [1,2] §

[1] CEA, DRF, Institut François Jacob, Molecular Imaging Research Center (MIRCen), F-92265 Fontenay-aux-Roses, France
[2] CNRS, CEA, Paris-Sud Univ., Univ. Paris-Saclay, Neurodegenerative Diseases Laboratory (UMR9199), F-92265, Fontenay-aux-Roses, France

Abstract

Alpha-synuclein (α-syn) and leucine-rich repeat kinase 2 (LRRK2) proteins are likely to play crucial roles both in sporadic and familial forms of Parkinson's disease (PD). The most prevalent mutation in LRRK2 is the G2019S substitution which induces neurotoxicity through an increase of its kinase activity. Interplay between LRRK2 and α-syn may be involved in the neurodegeneration of dopaminergic (DA) neurons in the substantia nigra (SNpc) in PD. Here, we aimed at studying whether LRRK2^{G2019S} could increase the neurotoxicity induced by a mutant form of α-syn (A53T mutation) *in vivo* in DA neurons. We used a co-infection approach with AAV2/6 vectors encoding α-syn^{A53T}, and the C-terminal part of LRRK2 (ΔLRRK2) containing the kinase domain with either the G2019S mutation (ΔLRRK2^{G2019}) alone or with the D1994A mutation (ΔLRRK2$^{G2019S/D1994A}$) that inactivates the kinase activity of LRRK2. AAVs were co-injected into the rat SNpc and histological evaluation was performed at 6 and 15 weeks post-infection (P.I.). A majority of SNpc neurons co-expressed ΔLRRK2 and α-syn^{A53T} after infection and all the LRRK2 forms were expressed at the same level. ΔLRRK2^{G2019S} alone produced no cell loss at 15 weeks P.I.. Results showed that co-expression of ΔLRRK2^{G2019S} and α-syn^{A53T} produced greater loss of DA neurons than that produced by α-syn^{A53T} alone. In contrast, LRRK2 constructs *in vivo* did not change cell loss induced by a different aggregating protein, the N-terminal domain of mutant huntingtin. We also show that the inactive form ΔLRRK2$^{G2019S/D1994A}$ did not change the toxicity of α-syn^{A53T} in comparison with the active form ΔLRRK2^{G2019S}. Thus, these results show that mutant LRRK2 may selectively facilitate α-syn toxicity in dopaminergic cells *in vivo* through a cell-autonomous mechanism involving its kinase activity.

Introduction

Parkinson's disease (PD) is a neurodegenerative disorder affecting approximately seven million people worldwide. Early in the course of the disease, the most obvious symptoms are movement-related, include shaking (resting tremor), rigidity, and slowness of movement. The neuropathological hallmarks of PD are characterized by a progressive loss of dopaminergic (DA) neurons in the substantia nigra *pars compacta* (SNpc) and the presence of neuronal aggregates (Lewy bodies) and dystrophic Lewy neurites containing the protein α-synuclein (α-syn) (Braak et Braak 2000). There exists no treatment to delay neurodegeneration. The cause of α-syn aggregation and preferential death of DA neurons are unknown. PD is mainly a sporadic neurodegenerative disorder but approximately 10% of the cases are of genetic origin. Among all the causative genes, mutations in *SNCA* coding for the α-syn protein and in LRRK2 (Leucin-rich repeat kinase 2) have been proved to associate with autosomal dominant (AD) PD (Lesage et Brice 2009).
Duplication, triplication and rare mutations (A53T (Polymeropoulos et al. 1997); A30P (Krüger et al. 1998); E46K (Zarranz et al. 2004)) in the *SNCA* gene have been found in families with dominantly inherited PD and are associated with early-onset forms of PD with an amplification of α-syn aggregation (Chartier-Harlin et al. 2004; Singleton et al. 2003). Compelling evidence indicate that α-syn is central in PD and plays a key role through different aggregated forms, including abnormally phosphorylated aggregates that produce multiple cellular alterations eventually leading to DA cell death (Saito et al. 2003).
Mutations in LRRK2 are the most common genetic cause of both familial and sporadic PD (Paisán-Ruíz et al. 2004; Zimprich et al. 2004). There are also variants in LRRK2 locus that are considered risk factors for developing PD. The most prevalent mutation in LRRK2 is the G2019S substitution accounting for 5–6% of autosomal-dominant (AD) familial and 1–2% of de novo generic PD cases (Gilks et al. 2005; Healy et al. 2008). Patients harboring the G2019S and other mutations are clinically indistinguishable from idiopathic PD cases, including the presence of Lewy bodies (LBs) in most cases (Biskup et West 2009; Yahalom et al. 2014). In general, although LRRK2 variants or mutations are considered risk factors of developing PD, the onset of symptoms in LRRK2 carriers has been found similar to that of idiopathic PD cases (Brockmann et al. 2011; Oosterveld et al. 2015). The mechanisms underlying LRRK2 neurotoxicity remain unknown. It is now generally admitted that the G2019S mutation increases LRRK2 kinase activity (both autophosphorylation and phosphorylation of exogenous kinase substrates) and that neurotoxicity originates from this increased activity (Lee et al. 2010; West et al. 2007). Moreover,

it was recently shown that LRRK2 was activated in the SNpc of idiopathic PD patients (Di Maio et al. 2018), highlighting the importance of LRRK2's kinase activity in the pathogenesis of both familial and sporadic forms of PD.
Because of the presence of LBs in symptomatic LRRK2 mutation carriers and the presence of LRRK2 in LBs, the hypothesis of a functional (and possibly physical) interaction between LRRK2 and α-syn has been suggested. Indeed LRRK2 toxicity may require the presence of α-syn and conversely, the presence of variants/mutant LRRK2 could increase the risk and/or impact on the α-synucleopathy in PD. Of importance, the level of kinase activity of LRRK2 could thus be a modifier of α-syn toxicity. If this turns out to be true, the therapeutic implication would be extremely important: the regulation of LRRK2 kinase activity could be theoretically beneficial in slowing disease progression not only in LRRK2 variants carriers but also in idiopathic PD. Recent experiments in transgenic mouse models of LRRK2 and α-syn support these hypotheses. In particular, results of experiments in genetic models of mutant LRRK2 or wild type LRRK2, in particular the effect of the pharmacological blockade of the kinase activity of $LRRK2^{G2019S}$ in these models, indicate that LRRK2 may increase α-syn toxicity (Bieri et al. 2019; Daher et al. 2014, 2015; Lin et al. 2009; Novello et al. 2018).
However, the mechanisms underlying the "protoxic" effect of LRRK2 (especially the G2019S mutation) on α-syn toxicity are not known. The exact role of the kinase domain is not totally demonstrated. Pharmacological interventions suggested that the kinase activity probably takes part in the functional interaction between the two proteins (for a review see Cresto et al. 2019). However, the requirement of the other functional domains of LRRK2, in particular the N-terminal domains that regulate many cellular functions through interactions with protein partners have not been ruled out. In addition, it is not known whether the potentiation of α-syn toxicity by the presence of $LRRK2^{G2019S}$ is related solely to a cell-autonomous mechanism. Alternatively, LRRK2-expressing cells that surround DA neurons, especially microglial cells and astrocytes, could also play a role. Indeed, pharmacological interventions with LRRK2 inhibitors or pan-cellular knock out or transgenic animals expressing wild type LRRK2 or mutant LRRK2 did not allow differentiating between cell-autonomous versus non cell-autonomous mechanisms *in vivo*.
We have previously shown that the C-terminal domain of LRRK2 (ΔLRRK2) alone possessed a kinase activity that was significantly increased by the G2019S mutation. ΔLRRK2 fragments did not phosphorylate Rab10, a well-known substrate of full length LRRK2. ΔLRRK2 is therefore not expected to behave as the full length protein. However, it was sufficient to induce a significant neurodegeneration *in vivo* when it bore the G2019S mutation, 6 months after its overexpression in the SNpc via AAV vectors (Cresto et al. In press). In the present study, in order to precisely address the above questions in a relevant cellular context, we studied the effect of this C-terminal domain of LRRK2 harboring the G2019S mutation ($\Delta LRRK2^{G2091S}$) or its inactive form (mutations G2019S plus D1994A, named DK) $\Delta LRRK2^{DK}$ on the neurotoxicity of α-syn with the A53T mutation ($\alpha\text{-syn}^{A53T}$). For this purpose, we performed experiments using AAVs allowing the over expression of the different forms of ΔLRRK2 and $\alpha\text{-syn}^{A53T}$ alone or in combination in DA neurons of the SNpc in adult rats. Quantitative histological evaluation showed that while $\Delta LRRK2^{G2091S}$ alone produced no loss of DA neurons, it could significantly increase $\alpha\text{-syn}^{A53T}$-induced neurotoxicity. This effect was not seen with the inactive form $\Delta LRRK2^{DK}$.

Materials and methods

Viral construction and production

Adeno-associated viral vector (AAV). Plasmids constructs were packaged into AAV2/6 capsids as described previously (Berger et al. 2015). Briefly, viral particles were produced by co-transfection of HEK-293T cells with (1) an adenovirus helper plasmid (pXX6-80), (2) an AAV packaging plasmid carrying the rep2 and cap8 genes and (3) the AAV2 expression vector containing the transgene. 72 hours following transfection, recombinant vectors were purified and concentrated from cell lysate and supernatant by ultracentrifugation on an iodixaniol density gradient followed by dialysis against PBSMK (0.5 mM MgCl2 and 1.25 mM KCl in PBS). Concentration of the vector stocks was estimated by real-time-PCR following the method described by Aurnhammer et al. (Aurnhammer et al. 2012) and expressed as viral genomes per ml of concentrated stocks (Vg/ml). AAVs coding for ΔLRRK2 (WT, G2019S, and "kinase dead), $\alpha\text{-syn}^{A53T}$ and GFP were produced.

Stereotaxic injection

Adult Sprague-Dawley rats (Charles River Laboratories) weighing ~250 g were housed under a 12 h light/12 h dark cycle, with *ad libitum* access to food and water, in accordance with European Community (Directive 2010-63/EEC) and French (Code Rural R214/87-130) regulations. Experimental procedures were approved by the local ethics committee and registered with the French Research Ministry (committee #44, approval #12-100 and APAFIS#1372-2015080415269690v2). For stereotaxic injections, the animals were deeply anaesthetised with 4% isoflurane followed by a mixture of ketamine (75 mg/kg) and xylazine (5 mg/kg), and placed in a stereotaxic frame. Recombinant adeno-associated viral vectors were injected unilaterally into the substantia nigra, at the following stereotaxic coordinates: +3.4 mm anterior to the interaural zero and ±2.0 mm lateral to bregma, at a depth of -7.8 mm relative to the skull, with the tooth bar set at -3.3 mm. We injected 4 µl of virus at a concentration of $2.5x10^{10}$ viral particles per site for single injection and in case of co-injection, $2.5x10^{10}$ vg of each vectors were injected for a total of $5x10^{10}$ viral particles per site, with a 34-gauge blunt-tipped needle linked to a 10 µl Hamilton syringe by a polyethylene catheter, at a rate of 0.25 µl/min, with an automatic pump (CMA-4004). The needle was left in place for five minutes and was then slowly withdrawn.

Tissue processing

For all procedures, rats were first deeply anaesthetised by isoflurane inhalation followed by the intraperitoneal injection of a lethal dose of sodium pentobarbital.

For immunohistochemistry, rats were transcardially perfused with 300 ml of 4% paraformaldehyde in phosphate buffer at a rate of 30 ml/min. After perfusion, the brain of each rat was removed quickly and immersed in ice-cold 4% paraformaldehyde for at least 24 h, before transfer to 15% sucrose for 24 hours and then 30% sucrose the next day, for cryoprotection. The brains were then cut into 40 µm sections on a freezing microtome (CM1900, Leica, Germany). Serials sections of the striatum and midbrain were stored in antifreeze solution (30% sucrose, 30% ethylene glycol in PBS) until use.

Immunohistological analysis and quantification

Immunohistochemistry. The sections were removed from the antifreeze solution and washed in PBS. Endogenous peroxidase activity was quashed by transferring these sections to 1% H_2O_2 for 30 minutes at room temperature (RT) and washing them three times with PBS, for 10 min each. The sections were then blocked by incubation with 4.5% normal goat serum for 30 min in PBS-T (0.2% Triton X-100 in PBS) and they were then incubated overnight with primary antibody in 3% normal goat serum in PBS-T, at 4°C, with gentle shaking (anti-tyrosine hydroxylase (TH) antibody: MAB318 clone LNC1, 1:3000; AB152: 1:1000, anti-hemagglutinin tag (HA), Covance clone 11, 1:1000; anti-α-synuclein, syn 211, 1:1000; anti-phospho-α-synS129, 1:5000). The next day, these sections were removed from the primary antibody solution, washed three times and incubated for 1 hour at room temperature with the appropriate biotinylated secondary antibody in PBS-T (Vector Laboratories, Burlingame, CA, USA, 1:1000). The sections were then washed and incubated with ABC complex solution in PBS-T (1:250, reagents A and B combined in a 1:1 ratio, Vector Laboratories) for 1 h. The sections were then incubated with DAB for 30 s to 1 min and mounted on slides, in Eukitt mounting medium.

Cell counting. Optical fractionators sampling was carried out on a Zeiss microscope AxioPlan. Midbrain dopaminergic neurons were outlined on the basis of TH immunolabelling, with reference to a coronal atlas of the rat brain (Paxinos and Watson, 6th edition). TH-positive cells were counted by unbiased stereology in the entire SNpc and the number of positive neurons per section was calculated with Mercator Software (Explora Nova, France). We placed 100 × 100 µm grids in a systematic random manner, 80 × 80 µm apart, with a 3 µm offset from the surface of the section. Quantification was performed on twelve serial sections spaced by 200 µm corresponding to the entire SNpc.
The phosphorylation of the α-syn in S129 (P-α-syn^{S129}) was evaluated by counting using stereology methods the number of positive-neurons for P-α-syn^{S129} in the SNpc. The SNpc was delimited using the Nissl staining and grids (250 x 250 µm) were placed spaced by 100 x 100 µm. Quantification was performed on six serial sections spaced by 400 µm corresponding to the entire SNpc. In the striatum, a threshold was applied to select only the positive-immunostaining for P-α-syn^{S129} and the quantification was done on three slices corresponding to the beginning, the middle and the end of the striatum.

Immunofluorescence. The procedure used was similar to that for immunohistochemistry, but without the incubation in 1% H_2O_2. The primary antibodies used for the immunofluorescence procedure were the same than previously described (IBA1, Dako, 1:1000). On the first day, sections were incubated with the primary antibody overnight at 4°C. The next day, they were incubated with a fluorescent secondary antibody: Alexa Fluor 594-labeled goat anti-rabbit IgG or Alexa Fluor 488-labeled goat anti-rabbit IgG (1:1000, Life Technologies) for 1 hour at RT. The sections were then washed and incubated overnight at 4°C with another primary antibody. Finally, they were incubated with a second fluorescent secondary antibody, Alexa Fluor 488-labeled goat anti-mouse IgG or 594-labeled goat anti-mouse IgG (1:1000, Life Technologies) for 1 hour at room temperature. The sections were stained with DAPI, washed and mounted in a fluorescence mounting medium. Images were acquired with a laser confocal microscope (SP8, Leica, Germany) or an epifluorescence microscopy (DM8000, Leica, Germany).

Colocalization. The percentage of colocalization between ΔLRRK2 and α-syn was determined by counting the number of cells co-expressing both ΔLRRK2 and α-syn proteins divided by the number of cells expressing α-syn alone. Images were acquired with a laser confocal microscope (SP8, Leica, Germany). On the same acquisitions, the expression levels of ΔLRRK2 and α-syn proteins were evaluated on three coronal sections in the substantia nigra. Twenty cells co-expressing both ΔLRRK2 and α-syn proteins were delineated per animal using image J software and the mean fluorescence intensity in the red and in the green channels (corresponding to ΔLRRK2 and α-syn proteins respectively) was measured in each cell.

Fluorescence intensity measurement. Striatal dopaminergic innervation at 15 weeks was quantified by measuring the fluorescence intensity of TH-immunoreactive terminals on three coronal striatal sections. These sections were observed by epifluorescence microscopy at a magnification of 63X, and the fluorescence intensity was determined with MorphoStrider software (Explora Nova, France).

Microglia area measurement. The area occupied by microglia was evaluated by confocal microscopy at a magnification of 20X in the dorso-medial part of the striatum and in the SN *pars reticulata*. A threshold was applied and the area of twenty microglia cells was measured per acquisition. Three acquisitions per animal were used.

Statistical analysis
Data were analysed by two-tailed, one-way analysis of variance (ANOVA) performed with Statistica software (Statsoft Inc., Tulsa, Oklahoma, USA) and, when appropriate, LSD post-hoc correction for multiple comparisons was applied. Unpaired Student's T-tests were

performed for pairwise comparisons. The annotations used to indicate the level of significance are as follows: *p<0.05; **p<0.01; ***p<0.001.

Results

Determination of the experimental conditions to detect a potential synergy between AAV- α-syn^{A53T} and AAV-ΔLRRK2^{G2019S} toxicity

We investigated whether LRRK2 could increase the toxicity of α-syn in DA neurons through cell-autonomous mechanisms. For this reason, we chose to use AAVs that allow selective expression in neuronal cells and produce efficient transduction of a large volume of brain tissue thanks to their good diffusion properties. In our previous work (Cresto et al. In press), we showed that the C-terminal part of LRRK2^{G2019S} (ΔLRRK2^{G2019S} : 1330-2527 aa) retains, at least in part, the biochemical properties of full length LRRK2^{G2019S}, including an increased kinase activity in comparison to wild type fragment. In addition, we found that the overexpression of the C-terminal part of ΔLRRK2^{G2019S} with AAVs in the adult rat SNpc produced partial (~30%) but significant loss of DA neurons at 25 weeks post-infection, whereas the overexpression of the wild type form of LRRK2 (ΔLRRK2^{WT}) was not toxic. In the present study, we used a similar approach and, to optimize the ΔLRRK2 constructs, we extended the cloned fragments to insert the serine 1292 (aa 1283-2527) (Fig. 1, A). This residue has been shown to play a key role in LRRK2^{G2019S} toxicity (Sheng et al. 2012). Biochemical analysis of cells transfected with these LRRK2 constructs showed that all three fragments were expressed at similar levels (Fig.1, B).
We studied the effects of AAV-ΔLRRK2^{G2019S}, AAV-ΔLRRK2^{WT} and AAV-ΔLRRK2$^{G2019S/D1994A}$ alone at 15 weeks P.I.. Each AAV was injected unilaterally into the SNpc (2.5x10^{10} vg). In addition to the three experimental groups, a control group received injections of vehicle (PBS/pluronic acid). The integrity of the nigrostriatal pathway was assessed using unbiased stereology to count the number of DA neurons which displayed Tyrosine Hydroxylase (TH) staining in the injected part of the SNpc (Fig. 1, C). Observation at low-magnification revealed no major loss of TH-positive cells in the different groups injected with AAVs coding for LRRK2 fragments. The total number of TH-positive cells in the SNpc did not differ significantly between the control group (PBS) and AAV-ΔLRRK2^{WT}, AAV-ΔLRRK2^{G2019S} or AAV-ΔLRRK2$^{G2019S/D1994A}$ (Fig. 1, D). Thus, these results suggested that these ΔLRRK2 fragments alone did not trigger significant neurodegeneration of DA neurons at 15 weeks P.I..
Since we asked whether AAVs coding for different ΔLRRK2 constructs could increase the toxicity of AAV- α-syn^{A53T}, we searched for an injection protocol leading to mild degeneration, in such a way that a potential "protoxic" effect of ΔLRRK2 constructs could be easily detected. We conducted pilot experiments to determine the appropriate dose (titers) of AAV- α-syn alone that would lead to progressive and partial loss of DA neurons. These experiments showed that a significant loss of DA neurons (~30%) could be obtained at 12 and 15 weeks after the infection with AAV- α-syn^{A53T} (2.5x10^{10} particles) (Supplementary Fig. 1, A-B). We also observed the presence of pS129 α-syn and ThioS positive aggregates in the surviving neurons of the SNpc, indicating an abnormal processing of α-syn in these animals (Supplementary Fig. 1, C).
Thus, these results indicated that the co-infection protocol with AAV- α-syn^{A53T} and AAV-ΔLRRK2^{G2019S} and the evaluation of DA cell loss at 15 week P.I. were suitable to detect a potential synergy of toxicity between the two pathological transgenes.

Effects of the co-infection with AAV- α-syn^{A53T} and AAV-ΔLRRK2^{G2019S}

We next asked with this co-infection paradigm (with 2.5x10^{10} particles for each vector) whether the presence of the different LRRK2 fragments (wild type, G2019S and G2019S/D1994A) in DA neurons could modify the toxicity of α-syn^{A53T}.
We first studied the neurotoxic effects produced by AAV- α-syn^{A53T} in presence or absence of AAV-ΔLRRK2^{G2019S} at 15 weeks P.I.. We characterized the co-localization of α-syn^{A53T} and LRRK2 fragments in the SNpc after co-infection, since we aimed at investigating the combined effects of α-syn^{A53T} and different LRRK2 fragments in neurons. Analysis using confocal microscopy showed that α-syn expression in the SNpc was high in TH positive neurons (Fig. 2, A). In average, 70% of neurons co-expressed α-syn^{A53T} and LRRK2 fragments (Fig. 2, B).
We evaluated the toxic effects of α-syn^{A53T} in presence or in absence of AAV-ΔLRRK2^{G2019S}. The AAV-α-syn^{A53T} alone produced a significant 38% loss of TH-positive cells as measured by unbiased stereology in the SNpc at 15 week P.I. (mean count +/- SEM: Control, 12,344 +/- 734; AAV-α-syn^{A53T}, 7,555 +/- 527). The co-injection of AAV- α-syn^{A53T} with AAV-GFP (as a control of viral load) produced a loss of DA neurons similar to that obtained with AAV-α-syn^{A53T} alone (6,601 +/- 360). Of interest, the co-infection with AAV- α-syn^{A53T} and AAV-ΔLRRK2^{G2019S} produced a larger loss of DA neurons (Mean counts +/- SEM: 5,585 +/- 355) that was statistically significant (Fig 3, A). In both α-syn^{A53T}/GFP and α-syn^{A53T}/ΔLRRK2^{G2019S} groups, we evaluated the impact of SNpc cell loss on the level of dopaminergic terminals in the dorso-medial striatum using TH-immunofluorescence (Fig. 4, A). These measurements were performed in the dorsal striatum which receives projection from the injected SNpc region. In comparison to the control group (PBS), the TH immunoreactivity in the striatum was reduced by 15% in both α-syn^{A53T}/GFP and α-syn^{A53T}/ΔLRRK2^{G2019S} groups. This small α-syn^{A53T}-induced loss of TH-positive fibres was similar in the GFP and ΔLRRK2^{G2019S} groups (Fig. 4, C).
We also counted the number of SNpc cells showing P-α-synS129 immunoreactivity in the different groups, a marker of an abnormal processing of α-syn (Fig. 3, C). The number of P-α-synS129 –positive cells was significantly lower in the group co-infected with AAV-α-syn^{A53T} and AAV-ΔLRRK2^{G2019S} than that of the groups infected with AAV-α-syn^{A53T} alone or in combination with AAV-GFP (Fig. 3, D). The P-α-synS129 immunoreactivity was also evaluated in the striatum and, consistent with the results obtained in the SNpc, we found lower

levels of aggregated α-syn in the striatum of rats co-infected with AAV-α-syn^{A53T} and AAV-ΔLRRK2^{G2019S} than in rats infected with AAV-α-syn^{A53T} / GFP (Fig. 3, E-F).

Differential effects of AAV-ΔLRRK2^{G2019S} and AAV-ΔLRRK2$^{G2019S/D1994A}$ on AAV-α-syn^{A53T} toxicity

We next investigated whether the effect of AAV-ΔLRRK2^{G2019S} on AAV-α-syn^{A53T}-induced toxicity was dependent on the kinase activity of the LRRK2 construct. To address this question, we compared the effects of ΔLRRK2^{G2019S} with those of the kinase dead form ΔLRRK2^{DK}. In these experiments, we chose an earlier time point P.I. (6 weeks).
We first compared the levels of transgene expression after infection with α-syn^{A53T} and AAV-ΔLRRK2^{G2019S} or AAV-ΔLRRK2^{DK}. Quantitative immunofluorescence analyses showed that almost the entire SNpc was infected by the AAV-α-syn^{A53T} when co-infected with either AAV-ΔLRRK2^{G2019S} or AAV-ΔLRRK2^{DK} (Fig. 5). We also re-evaluated the co-localisation of LRRK2-related transgenes and α-syn^{A53T} (Fig. 6). Results showed that 76% of neurons expressed both α-syn^{A53T} and ΔLRRK2 (Fig. 6, C), a result consistent with what we observed in the experiments described above (see Fig. 2). At higher magnification, we evaluated the level of fluorescence intensity corresponding to ΔLRRK2-HA staining. The results showed that ΔLRRK2^{G2019S} and ΔLRRK2^{DK} were expressed at the same level in SNpc neurons (Fig. 6, C). In addition, we found that the α-syn^{A53T} protein was expressed at the same levels in neurons co-expressing ΔLRRK2^{G2019S} and ΔLRRK2^{DK} (Fig. 6, C).
We then assessed the loss of DA neurons produced by AAV- α-syn^{A53T} when co-injected with either AAV-ΔLRRK2^{G2019S} or AAV-ΔLRRK2^{DK}. Results indicated that the loss of DA neurons induced by α-syn^{A53T} was significantly lower in presence of ΔLRRK2^{DK} than that in presence of ΔLRRK2^{GS} (Fig. 7, A-B). The number of cells with P-α-synS129 immunoreactivity was similar in the ΔLRRK2^{DK} and ΔLRRK2^{G2019S} groups (Fig. 7, C-D).
Finally, because of the role of neuroinflammation in neurodegeneration observed in α-syn^{A53T} models, we evaluated at this early time point (6 weeks P.I.) the status of microglial cells with immunohistochemistry using a validated marker of these glial cells, Iba1. Quantifications in the SN and in the striatum showed that, while α-syn^{A53T} alone produced microglial activation, ΔLRRK2^{G2019S} and ΔLRRK2^{DK} did not have any impact on the microglial activation induced by the mutant α-syn (supplementary Fig. 2).
Thus, these results indicated that the synergistic effect of ΔLRRK2^{G2019S} on the toxicity of α-syn^{A53T} towards DA neurons depends on its kinase activity.

Discussion

The mechanisms leading to the degeneration of DA neurons in PD patients carrying mutations of the *LRRK2* gene are unknown. It is generally established that LRRK2^{G2019S} leads to an increased kinase activity and that this abnormally increased kinase activity would lead to cell death (Greggio et al. 2006; Lee et al. 2010; Smith et al. 2006; West et al. 2007). Moreover, we have previously shown that the C-terminal domain of LRRK2 alone was sufficient to observe the toxic effect of the G2019S mutant in the SNpc of rats, 6 months after its overexpression in the SNpc via AAV vectors (Cresto et al. In press). In addition, a role of α-syn in LRRK2^{G2019S} toxicity has been suggested (Bieri et al. 2019; Daher et al. 2014, 2015; Lin et al. 2009; Novello et al. 2018). Indeed, neuropathological evaluation of the brain of PD patients with LRRK2 mutations shows the presence of bona fide LBs and Lewy neurites (Giasson et al. 2006). However, the specific role of the kinase activity in the crosstalk between LRRK2 and α-syn is controversial. In other words, how the kinase activity of LRRK2^{G2019S} mutation modulates α-syn neurotoxicity in the SNpc is unknown.
In the present work, we used an AAV approach to selectively target SNpc DA neurons and investigated how the C-terminal domain of LRRK2 harboring the G2019S mutation with increased kinase activity could modify the loss of DA neurons produced by overexpression of α-syn^{A53T} in the rat SNpc. In our experimental conditions, AAV-ΔLRRK2^{G2019S} alone did not produce loss of DA neurons and AAV-α-syn^{A53T} alone produced a partial loss of these cells. We found that the loss of DA cells produced by co-expression of ΔLRRK2^{G2019S} and α-syn^{A53T} was significantly higher than that measured in rats infected with AAV-α-syn^{A53T} alone or co-injected with a control vector (AAV-GFP). Conversely, overexpression of the inactive "kinase dead" form ΔLRRK2^{DK} at cellular levels similar to those of ΔLRRK2^{G2019S} did not change the toxicity of α-syn^{A53T}. These novel findings are further in support of the hypothesis that the C-terminal domain of LRRK2^{G2019S} augments the toxic effects of α-syn^{A53T} through the catalytic activity of its kinase domain.
The histological evaluation we performed after infection of the SNpc with AAV- α-syn^{A53T} and AAV-ΔLRRK2^{G2019S} showed that both transgenes were overexpressed in DA neurons. In both cases, approximately 70% of the SNpc was infected. After co-infection, co-localization of both transgenes was found in a majority of neurons in the SNpc. Neuropathological evaluation at 15 weeks after infection with AAV- α-syn^{A53T} indicated partial loss of DA neurons based on detection of TH-positive cells. This likely reflects neuronal loss, although it cannot be totally ruled out that, at least in part, the loss of TH-immunoreactivity is due to a marked reduction of the expression of this dopamine synthesis enzyme in absence of actual cell death. Cell count using other dopamine markers (e.g. VMAT) and cell staining (e.g. Nissl staining) may help to address this point.
The relevance of overexpressing the C-terminal domain of LRRK2 as compared to the full length protein is debatable. Indeed, ΔLRRK2^{G2019S} lacks N-terminal domains that are known to play crucial roles in LRRK2 function. As discussed elsewhere (Cresto et al. In press), biochemical characterization of ΔLRRK2^{G2019S} and ΔLRRK2^{WT} indicated that this LRRK2 fragment retains properties of full length LRRK2, including the ability to dimerize and the increase in kinase activity when the fragment harbors the G2019S substitution. However, we could not observe any phosphorylation of Rab10 by ΔLRRK2, indicating that the N-terminal part of LRRK2 is required for the phosphorylation of this particular substrate (Cresto et al. In press). Thus, it is conceivable that overexpression of ΔLRRK2^{G2019S} compared

to ΔLRRK2^{WT} leads to abnormal/increased phosphorylation of certain substrates, that at least in part are common with those of full length LRRK2, but it is not expected to behave exactly as the full length protein (Deng et al. 2008; Gloeckner et al. 2006; Greggio et al. 2008; Ito et Iwatsubo 2012). The increase of ΔLRRK2 kinase activity with the G2019S mutation could still produce cellular alterations and eventually death of neurons. Supporting this hypothesis, we previously showed that overexpression of the ΔLRRK2^{G2019S} fragment using AAVs triggers neurodegeneration of DA neurons at six month post-infection while the ΔLRRK2^{WT} fragment, expressed at similar high levels, was devoid of obvious neurotoxicity (Cresto et al. In press).

The advantage of the present AAV models, compared to the other existing transgenic models is that we could address the question of the potential exacerbation of α-syn^{A53T} toxicity by the kinase activity of LRRK2 directly in the SNpc (Melrose et al. 2010; Ramonet et al. 2011). We could directly investigate whether a functional interaction existed between AAV-α-syn^{A53T} and-ΔLRRK2^{G2019S} in DA neurons. Our results confirmed the existence of this interaction, since the overexpression of ΔLRRK2^{G2019S} significantly enhanced α-syn^{A53T} neurotoxic effects in the rat SNpc. Using transgenic animals, Lin and collaborators showed that the overexpression of LRRK2 (wild type or G2019S) in forebrain neurons (striatum and cerebral cortex) increased the toxicity of α-syn^{A53T} (Lin et al. 2009). In these double transgenic mice, significant degeneration of the striatum and cortex, and enhanced accumulation of α-syn aggregates were found. For technical reasons pathological transgenes were not expressed in the SNpc and no degeneration of DA was detected in these models. Probably, the CamKIIα promoter used to drive the expression of the tetracycline transactivator (tTA) that activates the TetO promoter of LRRK2 and α-syn^{A53T} transgenes in these mice is not active in SNpc DA neurons, since endogenous expression of CamKIIα in neurons of the SNpc is low compared to that seen in forebrain neurons. In LRRK2 knockout rats, the toxicity produced by AAV coding for α-syn is lower than that in wild type rats (Daher et al. 2015). Using crossbreeding of other transgenic models in which promoters driving LRRK2^{G2019S} and α-syn^{A53T} expression were different (Prion and CMV respectively), Daher and colleagues found no synergy between the transgenes (Daher et al. 2012). These observations and our present results suggest that the synergy between LRRK2 and α-syn may require expression of the two proteins in the same neurons to occur. Further supporting this view, we found that in our experimental set up, the co-expression of ΔLRRK2^{G2019S} and α-syn^{A53T} did not lead to more microglial activation than the expression of α-syn^{A53T} alone. Thus our results indicate that the synergy between LRRK2 and α-syn depends, at least in part, on cell-autonomous mechanisms. However, this does not rule out that in patients and other animal models, non-cell autonomous mechanisms could be also involved in the increased vulnerability of brains to α-syn when mutant LRRK2 is expressed in neurons and glial cells. For example, it has been recently shown that seeding of α-syn aggregates by exposure of neurons to α-syn fibrils is increased in neurons expressing mutant LRRK2 (Volpicelli-Daley et al. 2016; Bieri et al. 2019). The levels of LRRK2 activity in microglial cells may also regulate protoxic phenomenon associated with α-syn induced neuroinflammation (Daher et al. 2014; Maekawa et al. 2016; Russo, Bubacco, et Greggio 2014).

The neuronal mechanisms underlying the synergy between LRRK2 and α-syn are ill-defined. In particular, the exact role of the kinase domain of LRRK2 is unclear. It is generally accepted that the increased kinase activity of LRRK2^{G2019S} compared to wild type LRRK2, through increased phosphorylation of substrates, leads to neurodegeneration possibly through multifactorial cellular changes including disruption of microtubule assembly, mitochondrial defects, and alterations in protein translation (Rosenbusch and Kortholt 2016). However, the hypothesis of a key role of the increased kinase activity of LRRK2 mutations remains controversial. As already mentioned above, different transgenic rodent models expressing LRRK2^{G2019S} have been developed and extensively characterized. These models display no (or very limited) degeneration of DA cells in the SNpc. In fact, there exists no transgenic models which express very high levels of LRRK2^{G2019S} in the SNpc. The apparent lack of toxicity of LRRK2^{G2019S} in the SNpc is likely to be explained by the low level of expression of the transgene in transgenic models, since compelling evidence obtained from different experimental approaches clearly demonstrates that the higher the expression of LRRK2^{G2019S} is, the more severe the resulting toxicity gets. There exist rare evidence obtained *in vivo* that show a relationship between the increase kinase activity of LRRK2^{G2019S} and neurotoxicity. In the studies using HSV and adenovirus models (Dusonchet et al. 2011; Lee et al. 2010), as well as in our previous study with AAV-ΔLRRK2^{G2019S} (Noemie Cresto et al. In press), the overexpression of LRRK2^{G2019S} (or ΔLRRK2^{G2019S}) in the SNpc was found to produce a loss of DA neurons whereas the infection with wild type LRRK2 produced no toxicity.

Only a few studies addressed directly the role of the kinase in the interaction between α-syn and LRRK2 toxicity. It was shown that neuroinflammation and neurodegeneration produced by the infection of the SNpc with AAV-α-syn is significantly attenuated in LRRK2 KO rats compared to wild type littermates. In these experiments, the role of the kinase activity was not assessed (Daher et al. 2014). More recently, Daher showed that the toxicity of AAV-α-synuclein in the SNpc was higher in transgenic LRRK2^{G2019S} rats than in wild-type rats. Interestingly, in both genotypes, the treatment with the LRRK2 inhibitor PF-06447475 (PF) reduced the toxicity of α-syn (Daher et al. 2015). This suggested that the exacerbation of α-syn toxicity by LRRK2^{G2019S} could result from the increased catalytic activity of the kinase. However, LRRK2 inhibitors, including PF, produce destabilization of LRRK2, leading to reduced cellular levels of the protein (Lobbestael et al. 2016). Thus, protection by PF against combined α-syn/ LRRK2^{G2019S} toxicity could result from the reduction in LRRK2 levels rather that from actual inhibition of the catalytic activity of the kinase. In the present experiments, we found that whereas expression of ΔLRRK2^{G2019S} increased the toxicity of AAV-α-syn^{A53T} towards DA neurons, the overexpression of the inactive protein ΔLRRK2$^{G2019S/D1994S}$ produced no change towards the toxicity AAV-α-syn^{A53T}. In our experiments, we could check that the difference between the toxicity of ΔLRRK2^{G2019S} and that of ΔLRRK2^{DK} was not related to a difference in protein expression levels. Quantitative confocal analysis indicated that the levels of expression of the two proteins were similar in DA neurons *in vivo*. Thus, it is likely that the difference of effects between ΔLRRK2^{WT} and ΔLRRK2^{G2019S} mainly resides in their different kinase activities.

In conclusion, the present study suggests that the presence of the C-terminal part of LRRK2 with the G2019S mutation can potentiate the toxicity of α-syn^{A53T} in DA neurons *in vivo* and that this effect is kinase-dependent. Our "double hit" model in rats, which is relatively

simple to develop and handle, might be of interest to directly test the efficacy of new pharmacological or molecular therapies targeting LRRK2 and/or α-syn.

Figures

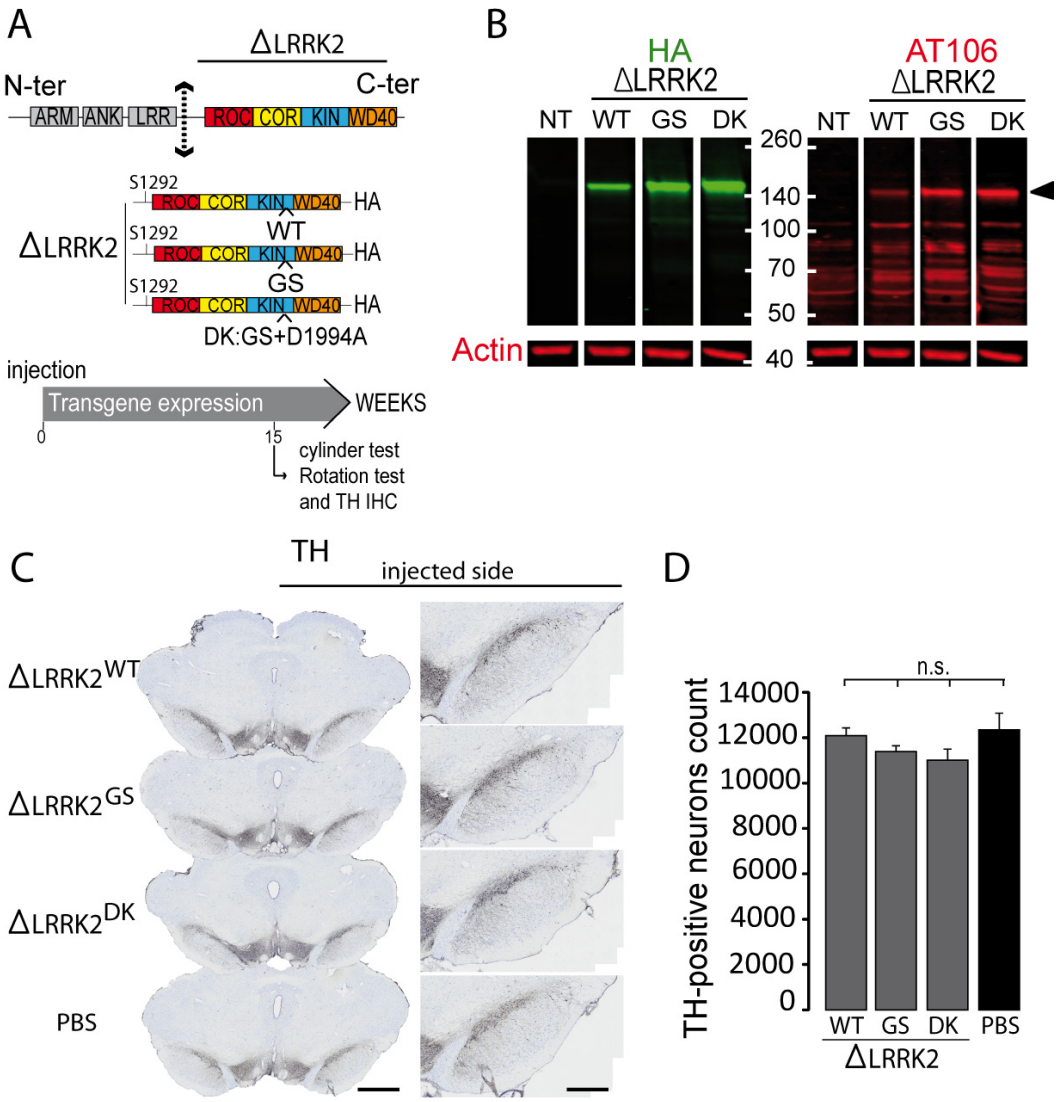

Figure 1: Immunohistochemistry for Tyrosine hydroxylase (TH) at 15 weeks P.I.. (A) The C-terminal fragment of LRRK2 called ΔLRRK2 was generated in different forms, WT, G2019S or dead kinase (DK). (B) Biochemical analysis of cells transfected with these ΔLRRK2 showed that all three fragments were expressed at similar levels (C-D) These fragments were cloned into an AAV and unilaterally injected into the rat SNpc. Fifteen weeks post-injection, TH immunohistochemistry was performed. The number of TH-positive neurons was evaluated by stereology, revealing no obvious toxicity of the LRRK2 fragments at 15 weeks post-infection. n=10 animal/group. ANOVA and PLSD *post hoc* test. n.s., not significant. Scale bar: 750µm, 400µm.

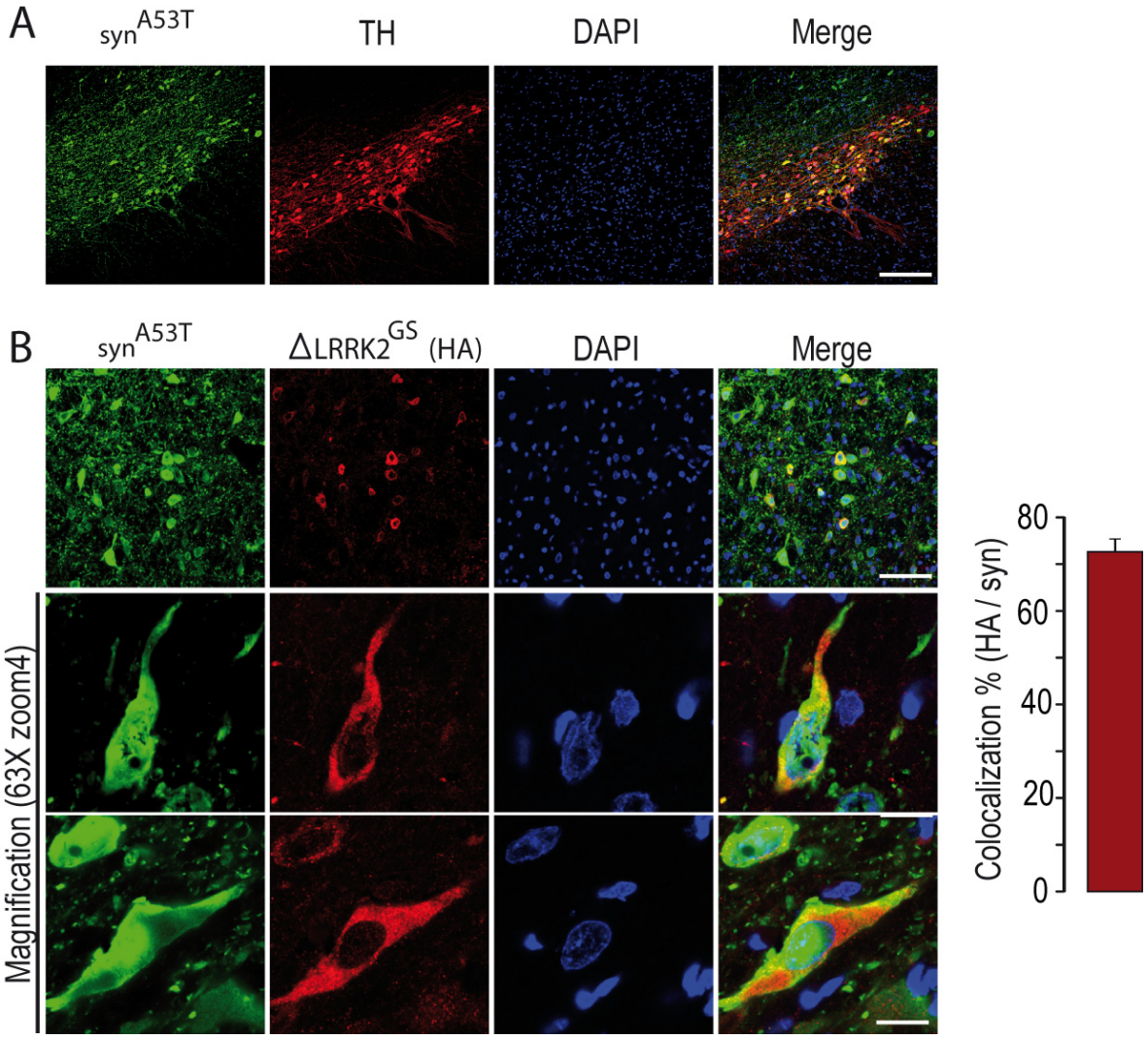

Figure 2: Histological evaluation of transgenes expression in the SNpc at 15 weeks P.I.. (A) The transduction of α-syn (in green) was evaluated in the SNpc. A TH staining, in red, was used to identify DA neurons. Scale bar: 500 µm. (B) The number of neurons expressing both α-syn and ΔLRRK2^{G2019S} was measured, higher magnification showed the cytoplasm localization of ΔLRRK2^{G2019S}. Scale bar 40X: 60 µm , 63X zoom 4: 10 µm.

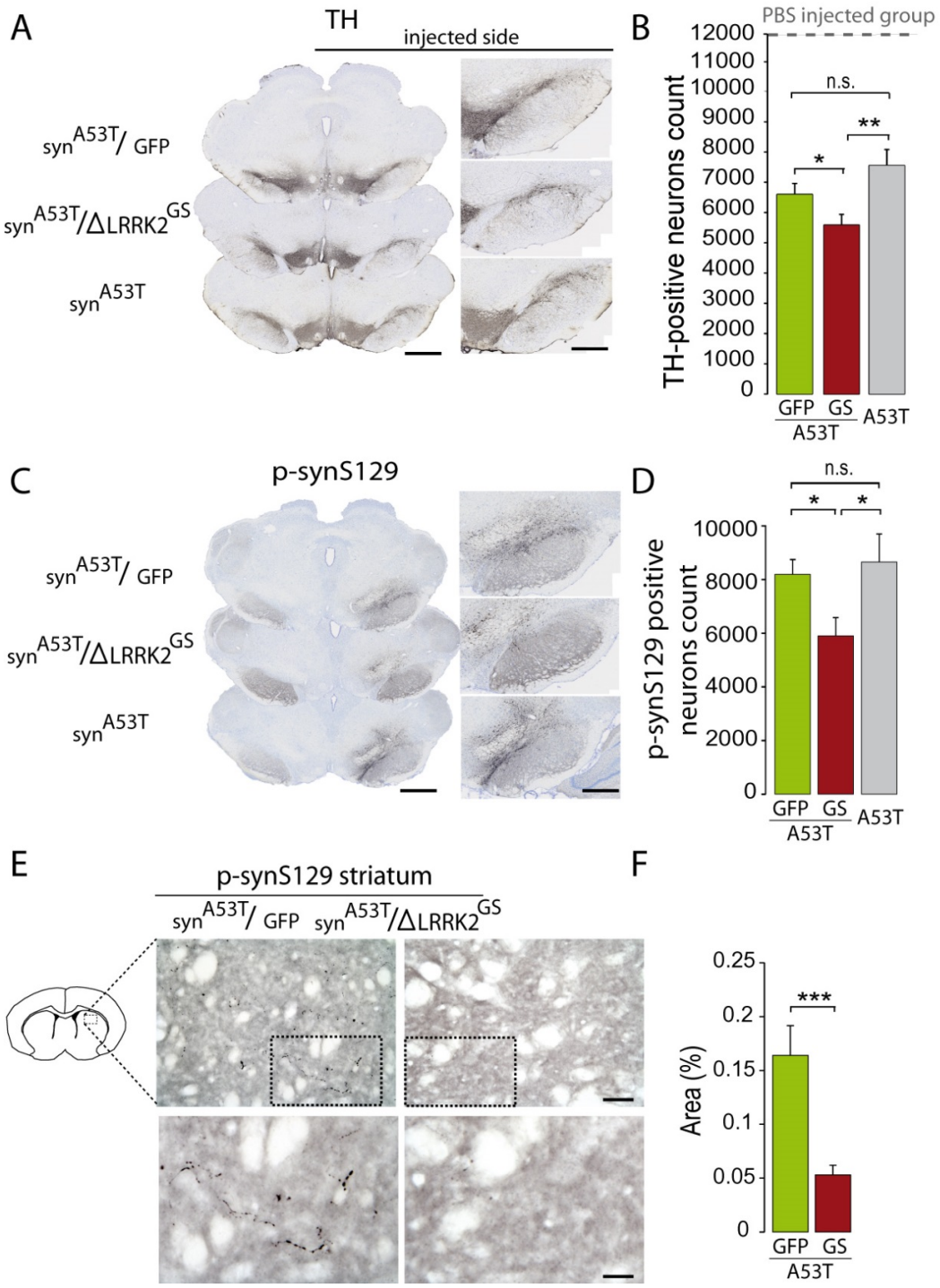

Figure 3: Immunohistochemistry for Tyrosine hydroxylase (TH) and phospho-α-synS129 aggregates at 15 weeks P.I.. (A-D) The number of TH-positive and P-α-synS129-positive neurons was evaluated by stereology in the SNpc. Scale bar: 750 µm, 400 µm (E-F) The percentage of area occupied by the P-α-synS129-positive staining was measured in the striatum at 15 weeks P.I.. n=10 animal/group. ANOVA and PLSD post hoc test. *, P<0.05; ***, P<0.001. Scale bar: 200 µm, 50 µm.

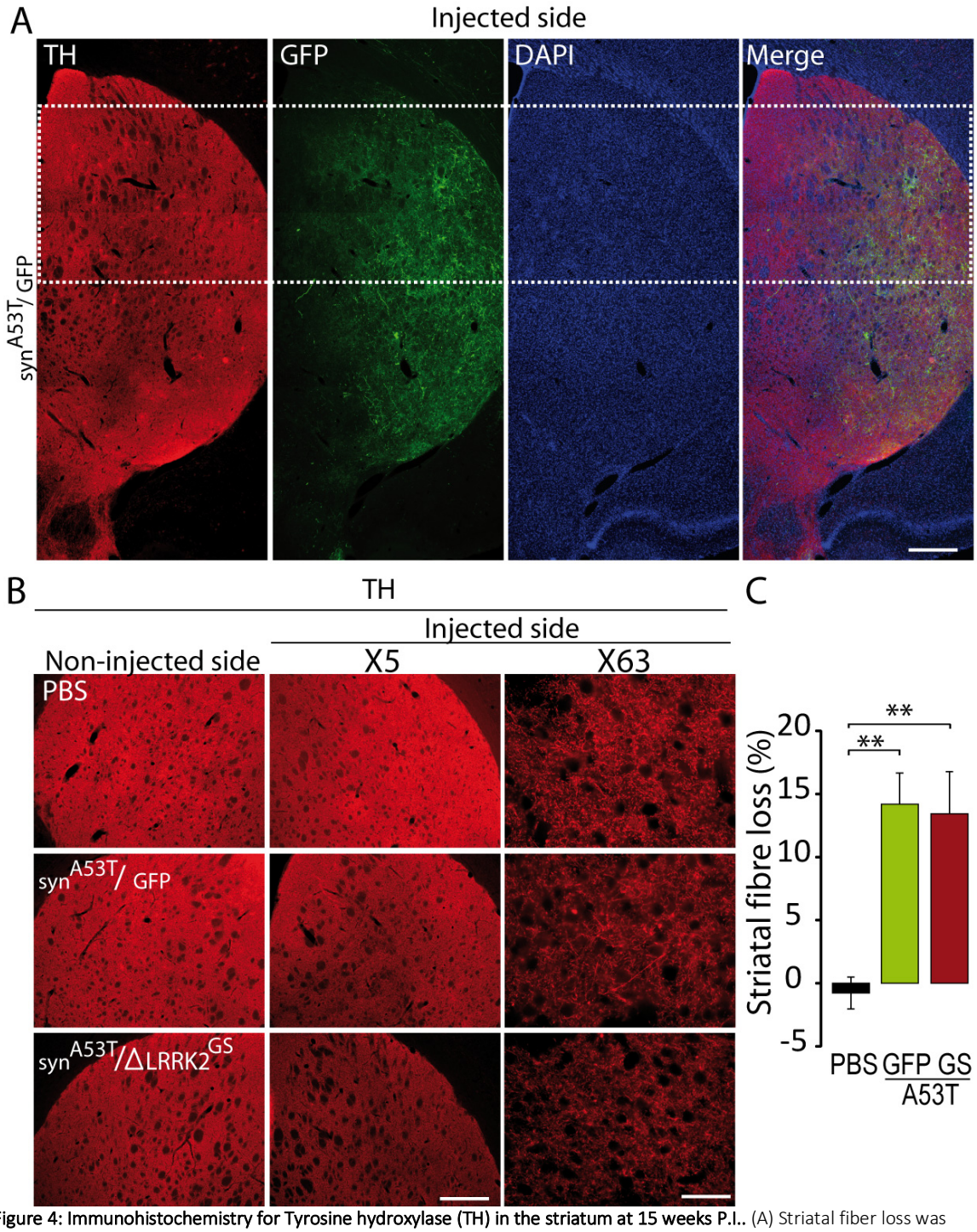

Figure 4: Immunohistochemistry for Tyrosine hydroxylase (TH) in the striatum at 15 weeks P.I.. (A) Striatal fiber loss was evaluated in the dorso-medial striatum using TH-immunofluorescence. Scale bar: 1000µm. (B-C) The mean grey value was quantified at the magnification X5. n=10 animal/group. ANOVA and PLSD post hoc test. **, P<0.01 (A-B) scale bar: 1000µm. (B-C) scale bar: 100µm.

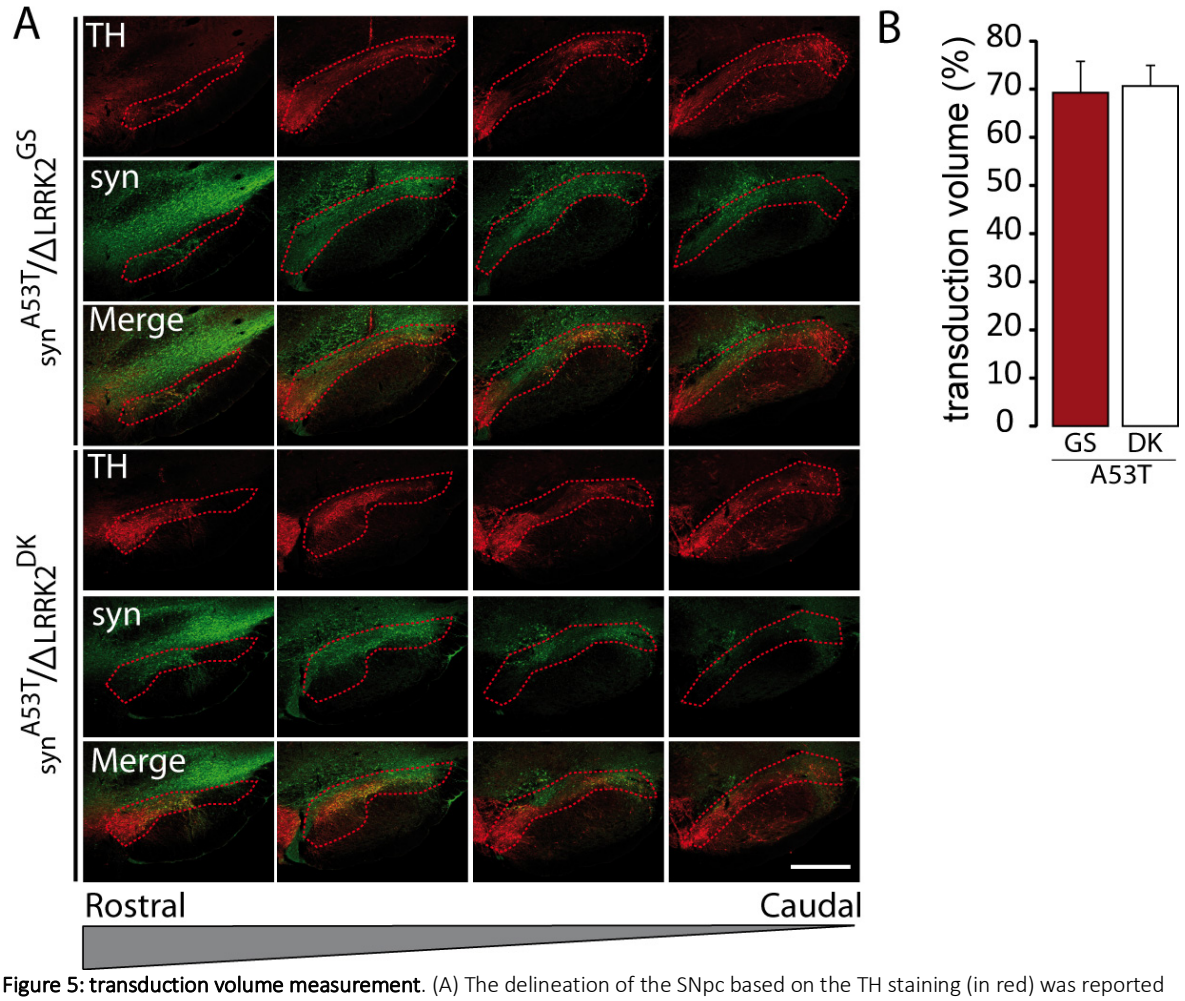

Figure 5: transduction volume measurement. (A) The delineation of the SNpc based on the TH staining (in red) was reported on the green channel corresponding to the α-syn protein to evaluate the transduced volume of the SNpc. Scale bar: 1000µm. (B) The quantification was done on the entire SNpc. n=8 animal/group.

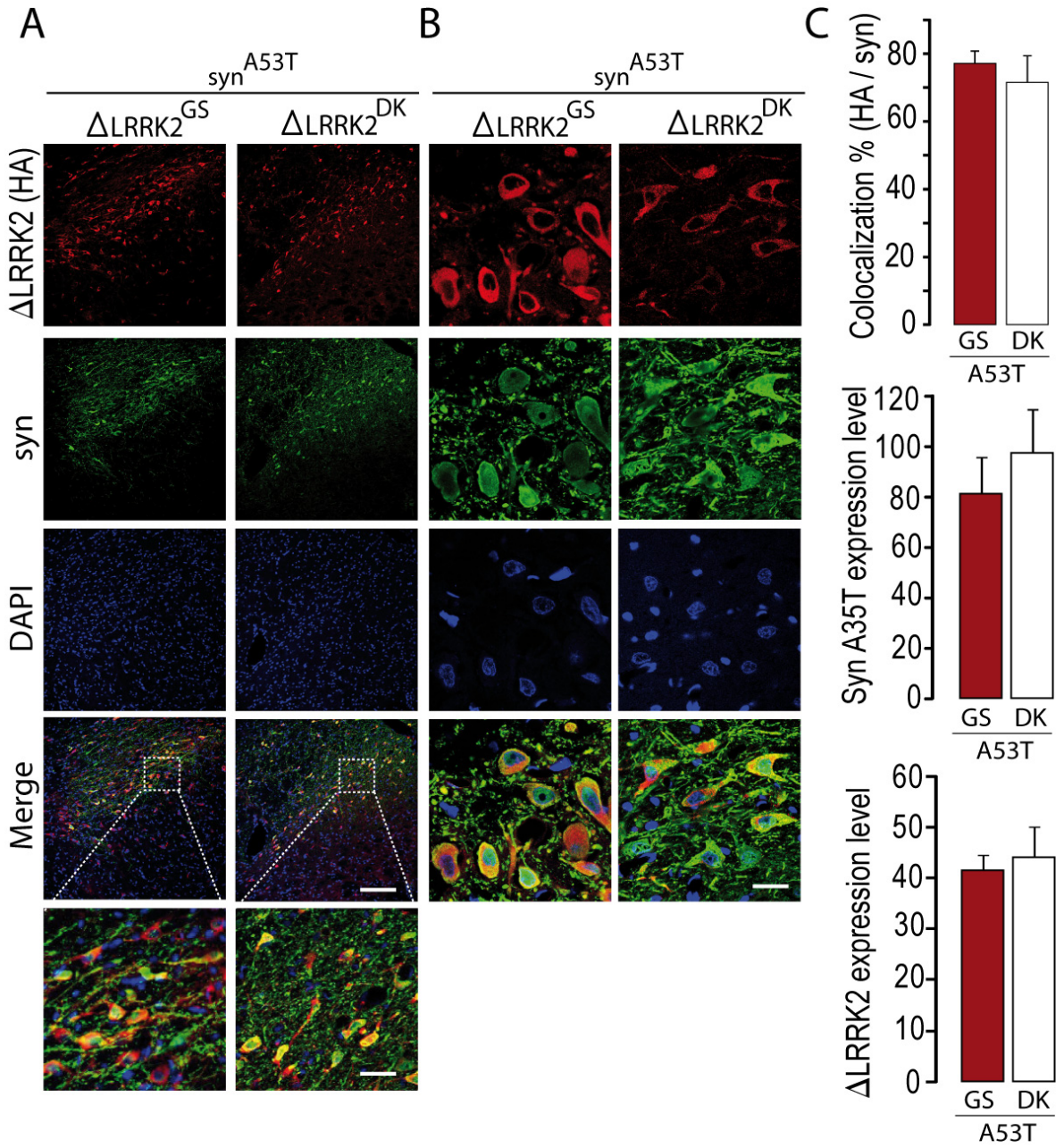

Figure 6: Colocalization and expression level. (A-B) At low and high-magnification, double immuno-fluorescence against HA (ΔLRRK2) and α-syn, showed that the majority of cells co-expressed both transgenes at similar levels. Scale bar: 200 µm, magnifications: 50 µm, 10µm. (C) The percentage of colocalization, and protein expression levels (mean grey fluorescence) were quantified in the different groups. n=8 animal/group.

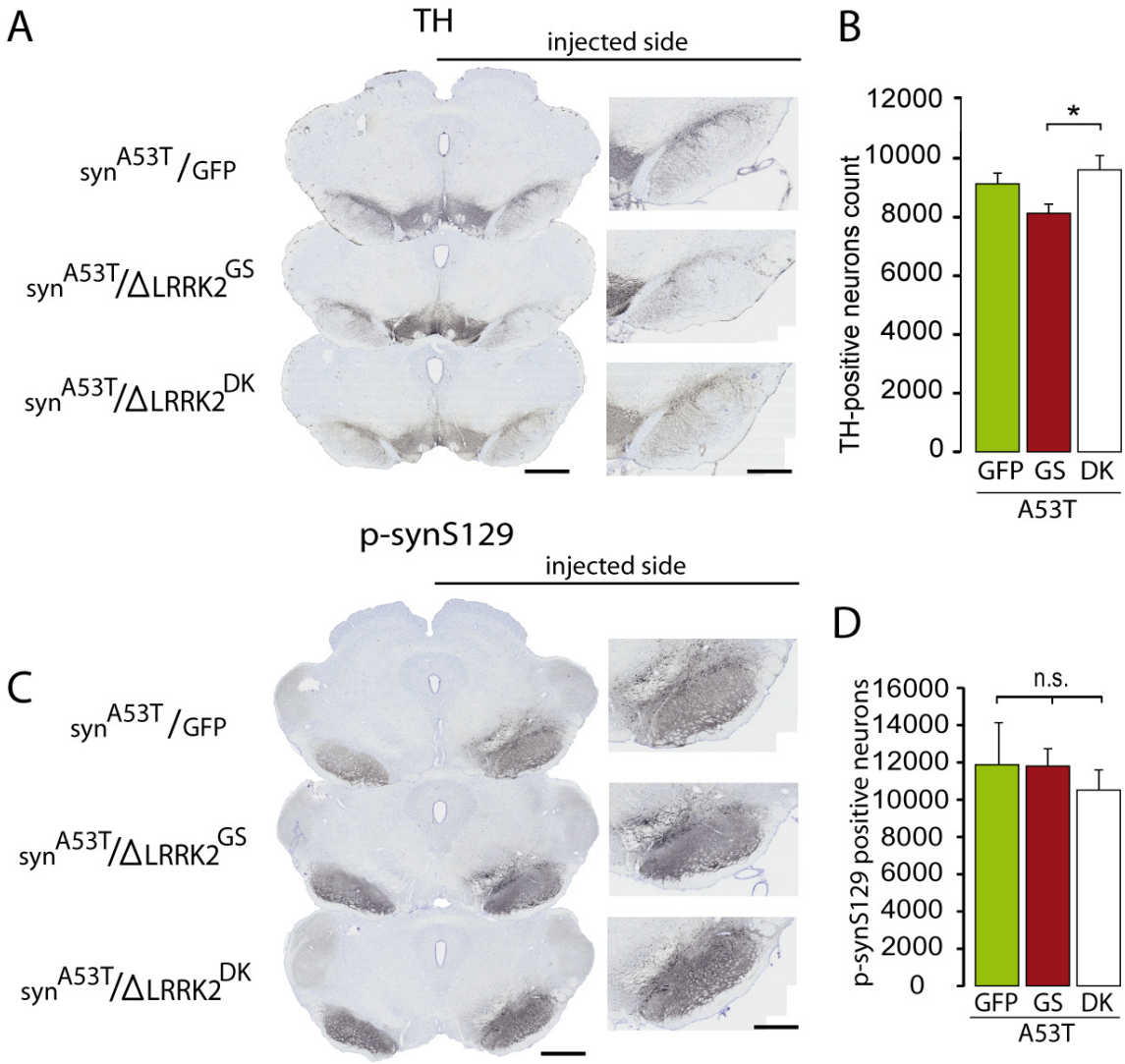

Figure 7: Immunohistochemistry for Tyrosine hydroxylase (TH) and phospho-α-synS129 aggregates at 6 weeks post-infection. (A-D) The numbers of TH-positive and P-α-synS129-positive neurons were evaluated by stereology in the SNpc. n=10 animal/group. ANOVA and PLSD post hoc test. P<0.05. Scale bar: 750µm, 400µm

Supplementary figures

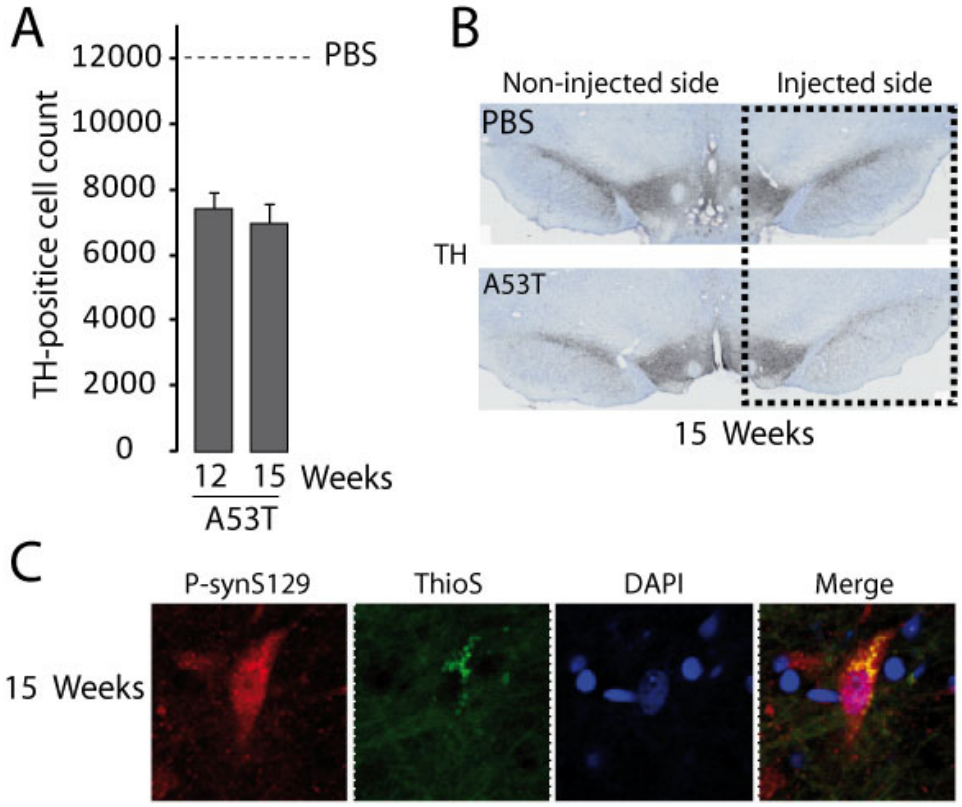

Supplementary Figure 1. Results of the pilot experiments carried out to set up the AAV-α-synA53T model characterized by partial degeneration of DA neurons in the SNpc of adult rats. AAV-α-syn^{A53T} was injected in the SNpc of rats. (A-B) Stereological count of the number of DA neurons in the SNpc, 12 and 15 weeks P.I.. (C) The presence of P-αsynS129 and thioflavin S positive aggregates was evaluated at 15 weeks P.I..

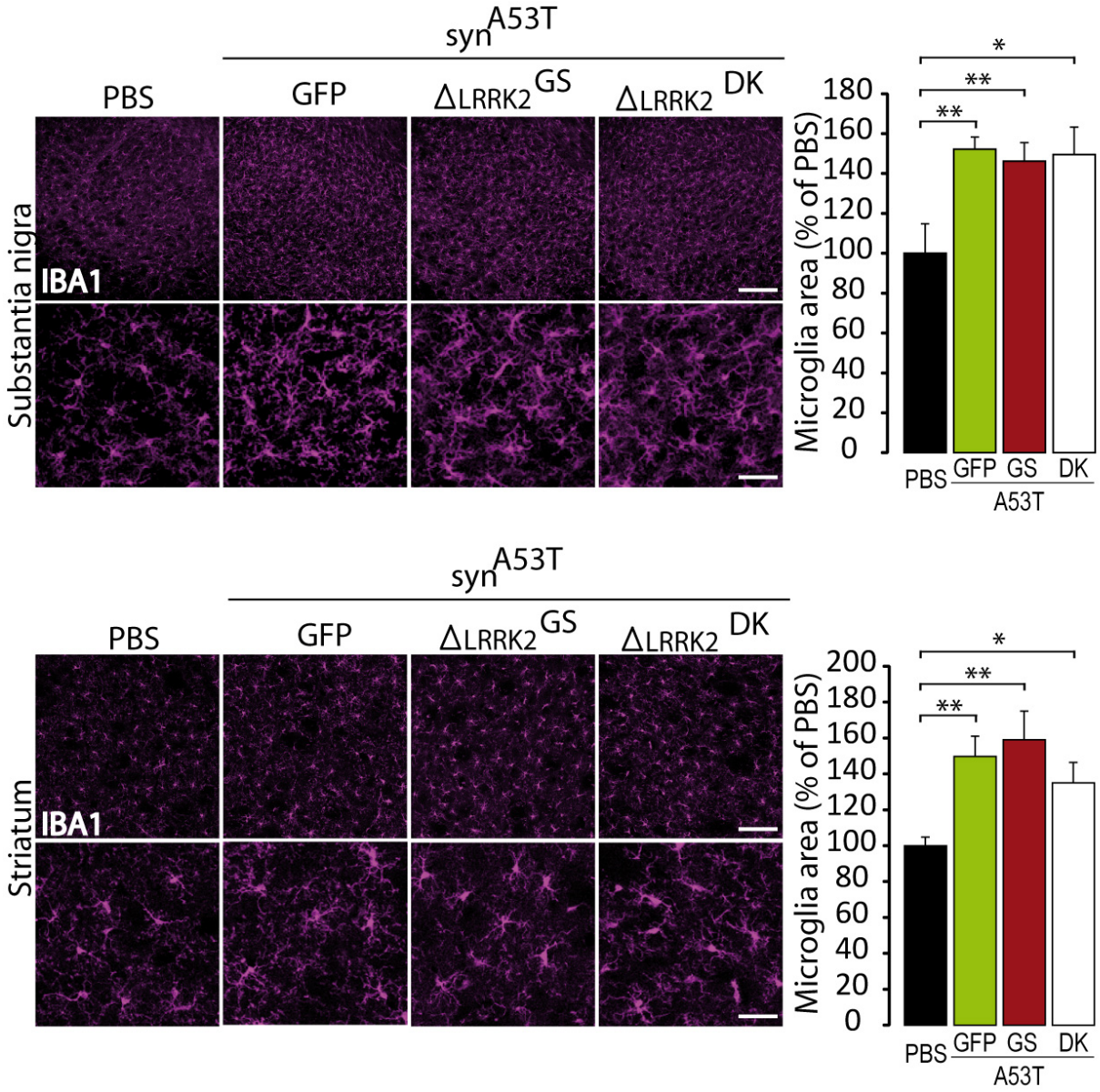

Supplementary Figure 2. (A-B) The microglial activation (microglia area) was evaluated based on the IBA1 staining in the SNpc and in the striatum (C-D). Results were expressed as percentage of control group (PBS). n=8 animal/group. ANOVA and PLSD post hoc test. P<0.05. Scale bar: 200 µm, magnifications: 50 µm.

Acknowledgements

This work was funded by rolling grants from the CEA and the CNRS.
The research generating these results received funding from la Fondation de France (AAP 2010, Engt 00016819 and AAP 2014, Engt 2014-0052580). Noemie Cresto is a recipient of a PhD fellowship from Association France Parkinson (2016).
This work benefited from a support from the national "Translational Research Infrastructure for Biotherapies in Neurosciences" (NeurATRIS, "Investissement d'Avenir", ANR-11-INBS-0011).

Conflict of Interest Statement

All authors declare that they have no conflict of interest

References

Aurnhammer, Christine, Maren Haase, Nadine Muether, Martin Hausl, Christina Rauschhuber, Ingrid Huber, Hans Nitschko, et al. 2012. « Universal Real-Time PCR for the Detection and Quantification of Adeno-Associated Virus Serotype 2-Derived Inverted Terminal Repeat Sequences ». *Human Gene Therapy Methods* 23 (1): 18‑28. https://doi.org/10.1089/hgtb.2011.034.

Berger, Adeline, Stéphanie Lorain, Charlène Joséphine, Melissa Desrosiers, Cécile Peccate, Thomas Voit, Luis Garcia, José-Alain Sahel, et Alexis-Pierre Bemelmans. 2015. « Repair of Rhodopsin mRNA by Spliceosome-Mediated RNA Trans-Splicing: A New Approach for Autosomal Dominant Retinitis Pigmentosa ». *Molecular Therapy* 23 (5): 918‑30. https://doi.org/10.1038/mt.2015.11.

Bieri, Gregor, Michel Brahic, Luc Bousset, Julien Couthouis, Nicholas J. Kramer, Rosanna Ma, Lisa Nakayama, et al. 2019. « LRRK2 Modifies α-Syn Pathology and Spread in Mouse Models and Human Neurons ». *Acta Neuropathologica* 137 (6): 961‑80. https://doi.org/10.1007/s00401-019-01995-0.

Biskup, Saskia, et Andrew B. West. 2009. « Zeroing in on LRRK2-linked pathogenic mechanisms in Parkinson's disease ». *Biochimica et Biophysica Acta (BBA) - Molecular Basis of Disease*, Parkinson's Disease, 1792 (7): 625‑33. https://doi.org/10.1016/j.bbadis.2008.09.015.

Braak, H., et E. Braak. 2000. « Pathoanatomy of Parkinson's Disease ». *Journal of Neurology* 247 (2): II3‑10. https://doi.org/10.1007/PL00007758.

Brockmann, Kathrin, Adriane Gröger, Adriana Di Santo, Inga Liepelt, Claudia Schulte, Uwe Klose, Walter Maetzler, et al. 2011. « Clinical and Brain Imaging Characteristics in Leucine-Rich Repeat Kinase 2-Associated PD and Asymptomatic Mutation Carriers ». *Movement Disorders: Official Journal of the Movement Disorder Society* 26 (13): 2335‑42. https://doi.org/10.1002/mds.23991.

Chartier-Harlin, Marie-Christine, Jennifer Kachergus, Christophe Roumier, Vincent Mouroux, Xavier Douay, Sarah Lincoln, Clotilde Levecque, et al. 2004. « Alpha-Synuclein Locus Duplication as a Cause of Familial Parkinson's Disease ». *Lancet (London, England)* 364 (9440): 1167‑69. https://doi.org/10.1016/S0140-6736(04)17103-1.

Cresto, Noémie, Camille Gardier, Francesco Gubinelli, Marie-Claude Gaillard, Géraldine Liot, Andrew B. West, et Emmanuel Brouillet. 2019. « The Unlikely Partnership between LRRK2 and α-Synuclein in Parkinson's Disease ». *The European Journal of Neuroscience* 49 (3): 339‑63. https://doi.org/10.1111/ejn.14182.

Cresto, Noemie, Marie-Claude Gaillard, Camille Gardier, Francesco Gubinelli, Elsa Diguet, Déborah Bellet, Laurine Legroux, et al. In press. « The C-terminal domain of LRRK2 with the G2019S mutation is sufficient to produce neurodegeneration of dopaminergic neurons in vivo ». *Neurobiology of Disease*, Sous presse.

Daher, João P. L., Hisham A. Abdelmotilib, Xianzhen Hu, Laura A. Volpicelli-Daley, Mark S. Moehle, Kyle B. Fraser, Elie Needle, et al. 2015. « Leucine-Rich Repeat Kinase 2 (LRRK2) Pharmacological Inhibition Abates α-Synuclein Gene-Induced Neurodegeneration ». *Journal of Biological Chemistry* 290 (32): 19433‑44. https://doi.org/10.1074/jbc.M115.660001.

Daher, João P. L., Laura A. Volpicelli-Daley, Jonathan P. Blackburn, Mark S. Moehle, et Andrew B. West. 2014. « Abrogation of α-synuclein–mediated dopaminergic neurodegeneration in LRRK2-deficient rats ». *Proceedings of the National Academy of Sciences of the United States of America* 111 (25): 9289‑94. https://doi.org/10.1073/pnas.1403215111.

Daher, João Paulo L., Olga Pletnikova, Saskia Biskup, Alessandra Musso, Sandra Gellhaar, Dagmar Galter, Juan C. Troncoso, et al. 2012. « Neurodegenerative phenotypes in an A53T α-synuclein transgenic mouse model are independent of LRRK2 ». *Human Molecular Genetics* 21 (11): 2420‑31. https://doi.org/10.1093/hmg/dds057.

Deng, Junpeng, Patrick A. Lewis, Elisa Greggio, Eli Sluch, Alexandra Beilina, et Mark R. Cookson. 2008. « Structure of the ROC domain from the Parkinson's disease-associated leucine-rich repeat kinase 2 reveals a dimeric GTPase ». *Proceedings of the National Academy of Sciences of the United States of America* 105 (5): 1499‑1504. https://doi.org/10.1073/pnas.0709098105.

Di Maio, Roberto, Eric K. Hoffman, Emily M. Rocha, Matthew T. Keeney, Laurie H. Sanders, Briana R. De Miranda, Alevtina Zharikov, et al. 2018. « LRRK2 Activation in Idiopathic Parkinson's Disease ». *Science Translational Medicine* 10 (451): eaar5429. https://doi.org/10.1126/scitranslmed.aar5429.

Dusonchet, Julien, Olexiy Kochubey, Klodjan Stafa, Samuel M. Young, Romain Zufferey, Darren J. Moore, Bernard L. Schneider, et Patrick Aebischer. 2011. « A Rat Model of Progressive Nigral Neurodegeneration Induced by the Parkinson's Disease-Associated G2019S Mutation in LRRK2 ». *The Journal of Neuroscience* 31 (3): 907‑12. https://doi.org/10.1523/JNEUROSCI.5092-10.2011.

Giasson, Benoit I., Jason P. Covy, Nancy M. Bonini, Howard I. Hurtig, Matthew J. Farrer, John Q. Trojanowski, et Vivianna M. Van Deerlin. 2006. « Biochemical and Pathological Characterization of Lrrk2 ». *Annals of Neurology* 59 (2): 315‑22. https://doi.org/10.1002/ana.20791.

Gilks, William P, Patrick M Abou-Sleiman, Sonia Gandhi, Shushant Jain, Andrew Singleton, Andrew J Lees, Karen Shaw, et al. 2005. « A common LRRK2 mutation in idiopathic Parkinson's disease ». *The Lancet* 365 (9457): 415‑16. https://doi.org/10.1016/S0140-6736(05)17830-1.

Gloeckner, Christian Johannes, Norbert Kinkl, Annette Schumacher, Ralf J. Braun, Eric O'Neill, Thomas Meitinger, Walter Kolch, Holger Prokisch, et Marius Ueffing. 2006. « The Parkinson Disease Causing LRRK2 Mutation I2020T Is Associated with Increased Kinase Activity ». *Human Molecular Genetics* 15 (2): 223‑32. https://doi.org/10.1093/hmg/ddi439.

Greggio, Elisa, Shushant Jain, Ann Kingsbury, Rina Bandopadhyay, Patrick Lewis, Alice Kaganovich, Marcel P. van der Brug, et al. 2006. « Kinase activity is required for the toxic effects of mutant LRRK2/dardarin ». *Neurobiology of Disease* 23 (2): 329‑41. https://doi.org/10.1016/j.nbd.2006.04.001.

Greggio, Elisa, Ibardo Zambrano, Alice Kaganovich, Alexandra Beilina, Jean-Marc Taymans, Veronique Daniëls, Patrick Lewis, et al. 2008. « The Parkinson Disease-Associated Leucine-Rich Repeat Kinase 2 (LRRK2) Is a Dimer That Undergoes Intramolecular Autophosphorylation ». *Journal of Biological Chemistry* 283 (24): 16906‑14. https://doi.org/10.1074/jbc.M708718200.

Healy, Daniel G, Mario Falchi, Sean S O'Sullivan, Vincenzo Bonifati, Alexandra Durr, Susan Bressman, Alexis Brice, et al. 2008. « Phenotype, genotype, and worldwide genetic penetrance of LRRK2-associated Parkinson's disease: a case-control study ». *The Lancet Neurology* 7 (7): 583‑90. https://doi.org/10.1016/S1474-4422(08)70117-0.

Ito, Genta, et Takeshi Iwatsubo. 2012. « Re-Examination of the Dimerization State of Leucine-Rich Repeat Kinase 2: Predominance of the Monomeric Form ». *Biochemical Journal* 441 (3): 987‑98. https://doi.org/10.1042/BJ20111215.

Krüger, Rejko, Wilfried Kuhn, Thomas Müller, Dirk Woitalla, Manuel Graeber, Sigfried Kösel, Horst Przuntek, Jörg T. Epplen, Ludger Schols, et Olaf Riess. 1998. « AlaSOPro Mutation in the Gene Encoding α-Synuclein in Parkinson's Disease ». *Nature Genetics* 18 (2): 106‑8. https://doi.org/10.1038/ng0298-106.

Lee, Byoung Dae, Joo-Ho Shin, Jackalina VanKampen, Leonard Petrucelli, Andrew B. West, Han Seok Ko, Yun Lee, et al. 2010. « Inhibitors of Leucine Rich Repeat Kinase 2 (LRRK2) Protect Against LRRK2-Models of Parkinson's Disease ». *Nature medicine* 16 (9): 998‑1000. https://doi.org/10.1038/nm.2199.

Lesage, Suzanne, et Alexis Brice. 2009. « Parkinson's Disease: From Monogenic Forms to Genetic Susceptibility Factors ». *Human Molecular Genetics* 18 (R1): R48‑59. https://doi.org/10.1093/hmg/ddp012.

Lin, Xian, Loukia Parisiadou, Xing-Long Gu, Lizhen Wang, Hoon Shim, Lixin Sun, Chengsong Xie, et al. 2009. « Leucine-Rich Repeat Kinase 2 Regulates the Progression of Neuropathology Induced by Parkinson's-Disease-Related Mutant Alpha-Synuclein ». *Neuron* 64 (6): 807‑27. https://doi.org/10.1016/j.neuron.2009.11.006.

Lobbestael, E., L. Civiero, T. De Wit, J.-M. Taymans, E. Greggio, et V. Baekelandt. 2016. « Pharmacological LRRK2 Kinase Inhibition Induces LRRK2 Protein Destabilization and Proteasomal Degradation ». *Scientific Reports* 6 (septembre): 33897. https://doi.org/10.1038/srep33897.

Maekawa, Tatsunori, Toshikuni Sasaoka, Sadahiro Azuma, Takafumi Ichikawa, Heather L. Melrose, Matthew J. Farrer, et Fumiya Obata. 2016. « Leucine-Rich Repeat Kinase 2 (LRRK2) Regulates α-Synuclein Clearance in Microglia ». *BMC Neuroscience* 17 (1): 77. https://doi.org/10.1186/s12868-016-0315-2.

Melrose, H. L., J. C. Dächsel, B. Behrouz, S. J. Lincoln, M. Yue, K. M. Hinkle, C. Kent, et al. 2010. « Impaired dopaminergic neurotransmission and microtubule-associated protein tau alterations in human LRRK2 transgenic mice ». *Neurobiology of disease* 40 (3): 503‑17. https://doi.org/10.1016/j.nbd.2010.07.010.

Novello, Salvatore, Ludovico Arcuri, Sandra Dovero, Nathalie Dutheil, Derya R. Shimshek, Erwan Bezard, et Michele Morari. 2018. « G2019S LRRK2 mutation facilitates α-synuclein neuropathology in aged mice ». *Neurobiology of Disease* 120 (June): 21‑33. https://doi.org/10.1016/j.nbd.2018.08.018.

Oosterveld, Linda P., John C. Allen, Ebonne Y. L. Ng, Soo-Hoon Seah, Kay-Yaw Tay, Wing-Lok Au, Eng-King Tan, et Louis C. S. Tan. 2015. « Greater Motor Progression in Patients with Parkinson Disease Who Carry LRRK2 Risk Variants ». *Neurology* 85 (12): 1039‑42. https://doi.org/10.1212/WNL.0000000000001953.

Paisán-Ruíz, Coro, Shushant Jain, E. Whitney Evans, William P. Gilks, Javier Simón, Marcel van der Brug, Adolfo López de Munain, et al. 2004. « Cloning of the Gene Containing Mutations that Cause PARK8-Linked Parkinson's Disease ». *Neuron* 44 (4): 595‑600. https://doi.org/10.1016/j.neuron.2004.10.023.

Polymeropoulos, Mihael H., Christian Lavedan, Elisabeth Leroy, Susan E. Ide, Anindya Dehejia, Amalia Dutra, Brian Pike, et al. 1997. « Mutation in the α-Synuclein Gene Identified in Families with Parkinson's Disease ». *Science* 276 (5321): 2045‑47. https://doi.org/10.1126/science.276.5321.2045.

Ramonet, David, João Paulo L. Daher, Brian M. Lin, Klodjan Stafa, Jaekwang Kim, Rebecca Banerjee, Marie Westerlund, et al. 2011. « Dopaminergic Neuronal Loss, Reduced Neurite Complexity and Autophagic Abnormalities in Transgenic Mice Expressing G2019S Mutant LRRK2 ». *PLoS ONE* 6 (4). https://doi.org/10.1371/journal.pone.0018568.

Rosenbusch, Katharina E., et Arjan Kortholt. 2016. « Activation Mechanism of LRRK2 and Its Cellular Functions in Parkinson's Disease ». *Parkinson's Disease* 2016: 7351985. https://doi.org/10.1155/2016/7351985.

Russo, Isabella, Luigi Bubacco, et Elisa Greggio. 2014. « LRRK2 and neuroinflammation: partners in crime in Parkinson's disease? » *Journal of Neuroinflammation* 11 (mars): 52. https://doi.org/10.1186/1742-2094-11-52.

Saito, Yuko, Akiko Kawashima, Nyoka N. Ruberu, Hideo Fujiwara, Shunichi Koyama, Motoji Sawabe, Tomio Arai, et al. 2003. « Accumulation of Phosphorylated α-Synuclein in Aging Human Brain ». *Journal of Neuropathology & Experimental Neurology* 62 (6): 644‑54. https://doi.org/10.1093/jnen/62.6.644.

Sheng, Zejuan, Shuo Zhang, Daisy Bustos, Tracy Kleinheinz, Claire E. Le Pichon, Sara L. Dominguez, Hilda O. Solanoy, et al. 2012. « Ser1292 Autophosphorylation Is an Indicator of LRRK2 Kinase Activity and Contributes to the Cellular Effects of PD Mutations ». *Science Translational Medicine* 4 (164): 164ra161-164ra161. https://doi.org/10.1126/scitranslmed.3004485.

Singleton, A. B., M. Farrer, J. Johnson, A. Singleton, S. Hague, J. Kachergus, M. Hulihan, et al. 2003. « Alpha-Synuclein Locus Triplication Causes Parkinson's Disease ». *Science (New York, N.Y.)* 302 (5646): 841. https://doi.org/10.1126/science.1090278.

Smith, Wanli W., Zhong Pei, Haibing Jiang, Valina L. Dawson, Ted M. Dawson, et Christopher A. Ross. 2006. « Kinase Activity of Mutant LRRK2 Mediates Neuronal Toxicity ». *Nature Neuroscience* 9 (10): 1231‑33. https://doi.org/10.1038/nn1776.

Volpicelli-Daley, Laura A., Hisham Abdelmotilib, Zhiyong Liu, Lindsay Stoyka, João Paulo Lima Daher, Austen J. Milnerwood, Vivek K. Unni, et al. 2016. « G2019S-LRRK2 Expression Augments α-Synuclein Sequestration into Inclusions in Neurons ». *The Journal of Neuroscience* 36 (28): 7415‑27. https://doi.org/10.1523/JNEUROSCI.3642-15.2016.

West, Andrew B., Darren J. Moore, Catherine Choi, Shaida A. Andrabi, Xiaojie Li, Dustin Dikeman, Saskia Biskup, et al. 2007. « Parkinson's Disease-Associated Mutations in LRRK2 Link Enhanced GTP-Binding and Kinase Activities to Neuronal Toxicity ». *Human Molecular Genetics* 16 (2): 223‑32. https://doi.org/10.1093/hmg/ddl471.

Yahalom, Gilad, Yael Orlev, Oren S. Cohen, Evgenia Kozlova, Eitan Friedman, Rivka Inzelberg, et Sharon Hassin-Baer. 2014. « Motor Progression of Parkinson's Disease with the Leucine-Rich Repeat Kinase 2 G2019S Mutation: Disease Progression in PD with G2019S Mutation ». *Movement Disorders* 29 (8): 1057‑60. https://doi.org/10.1002/mds.25931.

Zarranz, Juan J., Javier Alegre, Juan C. Gómez-Esteban, Elena Lezcano, Raquel Ros, Israel Ampuero, Lídice Vidal, et al. 2004. « The New Mutation, E46K, of α-Synuclein Causes Parkinson and Lewy Body Dementia ». *Annals of Neurology* 55 (2): 164‑73. https://doi.org/10.1002/ana.10795.

Zimprich, Alexander, Saskia Biskup, Petra Leitner, Peter Lichtner, Matthew Farrer, Sarah Lincoln, Jennifer Kachergus, et al. 2004. « Mutations in LRRK2 Cause Autosomal-Dominant Parkinsonism with Pleomorphic Pathology ». *Neuron* 44 (4): 601‑7. https://doi.org/10.1016/j.neuron.2004.11.005.

9. References

Abou Neel, E.A., Bozec, L., Knowles, J.C., Syed, O., Mudera, V., Day, R., Hyun, J.K., 2013. Collagen - Emerging collagen based therapies hit the patient. Adv. Drug Deliv. Rev. 65, 429–456.

Adams-Carr, K.L., Bestwick, J.P., Shribman, S., Lees, A., Schrag, A., Noyce, A.J., 2016. Constipation preceding Parkinson's disease: a systematic review and meta-analysis. J. Neurol. Neurosurg. Psychiatry 87, 710–716.

Adil, M.M., Vazin, T., Ananthanarayanan, B., Rodrigues, G.M.C., Rao, A.T., Kulkarni, R.U., Miller, E.W., Kumar, S., Schaffer, D. V., 2017. Engineered hydrogels increase the post-transplantation survival of encapsulated hESC-derived midbrain dopaminergic neurons. Biomaterials 136, 1–11.

Albert, K., Voutilainen, M., Domanskyi, A., Airavaara, M., 2017. AAV Vector-Mediated Gene Delivery to Substantia Nigra Dopamine Neurons: Implications for Gene Therapy and Disease Models. Genes (Basel). 8, 63.

Albrecht, D.S., Granziera, C., Hooker, J.M., Loggia, M.L., 2016. In Vivo Imaging of Human Neuroinflammation. ACS Chem. Neurosci. 7, 470–483.

Alegre-Abarrategui, J., Ansorge, O., Esiri, M., Wade-Martins, R., 2008. LRRK2 is a component of granular alpha-synuclein pathology in the brainstem of Parkinson's disease. Neuropathol. Appl. Neurobiol. 34, 272–283.

Algarni, M.A., Stoessl, A.J., 2016. The role of biomarkers and imaging in Parkinson's disease. Expert Rev. Neurother. 16, 187–203.

Andersson, C., Hamer, R.M., Lawler, C.P., Mailman, R.B., Lieberman, J.A., 2002. Striatal Volume Changes in the Rat Following Long-term Administration of Typical and Atypical Antipsychotic Drugs. Neuropsychopharmacology 27, 498.

Annerino, D.M., Arshad, S., Taylor, G.M., Adler, C.H., Beach, T.G., Greene, J.G., 2012. Parkinson's disease is not associated with gastrointestinal myenteric ganglion neuron loss. Acta Neuropathol. 124, 665–680.

Araki, M., Ito, G., Tomita, T., 2018. Physiological and pathological functions of LRRK2: implications from substrate proteins. Neuronal Signal. 2, NS20180005.

Avila Rodríguez, M.I., Rodríguez Barroso, L.G., Sánchez, M.L., 2018. Collagen: A review on its sources and potential cosmetic applications. J. Cosmet. Dermatol. 17, 20–26.

Barker, R.A., 2009. Parkinson's disease and growth factors – are they the answer? Parkinsonism Relat. Disord. 15, S181–S184.

Barker, R.A., Barrett, J., Mason, S.L., Björklund, A., 2013. Fetal dopaminergic transplantation trials and the future of neural grafting in Parkinson's disease. Lancet Neurol. 12, 84–91.

Barker, R.A., Drouin-Ouellet, J., Parmar, M., 2015. Cell-based therapies for Parkinson disease—past insights and future potential. Nat. Rev. Neurol. 11, 492–503.

Barrow, T.R., 2015. Cell replacement therapy in Parkinson's disease. Biosci. Horizons 8, hzv002–hzv002.

Bartels, A.L., Leenders, K.L., 2009. Parkinson's disease: The syndrome, the pathogenesis and pathophysiology. Cortex 45, 915–921.

Batassini, C., Broetto, N., Tortorelli, L.S., Borsoi, M., Zanotto, C., Galland, F., Souza, T.M., Leite, M.C., Gonçalves, C.-A., 2015. Striatal Injury with 6-OHDA Transiently Increases Cerebrospinal GFAP and S100B. Neural Plast.

Batchelor, P.E., Liberatore, G.T., Wong, J.Y.F., Porritt, M.J., Frerichs, F., Donnan, G.A., Howells, D.W., 1999. Activated macrophages and microglia induce dopaminergic sprouting in the injured striatum and express brain-derived neurotrophic factor and glial cell line-derived neurotrophic factor. J. Neurosci. 19, 1708–16.

Batista, C.R.A., Gomes, G.F., Candelario-Jalil, E., Fiebich, B.L., de Oliveira, A.C.P., 2019. Lipopolysaccharide-Induced Neuroinflammation as a Bridge to Understand Neurodegeneration. Int. J. Mol. Sci. 20, 2293.

Bender, A., Krishnan, K.J., Morris, C.M., Taylor, G.A., Reeve, A.K., Perry, R.H., Jaros, E., Hersheson, J.S., Betts, J., Klopstock, T., Taylor, R.W., Turnbull, D.M., 2006. High levels of mitochondrial DNA deletions in substantia nigra neurons in aging and Parkinson disease. Nat. Genet.

Bhat, S., Kumar, A., 2013. Biomaterials and bioengineering tomorrow's healthcare. Biomatter 3, e24717.

Bhidayasiri, R., Martinez-Martin, P., 2017. Clinical Assessments in Parkinson's Disease. In: International Review of Neurobiology. Elsevier Inc., pp. 129–182.

Billingsley, K.J., Bandres-Ciga, S., Saez-Atienzar, S., Singleton, A.B., 2018. Genetic risk factors in Parkinson's disease. Cell Tissue Res. 373, 9–20.

Bjorklund, A., Stenevi, U., 1979. Reconstruction of the nigrostriatal dopamine pathway by intracerebral nigral transplants. Brain Res. 177, 555–560.

Bjugstad, K.B., Lampe, K., Kern, D.S., Mahoney, M., 2010. Biocompatibility of poly(ethylene glycol)-based hydrogels in the brain: An analysis of the glial response across space and time. J. Biomed. Mater. Res. Part A 95A, 79–91.

Bjugstad, K.B., Redmond, D.E., Lampe, K.J., Kern, D.S., Sladek, J.R., Mahoney, M.J., 2008. Biocompatibility of PEG-Based Hydrogels in Primate Brain. Cell Transplant. 17, 409–415.

Blair, N.F., Frith, T.J.R., Barbaric, I., 2017. Regenerative Medicine: Advances from Developmental to Degenerative Diseases. In: Australasian Biotechnology. pp. 225–239.

Blesa, J., Phani, S., Jackson-Lewis, V., Przedborski, S., 2012. Classic and New Animal Models of Parkinson's Disease. J. Biomed. Biotechnol. 2012, 1–10.

Blesa, J., Przedborski, S., 2014. Parkinson's disease: animal models and dopaminergic cell vulnerability. Front. Neuroanat. 8, 1–12.

Blin, P., Dureau-Pournin, C., Foubert-Samier, A., Grolleau, A., Corbillon, E., Jové, J., Lassalle, R., Robinson, P., Poutignat, N., Droz-Perroteau, C., Moore, N., 2015. Parkinson's disease incidence and prevalence assessment in France using the national healthcare insurance database. Eur. J. Neurol. 22, 464–471.

Blum-Degena, D., Müller, T., Kuhn, W., Gerlach, M., Przuntek, H., Riederer, P., 1995. Interleukin-1β and interleukin-6 are elevated in the cerebrospinal fluid of Alzheimer's and de novo Parkinson's disease patients. Neurosci. Lett.

Bobela, W., Aebischer, P., Schneider, B.L., 2015. Alpha-synuclein as a mediator in the interplay between aging and Parkinson's disease. Biomolecules 5, 2675–2700.

Bohnen, N., Albin, R., 2011. The Cholinergic System in Parkinson's Disease. Behav Brain Res. 221, 564–573.

Boix, J., Padel, T., Paul, G., 2015. A partial lesion model of Parkinson's disease in mice - Characterization of a 6-OHDA-induced medial forebrain bundle lesion. Behav. Brain Res.

Borellini, L., Ardolino, G., Carrabba, G., Locatelli, M., Rampini, P., Sbaraini, S., Scola, E., Avignone, S., Triulzi, F., Barbieri, S., Cogiamanian, F., 2019. Peri-lead edema after deep brain stimulation surgery for Parkinson's disease: a prospective magnetic resonance imaging study. Eur. J. Neurol. 26, 533–539.

Bourin, M., 2018. Lewy Body Dementia: A Review. J. Neurosci. Neurosurg. 1, 2–4.

Braak, H., Rub, U., Gai, W.P., Del Tredici, K., 2003. Idiopathic Parkinson's disease: possible routes by which vulnerable neuronal types may be subject to neuroinvasion by an unknown pathogen. J. Neural Transm. 110, 517–536.

Braak, Heiko, Tredici, K. Del, Rüb, U., de Vos, R.A.., Jansen Steur, E.N.., Braak, E., 2003. Staging of brain pathology related to sporadic Parkinson's disease. Neurobiol. Aging 24, 197–211.

BrainMatTrain - Official Website, n.d. BrainMatTrain - Official Website [WWW Document]. URL http://curamdevices.ie/curam/research/eu-projects/brainmattrain/

Bravo-San Pedro, J.M., Niso-Santano, M., Gómez-Sánchez, R., Pizarro-Estrella, E., Aiastui-Pujana, A., Gorostidi, A., Climent, V., López de Maturana, R., Sanchez-Pernaute, R., López de Munain, A., Fuentes, J.M., González-Polo, R.A., 2013. The LRRK2 G2019S mutant exacerbates basal autophagy through activation of the MEK/ERK pathway. Cell. Mol. Life Sci. 70, 121–136.

Brodacki, B., Staszewski, J., Toczyłowska, B., Kozłowska, E., Drela, N., Chalimoniuk, M., Stepien, A., 2008. Serum interleukin (IL-2, IL-10, IL-6, IL-4), TNFα, and INFγ concentrations are elevated in patients with atypical and idiopathic parkinsonism. Neurosci. Lett.

Bruggeman, K.F., Moriarty, N., Dowd, E., Nisbet, D.R., Parish, C.L., 2019. Harnessing stem cells and biomaterials to promote neural repair. Br. J. Pharmacol. 176, 355–368.

Burrè, J., Sharma, M., Sudhof, T.C., 2015. Definition of a Molecular Pathway Mediating a-Synuclein Neurotoxicity. J. Neurosci. 35, 5221–5232.

Casano, A.M., Peri, F., 2015. Microglia: Multitasking Specialists of the Brain. Dev. Cell 32, 469–477.

Chang, S.-W., Shefelbine, S.J., Buehler, M.J., 2012. Structural and Mechanical Differences between Collagen Homo- and Heterotrimers: Relevance for the Molecular Origin of Brittle Bone Disease. Biophys. J. 102, 640–648.

Chattopadhyay, S., Raines, R.T., 2014. Collagen-based biomaterials for wound healing. Biopolymers 101, 821–833.

Chen-Plotkin, A.S., Albin, R., Alcalay, R., Babcock, D., Bajaj, V., Bowman, D., Buko, A., Cedarbaum, J., Chelsky, D., Cookson, M.R., Dawson, T.M., Dewey, R., Foroud, T., Frasier, M., German, D., Gwinn, K., Huang, X., Kopil, C., Kremer, T., Lasch, S., Marek, K., Marto, J.A., Merchant, K., Mollenhauer, B., Naito, A., Potashkin, J., Reimer, A., Rosenthal, L.S., Saunders-Pullman, R., Scherzer, C.R., Sherer, T., Singleton, A., Sutherland, M., Thiele, I., van der Brug, M., Van Keuren-Jensen, K., Vaillancourt, D., Walt, D., West, A., Zhang, J., 2018. Finding useful biomarkers for Parkinson's disease. Sci. Transl. Med. 10, eaam6003.

Chen, C., Weng, Y., Chien, K., Lin, K., Yeh, T., Cheng, Y., Lu, C., Wang, H., 2012. (G2019S) LRRK2 activates MKK4-JNK pathway and causes degeneration of SN dopaminergic neurons in a transgenic mouse model of PD. Cell Death Differ. 19, 1623–1633.

Chen, H., Burton, E.A., Ross, G.W., Huang, X., Savica, R., Abbott, R.D., Ascherio, A., Caviness, J.N., Gao, X., Gray, K.A., Hong, J., Kamel, F., Jennings, D., Kirshner, A., Lawler, C., Liu, R., Miller, G.W., Nussbaum, R., Peddada, S.D., Rick, A.C., Ritz, B., Siderowf, A.D., Tanner, C.M., Tröster, A.I., Zhang, J., 2013. Research on the Premotor Symptoms of Parkinson's Disease: Clinical and Etiological Implications. Environ. Health Perspect. 121, 1245–1252.

Chen, J.-H., Hsu, W.-C., Huang, K.-F., Hung, C.-H., 2019. Neuroprotective Effects of Collagen-Glycosaminoglycan Matrix Implantation following Surgical Brain Injury. Mediators Inflamm. 2019, 1–11.

Christine, C.W., Starr, P.A., Larson, P.S., Eberling, J.L., Jagust, W.J., Hawkins, R.A., VanBrocklin, H.F., Wright, J.F., Bankiewicz, K.S., Aminoff, M.J., 2009. Safety and tolerability of putaminal AADC gene therapy for Parkinson disease. Neurology 73, 1662–1669.

Collins, L.M., Toulouse, A., Connor, T.J., Nolan, Y.M., 2012. Contributions of central and systemic inflammation to the pathophysiology of Parkinson's disease. Neuropharmacology 62, 2154–2168.

Colombo, E., Farina, C., 2016. Astrocytes: Key Regulators of Neuroinflammation. Trends Immunol. 37, 608–620.

Corti, O., Lesage, S., Brice, A., 2011. What Genetics Tells us About the Causes and Mechanisms of Parkinson's Disease. Physiol. Rev. 91, 1161–1218.

Cotzias, G.C., Van Woert, M.H., Schiffer, L.M., 1967. Aromatic Amino Acids and Modification of Parkinsonism. N. Engl. J. Med. 276, 374–379.

Creed, R.B., Goldberg, M.S., 2018. New developments in genetic rat models of Parkinson's disease. Mov. Disord. 00, 1–13.

Cresto, N., Gardier, C., Gubinelli, F., Gaillard, M.-C., Liot, G., West, A.B., Brouillet, E., 2018. The unlikely partnership between LRRK2 and α-synuclein in Parkinson's disease. Eur. J. Neurosci. 49, 339–363.

Cuervo, A.M., 2006. Autophagy in neurons: it is not all about food. Trends Mol. Med.

Cuervo, A.M., Stafanis, L., Fredenburg, R., Lansbury, P.T., Sulzer, D., 2004. Impaired degradation of mutant α-synuclein by chaperone-mediated autophagy. Science (80-.).

Daher, J.P.L., 2017. Interaction of LRRK2 and α-Synuclein in Parkinson's Disease. pp. 209–226.

Daher, J.P.L., Pletnikova, O., Biskup, S., Musso, A., Gellhaar, S., Galter, D., Troncoso, J.C., Lee, M.K., Dawson, T.M., Dawson, V.L., Moore, D.J., 2012. Neurodegenerative phenotypes in an A53T α-synuclein transgenic mouse model are independent of LRRK2. Hum. Mol. Genet. 21, 2420–2431.

Damiano, M., Diguet, E., Malgorn, C., D'Aurelio, M., Galvan, L., Petit, F., Benhaim, L., Guillermier, M., Houitte, D., Dufour, N., Hantraye, P., Canals, J.M., Alberch, J., Delzescaux, T., Déglon, N., Beal, M.F., Brouillet, E., 2013. A role of mitochondrial complex II defects in genetic models of Huntington's disease expressing N-terminal fragments of mutant huntingtin. Hum. Mol. Genet. 22, 3869–3882.

Dawson, T.M., Ko, H.S., Dawson, V.L., 2010. Genetic Animal Models of Parkinson's Disease. Neuron 66, 646–661.

Deister, C., Schmidt, C.E., 2006. Optimizing neurotrophic factor combinations for neurite outgrowth. J. Neural Eng. 3, 172–179.

Delaville, C., Deurwaerdère, P. De, Benazzouz, A., 2011. Noradrenaline and Parkinson's Disease. Front. Syst. Neurosci. 5, 1–12.

DeLong, M., Wichmann, T., 2010. Changing views of basal ganglia circuits and circuit disorders. Clin. EEG Neurosci. 41, 61–67.

DeLong, M.R., Wichmann, T., 2007. Circuits and circuit disorders of the basal ganglia. Arch. Neurol. 64, 20–24.

DeMaagd, G., Philip, A., 2015. Parkinson's Disease and Its Management: Part 1: Disease Entity, Risk Factors, Pathophysiology, Clinical Presentation, and Diagnosis. P T 40, 504–32.

Devi, L., Raghavendran, V., Prabhu, B.M., Avadhani, N.G., Anandatheerthavarada, H.K., 2008. Mitochondrial Import and Accumulation of α-Synuclein Impair Complex I in Human Dopaminergic Neuronal Cultures and Parkinson Disease Brain. J. Biol. Chem. 283, 9089–9100.

Devine, M.J., Kaganovich, A., Ryten, M., Mamais, A., Trabzuni, D., Manzoni, C., McGoldrick, P., Chan, D., Dillman, A., Zerle, J., Horan, S., Taanman, J.-W., Hardy, J., Marti-Masso, J.-F., Healey, D., Schapira, A.H., Wolozin, B., Bandopadhyay, R., Cookson, M.R., van der Brug, M.P., Lewis, P.A., 2011. Pathogenic LRRK2 Mutations Do Not Alter Gene Expression in Cell Model Systems or Human Brain Tissue. PLoS One 6, e22489.

Di Maio, R., Barrett, P.J., Hoffman, E.K., Barrett, C.W., Zharikov, A., Borah, A., Hu, X., McCoy, J., Chu, C.T., Burton, E.A., Hastings, T.G., Greenamyre, J.T., 2016. α-Synuclein binds to TOM20 and inhibits mitochondrial protein import in Parkinson's disease. Sci. Transl. Med. 8, 342ra78-342ra78.

Dickson, D.W., 2018. Neuropathology of Parkinson disease. Parkinsonism Relat. Disord. 46, S30–S33.

Dinescu, S., Albu Kaya, M., Chitoiu, L., Ignat, S., Kaya, D.A., Costache, M., 2019. Collagen-Based Hydrogels and Their Applications for Tissue Engineering and Regenerative Medicine. In: Mondal, U.-P.D.M.I.H. (Ed.), Polymers and Polymeric Composites: A Reference Series. Springer International Publishing, pp. 1643–1664.

Domanskyi, A., Saarma, M., Airavaara, M., 2015. Prospects of Neurotrophic Factors for Parkinson's Disease: Comparison of Protein and Gene Therapy. Hum. Gene Ther. 26, 550–559.

Doty, R.L., 2012. Olfactory dysfunction in Parkinson disease. Nat. Rev. Neurol. 8, 329–339.

du Pré, B.C., Doevendans, P.A., van Laake, L.W., 2013. Stem cells for cardiac repair: an introduction. J. Geriatr. Cardiol. 10, 186–97.

Duchin, Y., Shamir, R.R., Patriat, R., Kim, J., Vitek, J.L., Sapiro, G., Harel, N., 2018. Patient-specific

anatomical model for deep brain stimulation based on 7 Tesla MRI. PLoS One 13, e0201469.

Dusonchet, J., Kochubey, O., Stafa, K., Young, S.M., Zufferey, R., Moore, D.J., Schneider, B.L., Aebischer, P., 2011. A Rat Model of Progressive Nigral Neurodegeneration Induced by the Parkinson's Disease-Associated G2019S Mutation in LRRK2. J. Neurosci. 31, 907–912.

Dutta, G., Zhang, P., Liu, B., 2008. The lipopolysaccharide Parkinson's disease animal model: mechanistic studies and drug discovery. Fundam. Clin. Pharmacol. 22, 453–464.

Duty, S., Jenner, P., 2011. Animal models of Parkinson's disease: a source of novel treatments and clues to the cause of the disease. Br. J. Pharmacol. 164, 1357–1391.

Engelender, S., Isacson, O., 2017. The Threshold Theory for Parkinson's Disease. Trends Neurosci. 40, 4–14.

Esteves, A.R., Swerdlow, R.H., Cardoso, S.M., 2014. LRRK2, a puzzling protein: Insights into Parkinson's disease pathogenesis. Exp. Neurol. 261, 206–216.

Fahn, S., 2018. The 200-year journey of Parkinson disease: Reflecting on the past and looking towards the future. Park. Relat. Disord. 46, S1–S5.

Ferreira, A.M., Gentile, P., Chiono, V., Ciardelli, G., 2012. Collagen for bone tissue regeneration. Acta Biomater. 8, 3191–3200.

Findley, L.J., 2007. The economic impact of Parkinson's disease. Parkinsonism Relat. Disord. 13 Suppl, S8–S12.

Fischer, D.L., Gombash, S.E., Kemp, C.J., Manfredsson, F.P., Polinski, N.K., Duffy, M.F., Sortwell, C.E., 2016. Viral Vector-Based Modeling of Neurodegenerative Disorders: Parkinson's Disease. In: Manfredsson, F. (Ed.), Gene Therapy for Neurological Disorders. Methods in Molecular Biology. Humana Press, New York, NY, pp. 367–382.

Floor, E., Wetzel, M.G., 2002. Increased Protein Oxidation in Human Substantia Nigra Pars Compacta in Comparison with Basal Ganglia and Prefrontal Cortex Measured with an Improved Dinitrophenylhydrazine Assay. J. Neurochem.

Flores-Martinez, Y.M., Fernandez-Parrilla, M.A., Ayala-Davila, J., Reyes-Corona, D., Blanco-Alvarez, V.M., Soto-Rojas, L.O., Luna-Herrera, C., Gonzalez-Barrios, J.A., Leon-Chavez, B.A., Gutierrez-Castillo, M.E., Martínez-Dávila, I.A., Martinez-Fong, D., 2018. Acute Neuroinflammatory Response in the Substantia Nigra Pars Compacta of Rats after a Local Injection of Lipopolysaccharide. J. Immunol. Res. 2018, 1–19.

Franco-Bocanegra, McAuley, Nicoll, Boche, 2019. Molecular Mechanisms of Microglial Motility: Changes in Ageing and Alzheimer's Disease. Cells 8, 639.

French, A.C., Thompson, A.L., Davis, B.G., 2009. High-Purity Discrete PEG-Oligomer Crystals Allow Structural Insight. Angew. Chemie Int. Ed. 48, 1248–1252.

Funayama, M., Hasegawa, K., Kowa, H., Saito, M., Tsuji, S., Obata, F., 2002. A new locus for Parkinson's disease (PARK8) maps to chromosome 12p11.2-q13.1. Ann. Neurol. 51, 296–301.

Gagne, J.J., Power, M.C., 2010. Anti-inflammatory drugs and risk of Parkinson disease: A meta-analysis. Neurology 74, 995–1002.

Galen, 1824. De trernore, palpitatione, convulsione, et rigore. In: Kuhn C.G. (Ed.), . Knobloch, Germany: Lipsiae.

Galvan, A., Wichmann, T., 2008. Pathophysiology of parkinsonism. Clin. Neurophysiol. 119, 1459–74.

Gao, H.-M., Hong, J.-S., 2008. Why neurodegenerative diseases are progressive: uncontrolled inflammation drives disease progression. Trends Immunol. 29, 357–365.

Gehrmann, J., 1996. Microglia: a sensor to threats in the nervous system? Res. Virol. 147, 79–88.

Gelders, G., Baekelandt, V., Perren, A. Van Der, 2018. Linking Neuroinflammation and Neurodegeneration in Parkinson's Disease. J. Immunol. Res. 2018.

Gelse, K., Pöschl, E., Aigner, T., 2003. Collagens - Structure, function, and biosynthesis. Adv. Drug Deliv. Rev. 55, 1531–1546.

Gerhard, A., Pavese, N., Hotton, G., Turkheimer, F., Es, M., Hammers, A., Eggert, K., Oertel, W., Banati, R.B., Brooks, D.J., 2006. In vivo imaging of microglial activation with [11C](R)-PK11195 PET in idiopathic Parkinson's disease. Neurobiol. Dis. 21, 404–412.

Ghosh, D., Mehra, S., Sahay, S., Singh, P.K., Maji, S.K., 2017. α-synuclein aggregation and its modulation. Int. J. Biol. Macromol. 100, 37–54.

Giasson, B.I., Duda, J.E., Quinn, S.M., Zhang, B., Trojanowski, J.Q., Lee, V.M.Y., 2002. Neuronal α-synucleinopathy with severe movement disorder in mice expressing A53T human α-synuclein. Neuron.

Gilsbach, B.K., Kortholt, A., 2014. Structural biology of the LRRK2 GTPase and kinase domains: implications for regulation. Front. Mol. Neurosci. 7, 1–9.

Giordano, C., Albani, D., Gloria, A., Tunesi, M., Batelli, S., Russo, T., Forloni, G., Ambrosio, L., Cigada, A., 2009. Multidisciplinary perspectives for Alzheimer's and Parkinson's diseases: hydrogels for protein delivery and cell-based drug delivery as therapeutic strategies. Int. J. Artif. Organs 32, 836–850.

Glass, C.K., Saijo, K., Winner, B., Marchetto, M.C., Gage, F.H., 2010. Mechanisms Underlying Inflammation in Neurodegeneration. Cell 140, 918–934.

Goedert, M., Compston, A., 2017. Parkinson's disease — the story of an eponym. Nat. Rev. Neurol.

Goedert, M., Spillantini, M.G., Del Tredici, K., Braak, H., 2013. 100 years of Lewy pathology. Nat. Rev. Neurol.

González Ballester, M.Á., Zisserman, A.P., Brady, M., 2002. Estimation of the partial volume effect in MRI. Med. Image Anal. 6, 389–405.

González, R.G., 2012. Clinical MRI of acute ischemic stroke. J. Magn. Reson. Imaging 36, 259–271.

Grealish, S., Diguet, E., Kirkeby, A., Mattsson, B., Heuer, A., Bramoulle, Y., Van Camp, N., Perrier, A.L., Hantraye, P., Björklund, A., Parmar, M., 2014. Human ESC-Derived Dopamine Neurons Show Similar Preclinical Efficacy and Potency to Fetal Neurons when Grafted in a Rat Model of Parkinson's Disease. Cell Stem Cell 15, 653–665.

Greenhalgh, A.D., David, S., 2014. Differences in the Phagocytic Response of Microglia and Peripheral Macrophages after Spinal Cord Injury and Its Effects on Cell Death. J. Neurosci. 34, 6316–6322.

Greenhalgh, A.D., Zarruk, J.G., Healy, L.M., Baskar Jesudasan, S.J., Jhelum, P., Salmon, C.K., Formanek,

A., Russo, M. V., Antel, J.P., McGavern, D.B., McColl, B.W., David, S., 2018. Peripherally derived macrophages modulate microglial function to reduce inflammation after CNS injury. PLOS Biol. 16, e2005264.

Groiss, S.J., Wojtecki, L., Sudmeyer, M., Schnitzler, A., 2009. Deep brain stimulation in Parkinson-s disease. Ther. Adv. Neurol. Disord. 2, 379–391.

Gundersen, V., 2010. Protein aggregation in Parkinson's disease. Acta Neurol. Scand. 122, 82–87.

Gupta, D., Tator, C.H., Shoichet, M.S., 2006. Fast-gelling injectable blend of hyaluronan and methylcellulose for intrathecal, localized delivery to the injured spinal cord. Biomaterials 27, 2370–2379.

Gustavsson, A., Svensson, M., Jacobi, F., Allgulander, C., Alonso, J., Beghi, E., Dodel, R., Ekman, M., Faravelli, C., Fratiglioni, L., Gannon, B., Jones, D.H., Jennum, P., Jordanova, A., Jönsson, L., Karampampa, K., Knapp, M., Kobelt, G., Kurth, T., Lieb, R., Linde, M., Ljungcrantz, C., Maercker, A., Melin, B., Moscarelli, M., Musayev, A., Norwood, F., Preisig, M., Pugliatti, M., Rehm, J., Salvador-Carulla, L., Schlehofer, B., Simon, R., Steinhausen, H.-C., Stovner, L.J., Vallat, J.-M., den Bergh, P. Van, van Os, J., Vos, P., Xu, W., Wittchen, H.-U., Jönsson, B., Olesen, J., 2011. Cost of disorders of the brain in Europe 2010. Eur. Neuropsychopharmacol. 21, 718–779.

Hauser, R.A., 2011. Future Treatments for Parkinson's Disease: Surfing the PD Pipeline. Int. J. Neurosci. 121, 53–62.

Hawkes, C.H., Del Tredici, K., Braak, H., 2009. Parkinson's disease: The dual hit theory revisited. Ann. N. Y. Acad. Sci. 1170, 615–622.

Hendrickx, D.A.E., van Eden, C.G., Schuurman, K.G., Hamann, J., Huitinga, I., 2017. Staining of HLA-DR, Iba1 and CD68 in human microglia reveals partially overlapping expression depending on cellular morphology and pathology. J. Neuroimmunol. 309, 12–22.

Herberts, C.A., Kwa, M.S.G., Hermsen, H.P.H., 2011. Risk factors in the development of stem cell therapy. J. Transl. Med. 9, 29.

Hesketh, M., Sahin, K.B., West, Z.E., Murray, R.Z., 2017. Macrophage Phenotypes Regulate Scar Formation and Chronic Wound Healing. Int. J. Mol. Sci. 18, 1545.

Hinkle, K.M., Yue, M., Behrouz, B., Dächsel, J.C., Lincoln, S.J., Bowles, E.E., Beevers, J.E., Dugger, B., Winner, B., Prots, I., Kent, C.B., Nishioka, K., Lin, W.L., Dickson, D.W., Janus, C.J., Farrer, M.J., Melrose, H.L., 2012. LRRK2 knockout mice have an intact dopaminergic system but display alterations in exploratory and motor co-ordination behaviors. Mol. Neurodegener.

Hirsch, E.C., Hunot, S., 2009. Neuroinflammation in Parkinson's disease: a target for neuroprotection? Lancet Neurol. 8, 382–397.

Hoban, D.B., Connaughton, E., Connaughton, C., Hogan, G., Thornton, C., Mulcahy, P., Moloney, T.C., Dowd, E., 2013a. Further characterisation of the LPS model of Parkinson's disease: A comparison of intra-nigral and intra-striatal lipopolysaccharide administration on motor function, microgliosis and nigrostriatal neurodegeneration in the rat. Brain. Behav. Immun. 27, 91–100.

Hoban, D.B., Newland, B., Moloney, T.C., Howard, L., Pandit, A., Dowd, E., 2013b. The reduction in immunogenicity of neurotrophin overexpressing stem cells after intra-striatal transplantation by

encapsulation in an in situ gelling collagen hydrogel. Biomaterials 34, 9420–9429.

Hornykiewicz, O., 2010. A brief history of levodopa. J. Neurol. 257, 249–252.

Horowski, R., Horowski, L., Phil, C., Vogel, S., Poewe, W., Kielhorn, F.-W., 1995. An Essay on Wilhelm von Humboldt and the Shaking Palsy: First Comprehensive Description of Parkinson's Disease by a Patient. Neurology 45, 565–568.

Hu, W., Wang, Z., Xiao, Y., Zhang, S., Wang, J., 2019. Advances in crosslinking strategies of biomedical hydrogels. Biomater. Sci. 7, 843–855.

Huang, X., Wu, C., Park, Y., Long, X., Hoang, Q.Q., Liao, J., 2018. The Parkinson's disease–associated mutation N1437H impairs conformational dynamics in the G domain of LRRK2. FASEB J. fj.201802031R.

Hulka, B.S., Wilcosky, T., 1988. Biological Markers in Epidemiologic Research. Arch. Environ. Heal. An Int. J. 43, 83–89.

Hunot, S., Dugas, N., Faucheux, B., Hartmann, A., Tardieu, M., Debré, P., Agid, Y., Dugas, B., Hirsch, E.C., 1999. FcεRII/CD23 Is Expressed in Parkinson's Disease and Induces, In Vitro, Production of Nitric Oxide and Tumor Necrosis Factor-α in Glial Cells. J. Neurosci. 19, 3440–3447.

Iturralde, M.P., 1990. Dictionary and Handbook of Nuclear Medicine and Clinical Imaging, Radiology. CRC Press.

J. Pratensis, 1549. De cerebri morbis hoc est ferme omnibus curandis. Basel: Petri.

Jackson-Lewis, V., Blesa, J., Przedborski, S., 2012. Animal models of Parkinson's disease. Parkinsonism Relat. Disord. 18, S183–S185.

Janezic, S., Threlfell, S., Dodson, P.D., Dowie, M.J., Taylor, T.N., Potgieter, D., Parkkinen, L., Senior, S.L., Anwar, S., Ryan, B., Deltheil, T., Kosillo, P., Cioroch, M., Wagner, K., Ansorge, O., Bannerman, D.M., Bolam, J.P., Magill, P.J., Cragg, S.J., Wade-Martins, R., 2013. Deficits in dopaminergic transmission precede neuron loss and dysfunction in a new Parkinson model. Proc. Natl. Acad. Sci. U. S. A.

Jang, H., Boltz, D.A., Webster, R.G., Smeyne, R.J., 2009. Viral parkinsonism. Biochim. Biophys. Acta - Mol. Basis Dis. 1792, 714–721.

Jankovic, J., 2002. Levodopa strengths and weaknesses. Neurology.

Jankovic, J., 2005. Motor fluctuations and dyskinesias in Parkinson's disease: Clinical manifestations. Mov. Disord. 20, S11–S16.

Jankovic, J., 2008. Parkinson's disease: clinical features and diagnosis. J. Neurol. Neurosurg. Psychiatry 79, 368–376.

Jankovic, J., Poewe, W., 2012. Therapies in Parkinson's disease. Curr. Opin. Neurol. 25, 433–447.

Jarraya, B., Boulet, S., Scott Ralph, G., Jan, C., Bonvento, G., Azzouz, M., Miskin, J.E., Shin, M., Delzescaux, T., Drouot, X., Herard, A.-S., Day, D.M., Brouillet, E., Kingsman, S.M., Hantraye, P., Mitrophanous, K.A., Mazarakis, N.D., Palfi, S., 2009. Dopamine Gene Therapy for Parkinson's Disease in a Nonhuman Primate Without Associated Dyskinesia. Sci. Transl. Med. 1, 2ra4-2ra4.

Jeon, B.S., Jackson-Lewis, V., Burke, R.E., 1995. 6-Hydroxydopamine Lesion of the Rat Substantia Nigra: Time Course and Morphology of Cell Death. Neurodegeneration.

Kalaitzakis, M.E., Graeber, M.B., Gentleman, S.M., Pearce, R.K.B., 2008. The dorsal motor nucleus of the vagus is not an obligatory trigger site of Parkinson's disease: a critical analysis of α-synuclein staging. Neuropathol. Appl. Neurobiol. 34, 284–295.

Kalia, L. V., Lang, A.E., 2015. Parkinson's disease. Lancet 386, 896–912.

Kalogeropulou, A.F., Zhao, J., Bolliger, M.F., Memou, A., Narasimha, S., Molitor, T.P., Wilson, W.H., Rideout, H.J., Nichols, R.J., 2018. P62/SQSTM1 is a novel leucine-rich repeat kinase 2 (LRRK2) substrate that enhances neuronal toxicity. Biochem. J. 475, 1271–1293.

Keller, J.N., Dimayuga, E., Chen, Q., Thorpe, J., Gee, J., Ding, Q., 2004. Autophagy, proteasomes, lipofuscin, and oxidative stress in the aging brain. Int. J. Biochem. Cell Biol.

Khaing, Z.Z., Thomas, R.C., Geissler, S.A., Schmidt, C.E., 2014. Advanced biomaterials for repairing the nervous system: what can hydrogels do for the brain? Mater. Today 17, 332–340.

Kneeland, J.B., Shimakawa, A., Wehrli, F.W., 1986. Effect of intersection spacing on MR image contrast and study time. Radiology 158, 819–822.

Koehler, P.J., Keyser, A., 1997. Tremor in latin texts of Dutch physicians: 16th-18th centuries. Mov. Disord. 12, 798–806.

Kopper, T.J., Gensel, J.C., 2018. Myelin as an inflammatory mediator: Myelin interactions with complement, macrophages, and microglia in spinal cord injury. J. Neurosci. Res. 96, 969–977.

Kordower, J.H., Chu, Y., Hauser, R.A., Freeman, T.B., Olanow, C.W., 2008. Lewy body–like pathology in long-term embryonic nigral transplants in Parkinson's disease. Nat. Med. 14, 504–506.

Kowal, S.L., Dall, T.M., Chakrabarti, R., Storm, M. V., Jain, A., 2013. The current and projected economic burden of Parkinson's disease in the United States. Mov. Disord. 28, 311–318.

Kowall, N.W., Hantraye, P., Brouillet, E., Beal, M.F., McKee, A.C., Ferrante, R.J., 2000. MPTP induces alpha-synuclein aggregation in the substantia nigra of baboons. Neuroreport 11, 211–213.

Kraus, M.F., Susmaras, T., Caughlin, B.P., Walker, C.J., Sweeney, J.A., Little, D.M., 2007. White matter integrity and cognition in chronic traumatic brain injury: a diffusion tensor imaging study. Brain 130, 2508–2519.

Kreutzberg, G.W., 1996. Microglia: a sensor for pathological events in the CNS. Trends Neurosci. 19, 312–318.

Kringelbach, M.L., Jenkinson, N., Owen, S.L.F., Aziz, T.Z., 2007. Translational principles of deep brain stimulation. Nat. Rev. Neurosci. 8, 623–635.

Krzyszczyk, P., Schloss, R., Palmer, A., Berthiaume, F., 2018. The Role of Macrophages in Acute and Chronic Wound Healing and Interventions to Promote Pro-wound Healing Phenotypes. Front. Physiol. 9, 1–22.

Kuhn, D.M., Francescutti-Verbeem, D.M., Thomas, D.M., 2006. Dopamine quinones activate microglia and induce a neurotoxic gene expression profile: Relationship to methamphetamine-induced nerve ending damage. In: Annals of the New York Academy of Sciences.

Lang, A.E., Gill, S., Patel, N.K., Lozano, A., Nutt, J.G., Penn, R., Brooks, D.J., Hotton, G., Moro, E.,

Heywood, P., Brodsky, M.A., Burchiel, K., Kelly, P., Dalvi, A., Scott, B., Stacy, M., Turner, D., Wooten, V.G.F., Elias, W.J., Laws, E.R., Dhawan, V., Stoessl, A.J., Matcham, J., Coffey, R.J., Traub, M., 2006. Randomized controlled trial of intraputamenal glial cell line-derived neurotrophic factor infusion in Parkinson disease. Ann. Neurol. 59, 459–466.

Lang, A.E., Lozano, A.M., 1998. Parkinson's Disease. N. Engl. J. Med. 339, 1044–1053.

Langston, J., Ballard, P., Tetrud, J., Irwin, I., 1983. Chronic Parkinsonism in humans due to a product of meperidine-analog synthesis. Science (80-.).

Langston, J.W., 2017. The MPTP Story. J. Parkinsons. Dis. 7, S11–S19.

Langston, J. William, Irwin, I., Langston, E.B., Forno, L.S., 1984. 1-Methyl-4-phenylpyridinium ion (MPP+): Identification of a metabolite of MPTP, a toxin selective to the substantia nigra. Neurosci. Lett. 48, 87–92.

Langston, J.W., Langston, E.B., Irwin, I., 1984. MPTP-induced parkinsonism in human and non-human primates - Clinical and experimental aspects. Acta Neurol. Scand.

Lanska, D.J., 2009. The history of movement disorders - Chapter 33, 3rd ed, Handbook of Clinical Neurology. Elsevier B.V.

Lau, L.M.L. de, Breteler, M.M.B., 2006. Epidemiology of Parkinson's disease. Lancet. Neurol. 5, 525–35.

Le, W., Wu, J., Tang, Y., 2016. Protective Microglia and Their Regulation in Parkinson's Disease. Front. Mol. Neurosci. 9, 1–13.

Lee, A., Hudson, A.R., Shiwarski, D.J., Tashman, J.W., Hinton, T.J., Yerneni, S., Bliley, J.M., Campbell, P.G., Feinberg, A.W., 2019. 3D bioprinting of collagen to rebuild components of the human heart. Science (80-.). 365, 482–487.

Lee, B.D., Dawson, V.L., Dawson, T.M., 2012. Leucine-rich repeat kinase 2 (LRRK2) as a potential therapeutic target in Parkinson's disease. Trends Pharmacol. Sci. 33, 365–373.

Lee, B.D., Shin, J.-H., VanKampen, J., Petrucelli, L., West, A.B., Ko, H.S., Lee, Y.-I., Maguire-Zeiss, K.A., Bowers, W.J., Federoff, H.J., Dawson, V.L., Dawson, T.M., 2010. Inhibitors of leucine-rich repeat kinase-2 protect against models of Parkinson's disease. Nat. Med. 16, 998–1000.

Lee, H.-H., Park, S.-C., Choe, I.-S., Kim, Y., Ha, Y.-S., 2015. Time Course and Characteristics of Astrocyte Activation in the Rat Brain after Injury. Korean J. Neurotrauma 11, 44.

Lee, Y., Dawson, V.L., Dawson, T.M., 2012. Animal Models of Parkinson's Disease: Vertebrate Genetics. Cold Spring Harb. Perspect. Med. 2, a009324–a009324.

Lee, Y., Lee, S., Chang, S.-C., Lee, J., 2019. Significant roles of neuroinflammation in Parkinson's disease: therapeutic targets for PD prevention. Arch. Pharm. Res. 42, 416–425.

Lees, A.J., 2007. Unresolved issues relating to the Shaking Palsy on the celebration of James Parkinson's 250th birthday. Mov. Disord. 22.

Lees, A.J., Tolosa, E., Olanow, C.W., 2015. Four pioneers of L-dopa treatment: Arvid Carlsson, Oleh Hornykiewicz, George Cotzias, and Melvin Yahr. Mov. Disord. 30, 19–36.

Lesage, S., Brice, A., 2009. Parkinson's disease: From monogenic forms to genetic susceptibility factors.

Hum. Mol. Genet.

Li, J.-Q., Tan, L., Yu, J.-T., 2014. The role of the LRRK2 gene in Parkinsonism. Mol. Neurodegener. 9, 47.

Li, J.-Y., Englund, E., Holton, J.L., Soulet, D., Hagell, P., Lees, A.J., Lashley, T., Quinn, N.P., Rehncrona, S., Björklund, A., Widner, H., Revesz, T., Lindvall, O., Brundin, P., 2008. Lewy bodies in grafted neurons in subjects with Parkinson's disease suggest host-to-graft disease propagation. Nat. Med. 14, 501–503.

Li, Q., Barres, B.A., 2018. Microglia and macrophages in brain homeostasis and disease. Nat. Rev. Immunol. 18, 225–242.

Li, Y., Liu, W., Oo, T.F., Wang, L., Tang, Y., Jackson-Lewis, V., Zhou, C., Geghman, K., Bogdanov, M., Przedborski, S., Beal, M.F., Burke, R.E., Li, C., 2009. Mutant LRRK2-R1441G BAC transgenic mice recapitulate cardinal features of Parkinson's disease. Nat. Neurosci. 12, 826–828.

Lin, C.C., Anseth, K.S., 2009. PEG hydrogels for the controlled release of biomolecules in regenerative medicine. Pharm. Res. 26, 631–643.

Lin, X., Parisiadou, L., Gu, X.L., Wang, L., Shim, H., Sun, L., Xie, C., Long, C.X., Yang, W.J., Ding, J., Chen, Z.Z., Gallant, P.E., Tao-Cheng, J.H., Rudow, G., Troncoso, J.C., Liu, Z., Li, Z., Cai, H., 2009. Leucine-Rich Repeat Kinase 2 Regulates the Progression of Neuropathology Induced by Parkinson's-Disease-Related Mutant α-synuclein. Neuron 64, 807–827.

Lin, X., Parisiadou, L., Sgobio, C., Liu, G., Yu, J., Sun, L., Shim, H., Gu, X.-L., Luo, J., Long, C.-X., Ding, J., Mateo, Y., Sullivan, P.H., Wu, L.-G., Goldstein, D.S., Lovinger, D., Cai, H., 2012. Conditional Expression of Parkinson's Disease-Related Mutant a-Synuclein in the Midbrain Dopaminergic Neurons Causes Progressive Neurodegeneration and Degradation of Transcription Factor Nuclear Receptor Related 1. J. Neurosci.

Lindvall, O., 2015. Treatment of Parkinson's disease using cell transplantation. Philos. Trans. R. Soc. B Biol. Sci. 370, 20140370.

Lindvall, O., 2016. Clinical translation of stem cell transplantation in Parkinson's disease. J. Intern. Med. 279, 30–40.

Lindvall, O., Backlund, E.-O., Farde, L., Sedvall, G., Freedman, R., Hoffer, B., Nobin, A., Seiger, Ak., Olson, L., 1987. Transplantation in Parkinson's disease: Two cases of adrenal medullary grafts to the putamen. Ann. Neurol. 22, 457–468.

Lindvall, O., Brundin, P., Widner, H., Rehncrona, S., Gustavii, B., Frackowiak, R., Leenders, K., Sawle, G., Rothwell, J., Marsden, C., Et, A., 1990. Grafts of fetal dopamine neurons survive and improve motor function in Parkinson's disease. Science (80-.). 247, 574–577.

Liu, G., Aliaga, L., Cai, H., 2012. α-synuclein, LRRK2 and their interplay in Parkinson's disease. Future Neurol. 7, 145–153.

Liu, M., Bing, G., 2011. Lipopolysaccharide Animal Models for Parkinson's Disease. Parkinsons. Dis. 2011, 1–7.

Liu, Z., Li, Y., Cui, Y., Roberts, C., Lu, M., Wilhelmsson, U., Pekny, M., Chopp, M., 2014. Beneficial effects of GFAP/vimentin reactive astrocytes for axonal remodeling and motor behavioral recovery in mice after stroke. Glia 62, 2022–2033.

Madl, C.M., Heilshorn, S.C., 2018. Engineering Hydrogel Microenvironments to Recapitulate the Stem Cell Niche. Annu. Rev. Biomed. Eng. 20, 21–47.

Madsen, D.H., Leonard, D., Masedunskas, A., Moyer, A., Jürgensen, H.J., Peters, D.E., Amornphimoltham, P., Selvaraj, A., Yamada, S.S., Brenner, D.A., Burgdorf, S., Engelholm, L.H., Behrendt, N., Holmbeck, K., Weigert, R., Bugge, T.H., 2013. M2-like macrophages are responsible for collagen degradation through a mannose receptor–mediated pathway. J. Cell Biol. 202, 951–966.

Manning-Boğ, A.B., Schüle, B., Langston, J.W., 2009. Alpha-synuclein-glucocerebrosidase interactions in pharmacological Gaucher models: A biological link between Gaucher disease and parkinsonism. Neurotoxicology 30, 1127–1132.

Manzoni, C., Mamais, A., Dihanich, S., McGoldrick, P., Devine, M.J., Zerle, J., Kara, E., Taanman, J.-W., Healy, D.G., Marti-Masso, J.-F., Schapira, A.H., Plun-Favreau, H., Tooze, S., Hardy, J., Bandopadhyay, R., Lewis, P.A., 2013. Pathogenic Parkinson's disease mutations across the functional domains of LRRK2 alter the autophagic/lysosomal response to starvation. Biochem. Biophys. Res. Commun. 441, 862–866.

Marchant, R.E., Miller, K.M., Anderson, J.M., 1984. In vivo biocompatibility studies. V. In vivo leukocyte interactions with Biomer. J. Biomed. Mater. Res. 18, 1169–1190.

Markey, S.P., Johannessen, J.N., Chiueh, C.C., Burns, R.S., Herkenham, M.A., 1984. Intraneuronal generation of a pyridinium metabolite may cause drug-induced parkinsonism. Nature 311, 464–467.

Marks, W.J., Bartus, R.T., Siffert, J., Davis, C.S., Lozano, A., Boulis, N., Vitek, J., Stacy, M., Turner, D., Verhagen, L., Bakay, R., Watts, R., Guthrie, B., Jankovic, J., Simpson, R., Tagliati, M., Alterman, R., Stern, M., Baltuch, G., Starr, P.A., Larson, P.S., Ostrem, J.L., Nutt, J., Kieburtz, K., Kordower, J.H., Olanow, C.W., 2010. Gene delivery of AAV2-neurturin for Parkinson's disease: a double-blind, randomised, controlled trial. Lancet Neurol. 9, 1164–1172.

Marks, W.J., Ostrem, J.L., Verhagen, L., Starr, P.A., Larson, P.S., Bakay, R.A., Taylor, R., Cahn-Weiner, D.A., Stoessl, A.J., Olanow, C.W., Bartus, R.T., 2008. Safety and tolerability of intraputaminal delivery of CERE-120 (adeno-associated virus serotype 2-neurturin) to patients with idiopathic Parkinson's disease: an open-label, phase I trial. Lancet Neurol. 7, 400–408.

Marques, O., Outeiro, T.F., 2012. Alpha-synuclein: from secretion to dysfunction and death. Cell Death Dis. 3, e350–e350.

Martin, I., Kim, J.W., Dawson, V.L., Dawson, T.M., 2014. LRRK2 pathobiology in Parkinson's disease. J. Neurochem. 131, 554–565.

Martinez-Vicente, M., Cuervo, A.M., 2007. Autophagy and neurodegeneration: when the cleaning crew goes on strike. Lancet Neurol. 6, 352–361.

Masliah, E., Rockenstein, E., Veinbergs, I., Mallory, M., Hashimoto, M., Takeda, A., Sagara, Y., Sisk, A., Mucke, L., 2000. Dopaminergic loss and inclusion body formation in alpha-synuclein mice: implications for neurodegenerative disorders. Science 287, 1265–9.

Mason, C., Dunnill, P., 2008. A brief definition of regenerative medicine. Regen. Med. 3, 1–5.

Mayeux, R., 2004. Biomarkers: Potential uses and limitations. NeuroRX 1, 182–188.

McGeer, P.L., Itagaki, S., Boyes, B.E., McGeer, E.G., 1988. Reactive microglia are positive for HLA-DR in

the substantia nigra of Parkinson's and Alzheimer's disease brains. Neurology 38, 1285–1285.

McKeith, I.G., Boeve, B.F., Dickson, D.W., Halliday, G., Taylor, J.-P., Weintraub, D., Aarsland, D., Galvin, J., Attems, J., Ballard, C.G., Bayston, A., Beach, T.G., Blanc, F., Bohnen, N., Bonanni, L., Bras, J., Brundin, P., Burn, D., Chen-Plotkin, A., Duda, J.E., El-Agnaf, O., Feldman, H., Ferman, T.J., Ffytche, D., Fujishiro, H., Galasko, D., Goldman, J.G., Gomperts, S.N., Graff-Radford, N.R., Honig, L.S., Iranzo, A., Kantarci, K., Kaufer, D., Kukull, W., Lee, V.M.Y., Leverenz, J.B., Lewis, S., Lippa, C., Lunde, A., Masellis, M., Masliah, E., McLean, P., Mollenhauer, B., Montine, T.J., Moreno, E., Mori, E., Murray, M., O'Brien, J.T., Orimo, S., Postuma, R.B., Ramaswamy, S., Ross, O.A., Salmon, D.P., Singleton, A., Taylor, A., Thomas, A., Tiraboschi, P., Toledo, J.B., Trojanowski, J.Q., Tsuang, D., Walker, Z., Yamada, M., Kosaka, K., 2017. Diagnosis and management of dementia with Lewy bodies. Neurology 89, 88–100.

McNaught, K.S.P., Olanow, C.W., 2006. Protein aggregation in the pathogenesis of familial and sporadic Parkinson's disease. Neurobiol. Aging 27, 530–545.

Melki, R., 2015. Role of Different Alpha-Synuclein Strains in Synucleinopathies, Similarities with other Neurodegenerative Diseases. J. Parkinsons. Dis. 5, 217–227.

Melki, R., 2018. Alpha-synuclein and the prion hypothesis in Parkinson's disease. Rev. Neurol. (Paris). 174, 644–652.

Melrose, H.L., Dächsel, J.C., Behrouz, B., Lincoln, S.J., Yue, M., Hinkle, K.M., Kent, C.B., Korvatska, E., Taylor, J.P., Witten, L., Liang, Y., Beevers, J.E., Boules, M., Dugger, B.N., Serna, V.A., Gaukhman, A., Yu, X., Castanedes-Casey, M., Braithwaite, A.T., Ogholikhan, S., Yu, N., Bass, D., Tyndall, G., Schellenberg, G.D., Dickson, D.W., Janus, C., Farrer, M.J., 2010. Impaired dopaminergic neurotransmission and microtubule-associated protein tau alterations in human LRRK2 transgenic mice. Neurobiol. Dis. 40, 503–517.

Meredith, G.E., Rademacher, D.J., 2011. MPTP mouse models of Parkinson's disease: An update. J. Parkinsons. Dis. 1, 19–33.

Meredith, G.E., Sonsalla, P.K., Chesselet, M.-F., 2008. Animal models of Parkinson's disease progression. Acta Neuropathol. 115, 385–398.

Michel, P.P., Hirsch, E.C., Hunot, S., 2016. Understanding Dopaminergic Cell Death Pathways in Parkinson Disease. Neuron 90, 675–691.

Mierzwa, A.J., Marion, C.M., Sullivan, G.M., McDaniel, D.P., Armstrong, R.C., 2015. Components of Myelin Damage and Repair in the Progression of White Matter Pathology After Mild Traumatic Brain Injury. J. Neuropathol. Exp. Neurol. 74, 218–232.

Mizuno, Y., Ohta, S., Tanaka, M., Takamiya, S., Suzuki, K., Sato, T., Oya, H., Ozawa, T., Kagawa, Y., 1989. Deficiencies in Complex I subunits of the respiratory chain in Parkinson's disease. Biochem. Biophys. Res. Commun. 163, 1450–1455.

Mogi, M., Harada, M., Narabayashi, H., Inagaki, H., Minami, M., Nagatsu, T., 1996. Interleukin (IL)-1β, IL-2, IL-4, IL-6 and transforming growth factor-α levels are elevated in ventricular cerebrospinal fluid in juvenile parkinsonism and Parkinson's disease. Neurosci. Lett. 211, 13–16.

Moriarty, N., Cabré, S., Alamilla, V., Pandit, A., Dowd, E., 2018a. Encapsulation of young donor age dopaminergic grafts in a GDNF-loaded collagen hydrogel further increases their survival, re-innervation

and functional efficacy after intra-striatal transplantation in hemi-Parkinsonian rats. Eur. J. Neurosci. 1–10.

Moriarty, N., Dowd, E., 2018. Brain repair for Parkinson's disease: is the answer in the matrix? Neural Regen. Res. 13, 1187.

Moriarty, N., Pandit, A., Dowd, E., 2017. Encapsulation of primary dopaminergic neurons in a GDNF-loaded collagen hydrogel increases their survival, re-innervation and function after intra-striatal transplantation. Sci. Rep. 7, 16033.

Moriarty, N., Parish, C.L., Dowd, E., 2018b. Primary tissue for cellular brain repair in Parkinson's disease: Promise, problems and the potential of biomaterials. Eur. J. Neurosci. 1–15.

Mortiboys, H., Johansen, K.K., Aasly, J.O., Bandmann, O., 2010. Mitochondrial impairment in patients with Parkinson disease with the G2019S mutation in LRRK2. Neurology 75, 2017–2020.

Nair, U., Klionsky, D.J., 2005. Molecular mechanisms and regulation of specific and nonspecific autophagy pathways in yeast. J. Biol. Chem.

Narendra, D., Walker, J.E., Youle, R., 2012. Mitochondrial Quality Control Mediated by PINK1 and Parkin: Links to Parkinsonism. Cold Spring Harb. Perspect. Biol. 4, a011338–a011338.

Newland, B., Dowd, E., Pandit, A., 2013. Biomaterial approaches to gene therapies for neurodegenerative disorders of the CNS. Biomater. Sci. 1, 556.

Nicodemus, G.D., Bryant, S.J., 2008. Cell Encapsulation in Biodegradable Hydrogels for Tissue Engineering Applications. Tissue Eng. Part B Rev. 14, 149–165.

Nikonova, E. V., Xiong, Y., Tanis, K.Q., Dawson, V.L., Vogel, R.L., Finney, E.M., Stone, D.J., Reynolds, I.J., Kern, J.T., Dawson, T.M., 2012. Transcriptional responses to loss or gain of function of the leucine-rich repeat kinase 2 (LRRK2) gene uncover biological processes modulated by LRRK2 activity. Hum. Mol. Genet. 21, 163–174.

Nuber, S., Harmuth, F., Kohl, Z., Adame, A., Trejo, M., Schönig, K., Zimmermann, F., Bauer, C., Casadei, N., Giel, C., Calaminus, C., Pichler, B.J., Jensen, P.H., Müller, C.P., Amato, D., Kornhuber, J., Teismann, P., Yamakado, H., Takahashi, R., Winkler, J., Masliah, E., Riess, O., 2013. A progressive dopaminergic phenotype associated with neurotoxic conversion of α-synuclein in BAC-transgenic rats. Brain.

Nussbaum, R.L., 2017. The Identification of Alpha-Synuclein as the First Parkinson Disease Gene. J. Parkinsons. Dis. 7, S45–S51.

Nutt, J.G., Burchiel, K.J., Comella, C.L., Jankovic, J., Lang, A.E., Laws, E.R., Lozano, A.M., Penn, R.D., Simpson, R.K., Stacy, M., Wooten, G.F., 2003. Randomized, double-blind trial of glial cell line-derived neurotrophic factor (GDNF) in PD. Neurology 60, 69–73.

O'Regan, G., Desouza, R.M., Balestrino, R., Schapira, A.H., 2017. Glucocerebrosidase Mutations in Parkinson Disease. J. Parkinsons. Dis. 7, 411–422.

Obeso, J.A., Rodríguez-Oroz, M.C., Benitez-Temino, B., Blesa, F.J., Guridi, J., Marin, C., Rodriguez, M., 2008. Functional organization of the basal ganglia: Therapeutic implications for Parkinson's disease. Mov. Disord. 23, 548–559.

Oertel, W.H., 2017. Recent advances in treating Parkinson's disease. F1000Research 6, 260.

Ohsawa, K., Kohsaka, S., 2009. Microglial Response to Injury. In: Encyclopedia of Neuroscience. Elsevier, pp. 861–864.

Okun, M.S., 2012. Deep-Brain Stimulation for Parkinson's Disease. N. Engl. J. Med. 367, 1529–1538.

Olsen, L.K., Dowd, E., McKernan, D.P., 2018. A role for viral infections in Parkinson's etiology? Neuronal Signal. 2, NS20170166.

Ono, K., Ikemoto, M., Kawarabayashi, T., Ikeda, M., Nishinakagawa, T., Hosokawa, M., Shoji, M., Takahashi, M., Nakashima, M., 2009. A chemical chaperone, sodium 4-phenylbutyric acid, attenuates the pathogenic potency in human α-synuclein A30P + A53T transgenic mice. Park. Relat. Disord.

Orive, G., Anitua, E., Pedraz, J.L., Emerich, D.F., 2009. Biomaterials for promoting brain protection, repair and regeneration. Nat. Rev. Neurosci. 10, 682–692.

Pain, S., Vergote, J., Gulhan, Z., Bodard, S., Chalon, S., Gaillard, A., 2019. Inflammatory process in Parkinson disease: neuroprotection by neuropeptide Y. Fundam. Clin. Pharmacol. 33, 544–548.

Paisán-Ruíz, C., Jain, S., Evans, E.W., Gilks, W.P., Simón, J., van der Brug, M., de Munain, A.L., Aparicio, S., Gil, A.M., Khan, N., Johnson, J., Martinez, J.R., Nicholl, D., Carrera, I.M., Peňa, A.S., de Silva, R., Lees, A., Martí-Massó, J.F., Pérez-Tur, J., Wood, N.W., Singleton, A.B., 2004. Cloning of the Gene Containing Mutations that Cause PARK8-Linked Parkinson's Disease. Neuron 44, 595–600.

Palfi, S., Gurruchaga, J.M., Lepetit, H., Howard, K., Ralph, G.S., Mason, S., Gouello, G., Domenech, P., Buttery, P.C., Hantraye, P., Tuckwell, N.J., Barker, R.A., Mitrophanous, K.A., 2018. Long-Term Follow-Up of a Phase I/II Study of ProSavin, a Lentiviral Vector Gene Therapy for Parkinson's Disease. Hum. Gene Ther. Clin. Dev. 29, 148–155.

Palfi, S., Gurruchaga, J.M., Ralph, G.S., Lepetit, H., Lavisse, S., Buttery, P.C., Watts, C., Miskin, J., Kelleher, M., Deeley, S., Iwamuro, H., Lefaucheur, J.P., Thiriez, C., Fenelon, G., Lucas, C., Brugières, P., Gabriel, I., Abhay, K., Drouot, X., Tani, N., Kas, A., Ghaleh, B., Le Corvoisier, P., Dolphin, P., Breen, D.P., Mason, S., Guzman, N.V., Mazarakis, N.D., Radcliffe, P.A., Harrop, R., Kingsman, S.M., Rascol, O., Naylor, S., Barker, R.A., Hantraye, P., Remy, P., Cesaro, P., Mitrophanous, K.A., 2014. Long-term safety and tolerability of ProSavin, a lentiviral vector-based gene therapy for Parkinson's disease: a dose escalation, open-label, phase 1/2 trial. Lancet 383, 1138–1146.

Papale, A., Cerovic, M., Brambilla, R., 2009. Viral vector approaches to modify gene expression in the brain. J. Neurosci. Methods 185, 1–14.

Papkovskaia, T.D., Chau, K.-Y., Inesta-Vaquera, F., Papkovsky, D.B., Healy, D.G., Nishio, K., Staddon, J., Duchen, M.R., Hardy, J., Schapira, A.H.V., Cooper, J.M., 2012. G2019S leucine-rich repeat kinase 2 causes uncoupling protein-mediated mitochondrial depolarization. Hum. Mol. Genet. 21, 4201–4213.

Pardo, J., Morel, G., Astiz, M., Schwerdt, J., Leon, M., Rodriguez, S., Herenu, C., Goya, R., 2014. Gene Therapy and Cell Reprogramming For the Aging Brain: Achievements and Promise. Curr. Gene Ther. 14, 24–34.

Parent, M., Parent, A., 2010. Substantia Nigra and Parkinson's Disease: A Brief History of Their Long and Intimate Relationship. Can. J. Neurol. Sci. / J. Can. des Sci. Neurol. 37, 313–319.

Park, M., Moon, Y., Han, S.-H., Kim, H.K., Moon, W.-J., 2019. Myelin loss in white matter hyperintensities and normal-appearing white matter of cognitively impaired patients: a quantitative

synthetic magnetic resonance imaging study. Eur. Radiol. 29, 4914–4921.

Park, S., Han, S., Choi, I., Kim, B., Park, S.P., Joe, E.-H., Suh, Y.H., 2016. Interplay between Leucine-Rich Repeat Kinase 2 (LRRK2) and p62/SQSTM-1 in Selective Autophagy. PLoS One 11, e0163029.

Parkinson, J., 2002. An Essay on the Shaking Palsy. J. Neuropsychiatry Clin. Neurosci. 14, 223–236.

Peelaerts, W., Bousset, L., Van der Perren, A., Moskalyuk, A., Pulizzi, R., Giugliano, M., Van den Haute, C., Melki, R., Baekelandt, V., 2015. α-Synuclein strains cause distinct synucleinopathies after local and systemic administration. Nature 522, 340–344.

Pekny, M., Nilsson, M., 2005. Astrocyte activation and reactive gliosis. Glia 50, 427–434.

Perlmutter, J.S., 2009. Assessment of Parkinson Disease Manifestations. Curr. Protoc. Neurosci. 49, 10.1.1-10.1.14.

Perlow, M., Freed, W., Hoffer, B., Seiger, A., Olson, L., Wyatt, R., 1979. Brain grafts reduce motor abnormalities produced by destruction of nigrostriatal dopamine system. Science (80-.). 204, 643–647.

Perry, G., Zhu, X., Babar, A.K., Siedlak, S.L., Yang, Q., Ito, G., Iwatsubo, T., Smith, M.A., Chen, S.G., 2008. Leucine-Rich Repeat Kinase 2 Colocalizes with α-Synuclein in Parkinson's Disease, but Not Tau-Containing Deposits in Tauopathies. Neurodegener. Dis. 5, 222–224.

Pickrell, A.M., Youle, R.J., 2015. The Roles of PINK1, Parkin, and Mitochondrial Fidelity in Parkinson's Disease. Neuron 85, 257–273.

Polymeropoulos, M.H., Lavedan, C., Leroy, E., Ide, S.E., Dehejia, A., Dutra, A., Pike, B., Root, H., Rubenstein, J., Boyer, R., Stenroos, E.S., Chandrasekharappa, S., Athanassiadou, A., Papapetropoulos, T., Johnson, W.G., Lazzarini, A.M., Duvoisin, R.C., Iorio, G. Di, Golbe, L.I., Nussbaum, R.L., 1997. Mutation in the α-Synuclein Gene Identified in Families with Parkinson's Disease. Science (80-.). 276, 2045–2047.

Pomfret, R., Miranpuri, G., Sillay, K., 2013. The Substitute Brain and the Potential of the Gel Model. Ann. Neurosci. 20, 118–122.

Price, A., Manzoni, C., Cookson, M.R., Lewis, P.A., 2018. The LRRK2 signalling system. Cell Tissue Res. 373, 39–50.

Przedborski, S., 2007. Neuroinflammation and Parkinson's disease 83, 535–551.

Przedborski, S., 2017. The two-century journey of Parkinson disease research. Nat. Rev. Neurosci.

Przedborski, S., Tieu, K., Perier, C., Vila, M., 2004. MPTP as a mitochondrial neurotoxic model of Parkinson's disease. In: Journal of Bioenergetics and Biomembranes.

Purves, D., Augustine, G.J., Fitzpatrick, D., Katz, L.C., LaMantia, A.S., McNamara, J.O., Williams, S.M., 2001. Circuits within the Basal Ganglia System. In: Neuroscience - 2nd Edition.

Puspita, L., Chung, S.Y., Shim, J., 2017. Oxidative stress and cellular pathologies in Parkinson's disease. Mol. Brain 10, 53.

Ramonet, D., Daher, J.P.L., Lin, B.M., Stafa, K., Kim, J., Banerjee, R., Westerlund, M., Pletnikova, O., Glauser, L., Yang, L., Liu, Y., Swing, D.A., Beal, M.F., Troncoso, J.C., McCaffery, J.M., Jenkins, N.A., Copeland, N.G., Galter, D., Thomas, B., Lee, M.K., Dawson, T.M., Dawson, V.L., Moore, D.J., 2011.

Dopaminergic Neuronal Loss, Reduced Neurite Complexity and Autophagic Abnormalities in Transgenic Mice Expressing G2019S Mutant LRRK2. PLoS One 6, e18568.

Ramprasad, M.P., Terpstra, V., Kondratenko, N., Quehenberger, O., Steinberg, D., 1996. Cell surface expression of mouse macrosialin and human CD68 and their role as macrophage receptors for oxidized low density lipoprotein. Proc. Natl. Acad. Sci. 93, 14833–14838.

Ratajczak, M.Z., Jadczyk, T., Pędziwiatr, D., Wojakowski, W., 2014. New advances in stem cell research: practical implications for regenerative medicine. Pol. Arch. Med. Wewn. 124, 417–26.

Recasens, A., Dehay, B., 2014. Alpha-synuclein spreading in Parkinson's disease. Front. Neuroanat. 8, 1–9.

Reichmann, H., 2010. Clinical criteria for the diagnosis of Parkinson's disease. Neurodegener. Dis. 7, 284–290.

Ricard-Blum, S., 2011. The Collagen Family. Cold Spring Harb. Perspect. Biol. 3, 1–19.

Rideout, H.J., Stefanis, L., 2014. The neurobiology of LRRK2 and its role in the pathogenesis of Parkinson's disease. Neurochem. Res. 39, 576–592.

Rizek, P., Kumar, N., Jog, M.S., 2016. An update on the diagnosis and treatment of Parkinson disease. Can. Med. Assoc. J. 188, 1157–1165.

Rocha, E.M., De Miranda, B., Sanders, L.H., 2018. Alpha-synuclein: Pathology, mitochondrial dysfunction and neuroinflammation in Parkinson's disease. Neurobiol. Dis. 109, 249–257.

Rockenstein, E., Mallory, M., Hashimoto, M., Song, D., Shults, C.W., Lang, I., Masliah, E., 2002. Differential neuropathological alterations in transgenic mice expressing α-synuclein from the platelet-derived growth factor and Thy-1 promoters. J. Neurosci. Res.

Russo, I., Bubacco, L., Greggio, E., 2014. LRRK2 and neuroinflammation: partners in crime in Parkinson's disease? J. Neuroinflammation 11, 52.

Sahin, G., Thompson, L.H., Lavisse, S., Ozgur, M., Rbah-Vidal, L., Dollé, F., Hantraye, P., Kirik, D., 2014. Differential dopamine receptor occupancy underlies L-DOPA-induced dyskinesia in a rat model of parkinson's disease. PLoS One.

Sanami, M., Sweeney, I., Shtein, Z., Meirovich, S., Sorushanova, A., Mullen, A.M., Miraftab, M., Shoseyov, O., O'Dowd, C., Pandit, A., Zeugolis, D.I., 2016. The influence of poly(ethylene glycol) ether tetrasuccinimidyl glutarate on the structural, physical, and biological properties of collagen fibers. J. Biomed. Mater. Res. Part B Appl. Biomater. 104, 914–922.

Sánchez-Pérez, A.M., Claramonte-Clausell, B., Sánchez-Andrés, J.V., Herrero, M.T., 2012. Parkinson's Disease and Autophagy. Parkinsons. Dis. 2012, 1–6.

Schapira, A.H.V., 2015. Glucocerebrosidase and Parkinson disease: Recent advances. Mol. Cell. Neurosci. 66, 37–42.

Schapira, A.H.V., Cooper, J.M., Dexter, D., Jenner, P., Clark, J.B., Marsden, C.D., 1989. Mithocondrial complex I deficiency in Parkinson's disease. Lancet 333, 1269.

Schapira, A.H. V., Cooper, J.M., Dexter, D., Clark, J.B., Jenner, P., Marsden, C.D., 1990. Mitochondrial

Complex I Deficiency in Parkinson's Disease. J. Neurochem. 54, 823–827.

Scudellari, M., 2016. A decade of iPS Cells. Nature 534, 310–312.

Sekuła, M., Zuba-Surma, E.K., 2018. Biomaterials and Stem Cells: Promising Tools in Tissue Engineering and Biomedical Applications. Biomater. Regen. Med.

Seol, W., 2010. Biochemical and molecular features of LRRK2 and its pathophysiological roles in Parkinson's disease. BMB Rep.

Shahmoradian, S.H., Lewis, A.J., Genoud, C., Hench, J., Moors, T.E., Navarro, P.P., Castaño-Díez, D., Schweighauser, G., Graff-Meyer, A., Goldie, K.N., Sütterlin, R., Huisman, E., Ingrassia, A., Gier, Y. de, Rozemuller, A.J.M., Wang, J., Paepe, A. De, Erny, J., Staempfli, A., Hoernschemeyer, J., Großerüschkamp, F., Niedieker, D., El-Mashtoly, S.F., Quadri, M., Van IJcken, W.F.J., Bonifati, V., Gerwert, K., Bohrmann, B., Frank, S., Britschgi, M., Stahlberg, H., Van de Berg, W.D.J., Lauer, M.E., 2019. Lewy pathology in Parkinson's disease consists of crowded organelles and lipid membranes. Nat. Neurosci. 22, 1099–1109.

Sheng, Z., Zhang, S., Bustos, D., Kleinheinz, T., Le Pichon, C.E., Dominguez, S.L., Solanoy, H.O., Drummond, J., Zhang, X., Ding, X., Cai, F., Song, Q., Li, X., Yue, Z., van der Brug, M.P., Burdick, D.J., Gunzner-Toste, J., Chen, H., Liu, X., Estrada, A.A., Sweeney, Z.K., Scearce-Levie, K., Moffat, J.G., Kirkpatrick, D.S., Zhu, H., 2012. Ser1292 Autophosphorylation Is an Indicator of LRRK2 Kinase Activity and Contributes to the Cellular Effects of PD Mutations. Sci. Transl. Med. 4, 164ra161-164ra161.

Sherman, M.Y., Goldberg, A.L., 2001. Cellular defenses against unfolded proteins: A cell biologist thinks about neurodegenerative diseases. Neuron.

Shimoji, M., Pagan, F., Healton, E.B., Mocchetti, I., 2009. CXCR4 and CXCL12 expression is increased in the nigro-striatal system of Parkinson's disease. Neurotox. Res.

Sidransky, E., Lopez, G., 2012. The link between the GBA gene and parkinsonism. Lancet Neurol. 11, 986–998.

Simmons, A., Tofts, P.S., Barker, G.J., Arridge, S.R., 1994. Sources of intensity nonuniformity in spin echo images at 1.5 T. Magn. Reson. Med. 32, 121–128.

Singh, N., Pillay, V., Choonara, Y.E., 2007. Advances in the treatment of Parkinson's disease. Prog. Neurobiol. 81, 29–44.

Sloan, M., Alegre-Abarrategui, J., Potgieter, D., Kaufmann, A.-K., Exley, R., Deltheil, T., Threlfell, S., Connor-Robson, N., Brimblecombe, K., Wallings, R., Cioroch, M., Bannerman, D.M., Bolam, J.P., Magill, P.J., Cragg, S.J., Dodson, P.D., Wade-Martins, R., 2016. LRRK2 BAC transgenic rats develop progressive, L-DOPA-responsive motor impairment, and deficits in dopamine circuit function. Hum. Mol. Genet. 25, 951–963.

Sofroniew, M. V., 2009. Molecular dissection of reactive astrogliosis and glial scar formation. Trends Neurosci. 32, 638–647.

Spader, H.S., Dean, D.C., Curt LaFrance, W., Raukar, N.P., Rees Cosgrove, G., Eyerly-Webb, S.A., Ellermeier, A., Correia, S., Deoni, S.C.L., Rogg, J., 2019. Prospective study of myelin water fraction changes after mild traumatic brain injury in collegiate contact sports. J. Neurosurg. 130, 1321–1329.

Spillantini, M.G., Crowther, R.A., Jakes, R., Hasegawa, M., Goedert, M., 1998. a-Synuclein in filamentous inclusions of Lewy bodies from Parkinson's disease and dementia with Lewy bodies. Proc. Natl. Acad. Sci. 95, 6469–6473.

Spillantini, M.G., Schmidt, M.L., Lee, V.M.-Y., Trojanowski, J.Q., Jakes, R., Goedert, M., 1997. alpha-Synuclein in Lewy bodies. Nature 388, 839–840.

Stadelmann, C., Timmler, S., Barrantes-Freer, A., Simons, M., 2019. Myelin in the Central Nervous System: Structure, Function, and Pathology. Physiol. Rev. 99, 1381–1431.

Steger, M., Diez, F., Dhekne, H.S., Lis, P., Nirujogi, R.S., Karayel, O., Tonelli, F., Martinez, T.N., Lorentzen, E., Pfeffer, S.R., Alessi, D.R., Mann, M., 2017. Systematic proteomic analysis of LRRK2-mediated Rab GTPase phosphorylation establishes a connection to ciliogenesis. Elife 6, 1–22.

Steger, M., Tonelli, F., Ito, G., Davies, P., Trost, M., Vetter, M., Wachter, S., Lorentzen, E., Duddy, G., Wilson, S., Baptista, M.A., Fiske, B.K., Fell, M.J., Morrow, J.A., Reith, A.D., Alessi, D.R., Mann, M., 2016. Phosphoproteomics reveals that Parkinson's disease kinase LRRK2 regulates a subset of Rab GTPases. Elife 5, 1–28.

Stocchi, F., Torti, M., 2017. Constipation in Parkinson's Disease. In: International Review of Neurobiology. Elsevier Inc., pp. 811–826.

Stoker, T.B., Barker, R.A., 2018. Regenerative Therapies for Parkinson's Disease: An Update. BioDrugs 32, 357–366.

Sullivan, A., O'Keeffe, G., 2016. Neurotrophic factor therapy for Parkinson's disease: past, present and future. Neural Regen. Res. 11, 205.

Sung, H.-Y., Park, J.-W., Kim, J.-S., 2014. The Frequency and Severity of Gastrointestinal Symptoms in Patients with Early Parkinson's Disease. J. Mov. Disord. 7, 7–12.

Sveinbjornsdottir, S., 2016. The clinical symptoms of Parkinson's disease. J. Neurochem. 1–7.

Takahashi, K., Yamanaka, S., 2006. Induction of Pluripotent Stem Cells from Mouse Embryonic and Adult Fibroblast Cultures by Defined Factors. Cell 126, 663–676.

Tieu, K., 2011. A Guide to Neurotoxic Animal Models of Parkinson's Disease. Cold Spring Harb. Perspect. Med. 1, a009316–a009316.

Titova, N., Qamar, M.A., Chaudhuri, K.R., 2017. Biomarkers of Parkinson's Disease. In: International Review of Neurobiology. Elsevier Inc., pp. 183–196.

Torres, E.M., Lane, E.L., Heuer, A., Smith, G.A., Murphy, E., Dunnett, S.B., 2011. Increased efficacy of the 6-hydroxydopamine lesion of the median forebrain bundle in small rats, by modification of the stereotaxic coordinates. J. Neurosci. Methods.

Trounson, A., McDonald, C., 2015. Stem Cell Therapies in Clinical Trials: Progress and Challenges. Cell Stem Cell 17, 11–22.

Ullah, F., Othman, M.B.H., Javed, F., Ahmad, Z., Akil, H.M., 2015. Classification, processing and application of hydrogels: A review. Mater. Sci. Eng. C 57, 414–433.

Ulusoy, A., Decressac, M., Kirik, D., Björklund, A., 2010. Viral vector-mediated overexpression of α-

synuclein as a progressive model of Parkinson's disease. In: Progress In Brain Research- Volume 184. Elsevier B.V., pp. 89–111.

Ünal-Çevik, I., Kılınç, M., Gürsoy-Özdemir, Y., Gurer, G., Dalkara, T., 2004. Loss of NeuN immunoreactivity after cerebral ischemia does not indicate neuronal cell loss: a cautionary note. Brain Res. 1015, 169–174.

Ungerstedt, U., 1968. 6-hydroxy-dopamine induced degeneration of central monoamine neurons. Eur. J. Pharmacol. 5, 107–110.

Valdés, P., Schneider, B.L., 2016. Gene Therapy: A Promising Approach for Neuroprotection in Parkinson's Disease? Front. Neuroanat. 10.

Van der Perren, A., Van den Haute, C., Baekelandt, V., 2014. Viral Vector-Based Models of Parkinson's Disease. In: Nguyen, H., Cenci, M. (Eds.), Behavioral Neurobiology of Huntington's Disease and Parkinson's Disease. Current Topics in Behavioral Neurosciences. Springer, Berlin, Heidelberg, pp. 271–301.

Vandenberghe, M.E., Hérard, A.-S., Souedet, N., Sadouni, E., Santin, M.D., Briet, D., Carré, D., Schulz, J., Hantraye, P., Chabrier, P.-E., Rooney, T., Debeir, T., Blanchard, V., Pradier, L., Dhenain, M., Delzescaux, T., 2016. High-throughput 3D whole-brain quantitative histopathology in rodents. Sci. Rep. 6, 20958.

Vaquer-Alicea, J., Diamond, M.I., 2019. Propagation of Protein Aggregation in Neurodegenerative Diseases. Annu. Rev. Biochem. 88, annurev-biochem-061516-045049.

Varaprasad, K., Raghavendra, G.M., Jayaramudu, T., Yallapu, M.M., Sadiku, R., 2017. A mini review on hydrogels classification and recent developments in miscellaneous applications. Mater. Sci. Eng. C 79, 958–971.

Vila, M., Vukosavic, S., Jackson-Lewis, V., Neystat, M., Jakowec, M., Przedborski, S., 2001. α-Synuclein Up-Regulation in Substantia Nigra Dopaminergic Neurons Following Administration of the Parkinsonian Toxin MPTP. J. Neurochem. 74, 721–729.

Visanji, N.P., Brotchie, J.M., Kalia, L. V, Koprich, J.B., Tandon, A., Watts, J.C., Lang, A.E., 2016. α-Synuclein-Based Animal Models of Parkinson's Disease: Challenges and Opportunities in a New Era. Trends Neurosci. 39, 750–762.

Vitte, J., Traver, S., Maués De Paula, A., Lesage, S., Rovelli, G., Corti, O., Duyckaerts, C., Brice, A., 2010. Leucine-Rich Repeat Kinase 2 Is Associated With the Endoplasmic Reticulum in Dopaminergic Neurons and Accumulates in the Core of Lewy Bodies in Parkinson Disease. J. Neuropathol. Exp. Neurol. 69, 959–972.

Volpicelli-Daley, L.A., Abdelmotilib, H., Liu, Z., Stoyka, L., Daher, J.P.L., Milnerwood, A.J., Unni, V.K., Hirst, W.D., Yue, Z., Zhao, H.T., Fraser, K., Kennedy, R.E., West, A.B., 2016. G2019S-LRRK2 Expression Augments α-Synuclein Sequestration into Inclusions in Neurons. J. Neurosci. 36, 7415–7427.

Wakabayashi, K., Tanji, K., Mori, F., Takahashi, H., 2007. The Lewy body in Parkinson's disease: Molecules implicated in the formation and degradation of α-synuclein aggregates. Neuropathology 27, 494–506.

Wakabayashi, K., Tanji, K., Odagiri, S., Miki, Y., Mori, F., Takahashi, H., 2013. The Lewy Body in Parkinson's Disease and Related Neurodegenerative Disorders. Mol. Neurobiol. 47, 495–508.

Walker, M.D., Volta, M., Cataldi, S., Dinelle, K., Beccano-Kelly, D., Munsie, L., Kornelsen, R., Mah, C., Chou, P., Co, K., Khinda, J., Mroczek, M., Bergeron, S., Yu, K., Cao, L.P. in., Funk, N., Ott, T., Galter, D., Riess, O., Biskup, S., Milnerwood, A.J., Stoessl, A.J., Farrer, M.J., Sossi, V., 2014. Behavioral deficits and striatal DA signaling in LRRK2 p.G2019S transgenic rats: a multimodal investigation including PET neuroimaging. J. Parkinsons. Dis.

Wang, B., Abraham, N., Gao, G., Yang, Q., 2016. Dysregulation of autophagy and mitochondrial function in Parkinson's disease. Transl. Neurodegener. 5, 19.

Wang, K., Bekar, L.K., Furber, K., Walz, W., 2004. Vimentin-expressing proximal reactive astrocytes correlate with migration rather than proliferation following focal brain injury. Brain Res. 1024, 193–202.

Wang, T.-Y., Bruggeman, K.F., Kauhausen, J.A., Rodriguez, A.L., Nisbet, D.R., Parish, C.L., 2016. Functionalized composite scaffolds improve the engraftment of transplanted dopaminergic progenitors in a mouse model of Parkinson's disease. Biomaterials 74, 89–98.

Wang, X., Yan, M.H., Fujioka, H., Liu, J., Wilson-Delfosse, A., Chen, S.G., Perry, G., Casadesus, G., Zhu, X., 2012. LRRK2 regulates mitochondrial dynamics and function through direct interaction with DLP1. Hum. Mol. Genet. 21, 1931–1944.

West, A.B., Moore, D.J., Biskup, S., Bugayenko, A., Smith, W.W., Ross, C.A., Dawson, V.L., Dawson, T.M., 2005. Parkinson's disease-associated mutations in leucine-rich repeat kinase 2 augment kinase activity. Proc. Natl. Acad. Sci. U. S. A. 102, 16842–16847.

Wichmann, T., DeLong, M.R., 2011. Deep-brain stimulation for basal ganglia disorders. Basal Ganglia 1, 65–77.

Widner, H., Tetrud, J., Rehncrona, S., Snow, B., Brundin, P., Gustavii, B., Björklund, A., Lindvall, O., Langston, J.W., 1992. Bilateral Fetal Mesencephalic Grafting in Two Patients with Parkinsonism Induced by 1-Methyl-4-Phenyl-L,2,3,6-Tetrahydropyridine (MPTP). N. Engl. J. Med. 327, 1556–1563.

Wirdefeldt, K., Adami, H.-O., Cole, P., Trichopoulos, D., Mandel, J., 2011. Epidemiology and etiology of Parkinson's disease: a review of the evidence. Eur. J. Epidemiol. 26, 1–58.

World Health Organization, 2006. Neurological disorders: a public health approach. Neurol. Disord. public Heal. challenges. 41–176.

Wright, A.D., Jarrett, M., Vavasour, I., Shahinfard, E., Kolind, S., van Donkelaar, P., Taunton, J., Li, D., Rauscher, A., 2016. Myelin Water Fraction Is Transiently Reduced after a Single Mild Traumatic Brain Injury – A Prospective Cohort Study in Collegiate Hockey Players. PLoS One 11, e0150215.

Xia, R., Mao, Z.H., 2012. Progression of motor symptoms in Parkinson's disease. Neurosci. Bull. 28, 39–48.

Xu, L., Pu, J., 2016. Alpha-Synuclein in Parkinson's Disease: From Pathogenetic Dysfunction to Potential Clinical Application. Parkinsons. Dis. 2016, 1–10.

Yasuhara, T., Kameda, M., Sasaki, T., Tajiri, N., Date, I., 2017. Cell Therapy for Parkinson's Disease. Cell Transplant. 26, 1551–1559.

Yeragani, V., Tancer, M., Chokka, P., Baker, G., 2010. Arvid Carlsson, and the story of dopamine. Indian

J. Psychiatry 52, 87.

Yin, J., Valin, K.L., Dixon, M.L., Leavenworth, J.W., 2017. The Role of Microglia and Macrophages in CNS Homeostasis, Autoimmunity, and Cancer. J. Immunol. Res. 2017.

Zeng, J.-H., Liu, S.-W., Xiong, L., Qiu, P., Ding, L.-H., Xiong, S.-L., Li, J.-T., Liao, X.-G., Tang, Z.-M., 2018. Scaffolds for the repair of bone defects in clinical studies: a systematic review. J. Orthop. Surg. Res. 13, 33.

Zhang, L., Niu, X., Sun, L., She, Z., Tan, R., Wang, W., 2018. Immune response of bovine sourced cross-linked collagen sponge for hemostasis. J. Biomater. Appl. 32, 920–931.

Zhang, Q., Chen, W., Tan, S., Lin, T., 2017. Stem Cells for Modeling and Therapy of Parkinson's Disease. Hum. Gene Ther. 28, 85–98.

Zimprich, A., Biskup, S., Leitner, P., Lichtner, P., Farrer, M., Lincoln, S., Kachergus, J., Hulihan, M., Uitti, R.J., Calne, D.B., Stoessl, A.J., Pfeiffer, R.F., Patenge, N., Carbajal, I.C., Vieregge, P., Asmus, F., Müller-Myhsok, B., Dickson, D.W., Meitinger, T., Strom, T.M., Wszolek, Z.K., Gasser, T., 2004. Mutations in LRRK2 Cause Autosomal-Dominant Parkinsonism with Pleomorphic Pathology. Neuron 44, 601–607.

université PARIS-SACLAY
ÉCOLE DOCTORALE
Signalisation et réseaux intégratifs en biologie (BIOSIGNE)

UNIVERSITÉ PARIS SUD
Comprendre le monde, construire l'avenir

Evaluation of an *in situ* polymerizing hydrogel scaffold as a brain delivery system for Parkinson's disease therapeutics

Abstract: Parkinson's disease (PD) is the second most common neurodegenerative disease, affecting 0.3% of general population, with an increasing rate of 1 to 2% in persons over 65. At the moment the only available pharmacological treatment (L-Dopa) focuses on mitigating symptoms; nowadays treatments to slow down the disease's progression, or suppress symptoms on the long term remain to be validated.

Cellular transplantation had showed encouraging results, but it has some limitation, including the poor survival of the grafted cells, strong immune response and rejection of the graft.

Biomaterials are materials used and adapted for medical applications and are designed to interact with different biological systems. Among them, collagen-based hydrogels recently gained attention in the field of regenerative medicine and cellular transplantation, being widely used for skin graft and wound healing, spinal cord regeneration, bones and tendon repair. To date, such promising approach has not been often investigated *in vivo* for neurodegenerative diseases as PD.

In this work we developed a rodent relevant model of PD that is able to show a progressive neurodegeneration of DA neurons in the SNpc. Using adeno-associated viral vector (AAV), we overexpressed the C-terminal domain of mutated LRRK2 form ($LRRK2^{G2019S}$) with or without mutant α-synuclein ($\alpha\text{-syn}^{A53T}$) in the SNpc. Our results showed that, while $LRRK2^{G2019S}$ alone did not produce any toxicity, $\alpha\text{-syn}^{A53T}$ co-expressed with LRRK2 G2019S produced a greater loss of dopaminergic cells in the SNpc. $\alpha\text{-syn}^{A53T}$ toxicity is likely to be facilitated by the kinase activity of mutant LRRK2 through a cell autonomous mechanism.

Once the neurodegenerative rat model of PD was developed and ready for testing the potential of the collagen scaffold as a delivery system, we proceeded with characterization of the hydrogel scaffold.

Using high field (11.7T) magnetic resonance imaging (MRI), and histological analysis we characterized our collagen-based hydrogel after *in vitro* and, *in vivo* polymerization after intracerebral injection in rats.

Our results indicate that collagen-based hydrogels can be safely injected into the brain without any major adverse effect and that MRI is a tool of choice for a direct and non-invasive *in vivo* follow-up of collagen hydrogel polymerization and grafting in the brain. The collagen scaffold showed a transitory and limited immune response localized around the site of injection.

These results suggest that our *in-situ* polymerizing collagen-based hydrogel could be safely employed as a delivery system for cells and/or molecules during neuronal transplantation.

Abstract: La maladie de Parkinson (MP) est la deuxième maladie neurodégénérative la plus répandue. Elle touche 0,3% de la population en général, avec un taux croissant de 1 à 2% chez les personnes de plus de 65 ans. À l'heure actuelle, le seul traitement pharmacologique disponible (L-Dopa) consiste à réduire la sévérité des symptômes moteurs; Plusieurs approches expérimentales sont actuellement à l'étude pour tenter de ralentir la progression de la maladie, ou réduire à long terme la sévérité des symptômes, mais avec un succès limité.

La transplantation cellulaire a déjà montré des effets encourageant dans les modèles animaux et en clinique, mais elle présente également plusieurs limites, notamment la faible survie des cellules greffées, une forte réponse immunitaire conduisant au rejet de la greffe. Les biomatériaux sont des matériaux utilisés et adaptés à des applications médicales. Ils sont conçus pour interagir avec différents systèmes biologiques. Parmi ceux-ci, les hydrogels à base de collagène ont attiré l'attention ces dernières années dans le domaine de la médecine régénérative et de la greffe cellulaire, largement utilisés pour la greffe de peau et la cicatrisation des plaies, la régénération de la moelle épinière, la réparation des os et des tendons. À ce jour, cette approche prometteuse n'a encore été étudiée que très rarement *in vivo* pour les maladies neurodégénératives telles que la MP.

Dans ce travail, nous avons développé un modèle pertinent de la MP pour les rongeurs, capable de montrer une dégénérescence progressive des neurones DA dans la SNpc. En utilisant un vecteur viral adéno-associé (AAV), nous avons surexprimé le domaine C-terminal de la forme LRRK2 mutée (G2019S) avec ou sans α-synucléine mutée ($\alpha\text{-syn}^{A53T}$) dans la SNpc. Nos résultats ont montré que, alors que $LRRK2^{G2019S}$ seule ne produisait aucune toxicité, l'α-syn co-exprimé avec $LRRK2^{G2019S}$ produisait une plus grande perte de neurones DA dans la SNpc par rapport à l'$\alpha\text{-syn}^{A53T}$ seule. La toxicité de l'a-syn est probablement facilitée par l'activité kinase du LRRK2 mutant par le biais d'un mécanisme « cell-autonomous ».

Une fois que le modèle neurodégénératif de la maladie de Parkinson a été développé et prêt à tester le potentiel du bio-polymère de collagène en tant que système d'administration, nous avons procédé à la caractérisation de l'échafaud en hydrogel.

En utilisant l'imagerie par résonance magnétique (IRM) à champ élevé (11,7 T) et l'analyse histologique, nous avons caractérisé notre hydrogel à base de collagène après polymérisation *in vitro* et, *in vivo*, après injection intracérébrale chez le rat.

Nos résultats indiquent que les hydrogels à base de collagène peuvent être injectés dans le cerveau sans effets délétères majeurs et que l'IRM est un outil de choix pour le suivi direct et non invasif de la polymérisation et de la greffe d'hydrogel de collagène. L'hydrogel de collagène a montré une réponse immunitaire transitoire et limitée essentiellement localisée autour du site d'injection.

Ces résultats suggèrent que notre hydrogel à base de collagène qui polymérise *in situ* pourrait être utilisé en toute sécurité comme système d'administration intracérébrale de cellules et / ou de molécules trophiques et/ou neuroprotectrices pour la MP.